ENHANCING BALLISTIC IMPACT RESISTANCE OF POLYMER MATRIX COMPOSITE ARMORS BY ADDITION OF MICRO AND NANO-FILLERS

A Thesis Submitted to the College of

Graduate and Postdoctoral Studies

In Partial Fulfillment of the Requirements

For the Degree of Doctor of Philosophy

In the Division of Biomedical Engineering

University of Saskatchewan

Saskatoon

By

Edison E. Haro

Permission to use

In presenting this thesis in partial fulfillment of the requirements for a postgraduate degree from the University of Saskatchewan, I agree that the Libraries of this University may make it freely available for inspection. I further agree that permission for copying of this thesis in any manner, in whole or in part, for scholarly purpose may be granted by the professors who supervised my thesis work or, in their absence, by the Head of the Department or the Dean of the College in which my thesis work was done. It is understood that any copying or publication or use of this thesis or part thereof for financial gain shall not be allowed without my written permission. It is also understood that due recognition shall be given to me and to the University of Saskatchewan in any scholarly use which may be made of any material in my thesis.

Requests for permission to copy or to make other use of material in this thesis in whole or part should be addressed to:

College of Graduate and Postdoctoral Studies
116 Thorvaldson Building,
110 Science Place
University of Saskatchewan
Saskatoon, Saskatchewan (S7N 5C9)
Canada

OR

Division of Biomedical Engineering
Room 2B60
57 Campus Drive
University of Saskatchewan
Saskatoon, Saskatchewan (S7N 5A9)
Canada

Abstract

Improving the ballistic impact resistance of hybrid polymer matrix composites through addition of micro- and nano-particles as fillers is the principal goal of this research. Development of light-weight ballistic plates, made of polymer matrix composites with improved ballistic resistance, can offer a solution of shielding with lighter, thinner, stronger and less expensive materials than the conventional ballistic plates. The use of micro- and nano-particles in low concentrations can achieve this goal without compromising the density or strength of the new armor plates.

Firstly, laminated hybrid composites consisting of aluminum alloy plates, epoxy resin and Kevlar® fabrics were developed. Shear thickening fluid (STF) made of nano-particles of colloidal silica (SiO_2) was impregnated into Kevlar® fabrics to determine its effect on the energy absorption behavior of the composites. STF decreased the tendency of Kevlar® fibers to rupture during projectile penetration, and thus, increased its impact energy absorption performance when compared to the samples made of Kevlar® neat fabrics (containing no STF). Similar laminated hybrid composites were subsequently built through impregnation of micro- and nano-particles of aluminum, gamma alumina, silicon carbide, colloidal silica and potato flour into Kevlar fabrics by mixing these particles with polyethylene glycol. The obtained laminates were evaluated to determine their impact resistance and energy absorption capabilities under ballistic impact. The plates containing aluminum and colloidal silica nano-powders have the highest energy absorption capability of between 679 up to 693 J for plate thickness and areal density of about 10.8 mm and 1.9 g/cm^2, respectively. These laminates can meet the protective requirements for levels IIA, II, and IIIA to resist ballistic impact from pistols caliber 9 mm.

In another approach, hybrid composite armor plates based on high density polyethylene (HDPE) were prepared by using 10 wt.% of Kevlar® short fibers, and 20 wt.% chonta palm wood, potato flour, colloidal silica or gamma alumina particles. Addition of colloidal silica and gamma alumina nano-particles improve stiffness by 43.5% and increase impact energy absorption capability by 20%, compared to control sample, which is HDPE containing 10 wt.% Kevlar® short fibers.

Hybrid bio-composites made of 10 wt.% Kevlar® short fibers and varying amount of chonta wood particles (10, 20, 30 wt. %), as additional reinforcement, were also developed and investigated. The hybrid composite plates containing 10 wt.% chonta palm wood micro-particles exhibited the

highest energy absorption capability of 62.4 J, which is equivalent to 19.5 % improvement over control specimens: HDPE reinforced with 10 wt.% Kevlar® short fibers.

Finally, bio-composites made of HDPE reinforced with varying fractions of micro-particles of chonta palm wood (10, 20, 25, and 30 wt. %) were developed and characterized. The ballistic impact performance of the biocomposites containing 25 wt.% chonta palm wood particles exhibited the highest energy absorption of 53.4 J, which represents a 41.3% improvement over the unreinforced HDPE specimens with similar thickness and density.

Acknowledgement

I would like to sincerely appreciate my supervisors Prof. Jerzy Szpunar and Prof. Akindele Odeshi for their guidance and endless support while carrying out this research project and in the course of writing this thesis. I wish to express my gratitude for their insights and comments that helped me to develop my research skills. I feel very fortunate for their unconditional support, I will always appreciate all they have done for me.

I also would like to thank my advisory committee members: Prof. Ike Oguocha, Prof. Duncan Cree, and Prof. Lope Tabil for their encouragements and their very constructive comments and discussions.

Additionally, I appreciate the valuable discussions and support from my friends and colleagues Xu Wen, A.A Tiamiyu and all members of the Advanced Materials and Renewable Energy (AMRE) group of the University of Saskatchewan.

Finally, I acknowledge the financial support of the Natural Science and Engineering Research Council of Canada (NSERC), the National Secretary of Science and Technology of the Ecuador (SENESCYT), and Ecuadorian Army.

Dedication

I want to dedicate this thesis to my lovely family, Vanessa, Ian and Erika, for their unconditional support, especially when the tasks many times seemed overwhelming, you have always been my inspiration to be strong and persistent, no matter how great the obstacles have been.

Also, to my beloved parents, the reason for what I become today and the achievements that I have accomplished. Thanks for your unconditional love and guide in all my challenges.

Table of Contents

List of Tables

List of Figures

Acronyms

HMMWV	High Mobility Multipurpose Wheeled Vehicle
STF	Shear Thickening Fluid
HDPE	High Density Polyethylene
NIJ	National Institute of Justice
PMC	Polymer Matrix Composites
CMC	Ceramic Matrix Composites
MMC	Metal Matrix Composites
ACM	Advanced Composite Materials
UHMWPE	Ultra High Molecular Weight Polyethylene
FML	Fiber Matrix Laminates
GLARE	Glass Reinforced Aluminium
ARALL	Aramid Reinforced Aluminum Laminates
PP	Polypropylene
PEG	Polyethylene Glycol
GFRP	Glass Fiber Reinforced Plastic
SEM	Scanning Electron Microscope
XRD	X-ray Diffraction
EDS	Energy Dispersive Spectroscopy
OM	Optical Microscope

Chapter 1: Introduction

1.1 Overview

In this chapter, the motivations for this study and the importance of improving the ballistic impact resistance and energy absorption performance of polymer matrix composite materials are briefly described. The main goal of this research and specific objectives of the study are presented. An overview of the content of this thesis is also highlighted.

1.2 Motivations for Research

The defense industry in conjunction with the scientific community has continued to show great interest in the development of protective armor systems (for both equipment and people) against threats in combat operations. One of the main threats is the impact of projectiles at medium and high speed. The efficiency of these systems depends strongly on their ability to resist impulsive loads and absorb energy. Therefore, it is critical to find new ways to improve the impact resistance of materials for protective armor application.

According to the Constitution of the Republic of Ecuador, article 158 (2008), the new missions assigned to the Ecuadorian Army in addition to the defense of the sovereignty and territorial integrity include contributions to public safety, risk management and national development. These activities require the use of tactical missions involving high-risk operations, especially in the fight against common and organized crimes such as drug and illegal chemical precursors trafficking, money laundering, kidnapping, extortion, guerrillas and other illegal armed groups including the Revolutionary Armed Forces of Colombia (FARC) and National Liberation Army (ELN).

For these reasons, the Ecuadorian Army has identified the need to protect their soldiers and tactical vehicles with effective protective armors and there is strong commitment to meet this need. Therefore, development of this research project becomes an institutional need to solve critical

issues in military operations of the Ecuadorian Army in order to accomplish their assigned tactical missions.

Currently, the commercially available, ballistic armor plates in the world market are heavy and with thickness exceeding 25 mm. The US Army uses vehicles HMMWV (high mobility multi-purpose wheeled vehicle) models M1151, M1152, M1165 and M1167 with weight up to 12,000 lbs, and with ballistic protection shielding against low caliber weapons (7.62 mm), 155 mm artillery explosions (above or below the vehicle), and improvised explosive protection of up to 12 lbs. TNT (trinitrotoluene) [1]. These tactical vehicles have been used in Afghanistan and Iraq with excellent results, considering that the land and climate conditions are arid and semiarid. However, those vehicles have not been tested under land and climate conditions of mountains and jungle. The Ecuadorian Army uses tactical vehicles HMMWV models M998 and M1152 without ballistic protection, which weigh between 3000 to 5200 lbs. Those vehicles work without problems in the muddy fields of the jungle and mountains where other kinds of heavy armored vehicles cannot have access. However, due to activities of narco-guerrilla and illegal armed groups which have increased the production, processing and transportation of narcotics in the border of neighbouring countries with Ecuador, the risk of tactical missions has increased. In many occasions, soldiers have had sudden encounters with the guerrillas, or they have been ambushed putting their lives at high risk. The use of tactical vehicles with ballistic protection and body armors for soldiers would reduce the risk to life and loss of life of soldiers. Injuries sustained by solders in combat operation against the criminals will also be drastically reduced. Due to new technological advances with respect to development of composite armor materials and their applications, it is possible to perform further investigations to develop light-weight ballistic plates made of polymer matrix composite that have high strength and low cost. They can be used as body armors for soldiers and as ballistic plates coupled to tactical vehicles that are involved in those high-risk missions.

1.3 Research Objectives

Improvement of the ballistic impact resistance of hybrid polymer matrix composite armors through addition of micro- and nano-particles as fillers and other reinforcements to increase the mechanical properties, impact resistance and ballistic energy absorption is the principal goal of this research. The use of micro- and nano-particles in low concentrations can achieve this goal without

compromising the density or the strength of the new armor plates. By considering the fact that polymer matrix composite armors can be developed using different types of matrices, such as thermosetting matrices (epoxy resins), and thermoplastic matrices (polymers) [2-6], different specific objectives have been identified towards realizing the main goal of the study. These are outlined as follows:

1. To determine the effect impregnation of laminated Kevlar® fiber reinforced thermosetting polymer composites with shear thickening fluid on their ballistic impact resistance and energy absorption capacity during impact.
2. To determine the effect of impregnation of woven Kevlar® fabrics with nano-fillers on the energy absorption behavior of hybrid composite laminates made from these fabrics.
3. To develop and characterize the mechanical behaviour and ballistic impact resistance of hybrid composites made of high density polyethylene (HDPE) and Kevlar® pulp mixed with nano-fillers.
4. To determine the effects of the addition of organic micro-particles (chonta palm wood) to Kevlar® short fibers reinforced HDPE on the mechanical properties and the dynamic impact resistance of the resulting hybrid composites;
5. To develop and evaluate the mechanical strength and ballistic impact resistance of new improved bio-composites made of chonta palm wood micro-particles and HDPE.

1.4 Thesis Overview

In this thesis, synthesis and characterization of polymer-based composites and hybrid laminates for use in protective armor are discussed. The thesis contains nine chapters. The motivation, scope and objectives of the research are presented in Chapter 1, while Chapter 2 contains a review of some of the most important works done in the area of composite materials manufacture for ballistic armor applications.

Details of the materials and methods used in this research study are provided in Chapter 3. These include the selection and properties of the materials used in the hybrid and composite materials manufacture and the manufacturing processes used. The procedures for mechanical characterization and microstructure analysis are discussed in this chapter.

Chapter 4 focusses on the influence of STF impregnation of Kevlar® fibers on the ballistic impact resistance of sandwich composite laminates made of alternate layers of woven Kevlar® fibers reinforces epoxy and AA 5086 H32 aluminum alloy plates. This aspect of the research work addresses the first specific objective and has been published in the *Composites: Part A*.

In Chapter 5, enhancement of the impact energy absorption capacity of hybrid composites, reinforced with woven Kevlar® fiber, by impregnation of the fiber with different nano-fillers such as silica carbide, aluminum powder, colloidal silica, gamma alumina, and potato flour in Kevlar® woven fibers is discussed. The hybrid composite laminates were built using a sandwich type configuration consisting of different layers of aluminum alloy, Kevlar® fiber woven impregnated with various micro- and nano-fillers and epoxy resin as bonding agent. Research findings discussed in this chapter have been published in the *International Journal of Impact Engineering*.

In Chapter 6, the effects of micro- and nano-particles additions as reinforcements on the strength and impact resistance of short Kevlar® fibers reinforced hybrid composites containing a thermoplastic HDPE matrix are discussed. Improvement in the dynamic impact response of the developed hybrid specimens as a result of the micro- and nano- particles additions is highlighted. This chapter has been published in *Journal of Polymer-Plastic Technology and Engineering*.

In Chapter 7, the effects of introduction of natural micro-particles (chonta palm wood) into short Kevlar® fibers reinforced HDPE are discussed. The high strain-rate compressive behaviour and ballistic impact resistance of the obtained hybrid composites are discussed. This chapter is currently under review by the *Journal of Dynamic Behavior*.

The ballistic impact behavior of biocomposite armors made of HDPE reinforced with chonta palm wood micro-particles are addressed in Chapter 8. The improvement in impact resistance and energy absorption capability as a result of this particulate reinforcement are investigated and discussed in this chapter. This chapter has been published by the *Journal of Defense Technology*.

Chapter 9 provides the summary of the work done, conclusions made from research findings and suggestions for further investigations.

Chapter 2: Literature Review

2.1 Overview

The scientific bases for enhancement of the performance of polymer composite armors through addition of micro- and nano-fillers are presented in this chapter. This will facilitate a better understanding of the research objectives. In the first section, body armors are described and classified according to their protection levels. The previous works done in the area of development of advanced composite materials, with enhanced impact resistance for application in body armors, are also reviewed. In addition, some important points of view that have not been established in the previous works (knowledge gaps), which support the research goals, are highlighted in this chapter.

2.2 Body armor classifications and level of protection

Military personnel and law enforcement officers are normally required to wear body armors depending the level of risk associated with their missions such as combat operations or fight against terrorism, delinquency (common and organized), drug trafficking, kidnapping, extortion, guerrillas and other illegal armed groups.

Depending on their ability to protect against bullets fired from weapons of different power, protective armor materials are classified by levels of protection according to NIJ Standards–0101.04, 0101.06 and 0108.01 [7-9] on a scale IIA, II, IIIA, III and IV (Table. 2.1).

Body armors that are developed to protect against levels IIA, II and IIIA are called soft body armors. Soft body armors are used normally in low risk missions. Although, those armors offer flexibility and lighter weight. However, they are designed to protect against low caliber weapons such as pistols with caliber bullets 9 mm, having an average weight of 125 g, velocities ranging from 373 to 441 m/s, and impact energy ranging from 537 to 1510 J [9, 10].

Table 2.1. Body armor level classification according to bullet calibers and velocities [8].

NIJ Standard 0101.06

Level	Caliber	Velocities
Level II A	9 mm 124 g. FMJ RN	373 m/s (1225 ft/s)
	40 S&W	352 m/s (1155 ft/s)
Level II	9 mm 124 g. FMJ RN	397 m/s (1305 ft/s)
	.357 Magnum 158 gr. JSP	435 m/s (1430 ft/s)
Level III A	357 Sig 125 g. FN	448 m/s (1470 ft/s)
	.44 Magnum 240 g. JHP	435 m/s (1430 ft/s)
Level III	7.62 mm NATO 148 g. (.308 Caliber) FMJ	847 m/s (2780 ft/s)
Level IV	30.06 166 g. (.30 Caliber) M2AP Armor piercing	877 m/s (2880 ft/s)

Soft body armors have the purpose of slowing down bullets through layers or interwoven fabrics, by spreading out the impact force between layers in the area impacted and avoiding the impact at a focused spot. These body armors are generally built with laminated configuration consisting of Kevlar®, Dyneema, or Spectra woven fibers to protect personnel (as bulletproof vests) up to level IIIA.

The ballistic levels of protection III and IV are achieved by hard body armors. The rigid ballistic plates in the levels III and IV are developed to resist more powerful weapons like rifles with 7.62 mm bullets weighing from 148 to 166 g, travelling at velocities ranging between 800 and 1100 m/s, and with an impact energy between 1960 and 3814 Joules [9, 10]. These kinds of rigid plates are typically made of high strength metallic alloys or ceramic materials, and they can be very heavy, inflexible, and with limited body covering, which compromise the tactical performance of the users with respect to mobility and agility.

In order to find a balance between level of protection, flexibility, mobility and lighter weight, composite materials with ballistic armor applications have been studied widely for protective armor applications. New technologies leading to improved composite materials can offer an efficient solution of shielding with lighter, thinner, stronger, and less expensive protective armor than the conventional ballistic vests.

2.3 Advanced composite materials used in ballistic armor applications

Composite materials are defined as a mixture of two or more materials (physically and mechanically different) in such a way that their combination can lead to improved properties that are not achievable in conventional monolithic materials [11, 12]. Normally, the components can be physically identified and separated from one another by an interface [13]. The basic components of composite materials are matrix material and reinforcing material. The matrix material is the continuous phase which can be a metal, polymer, ceramic, or carbon. The reinforcing component is a dispersed phase that is surrounded by the matrix, and it can be fibers or particles of different sizes (macro, micro or nano).The reinforcing materials can be organic or inorganic, or a combination of the two [14].

There are different ways of classifying composite materials; however, the most recognized classifications are detailed as follows:

- According to their matrix phase, composite materials can be classified as: polymer matrix composites (PMC), ceramic matrix composites (CMC), metal matrix composites (MMC) and carbon-based matrix composites [2, 14, 15].
- According to the type of reinforcing material (dispersed phase), composite materials can be classified as: continuous fiber-reinforced, fibrous fabric, braid reinforced, short fiber or whisker reinforced, particle reinforced, micro and nano-particle reinforced composites [2, 15].

Development of advanced composite materials with different kind of matrices for application in protective armor against high velocity impacts have continued to attract interests globally. Metal matrix composites (MMC's) have been developed by reinforcing metals with alumina and silicon carbide nano-particles to improve mechanical properties such as strength, stiffness, high temperature capability and wear resistance, which cannot be obtained by using just a monolithic metallic material [16, 17]. The most common metal matrices used to develop armor composites are aluminum and its alloys, titanium alloys, and magnesium alloys [3], while the most common MMC reinforcements are silica carbide (SiC), aluminum oxide (Al_2O_3), titanium boride (TiB_2), boron carbide (B_4C), and graphite [16]. Metal matrix composite armors consisting of AA 6061 aluminum alloy reinforced with silicon carbide (SiC) is reported to have improved impact resistance and enhanced stiffness, depending on the volume fraction of ceramic particle

reinforcement [16]. In another study, reinforcing AA 6061-T6 aluminum alloys is reported to lead to increase in both strength and stiffness but increase in susceptibility to adiabatic shear failure under impact loading at high strain rates [18]. The reinforcement of aluminum alloys with discontinuous SiC whisker and particles, was studied to develop potentially low-cost composites with high specific stiffness and improved mechanical properties, depending on the type, size, volume fraction, and aspect ratio of the reinforcing components (SiC) [19]. Metal matrix composites reinforced with nano-particles of carbides, nitrides, oxides, and nanotubes have been investigated and reported to have improved strength and wear resistance compared to monolithic metals (Al, Mg and Cu) such as wear resistance, and strength [20].

On the other hand, ceramic matrix composites (CMC) contain ceramic matrix which can be Al_2O_3, B_4C or SiC among others. The reinforcing components can be in form of whiskers, particles, or fibers, which are commonly made of SiC, Al_2O_3, Si_3N_4 and other ceramic fibers [3]. CMCs are conveniently separated into two categories: CMCs containing continuous reinforcements such fibers and CMCs containing discontinuous reinforcements such as particles, whiskers and short fibers [21]. CMCs have been investigated for use as protective armor ceramics plates for personnel and light vehicle against threats from low caliber weapons. This is promoted by using a composite ballistic armour system based generally on a ceramic front plate and a reinforced polymer back-plate. For example, Boron Carbide (B_4C) ceramic tiles have been used as a strike face combined with para-aramid and polymer matrix composites used as back-plate. It has been reported that ceramic tiles decelerate and degrade the impacting projectile by erosion and fracture; while, back plates absorb the residual impact energy and recollect fragments of the projectiles [21].

The development of ceramic armour systems for ballistic protection has been widely studied. Medvedovski [22] developed a composite armor consisting of a strike ceramic plate joined to an intermediate ceramic–polymer plate, and a polymer fibre lining as a backing material and tested it using low caliber weapons. He reported successful protection against these weapons in NIJ protection levels III and IV and concluded that increasing the thickness with an intermediate plate can enhance impact energy absorption capacity of the whole system. In another separate studies, Medvedovski [23, 24] examined the importance of correct choice of ceramic materials and manufacture procedures for achieving improved ability to dissipate ballistic energy. The effects of

alumina and carbide reinforcements on the microstructure and properties of the armor's systems developed were investigated by this author. It was concluded that the ballistic performance of the composite materials varies depending on the properties and microstructure of the reinforcing components, which also influence the crack propagation mechanism in the protective armor system [23, 24].

Protective CMC armor systems consisting of backing layers of Dyneema® fibers (SB21 and SB51) bonded to front ceramic plates of alumina and silicon carbide were developed by Garcia-Avila *et al.* [25] . The obtained composite armour plates were tested using low caliber weapons. Result of this investigation indicated that the use of silicon carbide offered 20% weight reduction in comparison with the use of alumina plates. The results of ballistic impact test suggest that a minimum ceramic layer thickness of 4 mm is necessary to stop the projectiles. In addition, it was reported that the fiber layer components (Dyneema®) collected bullet fragments and improved the ballistic impact resistance of the armor plates [25].

2.4 Polymer matrix composites designed for ballistic protection

Polymer matrix composites have two main components: an organic polymer as matrix and high strength fibres as the reinforcement. The fibers are the main component that carry the applied load. However, the matrix firmly bonds the fibers together and uniformly distribute the applied load to the fibers. The interaction achieved between components (matrix and reinforcements) directly affect the properties and performance of a composite material [14]. The main characteristics of PMCs are their high strength and high modulus with improved physical and chemical properties (in relation to their individual components) such as light weight, dimensional stability and chemical resistance [14, 15]. These properties enable production of lightweight armors, thereby improving the maneuverability of soldiers and tactical vehicles in combat operations [26]. Traditionally, PMCs have been classified according to their main components, namely the matrix material and the type of reinforcement.

1) The matrix used in the manufacture of a PMC can be a thermoplastic or a thermosetting polymer.

Thermoset polymers have their molecules chemically joined together by cross-linking. Once the curing reaction is completed resins cannot be melted or re-used again. The most common thermosets used in composite fabrication are: epoxies, polyesters, vinyl esters, phenolics, polyimides and cyanate ester. Commonly, thermosetting polymers have been used as the matrix for long continuous fibers reinforced plastic [3, 4, 6].

In thermoplastic polymers the molecules are not chemically joined together; thus, they can be heat-softened, melted, and reshaped many times as required. Typical thermoplastic polymers used as matrix materials in polymer based composites are nylons, polyethylene, polystyrene, polycarbonate, polyether, and polyacetals. These polymers have been used commonly to develop short fiber-reinforced plastic, which are generally fabricated by injection-molding, or extrusion processes [3, 4, 6].

2) PMCs can be classified based on the material used as reinforcement for the polymeric matrix; organic and inorganic fibers reinforced PMC, micro- and nano-particle fillers reinforced PMC or laminar composites with sandwich structures [2-6, 14].

Selection of suitable armor materials for ballistic resistance applications are very crucial, especially with respect to increasing the mobility and armor protection in high risk operations. Toughness is an important parameter in the selection an energy absorbing material that is resistant to the penetration of a harder body (i.e. ability to absorb work or energy). Thus, as it is shown in the Fig. 2.1, comparing Young's modulus and fracture toughness can be useful to selecting materials resistant to impact and that can absorb high impact energy [27].

The penetration resistance of a material is governed by the dynamic deformation mechanisms of both the projectile and target. The thickness, strength, ductility, toughness, and density of the target material, in addition to the velocity and hardness of the projectile, are crucial factors that determine ballistic impact performance. In Fig. 2.2, the energy absorption behavior of typical fibers in term of longitudinal wave speed are presented. It can be observed from this graph that the resistance to ballistic penetration of different fibers is highest to the upper right, where fibre materials such as Dyneema ultrahigh molecular weight polyethylene and Kevlar® (aramid) are located [27].

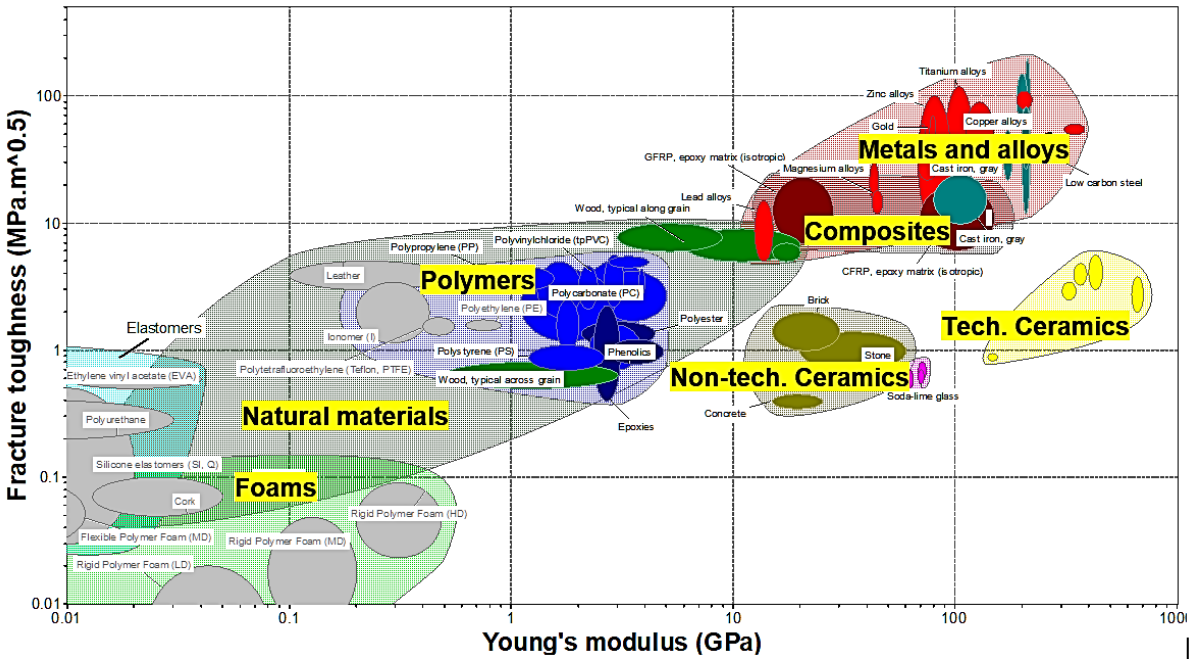

Fig. 2.1. Young's modulus and fracture toughness of common engineering materials [27].

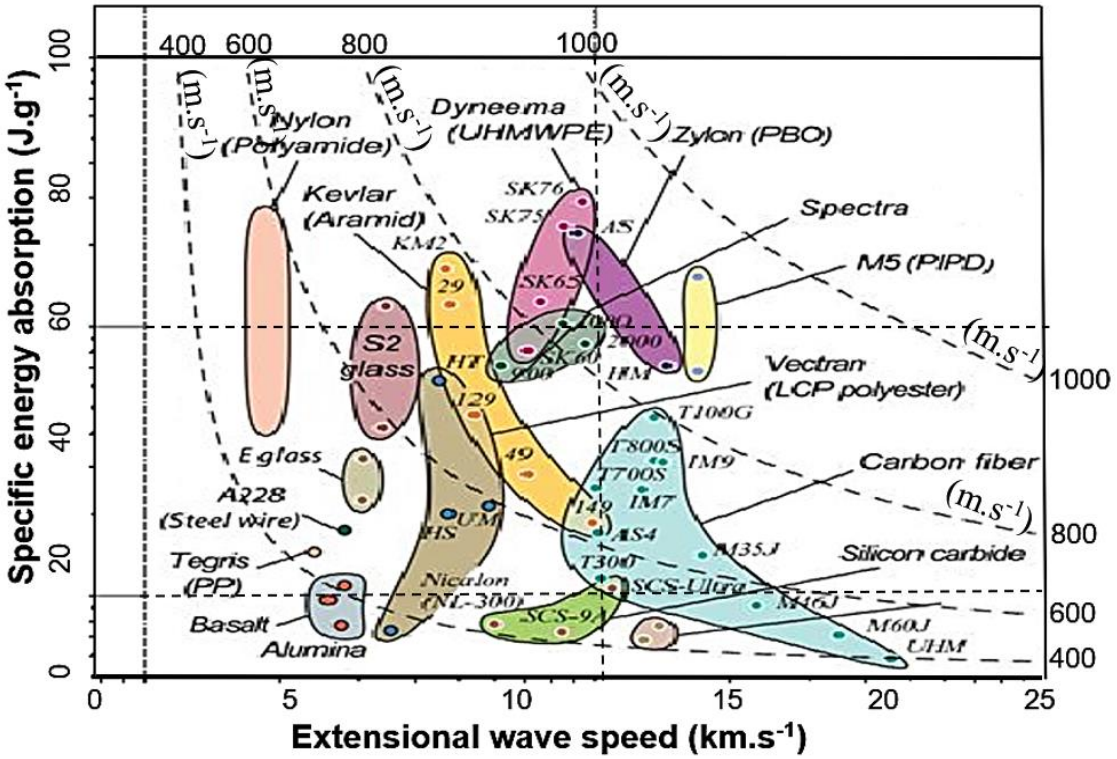

Fig. 2.2. Specific energy absorption of fibers versus extensional wave speed [27].

Varieties of synthetic fibers have been used to develop composite armors, out of which glass, carbon, Kevlar ®, Dyneema®, Spectra-UHMWPE and Boron fibers are the most commonly used [2-6, 14]. These fibers have been shown to resist high-velocity impacts ranging between 800 and 1000 m/s because they have a high tensile strength and high resistance to dynamic deformation/failure [27]. The polymer reinforcement with these fibers enhances ballistic impact resistance and energy absorption performance of the PMCs [26].

Ballistic response of thermoplastic-based composite armors made of polypropylene (PP) reinforced with Kevlar® fabrics in different structures (2D plain woven, 3D orthogonal and 3D angle interlock) was studied by Bandaru et. al. [26]. It was observed that 3D angle interlock specimens achieved the highest failure resistance under ballistic impacts with a velocity limit of 470 m/s and energy absorption capacity of up to 883.6 J [26]. A similar study was conducted by Zhang et. al. [28], in which UHMWPE was reinforced with three different types of woven structures, unidirectional, 2D plain-woven and 3D single-ply orthogonal woven fabrics. The results of the ballistic impact test conducted on the composite laminates indicated that unidirectional fiber reinforced UHMWPE absorbed the highest impact energy, thereby exhibiting the highest ballistic impact resistance of the developed and tested composite plates.

In another study, potential bullet-proof composites were developed using Kevlar®-29 fibers, Al_2O_3 powder and epoxy resin. These composites were subjected to ballistic impact tests while the relationship between target thickness and energy absorption behavior was experimentally determined and compared with theoretical results. For example, in both conditions, specimens with thickness of 18 mm were able to absorb around 600 J of impact energy, indicating that the developed composite materials can be used as armor materials [29]. A similar study was done by Sorrentino et. al. [30], who evaluated the ballistic performance of composite laminates made of Kevlar®-29 fibers impregnated with thermosetting resin. Experimental and analytical results were compared to validate a model that predicts the ballistic limit velocity in these kind of targets.

E-glass/phenolic composite laminates have also been studied for application as protective armor. Targets made of prepregs with thickness ranging from 5 to 30 mm were subjected to ballistic impact tests. Results indicated that failure mechanism is dependent on target thickness. For

example, thick specimens experienced tensile failure and delamination, while thin specimens experienced shear fracture of fibers [31]. In another study, ballistic impact performance of 2D plain weave E-glass/epoxy composites was evaluated using target thickness ranging from 4 to 30 mm. In this study, the results of ballistic limit velocity were found to range from 137.7 to 360.5 m/s depending on target thickness whereas failure was observed to be a result of friction, stretching and tensile failure of primary and secondary e-glass yarns, delamination as well as matrix cracking [32].

The constant need to improve the shielding capacity of polymer matrix composite armors against medium and high velocity impacts serves as the impetus for researchers to work with similar materials using different approaches and composites configurations and new reinforcing fillers to produce new improved armor composites. In that way, hybrid composite materials are developed and investigated for application in ballistic plates that offer a solution of shielding with lighter, thinner, stronger, and less expensive protective armor than the conventional ballistic vests.

2.4.1 Hybrid composite armors based on polymer matrix composites

Hybrid materials combine the properties of a matrix and two or more reinforcing components for a specific purpose [33]. Generally, the properties of the resulting hybrid composites are much better than those of their components [34]. Figure 2.3 illustrates the fact that hybrid materials can be created by a combination of several reinforcement options based on the specific characteristic of each. For example, hybrid materials designed to absorb the high amount of impact energy are commonly built using sandwich structures or laminates. These structures enable the choice of components with high strength, Young's modulus, and toughness. These can have polymeric, metallic or ceramic matrices reinforced with fibers, rubbers, shear thickening fluids, micro- and nano-particles or the combination of these [34].

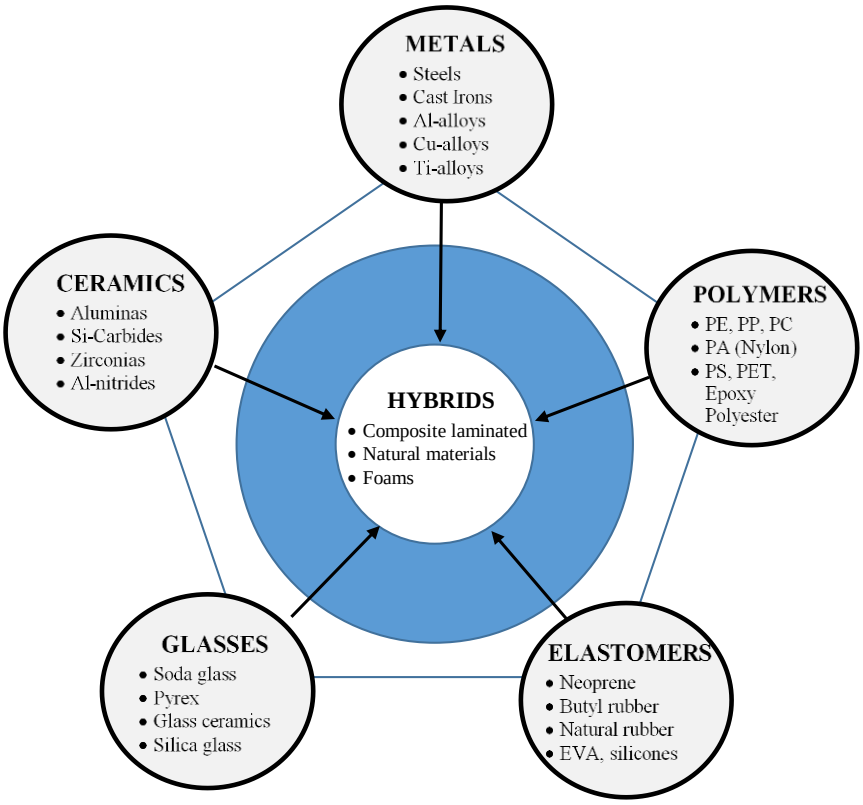

Fig. 2.3. Typical material combinations to develop hybrid composites [34].

The compatibility of components can be a crucial aspect in the design and performance of new hybrid materials. To achieve a positive hybridization, the components or materials chosen as matrix and reinforcements have to be compatible so that a strong bond can develop between them. In addition, the volume fraction of the reinforcing components and manufacturing process/parameters play important roles in the design and performance of hybrid composites [14]. The density and Young's modulus of the most common materials used as a matrix and reinforcing materials in hybrid composites are presented in Fig. 2.4. The empty areas that surround these materials offer opportunities to develop new hybrid composites for different purposes [34].

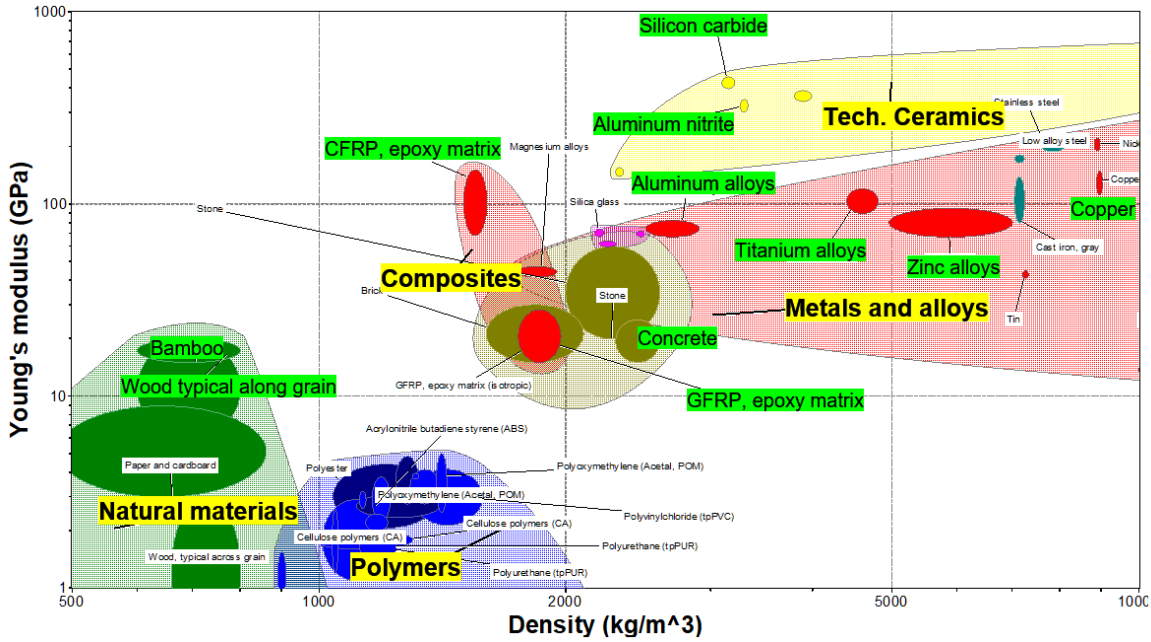

Fig. 2.4. Density vs Young's modulus to create new combinations of hybrid composites [34-36].

2.4.1.1 Hybrid matrix laminates

Hybrid fiber matrix laminates (FML's) provides a good choice of materials for application in protection against ballistic impact. These hybrid composites are multi-layered materials consisting of alternate layers of fiber reinforced plastic and thin metallic plates (Fig. 2.5). Hybrid composites laminates having a sandwich structure consisting of alternate layers of glass fiber reinforced aluminium (GLARE) and aramid fiber reinforced aluminum (ARALL) [37].

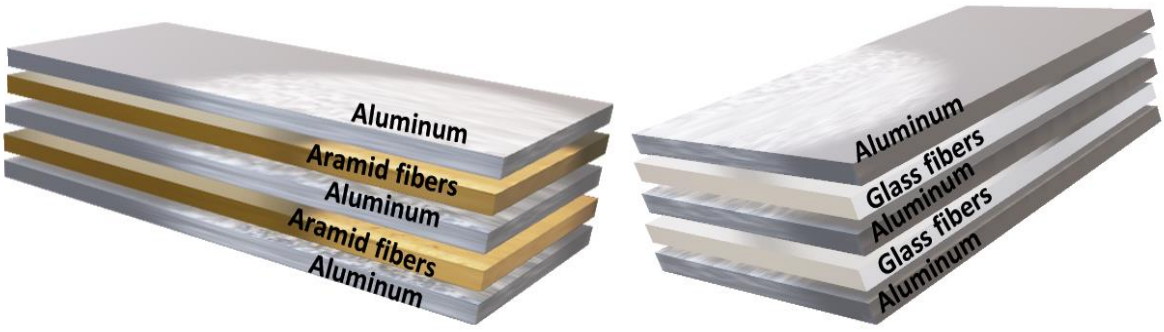

Fig. 2.5. Typical configurations of the hybrid fiber matrix laminates [37].

The factors affecting energy dissipation during ballistic impact of cross-ply GLARE 5 FML laminates consisting of 2024-T3 aluminum alloy/S2-glass/epoxy layers in different thicknesses have been investigated [38]. It was observed that thicker layers may enhance the amount of energy absorbed during ballistic impacts. The failure mechanism was reported to consist of bending, stretching, petaling and plugging in aluminum plates, and interfacial debonding and delamination between layers of aluminium and glass fibers. However, these failure mechanisms were reported to contribute to energy dissipation as the projectile penetrated the hybrid laminate targets. In another study Ramadhan [39] investigated the impact energy absorption capacity of hybrid laminates consisting of alternate layers of aluminum 6060-T6 and Kevlar® 29 fibers and reported its dependence on the stacking sequence and laminate thickness. The 506/HY 956 epoxy resin used in these hybrid composite laminates proved to be very efficient in resisting perforation of the plates during ballistic test [39].

Hybridization of two fibre types (Fig. 2.6) with a single matrix to develop new improved composites have been reported in previous studies. The goal of such configuration is to combine the properties of both fibres in the resulting hybrid composite [33]. For example, typical hybrid configurations of carbon/glass, carbon/Kevlar®, and Kevlar®/glass have been extensively investigated to develop new improve hybrid composites with improved mechanical properties [40-42]. Hybrids composite materials consisting of layers of glass fibre/carbon fibre/epoxy and aramid fibre/glass fibre/epoxy in different stacking configurations were investigated under ballistic impact loading conditions. It was reported that the impact resistance increased by up to 30% in comparison to composite consisting of only one type of woven fibre with similar number of layers [43-45].

In a previous study by E. Randjbaran [46, 47], hybrid composites made of Kevlar®, carbon, and glass woven fabrics configured in different stacking sequence, were developed and tested for ballistic impact response. Five different specimens were produced with similar shape and density. It was reported that the specimens with a stacking sequence of glass / carbon / Kevlar® / carbon / Kevlar® / glass possessed the highest amount of impact energy absorption, which is 95.17 J. However, the difference between this and energy absorbed by the configuration that possessed the least energy absorption capacity is only 0.16 J. The amounts of energy absorbed by the specimens with different configurations are close to each other.

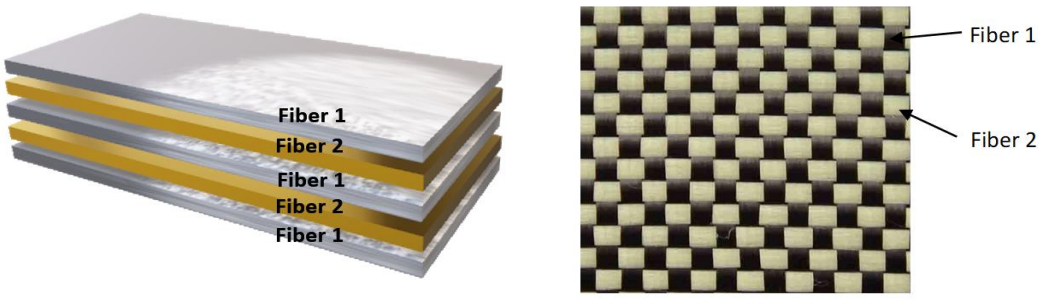

(a) (b)

Fig. 2.6. Typical hybrid configurations by using two fibre types: a) interlayer and b) intralayer [33].

2.4.1.2 Natural fiber reinforced hybrid polymer composites

Hybrid composites have been developed to contain varieties of natural materials which may be particles or fibers of woods, leaves, fruits, basts or stalks. These composites are called natural fiber reinforced hybrid polymer composites, since the natural filler materials are incorporated into a material system consisting of polymer reinforces with other fibers [48-52]. The most common natural fibers used as reinforcements or fillers in polymer-based composites include: kenaf, sisal, jute, hemp, abaca, oil palm, pineapple leaf, banana stem, bagasse, and coir fibers [53]. Depending on the classes of natural fibers used for polymer reinforcement and the way they are incorporated into the matrix, different natural fiber/filler-based hybrid composite can be produced for different industrial purposes [51]. Hybrid composites have been developed using non-woven kenaf fibres/Kevlar® epoxy in different configurations and subjected to ballistic impact tests using a 9 mm caliber projectile [54, 55]. The results of these experiments show that an arrangement of 14 layers of Kevlar® and 2 layers of kenaf offers the highest level of ballistic impact resistance. Thus, a positive hybridization of kenaf-Kevlar® in terms of energy absorbed was achieved. However, to increase ballistic properties of this kind of composites can be increased by increasing their thickness and areal density.

In a previous study, a hybrid composite was also produced using basalt, Kevlar®, and epoxy resin in order to improve ballistic performance of body armors and reduce weight. The results showed that hybrid laminates with basalt as interlayers between woven Kevlar® fibers improved the impact energy absorption capability and damage resistance [56]. Also, a vacuum infusion

technique was used to produce three hybrid composites containing basalt fibres and different combinations of glass/flax (GFB), glass/hemp (GHB) and hemp/flax (FHB). The combination GFB was reported to have the most improved properties compared to the other combinations [57]. Reis *et al.* [58] investigated the impact behavior and damage tolerance of composites made of Kevlar® and epoxy containing cork powder and nano-clays (Cloisite 30B) as reinforcing fillers. It was determined that nano-clay fillers addition enhanced the impact resistance and increased damage tolerance by 29%. In another study, glass fiber reinforced polymers (GFRP) made of S2-glass fiber fabrics, epoxy and impregnated with nano-clay and glass bubbles fillers, were tested under high energy impact loading, the energy resistance capacity was found ranged between 108 J and 206 J. The results showed that GFRP specimens containing 1 wt.% nano-clay absorbed the maximum impact energy [59].

2.4.2 Impregnation of micro- and nano-fillers in hybrid composite armors

The hybridization of composite materials, and specifically polymer composite armors by impregnation of organic or synthetic micro- and nano-particles (fillers) within textile fabrics have been another approach to producing improved lightweight soft body armors which are flexible and comfortable to wear.

The development of shear thickening fluid (STF) is a successful approach for improving the impact resistance of textile fabrics used in polymer reinforcement. STF is a non-Newtonian fluid formed by the combination of hard metal oxide particles suspended in a liquid polymer. This suspension increases the viscosity when the shear rate or applied stress is increased; therefore, STF is solidified at the point of the impact causing resistance to rupture [60]. In general, STF consists of colloidal silica particles mixed with polyethylene glycol as the solvent. However, there are other solvents such as ethylene glycol, polyvinylchloride, and glycerol that have low volatility and are thermally stable to maintain the STF properties [60, 61]. The main factors that may affect the rheological properties of STFs are particle shape, size distribution and volume fraction. In addition, the viscosity of the solvent is reported to affect the shear-thickening property of the mixture [60].

The main objective of the STF impregnation within textile structures is to enhance the impact resistance of fibrous materials. For example, the fabric ballistic performance was found to improve by 40 to 80% when Kevlar® was impregnated with STF [61, 62]. Lee, *et al.* [63] reported that the

impact resistance of Kevlar® fibers was enhanced by the impregnation with colloidal shear thickening fluid (STF) leading to superior ballistic protection when compared with Kevlar® laminates with no STF. Similarly, Kevlar® fabrics that is previously impregnated with colloidal silica (SiC) nanoparticles using polyethylene glycol (PEG) as the dispersing medium, was found to improve the impact energy absorption of Kevlar® fabrics [64]. It has been reported that about 20 to 50 layers of woven aramid fibers are required to produce a high ballistic performance required for protection. This can be further enhanced by impregnation with shear thickening fluid (STF) to reduce the layers of Kevlar® fabric required for a given level of protection by approximately 50% [63]. The energy dissipation of fabrics treated with STF was studied by Hasanzadeh et. al., [60], who associated the improvement achieved by impregnated fabrics to the shear-thickening behavior, increase in yarn friction (yarn pull-out energy), and better bonding and load transfer between woven Kevlar® layers.

From the review of literature, as highlighted above, there are several pieces of parameters that can be investigated to improve the ballistic impact resistance and energy absorption behavior of hybrid polymer matrix composites. These are detailed in the next section.

2.5 Information gaps identified from literature review

Some information gaps were identified in the literature. These include the following:

- There is no information on the ballistic impact response of STF-impregnated Kevlar® fabrics bonded with layers of aluminum alloy to form hybrid composite plates. It is very important to determine whether STF impregnation into fibers will allow such hybridization with metallic layers to produce high performance protective armor.
- It is necessary to expand knowledge on the ballistic impact response of hybrid composites plates consisting of aluminum alloy, epoxy and Kevlar® fabrics impregnated with various nano-fillers. In this case is important to evaluate whether other different nano-fillers (silica carbide, aluminum powder, colloidal silica, gamma alumina, and potato flour) may be impregnated into Kevlar® fibers using polyethylene glycol (PEG-400) as deposition medium, and if such infiltration will allow a positive hybridization with aluminum layers to produce high performance protective armour.

- The information about the hybridization of thermoplastic matrices reinforced by the combination of short fibers and micro- and nano-particulate reinforcements to produce hybrid composite armors have not widely reported. Thus, in this study, the performance evaluation of such hybrid composite armors under dynamic and ballistic impact will be investigated. Specimens will be made of different types of micro- and nano-fillers infiltrated in Kevlar® short fibers reinforced high-density polyethylene (HDPE).
- Limited information is available in the open literature on the dynamic impact response and the energy absorption behavior of bio-composites and hybrid bio-composites. In this study, bio-composites will be produced from hard wood palm micro-particles as reinforcement for HDPE. Hybrid bio-composites will be synthesized by the hybridization of Kevlar® pulp with organic micro-fillers in a HDPE matrix. Both materials will be tested under dynamic and ballistic impact loading conditions.

The Fig. 2.7 shows the different research approaches that will be used to fill the aforementioned knowledge gaps. As emphasized in Chapter 1, this research study focusses in improving the shielding capacity of polymer matrix composite armors by using addition of micro- and nano-particles as additional reinforcing components.

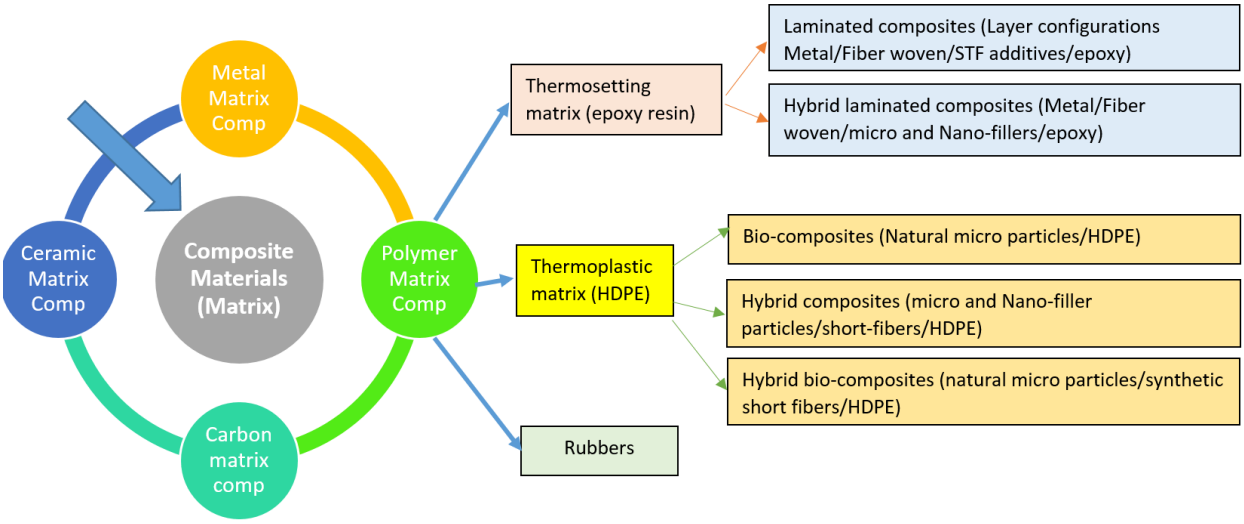

Fig. 2.7. Research approaches for improving the shielding capacity of polymer matrix composite armors.

Chapter 3: Materials and Methods

3.1 Overview

In this chapter, the materials used as reinforcing and matrix components in composite synthesis are described. In addition, the methods used for composites manufacture and characterization are presented. The materials characterization methods discussed in this chapter include: optical and scanning electron microscopy, water absorption measurement, X-ray diffraction, dynamic impact test and ballistic impact test.

3.2 Materials

3.2.1 Reinforcing materials and fillers

Hybrid composite laminates for protective armor applications developed in this study have different types of reinforcing and matrix materials. The first two studies that will be detailed in Chapters 4 and 5 use laminated layers of AA 5086-H32 aluminum alloy sheets and woven Kevlar® 49 (#281-38) with fibers reinforced epoxy (sandwich structure). In addition, micro- and nano-fillers, such as colloidal silica 406 (SiO_2), gamma alumina powder (Al_2O_3), uncoated aluminum powder UN1396, silicon carbide (SiC) and potato flour, were added in some composites as additional reinforcing components. A mixture of epoxy resin (LAM-125) and resin hardener (LAM-129) were used as the epoxy matrix component of the fiber reinforced polymer layers of the sandwich composites.

In the second phase of this research study, hybrid polymer composites and hybrid polymer biocomposites were manufactured using three different approaches. These studies will be discussed in the Chapters 6, 7, and 8. Different specimens were developed using high density polyethylene (HDPE), a common thermoplastic polymer. The reinforcing materials used were Kevlar® short fibers (#544 Kevlar®), nano-fillers and micro-particles of chonta palm wood (*Bactris gasipaes*).

3.2.1.1 Aluminum alloy AA 5086-H32

The aluminum alloy sheets (AA 5086-H32) used in this study were supplied by Onlinemetals.com (Seattle - US). The aluminum alloy sheets have a thickness of 1.6 mm and a nominal chemical composition of 95.4 Al, 0.05–0.25 Cr, 0.1max Cu, 0.5max Fe, 3.5–4.5 Mg, 0.2–0.7 Mn, 0.4max Si, and 0.25max Zn. The primary role of the AA 5086 aluminum alloy sheet is to act as rigid plates that support the fibrous materials and keep them in their relative positions within the hybrid laminates. They help to hinder propagation of crack through the fibers and also protect the fibers from environmental degradation. The aluminum plate enables uniform distribution of impact loads and enhances impact resistance of the laminates.

3.2.1.2 Kevlar® 49 woven fibers (#281-38)

Kevlar® 49 fibers also called aramid (aromatic polyamide) fibers, are organic fibers with low density and high specific tensile modulus and strength [3, 4]. Aramid fibers have been used as reinforcing constituents in many applications due to their high tensile strength and good resistance to the impact damage when compared to other polymeric fibers [3, 65]. As a result of these features, it has been used frequently in fiber reinforced polymer composites (FRP's) intended for military applications such as body armor and ballistic plates [3, 4, 65].

The cross-ply woven Kevlar® fiber 49 (#281-38) fabric used in this study was supplied by Aircraft Spruce (Ontario - Canada). The fabric has a thickness of 0.25 mm and a mass per unit area of about 169.8 g/m^2. The role of the Kevlar® fibers is to act as reinforcement and to enhance the mechanical properties (such as tensile and flexural strength) of the polymer matrix. Their high tensile strength prevents significant stretching and deflection of resultant composite materials during ballistic impact. These fibers slow down the projectile penetration through the initial resistance to tensile elongation, inter-laminar delamination and fiber pullout. In addition, their high strength and elastic modulus enhance the kinetic energy absorption and the transverse deformations during high-velocity impact [37, 66].

3.2.1.3 Kevlar® pulp (#544 Kevlar®)

Aramid short fibers (called aramid pulp) are short fibers with attached fibrils, which can provide efficient reinforcement for thermoset and thermoplastic polymers. These short fibers are available in different lengths, in the range 0.5 to 4 mm, and a diameter of about 5 to 20 µm, which allows a

uniform dispersion of aramid short fiber when mixed with different resins [4]. Kevlar® pulp (#544 Kevlar®), also called Kevlar® short fibers, produced by Fibre Glast Developments Corporation (Ontario - Canada), were used as primary reinforcement in some aspects of this study as will be reported in Chapters 6 and 7. The fiber length ranged between 0.5 and 1 mm. The density of Kevlar® pulp ranged between 0.04 and 0.16 g cm^{-3}.

3.2.1.4 Polyethylene glycol (PEG-400)

Polyethylene glycol (Carbowax PEG-400 NF) supplied by Fisher Chemical (Ontario - Canada), with a pH of 4.5–7.5 (5% sol) and a density of 1.13 g/cm^3, was the solvent used in dispersing the nano-fillers into the Kevlar® fabric. It is made of Carbowax (C_2H_4 on H_2O) and has low volatility and good thermal stability [67]. The use of PEG-400 enables an efficient dispersion of nano-fillers into Kevlar® fabrics [68].

3.2.1.5 Micro- and nano-filler materials

Fillers or solid additives are particles in micro or nano range sizes used in low concentrations, which are intentionally introduced to polymer composites to enhance or modify their mechanical and physical properties to obtain a composite with enhanced properties for specific applications. Typical materials used as particulate fillers can be organic or inorganic and they generally include wood flour, silica, alumina, glass, clay, limestone, and some synthetic polymers [69, 70]. The micro and nano-fillers used in this study are described below:

1. Colloidal silica 406 (SiO_2): The 406-colloidal silica, also called silicon dioxide or silica, manufactured by West System Inc. (Michigan - USA), was used as synthetic nano-fillers for composites reinforcement in this study. SiO_2 is an adhesive filler that has an average particle size of between 200 and 300 nm and a density of 0.048 g/cm^3. It is a thickening additive used as a strong gap filler. In polymer matrix composites manufacture, this nano-powder is widely used to improve mechanical and thermal properties [71]. When added dispersed in PEG, it becomes easy to impregnate colloidal silica into fibrous materials. Its infiltration into Kevlar® fibers improves the strength and impact resistance of the composite made from such fiber [68].

2. Gamma alumina powder (Al_2O_3): Gamma alumina powder (Al_2O_3) with a particle size of 0.05 μm, purchased from LECO Corporation (Hazel Grove - UK), was used in this investigation.

These ceramic nano-particles have been widely used for advanced structural applications and for reinforcing polymer matrix composites. They provide chemical stability, high elastic modulus, and good resistance to wear, in cutting tools, coatings, and in materials for military applications [21, 72]. The use of gamma alumina powder as filler in polymer matrix composites has been adopted in thermoplastic and thermosetting resins. For example, the addition of Al_2O_3 particles to polymer matrices during the manufacturing process enhanced the mechanical and physical properties of composite laminates made of Kevlar® 29/epoxy for ballistic armor applications [73]. Also. Talib *et al.* [29] concluded that a mixture of these particles with an epoxy resin infiltrated into Kevlar® layers can increase the level of energy absorbed by composite plates under high velocity impact.

3. Uncoated aluminum powder (UN1396): Pure aluminium metal powder is suitable for a range of applications when added to polyester or epoxy resin systems to produce polymer matrix composites. For example, Sarkar *et al.* [74] studied the effects of addition of aluminium powder on improvement of mechanical properties of woven glass epoxy composites, while Hamed [75] investigated the effects of aluminium powder impregnation into Kevlar® fibers reinforced PVC. In this study, uncoated aluminum powder UN1396, purchased from EM Science (USA) with 200 mesh (74 μm) size, were also applied as a micro additive or micro filler in sealing the voids between fiber bundles in Kevlar® fabrics during composite manufacture.

4. Silicon Carbide (SiC): SiC powders were supplied by Sigma-Aldrich Co. (Ontario - Canada) in the 200–450 mesh range (37–74 μm particle size), is another micro filler used in this study. It is an artificial abrasive material manufactured in electric resistance furnaces by the reaction of silica and carbon at high temperature. Commonly SiC particles have been used as reinforcing filler, abrasive in grinding and polishing materials, glassmaking and refractory agent. For example, when SiC micro-particles are incorporated into metallic alloys, it has been reported to result in metal matrix composites with improved oxidation resistance at high processing temperatures [3]. In another study, the effects of impregnation of SiC microparticles in Kevlar®, carbon, and S-glass fibers reinforced polymer composites were investigated by comparing the tensile and impact properties of the obtained materials. It was concluded that up to a loading level of 10 wt.% SiC, the composite can attain the maximum value of tensile

strength. Further addition of these particles will lead to decrease in tensile strength. With respect to impact properties, it was reported that the incorporation of 20 wt.% SiC microparticles in S-glass and Kevlar® fibers resulted in the maximum values of impact resistance [76].

5. Potato flour: This is a natural binder used in glues and as natural fillers in fibers to develop environmental friendly composites. In green polymer composites, natural organic fillers are used to fill the polymer matrix with these fillers coming from natural organic powders, fibers or starch, including potato and cassava natural fillers [77]. It was supplied by King Arthur Flour Company (Vermont – Canada). For example, biocomposites films have been prepared as reinforcing materials using potato starch/halloysite nanoclay; it was found that mechanical properties improved in the biocomposites developed [78]. In another study, potato starch has been used as a natural binding agent in composites made of palm fruit fibers for use as bullet proof plates in armored vehicles [79].

6. Chonta palm wood micro-particles (*Bactris gasipaes*): The components of natural fibers (hardwood fibers) are cellulose (45-50 wt.%), hemicellulose (21-35 wt.%) and lignin (22-30 wt.%) [3, 50]. These natural fibers are normally used as reinforcing components to produce natural fiber composites that are environment-friendly, less expensive, biodegradable, with low density compared with E-glass. However, in similar comparison, these natural composites show lower mechanical properties [3, 50]. The reinforcing material, chonta palm wood, used as the natural filler microparticles in the second phase of this study, is one of the hardest woods in the Amazon region and its applications in various fields have been discussed in previous studies [80, 81]. This natural fiber was provided by Indubalsa S.C. Ecuador in rectangular wood pieces; 150 mm long and 30 mm wide. The thickness ranged between 15 and 25 mm.

3.2.2 Matrix materials

Extensive researches have been carried out on the use of synthetic polymers to produce thermosetting and thermoplastic matrix composites. The main difference between both polymers is that thermoplastic polymers can be melted and reshaped (keeping same properties), while thermosetting polymers can not be reused again. The most known thermoset matrices are polyester,

epoxy, and vinyl ester while the most commonly used thermoplastic matrices in composites are: polypropylene, polyethylene, polystyrene and polyvinyl [3, 4, 50].

3.2.2.1 Thermosetting matrix

Epoxy resin has been used to build the specimens in experiments 1 and 2 in this study. Its characteristics are: high mechanical and thermal properties, high water resistance and long working time available [3, 4, 50]. Generally, a mixture of liquid epoxy resin and a curing agent create a complex three-dimensional network between components to obtain a solid epoxy polymer after polymerization (curing) is completed [3, 4].

Epoxy resin Pro-set (LAM-125) mixed with hardener (LAM-229) was used as the polymeric component of the hybrid composite laminates in this study. These resins were supplied by Aircraft Spruce (Ontario - Canada). Epoxy plays a critical role of bonding the various components of the laminates together. It has low viscosity and it is very effective in bonding Kevlar® and other fiber fabrics. Pro-set LAM-229 is a slow curing hardener, which requires 4 to 5 hours curing time at room temperature. This gives room for more processing time in the fabrication of composite materials with the epoxy resin. The resin mixed with hardener also bonds the aluminum plates with the Kevlar® fiber fabrics to achieve a completely rigid structure.

3.2.2.2 Thermoplastic matrix

High-density polyethylene (HDPE) are semi-crystalline thermoplastics that can be used using different composites manufacturing techniques including extrusion, compression and injection molding, which can combine the polymer with reinforcing fibers to develop high performance thermoplastic composites [3, 4]. HDPE is lightweight and it possesses good resistance to organic solvents, low moisture absorption, good fatigue and wear resistance, good bonding properties, high stiffness, good impact strength and good toughness [3, 50].

HDPE, SCLAIR® 2909 was used in the investigations reported in Chapter 3, 4 and 5. It was supplied by NOVA Chemicals (Alberta - Canada). This thermoplastic polymer has a density of 0.962 g cm^{-3} and melt mass flow rate (MFR) of 1.3 g min^{-1} (D 1238-79 ASTM standard) at 190°C. HDPE has better energy absorption capacity, stiffness, yield behavior and tensile strength

compared with the low-density polyethylene (LDPE) and low linear-density polyethylene (LLDPE) under dynamic compressive loading [82].

3.3 Manufacturing processes

3.3.1 Hybrid thermosetting composite armors

Hand lay-up technique was used to manufacture hybrid composite armors using based on epoxy matrix. Two different composite configurations were adopted. These procedures will be provided in detail in Chapters 4 and 5. Hand lay-up technique involves assembly of successive layers of epoxy resin-impregnated woven fibers in a sandwich configuration [4, 15]. Sandwich construction provides a convenient method to obtain high stiffness, good impact resistance and damage tolerance at minimal weight for diverse applications [4, 69].

The first hybrid composites developed in this study, are laminated hybrid materials made of 5086-H32 aluminum alloy, epoxy and Kevlar® fabrics impregnated with shear thickening fluid (Chapter 4). The second experiment study involves manufacture and characterization of hybrid composites laminates made of a multilayer configuration of aluminum alloy/Kevlar® fiber woven/micro- and nano-fillers/epoxy resin (Chapter 5). The first stage in the manufacturing process for these specimens involves cutting the AA 5086 Al-H32 aluminum alloy sheet into 15 cm x 15 cm square pieces. Their surfaces were degreased and grinded with SiC emery paper to remove surface oxide layer. They were subsequently cleaned with ethyl alcohol and dried in readiness for use in the manufacture of the hybrid composite laminates. The Kevlar® fibers were cut into the same dimensions as the aluminum plates. Table 3.1 shows properties of the materials used in the manufacture of the hybrid composite materials intended for protective armor use in this study.

Table 3.1. Mechanical properties of materials used in the hybrid composite materials manufacture [99].

Properties	AA 5086-H32 aluminum alloy	Kevlar® fibers 49 #281-38	Epoxy resin mixed with Hardener (LAM-125 / LAM-229)
Thickness (mm)	1.6	0.254	-
Dimensions (cm)	15.2 x 15.2	15.2 x 15.2	-
Area density (g/cm^2)	0.844	0.017	-
Density (g/cm^3)	2.66	1.44	1.14 / 0.96
Modulus of Elasticity (GPa)	71.0	131	3.92
Ultimate Tensile strength (MPa)	294 - 298	3600 - 4100	58
Yield strength (MPa)	221.32 - 226.14	1240 MPa	110 MPa
Elongation (%)	8 - 13.5 %	0.028	0.017

The shear thickening fluid (STF) preparation and impregnation into Kevlar® fibers, for the two experiments are different. In the first experiment to produce hybrid materials consisting of 5086-H32 aluminum alloy, epoxy reinforced with Kevlar® fabrics impregnated with STF (Chapter 4), STF, polyethylene glycol (Carbowax TM PEG- 400) and colloidal silica (SiO_2) were mixed together in a ratio of 2:1 and stirred using a magnetic stirrer rotating at 1200 RPM for 3 h at room temperature. The mixing ratio of 2:1 makes it possible to achieve the desired a non-Newtonian fluid (STF) that increases its viscosity with increasing shear-rate [67]. After preparation, the STF was diluted with ethyl alcohol using a ratio of 3:2 and held for 2 h. The cut Kevlar® fiber fabrics were then impregnated with the STF. It was ensured that the proportion of STF infiltrated into the fiber approximately were the same for each cut fabric. Kevlar® fabrics were weighed before and after STF impregnation in order to ensure the same proportion of STF was infiltrated into the fiber fabrics. The fiber layers were dried for 72 h at room temperature until all the ethanol solvent was completely evaporated.

In the second experiment, which involved manufacture of multilayer configuration of Al alloy/Kevlar® fiber woven/micro- and nano-fillers/epoxy resin, polyethylene glycol (Carbowax™ PEG-400) and the fine particles of fillers were mixed together using a constant proportion of 100 ml of PEG-400 to 50 g of the fillers for all targets. While only colloidal silica was investigated in the first experiment, different types of fillers were used in experiment 2. The mixtures were mixed thoroughly using a magnetic stirrer rotating at 1200 RPM for 3 hours at room temperature. The mixtures of nano-fillers and PEG were thereafter diluted in 100 ml of ethyl alcohol for 2 hours.

The same procedure was used for different micro-fillers except for the samples made with potato flour that was already a diluted solution. Different STF containing different type of micro or nanofillers were impregnated into the Kevlar® fabrics individually on the both sides using the same amount of solution and on the same quantity of Kevlar® fabrics. For example, 250 g of STF containing different nano-fillers diluted in ethyl alcohol solution were impregnated in 20 layers of woven Kevlar® fabric. The same proportion was used for all composite plates produced. Kevlar® fabrics were weighed before and after STF impregnation in order to ensure the same amount of STF (with nano-fillers) were impregnated into the fabrics.

For both experiments, the impregnated fiber fabrics were then dried for 72 hours at room temperature (22 °C) until all the ethanol residues were completely evaporated. Hand lay-up method was used to fabricate the hybrid laminates. Fig. 3.1 provides a schematic representation of the configuration of the hybrid composite laminates. As mentioned earlier, the difference in the second experiment is the impregnation of the Kevlar® fibers with different kinds of micro- and nano-fillers.

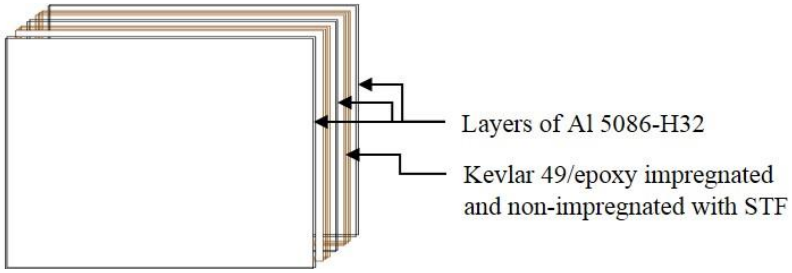

Fig. 3.1. Sample

The bonding of layers in the hybrid was enabled with the adhesive nature of the epoxy resin. Epoxy resin (LAM-125) and hardener (LAM-229) were mixed in a proportion of 4:1 according to the supplier's specifications and used to bond Kevlar® fiber layers (impregnated or not-impregnated with STF and micro- and nano-fillers) to the AA 5086-H32 aluminum alloy sheets to form a laminated structure. The hybrid composite plates were subjected to a compressive pressure of 1600 Pa using a laminating press for 24 h at room temperature. The application of pressure was to ensure a proper bonding of fiber layers with the metallic sheets and also to ensure homogeneous distribution of the epoxy resins within the laminates.

3.3.2 Hybrid thermoplastic composite armors

The hybrid composite armors containing a thermoplastic matrix (HDPE) were produced in three different plate configurations. These experiments are discussed in great details Chapters 6, 7 and 8. Experiment #3, as part of the second phase of this study, involves manufacture of hybrid polymer composite armor plates that consist of HDPE matrix reinforced with Kevlar® short fibers and micro- and nano-fillers as additional reinforcements (Chapter 6). Experiment #4 deals with hybrid biocomposites with a configuration that consist of HDPE reinforced with Kevlar® pulp and chonta palm micro-particles (Chapter 7). The last experiment (#5) involves manufacture of biocomposites made of HDPE reinforced with only micro-particles of chonta palm wood (Chapter 8). All these experimental specimens were made with similar manufacturing procedure as provided in the subsequent paragraphs.

The as-received HDPE pellets were first milled in a grinder (Retsch GmbH 5657 HAAN, West Germany) using a 1 mm sieve. This initial milling of HDPE was done to ensure homogeneous mixing of HDPE with Kevlar® pulp and the micro- and nano-fillers subsequently. To avoid a change in the properties of HDPE due to temperature rise during milling, a continuous flow of carbon dioxide gas (CO_2) was maintained as the polymer was milled. Prior to mixing with milled HDPE, the moisture in the Kevlar® pulp was removed by heating at 105°C in an electric oven for 24 h.

The as-received rectangular pieces of the chonta palm wood were cleaned and cut into small chips. The initial moisture content of the wood chips was measured using a Wagner moisture meter (MMC220, Oregon - US). This was determined to be 40 wt.% before drying and a significant reduction in moisture content was therefore necessary. The wood chips were heat-treated at 105°C for 24 h to reduce the moisture content. The dried chonta palm pieces were then milled using the Retsch knife grinding mill with a sieve size of 0.75 mm. The obtained chonta palm wood powder was not chemical treated and had particle sizes in the range between 500 and 750 μm. These chonta palm powder was further dried in Supermatec (Hotpack) industrial electric oven for 24 h at 105 ^{o}C in order to reduce the moisture content of the wood microparticles to less than 1 wt.%. Moisture content was obtained by measuring the initial weight of wood chips (before milling) and the final weight of wood powder (after milling and drying process). A higher percentage of moisture will result in a porous composite.

Preliminary mixing of the components (micro- and nano-fillers/Kevlar® pulp/HDPE) before the extrusion process was done using a rotatory type mixer (National Hardware, Dresden, ON) operated at a speed of 90 rpm for 15 min. After the preliminary mixing process, the material was extruded in a parallel twin screw extruder (SHJ-35, Akron Inc., Batavia, OH). The extrusion process has been frequently used to produce hybrid composites consisting of reinforcing fillers and thermoplastic matrices [53, 83-86]. The goal of the extrusion process is to produce a uniform distribution of the reinforcements (fillers/Kevlar® pulp) within the HDPE matrix. During the extrusion process, the mix was fed from the hopper into the barrel of the extruder through a feed throat. A screw rotating at 215 rpm drove the mixture through the barrel. The mixture gradually melted due to the heat generated by the heaters in the barrel and from the friction generated by the rotating screw. The molten mixture was then made to pass through a sieve pack to remove the contaminants. The operating parameters such as motor current, melt pressure, motor speed, and feeder speed are 13.1 A, 0.5 MPa, 215 and 50 rpm, respectively. The line temperature was varied in the following sequential order 140, 150, 155, 160, 170, 175, 180, 185, and 220°C. The molten mixture was passed through a long needle-shaped die and hardened by a subsequent cooling by water immersion and air flow to form long noodles. An overview of the equipment used in the extrusion process is provided in Fig. 3.2.

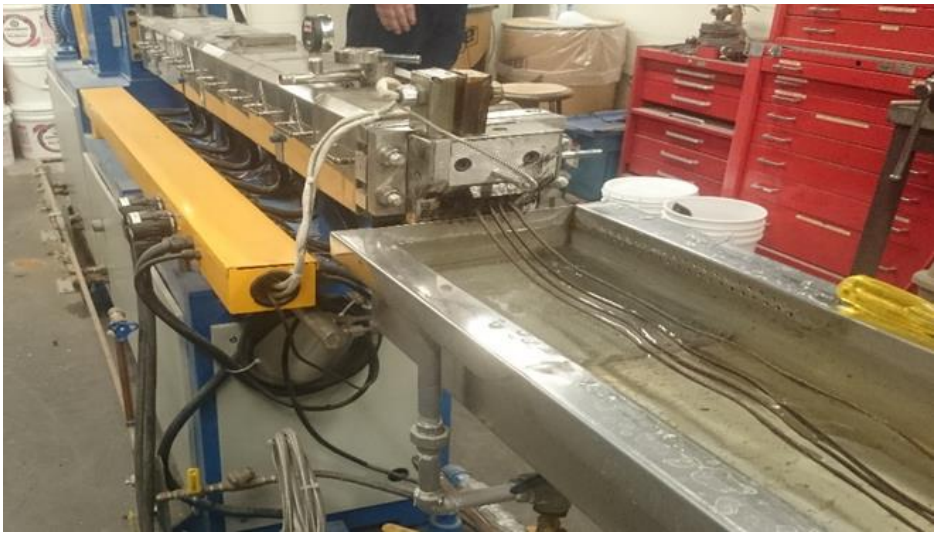

Fig. 3.2. Extrusion process during hybrid thermoplastic composites

The long noodles obtained from the extrusion process were pelletized using a cooling strand LQ-60 pelletizer to obtain cylindrical pellets with thickness ranging from 2 to 5 mm. These pellets

were dried in an electric oven at 75°C for 48 h, after which they were subsequently cured in a fluid bed dryer at 55°C for 30 min to eliminate any remaining moisture. The pellets were weighed before and after drying. The moisture content of the pellets was estimated to be to have reduced to about 0.6 wt.%. Finally, the cylindrical pellets were subjected to hot compression to form test specimens in a square mold of 20 cm x 20 cm x 0.5 cm using a Drake compression molding machine (J.B. Miller Machinery & Supply Co., Toronto, ON, Canada). During compression molding, 200 g of mixed material (pellets) were compressed at a constant pressure of 8.08 MPa at 160°C for 10 min. The resulting hybrid composite plates were water-cooled for 30 min while the applied pressure was maintained to ensure good dimensional stability. Different test specimens were cut from the obtained plates according to the relevant test standards. The manufacturing process is similar for production of hybrid materials that contain additions of different types of micro- and nano-fillers to Kevlar® pulp reinforced HDPE [87].

In the case of the micro-particles of chonta palm wood, thermal degradation of lignin wood materials will not occur at the selected compression temperature since lignin decomposes at temperatures ranging from 200-500°C [88]. Its original properties will therefore be retained during the elevated temperature thermoplastic forming.

3.4 Characterization methods and experimental procedures

3.4.1 Microstructural analysis

Microstructural analysis of the laminated hybrid composites (experiments #1 and #2), was performed using Hitachi SU-6600 scanning electron microscope (SEM) at accelerated voltage of 3.0 kV. The microscopic analysis was used for determination of the distribution of nano-fillers and the quality of the adhesion between the nano-fillers and the Kevlar® fiber surface. The picture of the SEM used in this study is provided in Fig. 3.3.

Fig. 3.3. Scanning electron microscope (Hitachi SU-6600).

The microstructural evaluation of the obtained hybrid thermoplastic composites (experiments #3, #4 and #5), was done with same equipment operating at an accelerated voltage of 15.0 kV. Specimens were gold coated using Edwards S150B sputter coater to ensure conductivity and high-quality micrographs. Energy dispersive spectroscopy (EDS) was used to map the distribution and relative proportion (intensity) of nano-fillers over selected scanned areas of the composite containing colloidal silica and gamma alumina particles. The SEM images provided information on the distribution of micro- and nano-particles in the composites and on the failure mode in materials under dynamic impact and ballistic impact loading.

3.4.2 Water absorption test

The water absorption test for the hybrid thermoplastic composites (experiments #3, 4 and 5), was performed according to ASTM D570 standard [89]. Rectangular specimens, 76.2 mm long by 25.4 mm wide and 5 mm thickness, were immersed in distilled water at 22°C for 2 and 24 h. The samples were weighed before and after immersion. The amount of water absorbed was determined using the following formula.

$$WA\ (\%) = \frac{W_1 - W_0}{W_1} \times 100\% \qquad 3.1$$

where WA is the water absorbed (%), W_0 and W_1 represent the weights before and after water immersion (gm).

3.4.3 Crystallographic structure analysis

The crystallographic structure of the hybrid thermoplastic composites produced in this study (experiments #3, 4 and 5) was analyzed using Bruker D8 discover X-ray diffractometer (XRD) with Cr Kα radiation (λ = 2.29 Å) with the source operating at 40 kV and 40 mA (Fig. 3.4). The angular range (2θ) for the area detector varied from 10° to 110°. The scanning step size of 0.01° and scanning rate of 2°/min were used to investigate the crystallographic orientations along the compression axis of the hybrid composites. Rectangular specimens 10mm x 10mm x 5 mm were used for the XRD analysis.

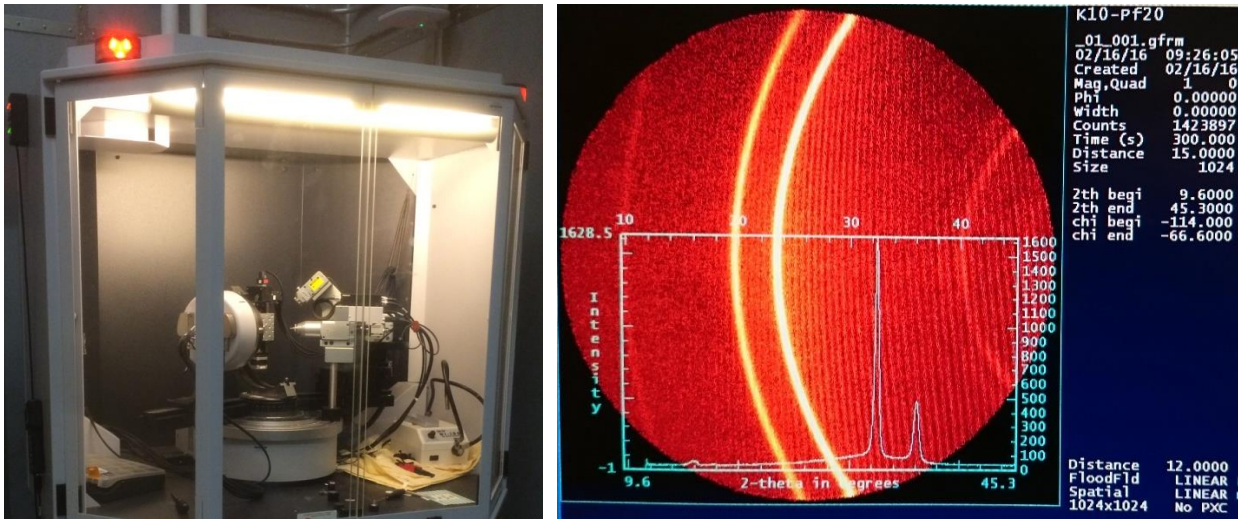

Fig. 3.4. Bruker D8 discover X-ray diffractometer (XRD).

3.4.4 Tensile strength

The tensile strength and the Youngs modulus of the specimens in experiments #3, 4, and 5, were determined using 5500 R model Instron universal testing machine (Norwood, MA, US) (Fig. 3.5) at room temperature according to ASTM D638 (type IV) standard [90]. The average dimensions of the tensile test specimens are 196 mm (length) x 13.4 mm (width) x 5 mm (thickness). The dog-bone specimens were tested at a cross-head speed of 5 mm min^{-1}. A high-resolution extensometer

with a fixed gage length of 50 mm was attached to the test specimens to obtain reliable strain measurements for Young modulus determination.

Fig. 3.5. Tensile test system.

3.4.5 Dynamic impact test

The dynamic impact test was conducted using an instrumented split Hopkinson pressure bar (SHPB). This equipment, also known as Kolsky Bar, is generally used to characterize the dynamic mechanical response of materials under high strain-rate loading ranging between 10^2 - 10^4 s^{-1} [91].

The bar is schematically presented in Figure 3.6. The dimension of the rectangular impact test specimens is 10 x 10 x 5 mm^3. The specimens were rapidly compressed on their square surfaces between the incident and transmitter bars when a striker bar fired by a light gas gun struck the incident bar.

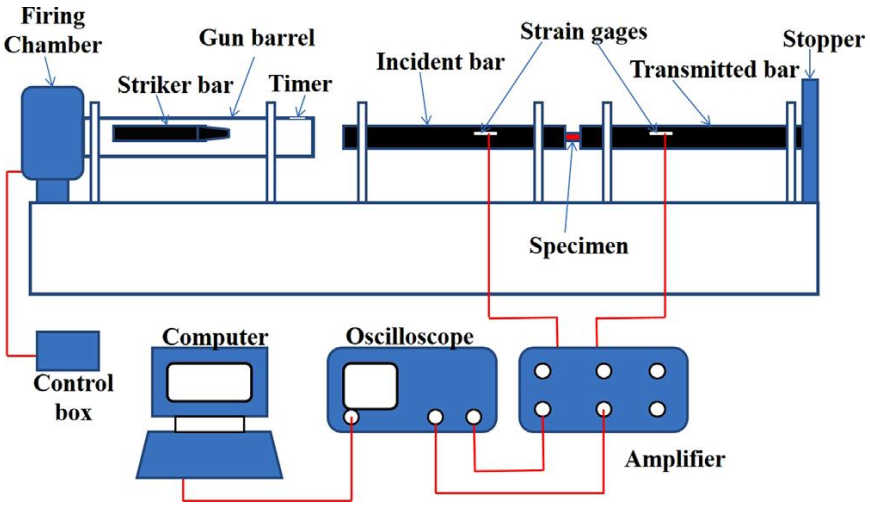

Fig. 3.6. Schematic representation of split Hopkinson pressure bar system used in this study.

Both the incident and transmitter bars (19 mm in diameter) were made of 7075-T651 aluminum alloy. In this study, the striker bar was fired at pressures of 50, 60, and 70 kPa, striking the incident bar at a momentum of 4.0, 6.8 and 8.7 kg. m s^{-1}, respectively. The impact momentums generated strain rates ranging between 900 and 2,800 s^{-1} in the specimens. The elastic waves produced by the impact travels through the bars and were captured by strain gages mounted on them. These were amplified by the strain amplifier and recorded on a mixed signal digital oscilloscope connected to the strain amplifier. More detailed description of this equipment is provided elsewhere [87, 91, 92]. Based on the strain pulses captured by the strain gages, the stress (σ), strain (ε) and strain rates $(\dot{\varepsilon})$ were calculated using empirical equations (3.2)-(3.4) [91-93]:

$$\sigma = \left(\frac{A_B}{A_S}\right) E_B * \varepsilon_T \tag{3.2}$$

$$\varepsilon = -2\left(\frac{C_B}{L_S}\right)\int_0^t \varepsilon_R dt \tag{3.3}$$

$$\dot{\varepsilon} = -2\left(\frac{C_B}{L_S}\right)\varepsilon_R \tag{3.4}$$

where A_B and A_S are the cross-sectional areas of the bars and specimen respectively. ε_T and ε_R are the transmitted and reflected strain pulses respectively, C_B is the velocity of elastic waves in the

bars, E_B is the elastic modulus of the bar material. L_S and t represent the initial length of the specimen and deformation time, respectively.

3.4.6 Ballistic impact test

The ballistic impact resistance of the targets developed was evaluated according to the NIJ 0101.06 and 0108.01 standards for protective armor materials [9, 10]. For the experiments 1 and 2, ballistic tests were performed by high-velocity impacts on the 15 cm x 15 cm square target plates developed in this study. Fig. 3.7 shows a schematic representation of the ballistic impact testing system. The ballistic impact tests were carried out using a rifle caliber 270 Winchester and ammunitions of 150 g power point with an average mass of 9.72 g. For the experiments 3, 4, and 5, the ballistic impact tests were conducted on square target plates (20 x 20 cm) with a thickness of 5 mm using a semi-automatic Beretta C x 4-Storm rifle. The ammunition used was 9 mm Luger (type FMJ) with a mass of 124 g. According to NATO specifications, the muzzle velocity and muzzle energy of this weapon are 381 m s^{-1} and 582 J, respectively [94, 95].

In the first experiment, six shots were fired on each target from a distance of 15 m. This distance is suitable to achieve stability and obtain reliable ballistic performance data [96]. In the second experiment, in order to determine the initial velocity, two targets were developed, and four shots were fired at each target (8 shots in total). In subsequent tests to determine energy absorption for each category of laminate, three targets were developed, and two shots were fired at each target making a total of six shots for each type of plate. Shots were fired also from a distance of 15 m to penetrate the plate on one side and exit on the other side. In the remaining experiments 3, 4, and 5, six shots were fired at each target from a distance of 5 m with a similar ballistic testing system.

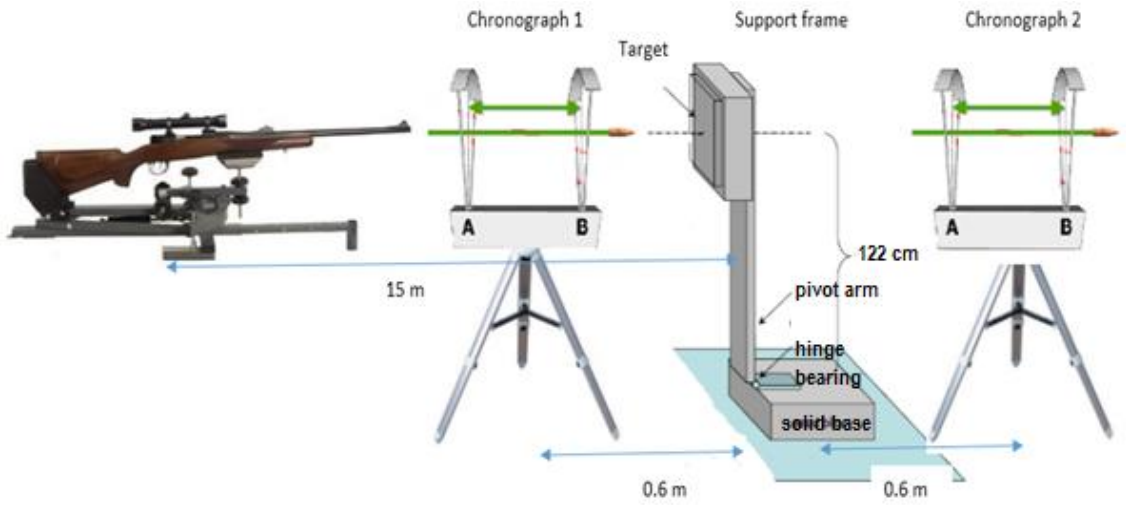

Fig. 3.7. Graphical representation of the ballistic testing system.

The muzzle velocity of 868 (m/s) and muzzle energy of 3667 (J/s) were achieved from the ammunition weighing 9.72 according to NATO standards [94, 95]. The initial and residual velocities of the projectiles were respectively measured before and after impact in order to determine the energy absorption by the targets. Ballistic precision chronographs (Caldwell) were used to measure the entry velocity and residual velocity of the projectiles after impacts. These chronographs are able to measure the projectile velocity ranging from 1 to 3000 m/s. Caldwell achieves this level of accuracy by using a high speed 48 MHz processor. The impact energy, residual energy, and absorbed energy were calculated based on the initial velocity of the projectile of mass *m* before impact (V_i) and its residual or exit velocity (V_r) after perforating the target as follows [97, 98]:

$$\text{Initial (Impact) Energy (J)} = \frac{1}{2}mV_i^2 \qquad 3.5$$

$$\text{Residual energy of projectile after impact (J)} = \frac{1}{2}mV_r^2 \qquad 3.6$$

$$\text{Energy absorbed or dissipated (J)} = \frac{1}{2}mV_{initial}^2 - \frac{1}{2}mV_{residual}^2 \qquad 3.7$$

$$\%\,\text{Energy dissipated} = \left(\frac{\text{Dissipated energy (J)}}{\text{Initial energy}}\right) X\,100 \qquad 3.8$$

The energy absorption for different target configurations are the same as the dissipated energy by the target, and which provides an indication of which target can dissipate more impact energy.

These are used for classification of the ballistic resistance of the materials according to NIJ 0108.01 standard. The energy absorption was also compared with the velocity and energy specifications for different low caliber weapons according to NATO standards. After the ballistic impact tests, the entry and the exit sides of the targets were analyzed in relation to the depth of penetration as well as the size of perforation at the entry and exit sides of the targets in order to determine the relations between, thickness, density, and penetration distance in the specimen. Detailed microstructural study of the specimen before and after the impact tests were conducted using optical and scanning electron microscopy (SEM) in order to evaluate the delamination and cracking mechanisms in the hybrid laminates during ballistic impact. In addition, penetration channels were cut along the centerline for analysis using SEM in order to determine the extent of the impact damage in various components of the laminates.

Chapter 4: Ballistic Impact Response of Laminated Hybrid Materials Made of 5086-H32 Aluminum alloy, Epoxy and Kevlar® Fabrics Impregnated with Shear Thickening Fluid

4.1 Overview

The objective of this chapter is to determine the influence of woven Kevlar® fibers impregnation with shear thickening fluids (STF) on mechanical behaviour and ballistic impact resistance of laminated composites made of alternate layers of aluminum plates and woven Kevlar® fibers reinforced epoxy. The research findings reported in this chapter have been published as manuscript #1 as follows:

Haro, E.E., Szpunar, J.A., Odeshi, A.G., "Ballistic impact response of laminated hybrid materials made of 5086-H32 aluminum alloy, epoxy and Kevlar® fabrics impregnated with shear thickening fluid, *Composites Part A Applied Science and Manufacturing*, vol. 87, pp. 54–65, 2016 [99].

The contributions of the PhD candidate are 1) experimental design, 2) preparing and processing all the samples; 3) physical, microstructural and mechanical characterization of the composites and 4) development of the manuscripts original manuscripts for publication. The manuscript was reviewed by my supervisors before it was submitted for publication in this journal.

The differences between this chapter and the published paper are: 1) The descriptions of the materials and target preparation have been removed from this chapter. This is to avoid duplication since this aspect is covered in Chapter 3 of this thesis. 2) The table depicting the mechanical properties of materials, and the figures corresponding to sample configuration and representation of the ballistic testing system, also have likewise been removed to avoid repetition. The references of the manuscript are listed at the end of this thesis. The copyright permission of use this paper is provided in the Appendix section.

4.2 Abstract

The ballistic impact behavior of hybrid composite laminates synthesized for armor protection was investigated. The hybrid materials, which consist of layers of aluminum 5086-H32 alloy, Kevlar® 49 fibers impregnated with shear thickening fluid (STF) and epoxy resin were produced in different configurations using hand lay-up technique. The hybrid materials were impacted by projectiles (ammunitions of 150 gr power-point) fired from a rifle Remington 7600 caliber 270 Winchester to strike the target at an average impact velocity and impact energy of 871 m/s and 3687 J, respectively. The roles of the various components of the hybrid materials in resisting projectile penetration were evaluated in order to determine their effects on the overall ballistic performance of the hybrid laminates. The effects of hybrid material configuration on energy dissipation during ballistic impacts were investigated in order to determine a configuration with best performance for application as protective armor. The energy dissipation capability of the hybrid composite targets was compared with the initial impact energy of low caliber weapons (according to NATO standards) in order to determinate the protection level achieved by the developed hybrid laminates. Deformation analysis and penetration behavior of the targets were studied in different stages; the initial (on target front faces), intermediate (cross-section), and final stages (target rear layers). The influence of target thickness on the ballistic impact response of the laminates were analyzed. Differences in ballistic behavior were observed for samples containing Kevlar® impregnated with STF and those containing no STF. Finally, mechanisms of failure were investigated using scanning electron microscopic examination of the perforations.

Keywords: protective armor, hybrid laminates, composite materials, ballistic impact, armor penetration.

4.3 Introduction

The defense industry and materials scientists have continued to show considerable interest in development of improved protective systems for equipment and military personnel against threats in combat operations. One of the main threats is the impact of projectiles at medium and high speed. The effectiveness of these systems depends critically on their ability to resist impulsive loads and absorb energy. Depending on their ability to protect against bullets fired from different caliber weapons, protective armor materials are classified, according to NIJ0108.01 and

NIJ0101.04 standard (US National Institute of Justice), on a scale IIA-II-IIIA-III and IV [9]. Protective materials belonging to category IIA, II and IIIA are called soft body armors. They are designed to protect against smaller weapons such as pistols with caliber bullets 9 mm having an average weight of 125 g, velocities ranging from 373 to 441 m/s, and impacts energy from 537 to 1510 J. The rigid ballistic plates in the levels III and IV are developed to resist more powerful weapons like rifles with 5.56 and 7.62 mm bullets that weigh 148 to 166 g, travelling at velocities ranging between 800 and 1100 m/s, and with impact energy of between 1960 and 3814 Joules [10].

Soft body armors are generally built with single layers of Kevlar®, Dyneema or Spectra fibers to protect personnel as bulletproof vests up to level IIIA. They are produced to have minimum weight and thickness. The main function of the ballistic vests is to protect the human torso from the impact energy of bullets and reduce the possibility of their penetration into the body. The low energy dissipation by soft body armors that are developed with only fiber layers can produce a blunt injury from ballistic impact. This injury is called behind armor blunt trauma (BABT) and in extreme cases can be very grave resulting even in death [100]. Several torso models were investigated (clay model, ballistic gelatin, animal models, and human cadavers) to collect the information on the transfer of energy and pressure wave propagation (maximum depth of 44 mm) during ballistic impacts, and the effects (injuries) that these impacts produce on the organs [101]. Two factors that contribute to ballistic performance in layers of Aramid and Twaron fabrics were investigated: trauma depth and its diameter produced by ballistic impacts and it was proved that the number of fiber layers used determines the level of protection or injuries caused to the human body during exposure to ballistic impact [102]. For military purposes it is known that the human body can absorb around 80 J during high-velocity impact from light weapons with a high probability of tissue damage [103]. According to Merkle *et al*. [101] and based on the body armor standards, the bullets must be stopped by the vest and the deformation produced at the back of the vest (penetration depth) should not be more than 44 mm for an effective protection. If this limit is exceeded, the body can suffer severe injuries. One of the primary objectives of this research is to reduce the BABT effects produced by soft body armour by ballistic impact.

Advanced composite materials consisting of polymers, metals or ceramic reinforced with fibers or particles are often studied for use in protective armour. The objective is to produce high structural integrity and an enhanced ability to stop the penetration of projectiles in armor plates [104]. Fibers

such as Dyneema, Spectra (UHMWPE fibers), and Kevlar® (aramid fibers) have been shown to resist high-velocity impacts ranging between 800 and 1000 m/s because they have a high resistance to dynamic deformation [27]. They can, therefore, be used to reinforce polymers to produce composite materials with a good resistance to failure under ballistic impact. Multilayer composites differ in the number of materials that are used in the layers and the arrangement of various components (configuration) based on the specific need. These layered structures are commonly used in dynamic impact applications where the matrix components are light metals (Al, Mg, or Ti alloys) and the reinforcement components are impact resistant fibers. Typical structures used for protection against the dynamic impact are fiber metal laminates (FMLs), metal matrix composites (MMCs), polymer matrix composites (PMCs), and ceramic matrix composites (CMCs) [97]. In addition, multilayer armor systems (MAS) generally consist of a ceramic layer (front) bonded to Kevlar® fabric plies (middle) and an aluminum alloy layer at the back and are built for protection against heavy bullets impact [105].

Ashby *et al.* [27] described the hybrid material to consist of two or more materials with a shape or scale designed to produce a combination of properties needed to achieve a well-defined objective. It is possible to improve the multilayer structures by combining properties of different materials such as metallic alloys, fibers, natural materials, and even by modifying their structure or grain size, which is a very good approach for improving properties like stiffness, strength and damage tolerance [34]. Hybrid laminates consisting of Kevlar®-29/ epoxy and 6060-T6 aluminum alloy sheets produced using different stacking configurations were subjected to ballistic impact at velocities ranging between 180 and 400 m/s. The highest energy absorption of 358 J was observed when aluminum plate was placed at the back (bullet's exit side) of the hybrid plate [39]. However, it is important to determine the possibility of further enhancing the ballistic impact resistance through the impregnation of the fiber with shear thickening fluids (STF). This can lead to laminate structures with improved resistance to ballistic impact damage. Reinforcements with about 20 to 50 layers of woven aramid fibers are required to produce a high ballistic performance with respect to protection and energy absorption. These properties can be further enhanced by impregnation with shear thickening fluid (STF) to reduce the number of layers of Kevlar® fabric by approximately 50% [63]. STF is a combination of hard metal oxide particles suspended in a liquid polymer and has a behavior similar to non-Newtonian fluid whose viscosity increases when shear stress is applied. The components used are polyethylene glycol (PEG) and colloidal silica. STF at

the very moment of impact shows a solid-like behavior and return to its fluid state after impact [62, 106, 107].

In a study by Majumdar *et al.* [64] a soft composite materials was developed using STF in different concentrations (50%, 60% and 70% of silica nanoparticles in PEG) and infiltrated into Kevlar® fabrics. A 0.380 caliber revolver was used for a low-velocity (165.2 m/s) impact test of the Kevar fabric impregnated with STF. It was observed that higher STF concentration enhanced the impact energy absorption capacity of the Kevlar® fabric. The results of other investigations also show that STF impregnation enhances the impact resistance of fibrous materials and enable reduction of the number of layers required for adequate protection [61, 62]. In these studies, the ballistic performance of Kevlar® fabrics were reported to improve by 40 to 80% when impregnated with STF. Lee *et al.* [63] reported that the impact resistance of Kevlar® fibers is enhanced by the impregnation of a colloidal shear thickening fluid (STF) leading to superior ballistic protection when compared with Kevlar® laminates with no STF. Findings from these studies indicated improved resistance of Kevlar® fibers impregnated with STF to ballistic impact. However, information on the use of STF in the configurations of hybrid laminates containing metals and fibers is very limited.

Developing armour plates with hybrid materials can offer a protective shield that is lighter, thinner, stronger, and less expensive than protective armor made by conventional armour materials. The objective of this study is to develop a novel hybrid composite laminates that can combine the properties of the 5086-H32 Aluminum alloy, Kevlar®-49/epoxy composite and shear thickening fluid (STF). Although many studies have been conducted on the effects of STF impregnation on the ballistic performance of Kevlar® fabrics. However, there is no information on the ballistic impact response of STF-impregnated Kevlar® fabrics bonded with layers of aluminum alloy to form hybrid composite plates. It is very important to determine whether STF impregnation into fibers will allow such hybridization with metallic layers to produce high performance protective armor. In this study therefore, the effects of STF impregnation on the ballistic impact resistance of the hybrid laminates are determined. The penetration resistance and energy absorption in the obtained hybrid laminates during ballistic impacts are evaluated and discussed.

4.4 Configuration and preparation of targets

Table 4.1 shows the compositions and configurations of the prepared hybrid composite laminates. In each category, three specimens with the same number of layers and similar configuration are prepared. The specimens were used to compare the ballistic impact resistance of hybrid plates made of Kevlar® impregnated with STF (colloidal silica) and those made of Kevlar® without STF, which were processed and tested under the same condition. The weight and thickness of the plates were measured, and the results showed that plates containing impregnated STF have a higher average weight (17–22%) and a higher thickness (10–15%) than those with no STF impregnation. Homogeneous distribution of the silica nanoparticles into the fibers depend on the size and distribution of these particles.

Table 4.1. Configurations of the manufactured hybrid laminates (targets).

Targets	Samples containing STF			Samples containing no STF		
	Al/K20/Al	Al/K10/Al/K10/Al	Al/K10/Al/K10/ Al/K10/Al	Al/K20/Al	Al/K10/Al/K10/Al	Al/K10/Al/K10 /Al/K10/Al
Al 5086-H32 (g)	190	285	380	190	285	380
Kevlar® (g)	75	75	112.5	75	75	112.5
Weight K/STF dried (g)	208	208	312	-	-	-
Epoxy Resin (ml)	100	100	150	100	100	150
Weight of Target (g)	394	486	688	332	432	618
Target thickness (mm)	10.5	11.8	16.4	8.1	9.4	13.6
Target areal density (g/cm^2)	1.75	2.16	3.06	1.48	1.92	2.75

Al = Aluminum 5086-32 alloy [Thickness = 1.6 mm]; K20 = 20 Layers of woven Kevlar® fiber cloth

As a result, the concentration of the solutes and solvents in the STF has a direct relation to the impregnation efficiency of the fibers with STF [108]. Fig. 4.1 shows scanning electron microscopic (SEM) images of woven Kevlar® fiber cloth with containing impregnated STF and that impregnated with STF after evaporation of the solvent. Fig. 4.1b confirms a complete impregnation of the Kevlar® fibers with the STF.

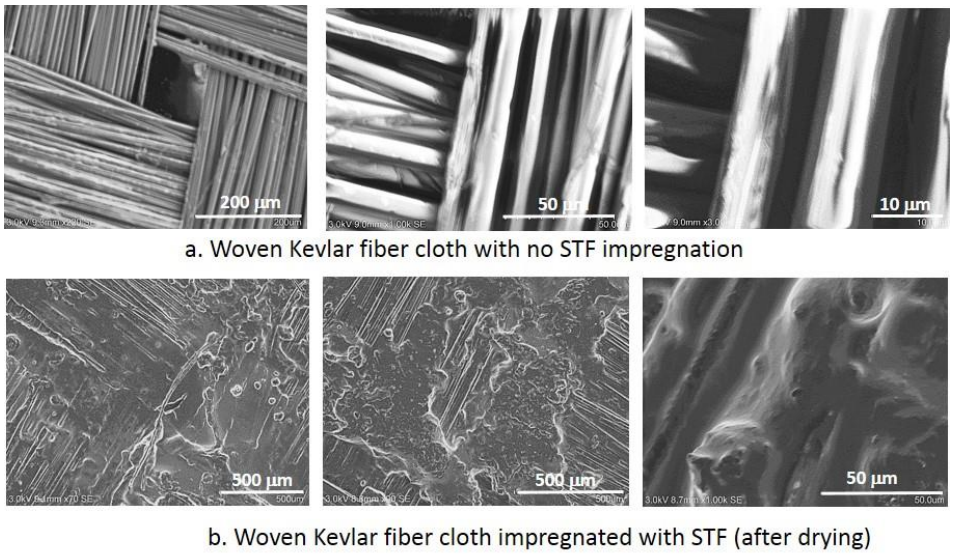

Fig. 4.1. Scanning electron micrographs of the woven Kevlar® cloth (a) before and (b) after impregnation with STF.

4.5 Results and discussion

4.5.1 Evaluation of the interaction of components

The main function of the AA 5086 aluminum alloy is to support the reinforcing Kevlar® fibers and provide with the necessary stability. Aluminum alloys in conjunction with resin-hardeners can hold the fibers together. Aluminum plates protect the fibers from the environment, and distribute the loads evenly so that all fibers are subjected to the same amount of strain [109].

The Kevlar® fibers serve as reinforcement for an enhanced resistance to bullet penetration. They enhance the mechanical properties such as tensile and flexural strength. Their high tensile strength makes it possible to significantly resist stretching forces during fiber deflection produced by ballistic impacts. Kevlar® fiber is particularly important in slowing down the projectile through initial tensile elongation, inter-laminar delamination, and fiber pull out during projectile penetration [27].

The colloidal silica in STF is a thickening additive that serves as a strong filler to improve strength, abrasion resistance, and ballistic performance of the hybrid laminate ensemble. The epoxy provides a strong bond between the components of the hybrid composite laminates. SEM

micrographs of the transverse sections of manufactured hybrid material (Fig. 4.2) confirms a strong adhesion between the metallic and nonmetallic components [63, 68, 110].

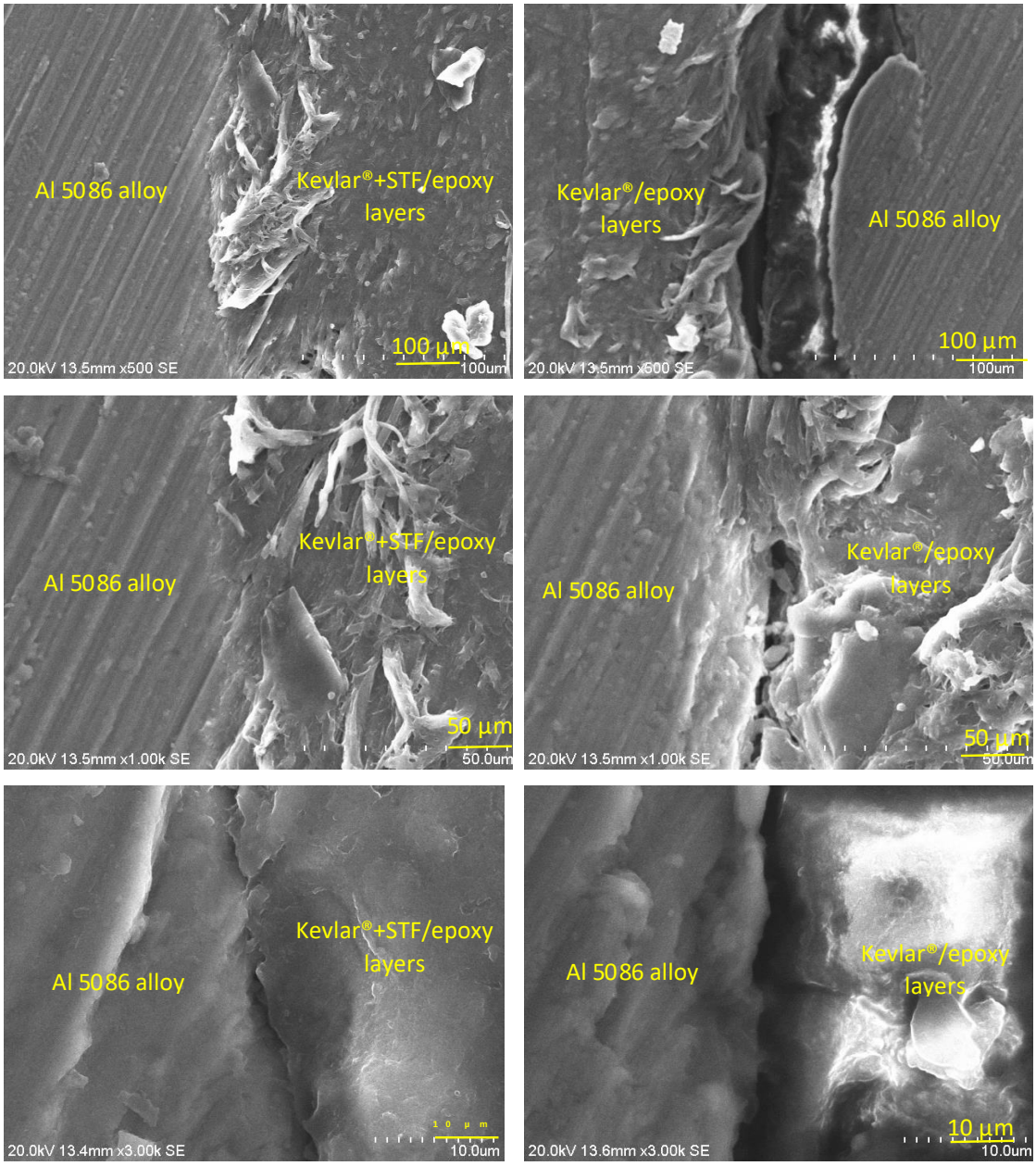

Hybrid composite samples containing STF Hybrid composite samples containing no STF

Fig. 4.2. SEM pictures comparing the interface bonding between the metallic and non-metallic components of hybrid laminate targets.

4.5.2 Energy absorption (dissipation) by the targets during ballistic impact tests

From an earlier study on energy dissipation in targets during ballistic impact, it was reported that fraction of the kinetic energy of the projectile is converted into heat while the remaining is absorbed by the target and utilized in its deformation [110]. The absorbed energy by the target represents kinetic energy loss due to elastic and plastic deformations. The residual energy is the kinetic energy of the projectile after perforating the target [109]. Figure 4.3 shows the relationship between the targets configuration on one hand, and the residual energy and absorbed energy on the other hand. It is evident that the targets treated with STF have better response to absorb energy in the range from 685 to1037 J, with an average standard deviation of 65.6 J, compared to those with no STF impregnation (507-907 J), and an average standard deviation of 70 J. The residual energy of the target containing STF impregnation ranged between 2650 J and 3002 J. This is lower for plates containing no STF impregnation in which the residual energy varies in the range: 2780 - 3180 J.

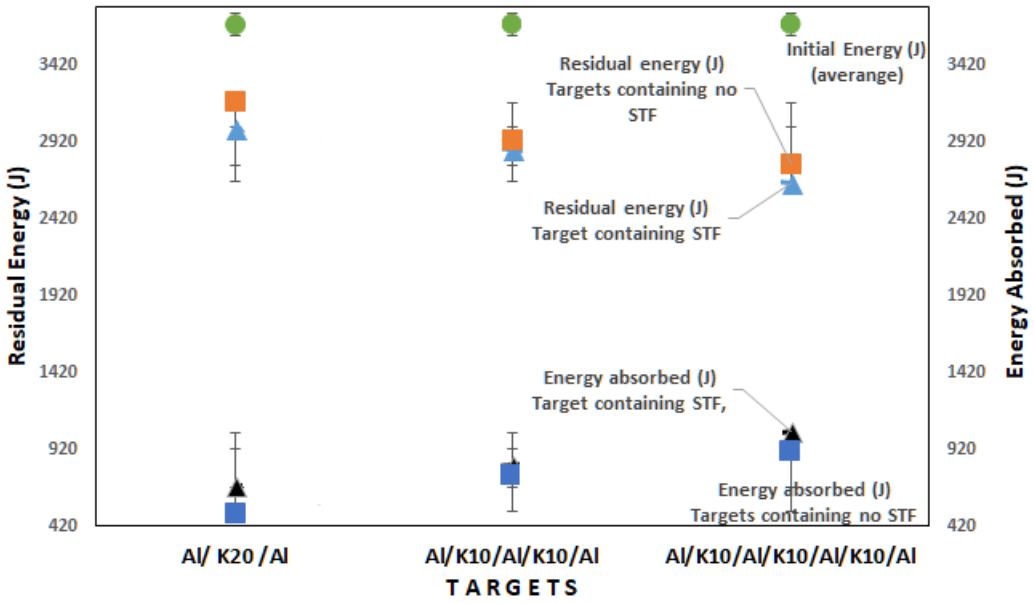

Fig. 4.3. Effects of hybrid material configuration and shear thickening fluid impregnation on residual and absorbed energy.

The amount of energy absorbed is about 130 to 178 J higher for STF-containing samples, implying better resistance to ballistic impact. The capacity to absorb energy in STF-containing targets with less area density in relation to the samples containing no STF is in agreement with the results of the investigations carried out by Lee *et al.*[63]. The results obtained in this study align with those

obtained from ballistic impact testing and stabbing resistance resting of soft protective armor (clothes) made with and without STF impregnation. Absorption of impact energy was enhanced under both test conditions for the cloth containing STF impregnation. Consequently, the number of Kevlar® fabric layers required for protection was reduced by between 20 and 40% with STF impregnation [61, 63, 111].

Figure 4.4 provides the relationship between the target's areal density and the percentage energy dissipated. The energy absorption by the targets with STF is greater than that for the targets containing no STF. The areal density differences between specimens only ranged between 10% and 15%. These results agree with the findings of Y. S. Lee *et al.* [63] in which the impregnated fibers with STF were reported to have an areal density similar to that of Kevlar® with no STF impregnation. They also reported that impregnation of Kevlar® fabric with STF enhanced the energy absorption capability and the flexibility of the targets. In this study, we observed that whereas the hybrid laminate with configuration Al/K10/Al/K10/Al/K10/Al containing STF dissipated about 28 % of the initial energy of the projectile, target with the same configuration but containing no STF dissipated 24 % of the initial energy. Improvement in energy absorption with STF impregnation can be attributed to microstructural change in the impregnated colloidal silica in the shear thickening fluid that creates particle clusters (hydro clusters) [63]. These clusters enhance the hydrodynamic stress by increasing the viscosity in the suspension during dynamic impacts.

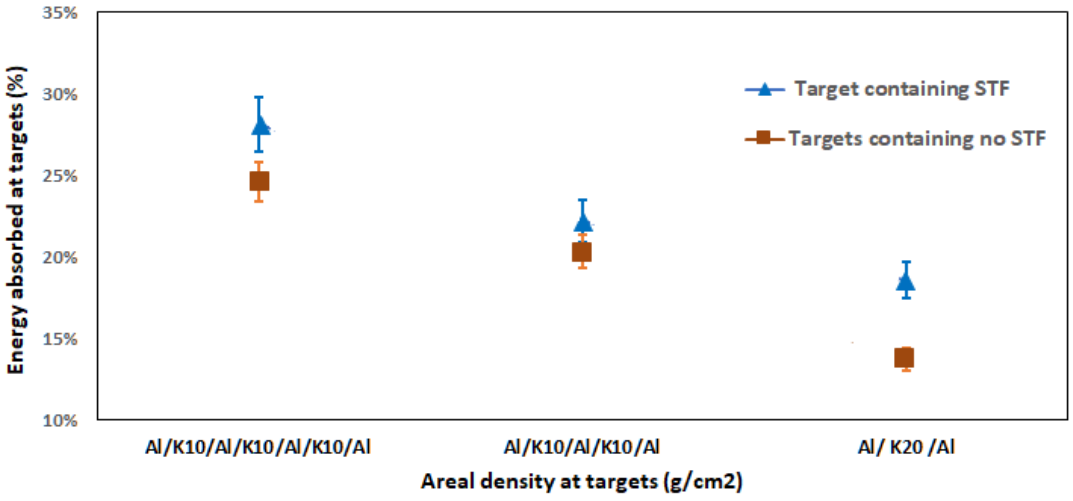

Fig. 4.4. Energy dissipated in relation to the area density of the targets

The results of microstructural investigation of the Kevlar® fabrics indicate that the fabrics not treated with STF have empty spaces between fiber bundles. This can contribute to the observed lower effectiveness of the targets with no STF in resisting bullet penetration during ballistic impact. On the other hand, the targets built with Kevlar® impregnated with STF has the empty space between fibers bundles completely filled with particles of colloidal silica. This underscores the significant effect of STF impregnation of the Kevlar® fabrics in producing a consolidated hybrid structure and increasing the energy absorption during impact. This impregnation can enhance the fiber elongation, increases the delamination resistance, and fiber breakage contributing to increase in the amount of energy absorbed during the projectile penetration. In so doing, there will be greater resistance to posterior crack propagation through load distribution between aluminum/resin matrix and the Kevlar® fibers. As more yarns are involved in the absorption of the impact energy, the resistance to projectile penetration of target will increase.

4.5.3 Comparison of the initial impact energy from different light weapons with the energy dissipated from the developed hybrid composite laminates.

The initial velocity and impact energy of low caliber weapons, have been recorded according to NATO standard specifications [94, 95]. Although, the shape and material characteristics of the bullets are different for each weapon, the energy of impact can be compared with the results of the energy absorption obtained in the experimental investigations in this study as summarized in Table 4.2.

Table 4.2. Results of the ballistic impact test of the hybrid materials (targets).

Targets	Samples containing STF			Samples containing no STF		
	Al/K20 /Al	Al/K10/Al/K10/Al	Al/K10/Al/K10/Al/K10/Al	Al/K20 /Al	Al/K10/Al/K10/Al	Al/K10/Al/K10/Al/K10/Al
Initial velocity (m/s) (average)	871	871	871	871	871	871
Residual impact velocity average (m/s)	786	768	738	809	777	756
Initial energy average (J)	3687	3687	3687	3687	3687	3687
Residual impact energy average (J)	3002	2867	2650	3180	2937	2780
Absorbed energy average (J)	685	820	1037	507	750	907
St. deviation Absorbed energy (J)	99.7	95.67	83.9	113.1	149	92.4
Absorbed energy average (%)	19%	22%	28%	14%	20%	25%
Energy dissipated per unit area (J/cm2)	3.04	3.64	4.61	2.25	3.33	4.03
Energy absorption per unit thickness (J/mm)	65	69	63	63	80	67

The initial energy (3687 J, standard deviation of 53.1 J) applied in the current study is higher than the initial impact energy presented in Table 4.3. The energy dissipated in each target is presented in Fig. 4.5 in the form of horizontal lines, and the initial impact energy of several low caliber weapons presented as the vertical bars in the bar chat. Based on experimental findings and calculations, it is possible to suggest that the targets built with Al/K20/Al (Kevlar® untreated with STF) cannot resist any ballistic impact from those weapons. The configuration Al/K20/AL impregnated with STF can resist only bullets from pistol HK and Parabellum 9 mm The Al/K10/Al/K10/Al laminate with STF impregnation can resist all kinds of pistols up to the Beretta M9 (caliber 9 mm). The rest of samples Al/K10/Al/K10/Al (STF), and Al/K10/Al/K10/Al/K10/Al (treated and untreated with STF) can respectively absorb energies of 819 J, 907 J, and 1036 J. These are enough to provide sufficient protection for pistols (9 mm). Nevertheless, they are not able to resist shots from caliber 5.56 mm rifles and higher. It is evident from this study that configuration of the hybrid laminates in addition to STF impregnation determine the level of protection achievable against low caliber weapons listed in Table 4.3.

Table 4.3. Initial velocity and energy of low caliber weapons [94].

Low caliber weapons	Cartridge (mm)	Cartridge weight (g)	Bullet weight (g)	Velocity (m/s)	Energy (J)
270 Winchester rifle	7.06	150	9.72	869	3667
AK-47 rifle	7.69 * 39	24	8	715	2045
M14 rifle	7.62 * 51	25.4	9.33	838	3275
FAL rifle	7.62	24	9.5	823	3217
M16 rifle	5.56 * 45	12.31	4.02	991	1974
HK rifle	5.56		4.1	936	1796
AUG rifle	5.56		4	940	1767
Beretta M9 pistol	9 * 19	8.1	4.1	600	756
HK pistol	9	7.45	4.5	390	570
Parabellum pistol	9	9.5	5.2	460	561

Reference: NATO EPVAT testing, Quick LOAD, SAAMI, standard

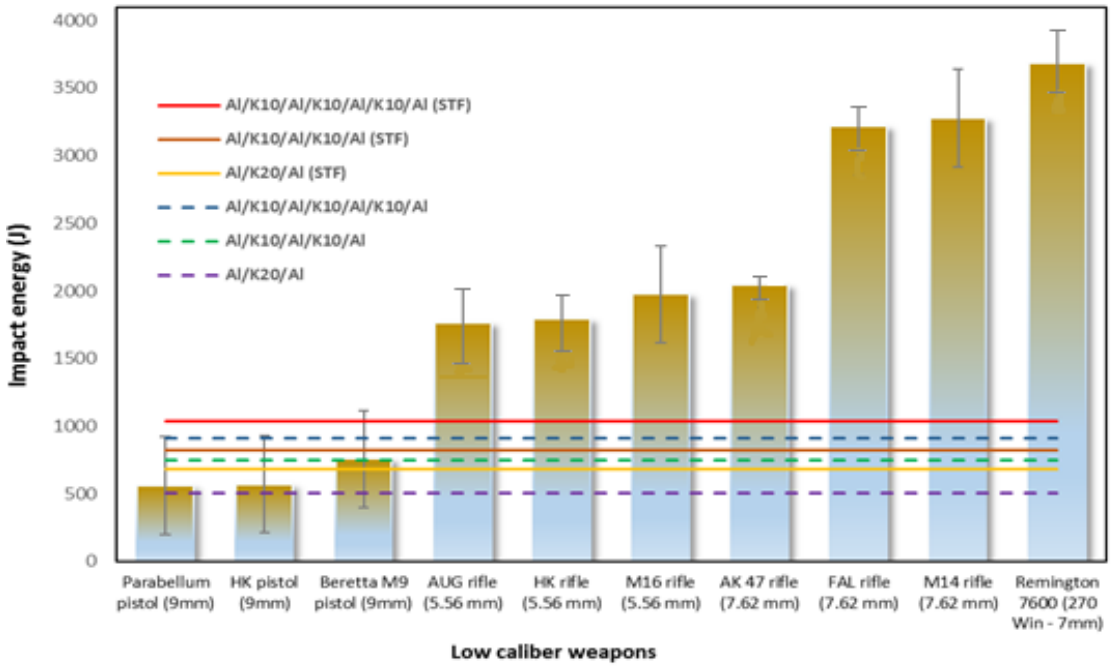

Fig. 4.5. Dissipated impact energy from targets vs initial energy from low caliber weapon.

4.5.4 Deformation analysis and projectile penetration of targets

Experimental data providing information on penetration of targets during ballistic impacts are summarized in Table 4.4. The average diameter of the crater on the entry and the exit sides were measured as well as the total penetration depth. Figure 4.6 shows the morphology of the perforation on the hybrid ballistic plates after projectile penetration (270 Winchester - 150 gr power-point).

Table 4.4. Projectile penetration of the targets dimensions of perforation.

Targets	Average energy absorbed (J)	Specific energy absorbed (J/(g/cm2))	Average initial thickness (mm)	Average entry diameter of crater, D in (mm)	Average Exit diameter of crater, D out (mm)	Total penetration height (mm)
Al/K10/Al/K10/Al/ K10/Al (STF)	1037	339	16.40	9.35	19.94	36.31
Al/K10/Al/K10/Al (STF)	820	379	11.80	9.12	20.01	27.58
Al/K20/Al (STF)	685	391	10.50	8.83	15.78	24.17
Al/K10/Al/K10/Al/ K10/Al	907	330	13.60	9.44	24.92	36.43
Al/K10/Al/K10/Al	750	390	9.40	9.73	17.16	27.37
Al/K20/Al	507	342	8.10	9.08	14.89	21.06

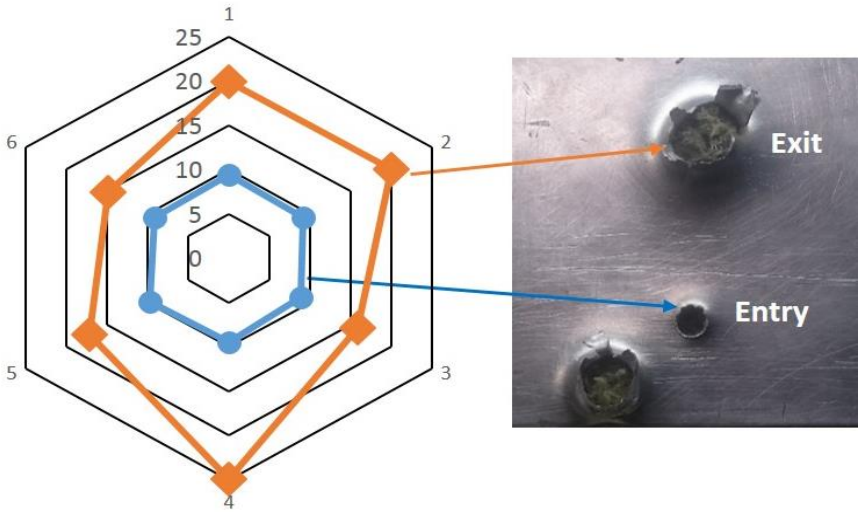

Fig. 4.6. Morphology of cross section of penetration channel at the entry and exit sides of the targets.

A cylindrical shape perforation orifice can be observed. The diameter of the circular hole produced by the projectile of diameter 7.06 mm at the entry side of all the targets ranged between 8.8 and 9.7 mm. In contrast, the diameter of the exit side of the perforation is more scattered and vary widely between 14.8 mm and 24.9 mm forming open petals after complete projectile penetration. The petal shaped appearance depends on several factors such as the target configurations, thickness, STF impregnation, arrangement of aluminum and Kevlar® layers (configuration). All targets were completely perforated by the projectiles. Similar patterns of perforation were also observed in the penetration channels in Al-7017 alloy backing plates in which the residual depth of penetration and the ductile-hole growth were measured [112]. In addition, STF-containing samples showed better stability after several shots were fired at the targets (Fig. 4.7a). Delamination effect was not observed in the targets because of improved bonding between layers of Aluminum and Kevlar® impregnated with STF (Fig. 4.7b). On the other hand, targets with Kevlar® fabric that was not impregnated with STF experienced delamination between the fiber and the aluminum plate as presented in Fig. 4.7b.

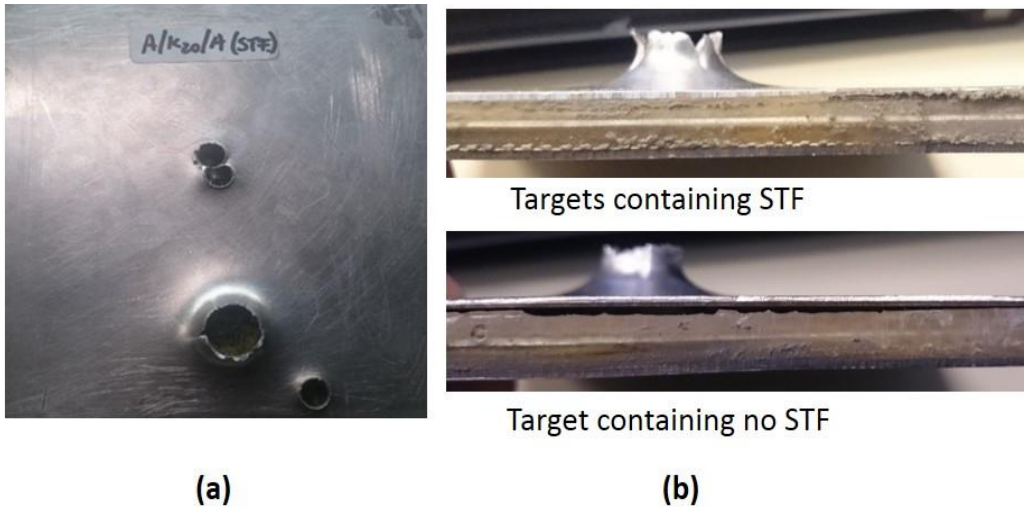

Fig. 4.7. (a) Perforation of the hybrid laminae target by bullets and (b) side view of craters showing stability of targets after ballistic impacts.

4.5.5 The influence of target's thickness

Thickness is an important factor that can influence the energy absorption during ballistic impact, and it depends on the configuration and number of layers of each component of the target. The target's thickness and the configuration are provided in the Table 4.1. The specimens made with fibre with no STF impregnation has smaller thickness compares with those containing STF. About 20 % increase in the target's thickness occurred with STF impregnation. The penetration depth for each target during ballistic impact depends on several factors that include sample thickness and configuration. Ballistic impacts produce a wide range of scattered diameter for different penetration depths in a transverse section (21.1 - 36.4 mm). The specimens' capacity to absorb energy per unit thickness (measured by energy absorbed per unit mm of the thickness) are presented in Fig. 4.8. For example, targets with configuration Al/K10/Al/K10/Al (Kevlar® with no STF impregnation) absorbed 80 J/mm but could only absorb a maximum total energy of 750 J. In contrast, targets with the same configuration containing STF were able to absorb energies per unit length and total energy of 69J/mm and 819 J, respectively.

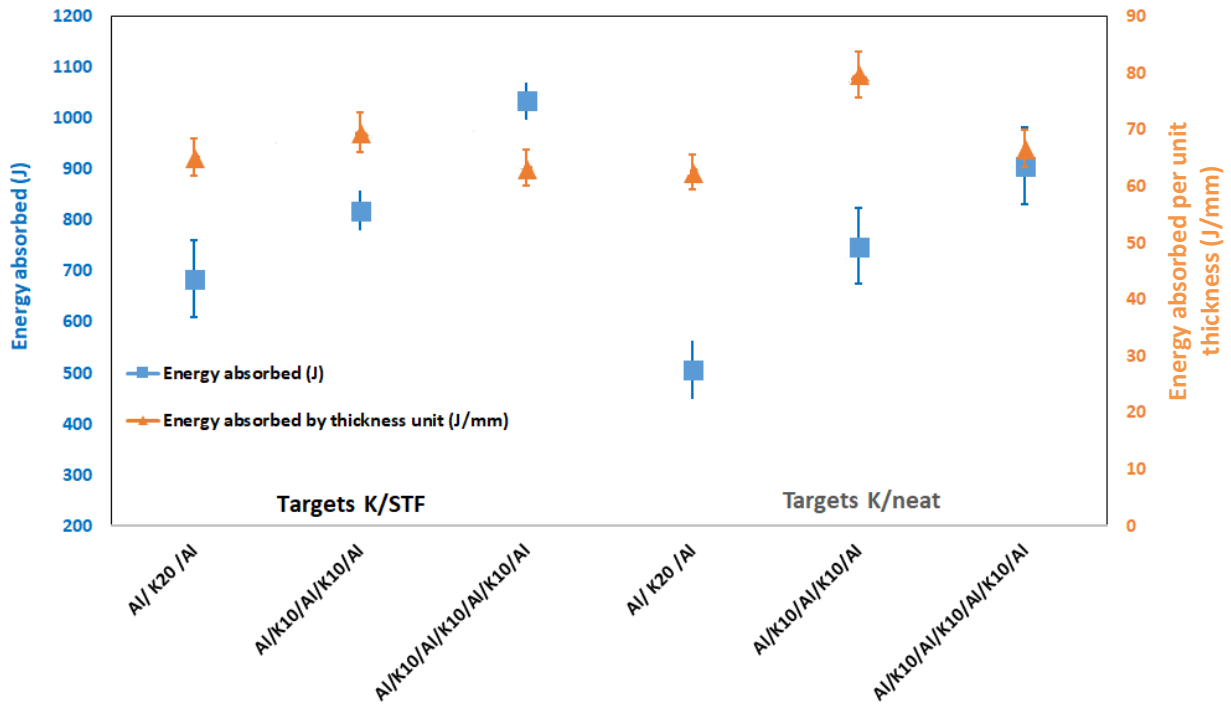

Fig. 4.8. Relation between energy absorbed per unit thickness and dissipated energy during ballistic impacts at the specimens.

4.5.6 Energy absorption and failure analysis during ballistic impacts

The mechanisms of energy absorption and the impact damage evolution sequence produced by ballistic impacts were investigated using scanning electron microscope. The failure of the targets occurred by a combination of perforation, plastic deformation and delamination. Perforation of the targets depends on their thickness and the material properties of the hybrid laminates. The extent of plastic deformation depends on shape of projectile's nose, impact velocity and the impact resistance of the target. The kinetic energy of the projectile is transformed into heat and work on impact. Microscopic analyses were made on the transverse section of the perforation that was cut parallel to the penetration channels (Fig. 4.11). The damage produced between various layers of Aluminum, Kevlar® (treated and non-treated with STF), and the epoxy resin matrix can be observed in Fig. 4.9.

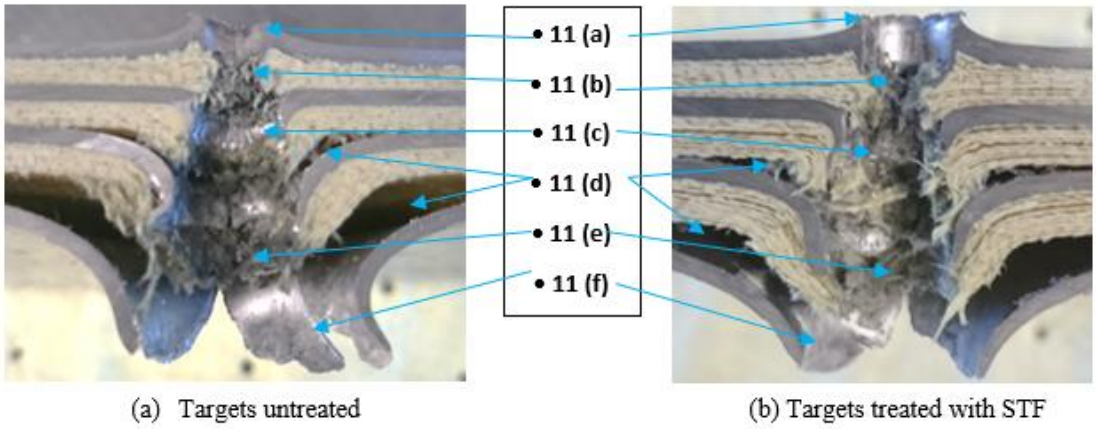

Fig. 4.9. Mechanism of energy absorption during ballistic impact.

The sequence observed shows an initial indentation on the Aluminum frontal face produced by a localized stress during the initial contact with the projectile (Fig. 4.9a), which created a small puncture due to projectile pressure. The initial penetration on the first aluminum plate (average diameter 8.83 to 9.44 mm) and the initial fracture of the fibers were produced by the compressive force from the projectile (Fig. 4.9b). This created a ductile enlarged crater resulting in shear plugging, tensile loading and fracture of the first fiber yarn. Shear, tensile and compressive forces were generated by the projectile as it penetrated the target leading to fragmentation of Kevlar® fibers and expulsion of the fragments from perforation channel. Internal cracking also occurred in aluminum plates as they deform during projectile penetration (Fig. 4.9c). Difference in tensile response of the Kevlar® fabrics to projectile penetration were observed for the Kevlar® fabric impregnated with STF and those containing no STF. For instance, Kevlar® fibers containing no STF suffered a high yarn pullout, debonding, plastic deformation, and fracture and fiber fragments expulsion during projectile penetration. On the other hand, for the targets containing fibers impregnated with STF, the intensity of fibre pulls out was less due to better adhesion within the fiber bundles and with the aluminum plate. As a result, targets with STF impregnation exhibited more ductility and better resistance against projectile penetration.

Delamination between Kevlar® layers and in greater proportion between aluminum plates and Kevlar® layers can be observed in Fig. 4.9d. Such delamination is an effect of the elastic wave propagation and force distribution in the target where the fibers serve as the reinforcement. Delamination occurred at the interfaces between layers of aluminum alloy and Kevlar® fabrics, the intensity of which increased with projectile penetration. Investigations indicate that the

Kevlar® fabric with no STF impregnation has a weak bonding between fabric layers. However, for targets treated with STF, the delamination occurred less intensively. Shear forces and dynamic friction between layers increases as the projectile penetrated the target. The deformation leading to absorption of impact energy reached the maximum level in last layer of the Kevlar® fiber before the exit of the projectile (Fig. 4.9e). The aluminum sheet at exit side of the target deformed extensively showing radially and circumferentially propagating cracks forming sheet of open petals. The radial fracture produces a wrinkle in each petal, which finally takes a form of a highly deformed tip. This shape depends on the extent of energy absorption; the more the energy absorbed by the target, the greater is the deformation. The depth penetration of the channels (Fig. 4.9f) formed by the projectiles depend on the penetration resistance and the energy absorbed by the targets. The results obtained in this study agree with those obtained from other studies on ballistic response of carbon composite materials in relation to energy absorption sequence and impact damage evolution [97, 113]. The delamination studies conducted on fiber metal laminates (FMLs) showed that an interfacial fracture between the aluminum and glass fiber layers was caused by shear forces [114].

Photographic investigation of the surface of perforations provided information on the mode of fracture and the sharp-nosed projectile perforated the hybrid laminates during ballistic impact test. At the initial stage of penetration, a ductile crater enlargement is observed. Linear deformation bands are features of initial perforation of the aluminum front face layer and they propagate linearly across the transverse section. Horizontal striations are also produced by the lands and groves that come from the rifling process of the ogive. Figure 4.10 shows the impression marks of the bullet as it travels through the barrel. In Fig. 4.10a high plastic deformation is observed in the penetration channels, which is characterized by deformation bands. Vertical striations that come from the initial reaming of the barrel are observed on the surface. Figure 4.10b indicate plastic deformation leading to formation of a petal in the point of exit of the projectile from the last layer of aluminum plate.

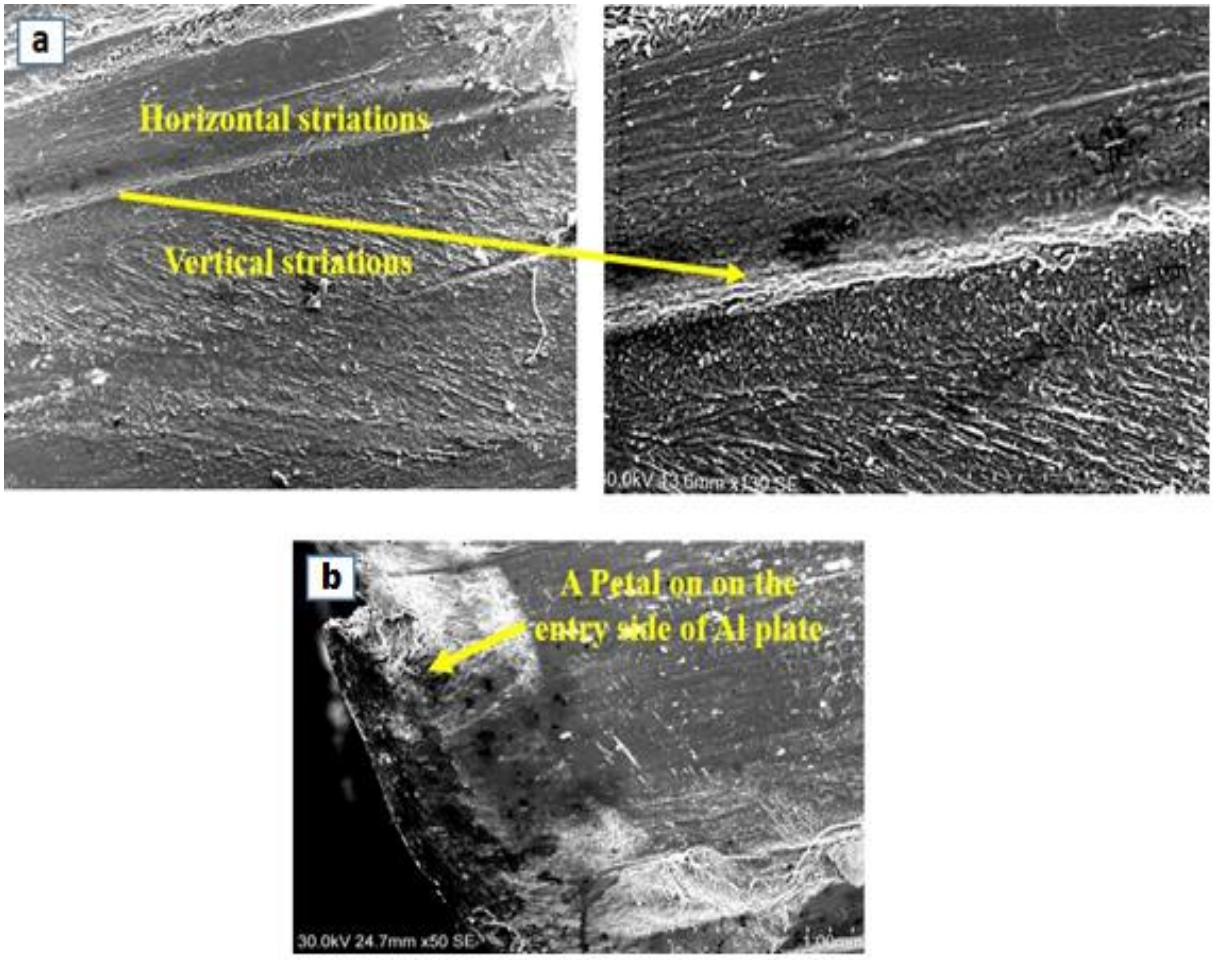

Fig. 4.10 Fracture surface along perforation in the target

Figure 4.11 shows the aluminum plates after complete penetration of the projectile through the target. A radial cracking caused by the projectile propagated in the circumferential direction by forming sheets of open petals (Fig. 4.11a). The circular deformation bands shown in the Fig. 4.11b on the aluminum petals may be a result of a near-adiabatic heating that occurred during the ballistic impact. The heat generated must have led to intense thermal softening along narrow bands in the aluminum sheet leading to strain localization along those bands. Shear bands caused by localization of deformation were observed in AA 6061-T6 and 5083-H131 aluminum alloys subjected dynamic impact load [115].

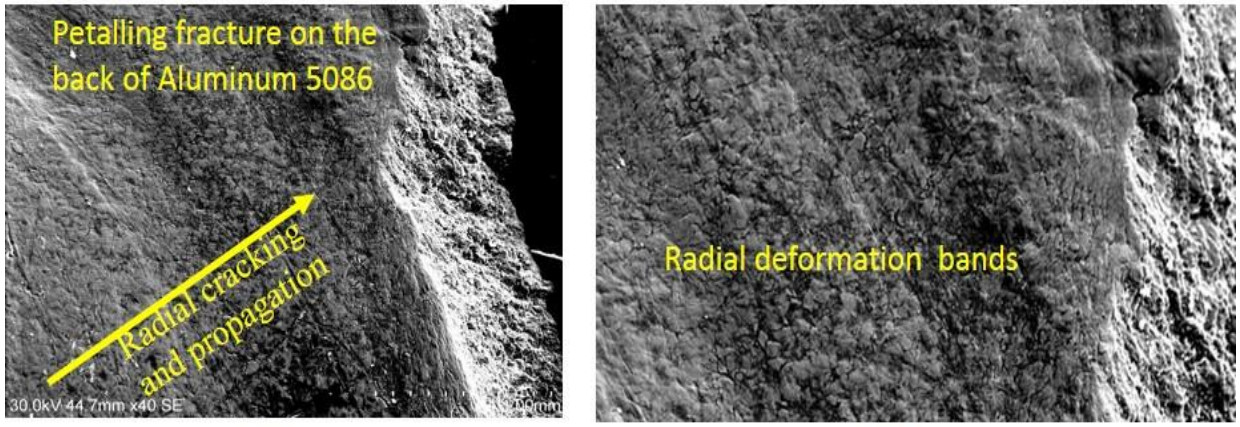

Fig. 4.11. Radial cracking and deformation bands on the open petals formed on the rear side aluminum plates at the exit point of the projectile.

4.6 Conclusions

Hybrid laminates made of layers of aluminum 5086-H32 and Kevlar®/epoxy composites were fabricated in different configurations and subjected to ballistic impact testing. The effects of laminate configuration and shear thickening fluid (STF) impregnation into the fibers on the ballistic performance were evaluated. The configuration of the hybrid composite laminates has significant influence on its resistance to perforation by the projectile. The hybrid composite laminates made with Kevlar® fabric impregnated with STF (colloidal silica) have higher energy absorption capability than those containing no STF impregnation. The results indicate that most of the laminate configurations developed should meet the protective requirements for levels IIA, II, and IIIA, which means they are able to resist the impact from pistols of 9 mm with an energy absorption ranging from 507 to 1037 J. The mode of failure leading to projectile penetration is the same irrespective of target configuration. Fracture surfaces contain horizontal and vertical striations as well as deformation bands that propagated across the transverse section of the aluminum plates. The tendency of Kevlar® fibers to rupture during projectile penetration decreased when impregnated with STF. The energy absorption capability of the hybrid laminates improved with STF addition. Plastic deformation, radial and circumferential cracking aluminum produced open petals at the exit side of the target.

Chapter 5: The Energy Absorption Behavior of Hybrid Composite Laminates Containing Nano-fillers under Ballistic Impact

5.1 Overview

In the previous chapter, the shear thickening fluids (STF) made of colloidal silica nano-particles, was infiltrated into woven Kevlar® fibers used in reinforcing epoxy resin. It was concluded that impregnating the Kevlar® fibers with STF improve the ballistic impact resistance of laminated hybrid materials. Therefore, the purpose of this chapter is to study the influence of several different micro- and nano-fillers used in developing new STF for impregnating Kevlar® woven fibers on the ballistic performance of hybrid composite laminates made from the impregnated Kevlar® fibers.

The research findings reported in this chapter have been published as manuscript #2 in the Journal paper:

E. E. Haro, A. G. Odeshi and J. A. Szpunar, "The energy absorption behavior of hybrid composite laminates containing nano-fillers under ballistic impacts.", *International Journal of Impact Engineering.*, vol. 96, pp. 11-22, 2016 [116].

The contributions of the PhD candidate in this manuscript are 1) experimental design, 2) preparing and processing all the samples, 3) materials characterization, analysis of test results, and 4) development of the manuscript for publication. The manuscript was reviewed by my supervisors before it was submitted for publication in this journal. To avoid repetition of information provided in Chapter 3 of this thesis, the descriptions of the materials and target preparation have been removed from this chapter. The references of the manuscript are removed and listed at the end of this thesis. The copyright permission for use of this paper is attached in the Appendix section.

5.2 Abstract

Hybrid composite laminates consisting of woven Kevlar® fiber fabric, epoxy and AA 5086-H32 aluminum sheets were produced and the effects of addition of different micro and nano-fillers to the fiber on ballistic response of the hybrid laminates were investigated. The micro and nano-fillers used in this study are powders of aluminum, gamma alumina, silicon carbide, colloidal silica and potato flour. They were introduced into the Kevlar® fabrics by mixing with polyethylene glycol (PEG-400), followed by impregnation of the Kevlar® fabric with the mixture and drying to eliminate the solvent. The energy absorption by the hybrid composite laminates containing the various nano-fillers under ballistic impact were determined and compared with laminate containing no nano-filler impregnation. The ballistic impact resistance of the produced hybrid composite laminates was tested according to NATO standards using a caliber 270 Winchester rifle. The projectile penetration and the resulting perforations of the hybrid laminates were studied in order to determine the influence of the deposited nano-fillers on Kevlar® fibers on their energy absorption and impact resistance. The relationship between areal density and energy absorbed are discussed to determine which specimens perform better under ballistic impact. Protection levels achieved by targets were analyzed in relation to the initial impact energy from low caliber weapons. The results indicate that the ballistic impact resistance and impact energy absorption capacity of the hybrid composite laminates were enhanced by deposition of micro and nano-fillers into surface of the Kevlar® fibers fabrics. The highest impact energy absorption capacity was achieved by deposition of aluminum powder followed be colloidal silica and silicon carbide powder in that order. Addition of gamma alumina powder and potato flour have produced the least effect of enhancing the impact energy absorption capability of the laminates. These findings indicate that introduction of micro- and nano-fillers coating on Kevlar® fabrics using PEG-400 offers a promising method for strengthening interfacial bonding between the matrix and fibers in hybrid composite laminates.

Keywords: hybrid composites, energy absorption, ballistic impact, protective armor, composite materials, nano-fillers.

5.3 Introduction

Improving the shielding capacity of protective armor materials against ballistic impact has continued to attract the interest of the scientific community. Development of hybrid composite laminate structures can offer a solution of providing protective shields that are lighter, leaner, and more potent than the conventional protective armor plates made of monolithic materials. Hybrid materials consist of layer of two or more existing materials configured in such a way that allows the superposition of their properties to meet targeted service requirements [34]**.** In hybrid composites, improved multilayer structures combining properties of widely diverse materials such as metal alloys, fibers, natural materials, and even nanoparticles are made possible in order to achieve protective armor with enhanced protection capability [27]. The motivation for the increased interest in the use of nanoparticles with dimensions ranging from 1 to 100 nm in engineering applications include their unique surface strengthening effect in metal alloys, ceramics, fibers, and even polymers leading to increase in mechanical properties such as strength and stiffness, thermal properties, among others. Nanoparticles in low concentrations can achieve these purposes without compromising the density, toughness or the manufacturing process [117-119].

Most of the studies on armor vests used in ballistic protection have reported ways of improving the resistance of Kevlar® fibers to ballistic impact failure. One of the most common ways of achieving this is through impregnation of the Kevlar® fabrics with shear thickening fluid (STF). STF consists of oxide particles suspended in a liquid polymer. It behaves as a non-Newtonian fluid whose viscosity increases when shear stress is applied. The components of STF are polyethylene glycol and colloidal silica. STF assumes a solid-like behavior at the moment of impact loading. After impact loading, they return to their fluid state [106, 107]. Colloidal silica particles create a sealing coat, which enhances the resistance of the woven fibers to ballistic impact. Infiltration of aramid fiber fabrics with STF results in a microstructural change as the colloidal silica in the STF create particle clusters (hydro clusters), which enhance the hydrodynamic stress in the suspension and increase the capacity to resist ballistic impact [61, 62]. Experimental investigations have proved that the resistance of Kevlar® fabrics to ballistic penetration is improved by impregnation with silica particles (size 450 nm) dispersed in ethylene glycol. In addition, it was established that this impregnation enhanced the material flexibility and reduced the required thickness for adequation protection when compared with Kevlar® fabrics with no STF-

impregnation [63]. According to Majumdar *et al.* [62], the higher the STF concentration, the better the capacity for impact energy absorption by fibrous materials, and the lower will be the number of fiber layers required for the needed protection. STF increases the friction between the yarns during ballistic impacts and reduces the number of Kevlar® layers used in composite laminates by between 40 and 80% [97]. About 50% increase in energy absorption capacity was reported when Kevlar® was impregnated by STF in comparison with composites made of Kevlar® fabric that is not treated with STF [120].

In another study, the use of aluminum oxide (Al_2O_3) nano-fillers in epoxy resin reinforced with Kevlar® 29 fabrics was reported to improve the performance of bulletproof vest made of this composite material. Composite plates of different thickness were used to show the level of energy absorption by each plate during ballistic impact testing. The results showed that by using a stacking sequence of 30 layers cross–ply laminates, a highest energy absorption was achieved with an impact velocity of 400 m/s [29]. In the same way, epoxy resin filled with oxide nanoparticles of silane modified iron (III) was impregnated into Kevlar® fibers to create reinforced composite laminates; the oxide nanoparticle impregnation resulted in a significant enhancement of the tensile strength of the laminates [121]. Also, Kevlar® fibers impregnated with epoxy resin filled with cork powder, cork/clays, and clays were compared with specimens made of epoxy resin reinforced with Kevlar®. Previous research findings indicated that addition of cork powder to polyester resin reduces the flexural strength, and that the addition of the fillers can change the mechanical behavior of the matrix. However, for both kinds of specimens similar fatigue strength was observed [122]. In another experiment, the results indicated that fillers impregnation enhances the impact resistance by 4.5% for laminates filled with cork, by 10.4% for laminates filled with cork/clay and by 16.1% for laminates filled with clay [58]. When carbon fibers were coated with carbon nanotubes as nano-fillers in an epoxy resin, the fiber surface area increased, which provided a stronger interfacial bonding between the CNT/carbon fiber/epoxy matrix [123-125]. Hybrid nano-composites developed using different configurations of fiberglass/epoxy/nano-clay and fiberglass/epoxy/nano graphene were subjected to ballistic impacts from pistol of calibers 38 and 9 mm, and the results showed that hybrid nano-composites are able to absorb impact energy ranging from 284 J to 446 J, and that nano-clay and graphene additions into the epoxy matrix increase the energy absorption capacity of the hybrid nano-composites [126].

In another study, woven carbon fibers were reinforced with a polymer/epoxy matrix containing dispersed short multi-walled carbon nanotubes and significant improvement in inter-laminar damage tolerance was achieved with the carbon nanotubes addition (0.5 wt. %) to the epoxy matrix. The static interlaminar shear strength of the hybrid composite was found to increase by 20%, and interlaminar fracture toughness (Mode I) by 180% in relation to the samples without nano-reinforcement [127]. In an effort to improve the impact resistance of a carbon fibre reinforced plastic (CFRP), about 0.5% by weight of multi-wall carbon nanotubes (MWCNTs) were dispersed in the epoxy matrix (Bisphenol A). The MWCNTs inclusion enhanced the fracture resistance and ballistic impact performance (energy absorption capability) of the CFRPs [128]. Addition of carbon nanotubes (CNTs) and nano-sized core shell rubber particles (CSR) to Kevlar® fiber reinforced epoxy also led to improvement in impact energy absorption capacity [129]. Different techniques of nano-particles' dispersion have been employed to enhance interfacial bonding between matrix and fibers. For example, CNTs particles were impregnated directly on carbon fibers through immersion in an aqueous suspension prepared with CNTs, which led to better results compared to that other dispersion techniques such as CNTs mixed with epoxy resin or spraying methods [130].

Although many studies have been conducted on the effects of STF, CNTs, and Al_2O_3 impregnation into the resin matrix of fiber reinforced plastics on their ballistic impact resistance. However, there is no information on the ballistic impact response of hybrid composites plates consisting of aluminum alloy, epoxy and Kevlar® fabrics impregnated with other nano-fillers. It is very important to determine whether nano-fillers impregnation into fibers will allow such hybridization with metallic layers to produce high performance protective armor. In this study, nano-fillers of silica carbide, aluminum powder, colloidal silica, gamma alumina, and potato flour were mixed with a solution of polyethylene glycol (PEG-400) and were then infiltrated into Kevlar® fabrics in order to improve the energy absorption capacity of the resulting hybrid composite laminates. This is a new infiltration method of micro and nano fillers into fabric fibers and the feasibility of deposition using Polyethylene glycol (PEG-400) will be evaluated. The objective of this study is to improve the ballistic impact resistance and toughness of the hybrid composite laminates by addition of these nano-fillers to reinforce the Kevlar® fiber components without significantly altering the material's physical properties such as weight, thickness or density. The capacity of the obtained hybrid composite laminates to absorb energy, as a function of the type of the applied

nano-fillers was determined by conducting ballistic impact testing using a 270 caliber Winchester rifle and 150 gr power point ammunitions with an average mass of 9.72 g.

5.4 Configuration and preparation of targets

Table 5.1 shows the components and the configuration of the various hybrid composite plates produced for investigation in this research study. In each plate, two aluminum sheets surround 20 Kevlar® layers, which were previously treated by impregnation with nano-fillers or not. The weight and thickness of plates containing impregnated nanofillers are higher than those containing no nano-filler. These physical properties also vary depending on the type of the nano-fillers used.

Table 5.1. Experimental data sheet showing laminates' composition, configuration and their physical properties.

Targets configuration K20 + STF (nano-filler solutes metallic, ceramic and naturals)						
	Al/ K20 /Al (K untreated)	Al/ K20 /Al (silica carbide)	Al/ K20 /Al (potato flour)	Al/ K20 /Al (aluminum powder)	Al/ K20 /Al (colloidal silica)	Al/ K20 /Al (alumina)
Al 5086 thickness 1.6mm (g)	190	190	190	190	190	190
weight only K pure (g)	75	75	75	75	75	75
STF solutes (ml)	0	150	150	150	150	150
Additives (g)	0	50	50	50	50	50
PEG-400 (ml)	0	100	100	100	100	100
Ethyl alcohol used (ml)	100	100	0	100	100	100
Resin used (ml) (4:1)	100	100	100	100	100	100
Target weight measured (g)	332	378	386	390	398	434
Target thickness (mm)	8.1	9.7	9.5	10.8	10.6	11.8
Target areal density (g/cm^2)	1.5	1.7	1.7	1.7	1.8	1.9

Al = Aluminum 5086-32 alloy; K20 = 20 Layers of woven Kevlar fiber cloth (i.e. the figures following K indicate the number of fiber layers); K untreated = Kevlar containing no impregnated nano-fillers.

The comparative values of the weight, thickness, and areal density of various specimens developed for various hybrid laminates can be clearly observed in Fig. 5.1. Such variations can be attributed to variation in the nano-filler residue after the evaporation of PEG- 400 during the drying of the fibers, and the difference in resin absorption capability of treated and untreated Kevlar® fabric layers. For instance, targets with Kevlar® neat showed greater resin absorption than targets with Kevlar® containing impregnated nano-fillers. The samples treated with gamma alumina powder have the highest thickness, mass and areal density. The areal density was calculated by dividing the density with the surface area of the plate. An areal density of 1.5 g/cm^2 was obtained for specimens made of Kevlar® with no nano-filler impregnation, which is lower than that of those

plates made with Kevlar® impregnated with nano-fillers. The plates made with Kevlar® impregnated with gamma alumina nano-powders have the highest areal density (average of 1.9 g/cm^2). The laminates containing potato flour, aluminum powder, and silica carbide have the same average areal density of 1.7 g/cm^2 while those containing colloidal silica have an average areal density of 1.8 g/cm^2.

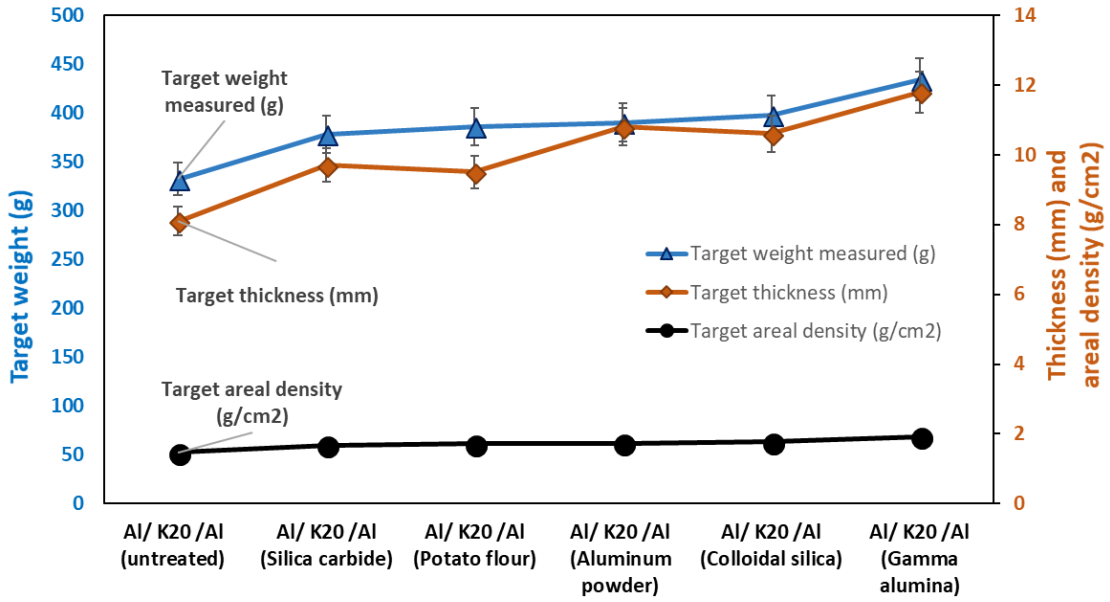

Fig. 5.1. Mass, thickness and areal density of the developed hybrid laminate as a function of the applied nano-filler.

The energy absorption by each produced hybrid plate was calculated in order to enable classification of the plates according to NIJ 0108.01 standard for ballistic resistant materials. With that, the calculated energy absorption for each material can be compared with the velocity and energy specifications of different low caliber weapons according to NATO standards [94].

5.5 Results and discussion

5.5.1 Effects of target configuration and filler addition on absorbed and residual energy

The results of previous studies have shown that the kinetic energy of a projectile is transformed into work and a fraction of the initial energy is absorbed in deforming the target. The absorbed energy by the target represents the loss in kinetic energy through elastic and plastic deformations while the residual kinetic energy is the projectile energy that remains after the ballistic impact [131]. The effects of the applied nano-fillers on the energy absorption capability of the hybrid

composite plates produced in this study are provided in Table 5.2. The average initial velocity of 871 m/s, with a standard deviation of 6.70 m/s, was recorded by the ballistic chronograph, which is comparable to the muzzle velocity of 869 m/s for the same ammunition as provided in NATO specifications. This average initial velocity was chosen to produce similar initial conditions for all of the targets.

Table 5.2. Ballistic impact data sheet for various laminate targets produced.

Targets	INITIAL velocity average (m/s)	INITIAL Energy average (J)	RESIDUAL Velocity Average (m/s)	RESIDUAL Energy Average (J)	Velocity absorbed (m/s)	Energy absorbed (J)	Energy absorbed (%)
Al/ K20 /Al (aluminum powder)	871	3687	785	2994	86	693	18.8%
Al/ K20 /Al (colloidal silica)	871	3687	787	3008	84	679	18.4%
Al/ K20 /Al (silicon carbide)	871	3687	788	3021	83	666	18.1%
Al/ K20 /Al (potato flour)	871	3687	803	3134	68	553	15.0%
Al/ K20 /Al (gamma alumina)	871	3687	804	3144	67	543	14.7%
Al/ K20 /Al (untreated)	871	3687	809	3180	62	507	13.7%

The residual and absorbed energy for targets containing different nano-fillers are graphically displayed in Fig. 5.2. Specimens containing Kevlar® fabric infiltrated with aluminum powder exhibit the highest energy absorption (693 J) which represents a 18.8% of the initial energy, followed by targets made of Kevlar® fabrics impregnated with colloidal silica (679 J) and silicon carbide (666 J) particles. The energy absorption of the laminates containing colloidal silica and silicon carbide particles are only 0.39% and 0.73% lower than that containing aluminum powder, respectively. The targets specimens containing impregnated potato flour and gamma alumina were able to absorb 553 J and 543 J, respectively. The lowest energy absorption of 507 J was determined for plates made of Kevlar® fabric with no nano-filler impregnation. These results suggest that deposition of nano-fillers on Kevlar® fabrics used in producing hybrid composite laminates improved the energy absorption capability of the laminates. Kostopoulos *et al.* [128] also reported that CNT inclusion in the matrix of CFRP composites increases their energy absorption capability and impact damage resistance.

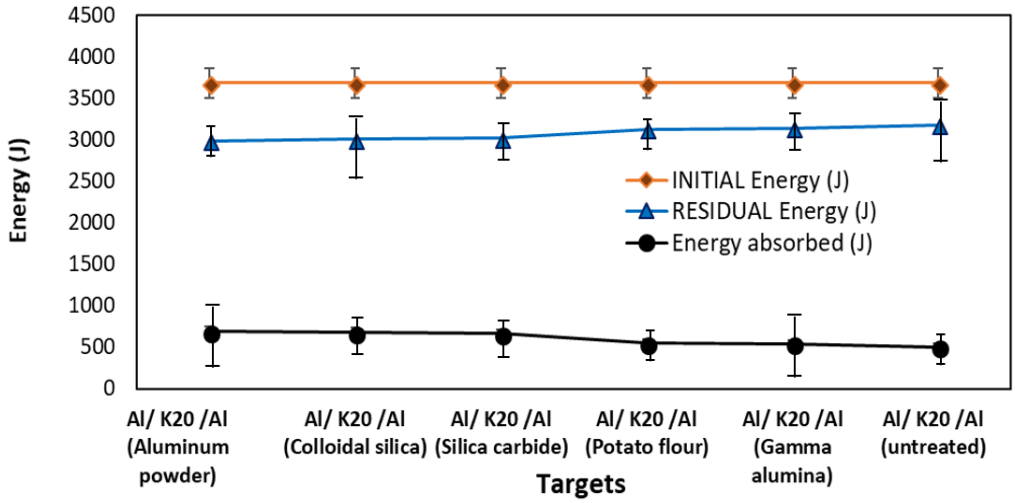

Fig. 5.2. Residual and dissipated energy during ballistic impact.

A comparative analysis of the correlation between the areal densities of the targets and their energy absorption during ballistic impact are presented in Fig. 5.3. Both the energy absorption and the areal density of targets containing Kevlar® fabric with no nano-filler addition are less than those of the other targets containing nano-fillers. On the other hand, specimens containing gamma alumina powder impregnation have low energy dissipation but the highest areal density of all targets. Targets with higher energy absorption (aluminum powder, silica carbide and colloidal silica) have a similar average areal density of 1.7 g/cm^2. A previous study by Y. S. Lee, *et al.* [63] also indicated that whereas impregnated fibers with STF had an areal density similar to that of Kevlar® with no STF impregnation, Kevlar® containing impregnated STF has reduced thickness and absorbed more impact energy. The impact energy absorption has been reported in other ballistic impact tests and stabbing experiment to increase by about 30 and 40% with STF impregnation in comparison with specimens made with Kevlar® neat, i.e. with no impregnation with STF or any other nano filler [61, 63, 111]. Avila *et al.* [126] also reported an improvement in the energy absorption capability of fibre reinforced epoxy composite by the addition of nanoparticles of clay and graphene. The addition of the nanoparticles was observed to strengthen fiber/matrix bonding and they acted as barrier to crack propagation leading to increase in penetration resistance.

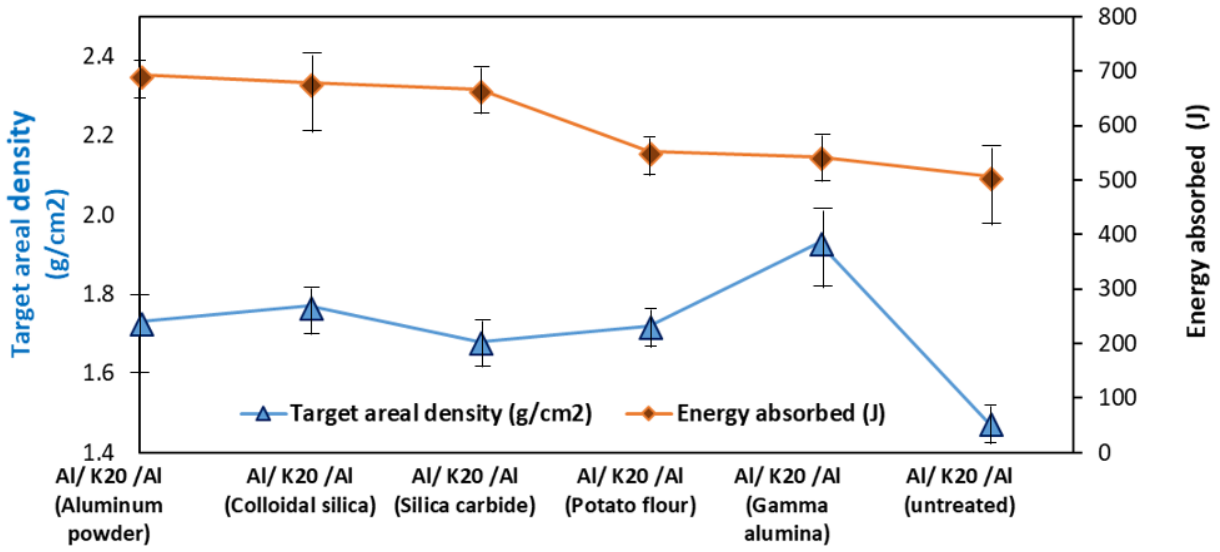

Fig. 5.3. Relationship between the absorbed energy and areal density of targets.

In the current investigation, the thickening fluids formed by nano-fillers and PEG-400 coated the Kevlar® fibers and produced a nano-filler sealing on the fiber layers in the hybrid laminate structure. The nano-filler impregnation enhanced the amount of energy absorbed during the projectile penetration. Therefore, treatments of Kevlar® fabrics with thickening fluids containing nano-fillers enhanced the ballistic impact resistance of the fabrics. As a result, failure resistance and the energy absorption are greater. This suggests that deposition of nano-fillers coating on Kevlar® fabrics using PEG-400 offers a promising method for strengthening the interfacial bonding between the matrix and fibers in hybrid composite laminates.

5.5.2 Energy absorbed by the targets vs the initial impact energy of projectiles fired by different light weapons

The initial velocity and energy specifications of nine low caliber weapons according to NATO standard specifications [95] are presented in Table 5.3. The initial energy of 3687 J used in this study is higher than the energy specifications shown in this table. Thus, the results obtained in this experiment can be compared with the data provided in Table 5.3.

Table 5.3. Velocity and energy specifications of low caliber weapons [94].

Low caliber weapons	Cartridge (mm)	Cartridge weight (g)	Bullet weight (g)	Velocity (m/s)	Energy (J)
270 Winchester rifle	7.06	150	9.72	869	3667
AK-47 rifle	7.69 * 39	24	8	715	2045
M14 rifle	7.62 * 51	25.4	9.33	838	3275
FAL rifle	7.62	24	9.5	823	3217
M16 rifle	5.56 * 45	12.31	4.02	991	1974
HK rifle	5.56		4.1	936	1796
AUG rifle	5.56		4	940	1767
Beretta M9 pistol	9 * 19	8.1	4.1	600	756
HK pistol	9	7.45	4.5	390	570
Parabellum pistol	9	9.5	5.2	460	561

Reference: NATO EPVAT testing, Quick LOAD, SAAMI, standard

The horizontal lines in the Fig. 5.4 represent the absorbed energy determined for each hybrid laminate tested. The initial impact energy of ten low caliber weapons is presented in vertical bars. The results indicate that hybrid composite laminates built with the configuration Al/K20/Al and Kevlar® that is untreated with nano-fillers, and those containing Kevlar® impregnated with potato flour or gamma alumina powder cannot resist the ballistic impacts from those weapons. The reason for that is that the energy they can absorb are below the initial energy produced by lowest calibre HK and Parabellum pistols (9mm) which are 570 J and 561 J, respectively. The configuration Al/K20/AL containing impregnated aluminum powder, colloidal silica, and silica carbide are able to absorb impact energy ranging from 666 J to 693 J. This means that they can resist bullets from pistol HK and Parabellum 9mm, but they are not able to resist shots from pistols Beretta M9, whose initial impact energy is 756 J; and also, from rifles caliber 5.56 mm and higher caliber weapons.

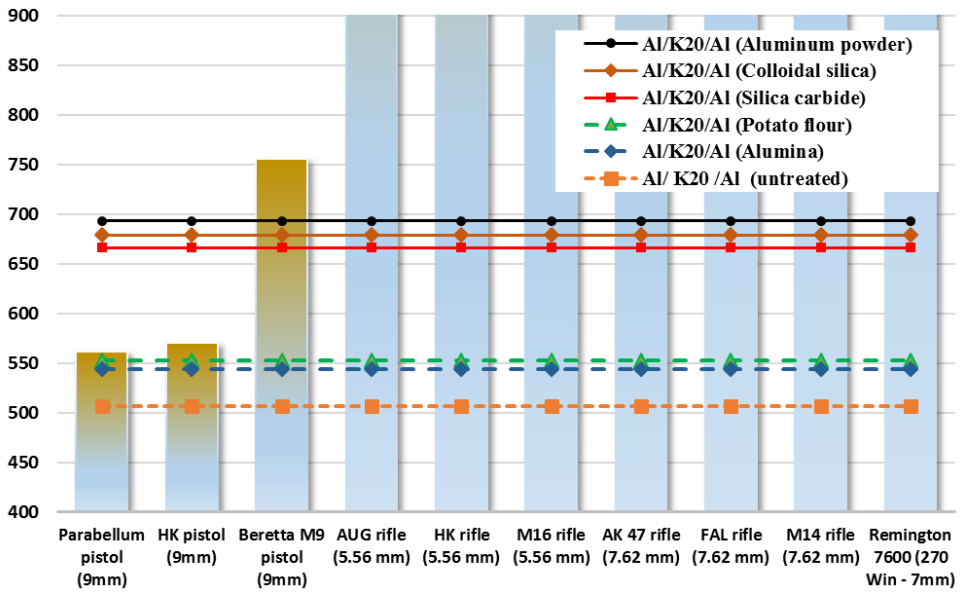

Fig. 5.4. Absorbed impact energy by targets vs initial energy of different low caliber weapons.

5.5.3 Analysis of deformation and penetration behavior of the targets

The projectile penetration data for the various hybrid laminates during the ballistic impact testing are presented in Table 5.4. The average diameter of the crater entry on the front face, and the average diameter of the crater exit on the back face were measured.

Table 5.4 Penetration morphology in the laminate after ballistic impact

Targets	Energy absorbed (J)	Initial target thickness (mm)	Target areal density (g/cm^2)	Entry crater diameter (mm)	Exit crater diameter (mm)	Penetration depth (mm)
Al/ K20 /Al (Al powder)	693	10.8	1.7	9.4	13.5	25.2
Al/ K20 /Al (Colloidal silica)	679	10.6	1.8	8.8	15.8	24.2
Al/ K20 /Al (Silicon carbide)	666	9.7	1.7	9.4	15.2	23.7
Al/ K20 /Al (Potato flour)	553	9.5	1.7	9.0	15.0	22.3
Al/ K20 /Al (Gamma alumina)	543	11.8	1.9	9.1	14.5	26.1
Al/ K20 /Al (untreated)	507	8.1	1.5	9.1	14.9	21.1

The total depth of penetration (Fig. 5.5) on the transverse section of each specimen was measured as well. Figure 5.6 shows the morphology of penetration channel at the entry and exit sides of the targets that were produced by the projectile (diameter 7.06 mm) ogive (spitzer ogive shape). The

diameter of the crater (perforation) at the entry side ranged between 8.8 mm to 9.4 mm for all targets. The exit diameter of the crater on the back side ranged between 13.5 mm and 15.8 mm, forming an open petal after complete projectile penetration. The petal shaped appearance depends on several factors such as the target configurations, thickness, nano-filler impregnation and type of nano-filler used and the energy asorption capability of the aluminum and Kevlar® fabric components.

Fig. 5.5. Total depth penetration channel on the transverse section of the targets.

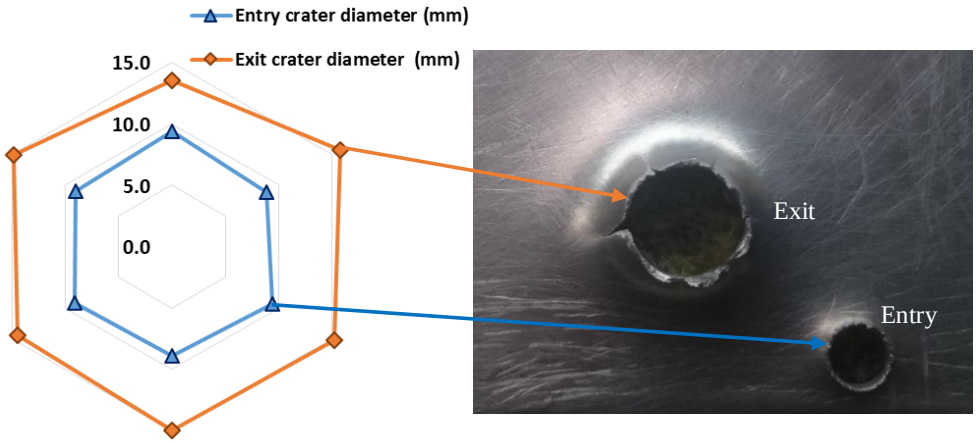

Fig. 5.6. Morphology of penetration channel at the entry and exit sides of the targets.

The morphology of the crater at the entry and exit side can be more clearly seen in Fig. 5.7. Similar morphology was observed in the craters of GLARE specimens made of 2024-T3 aluminum layers, E-glass fibers and epoxy resin during ballistic impact testing; a petal shape was observed on the back aluminum layers. Although as the impact energy were increased, larger petals were observed, but behavior was determined to be similar for all targets [132].

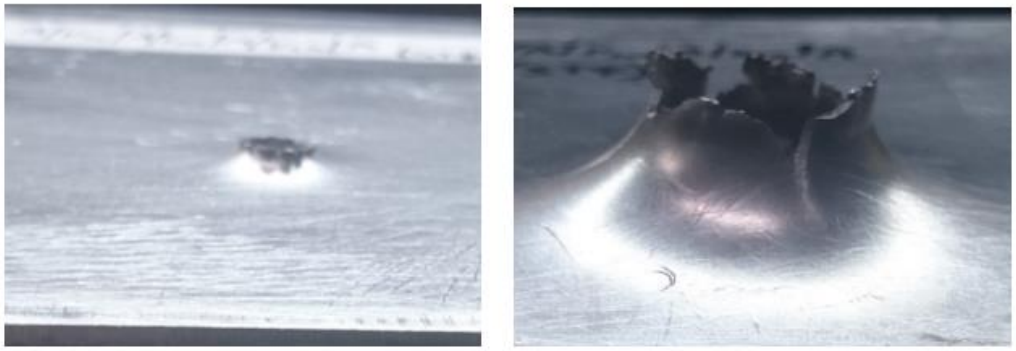

(a) front (b) rear

Fig. 5.7. Rear and front faces of targets after ballistic impacts.

The total depth of penetration depends basically on two factors: the thickness and the configuration of the targets. The penetration depths on the transverse sections of hybrid laminate targets produced in this study are provided in Table 5.4. They ranged between 21.1 mm and 26.1 mm. In addition, it can be concluded that targets made of Kevlar® neat, which have the lowest thickness and low energy absorption capacity, have the lowest penetration depth of 21.1 mm. Thus, this implies that these targets have less resistance to the projectile penetration. The targets containing Kevlar® fabric infiltrated with potato flour have penetration depth of 22.3 mm. Laminates with better ballistic performance in terms of penetration depth are those targets containing impregnated aluminum powder, colloidal silica, and silica carbide powder. They showed penetrations depths of between 23 and 25 mm. Targets with gamma alumina exhibited the highest penetration depth of 26.1 mm, but a low energy absorption. This may also be due to the fact that they have the highest thickness compared to the other laminates.

5.5.4 Targets' thickness and weight influence on ballistic response

Thickness is an important factor in the energy absorption capability of targets during ballistic impact. The thickness of a target made of hybrid laminates usually depends on the configuration and the number of layers of each component of the laminate. The thickness of the hybrid laminate targets produced in this study are provided in the Table 5.1. Laminates containing 20 layers of untreated Kevlar® fabric (i.e. no infiltration with nano-filler) have an average thickness of 8.1 mm in comparison with those made of Kevlar® treated with nano-fillers, whose thickness range between 9.5 and 11.8 mm. Figures 5.8 and 5.9 provide the relationship between weight and thickness in relation to the energy absorbed by the laminates, respectively. Weight and thickness

are higher for the targets treated with gamma alumina powder than other laminates as can be observed in the graphs. Despite that, they are not capable of absorbing more impact energy than the targets containing other nano-powders. Targets containing impregnated silica carbide exhibited a top ballistic performance because their average energy absorption of 666 J this was obtained with the lowest density (weight 378 g and thickness 9.7 mm) in comparison to targets containing other nano fillers.

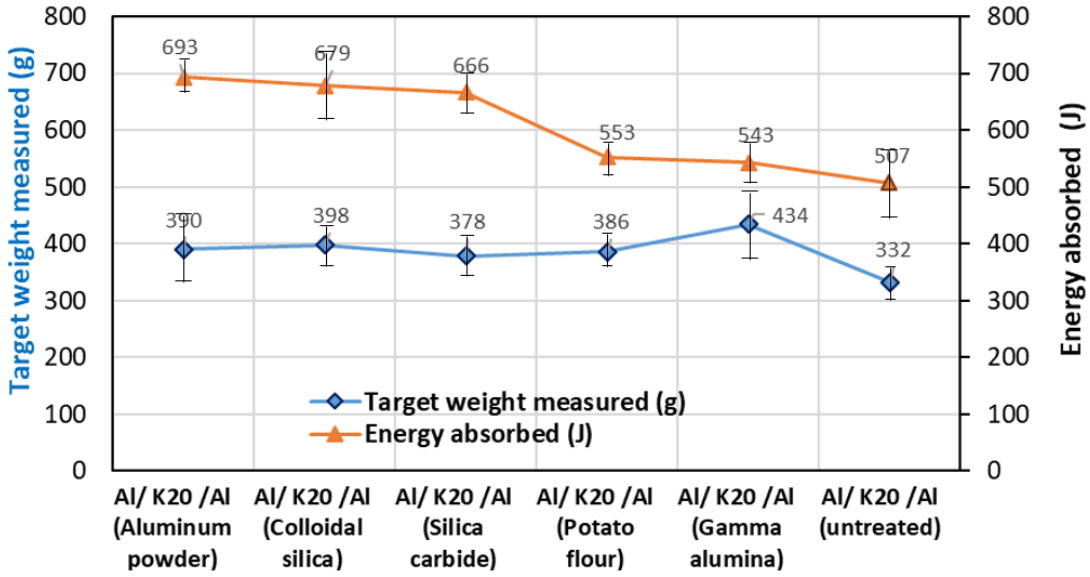

Fig. 5.8. Relation between the absorbed energy and target weight.

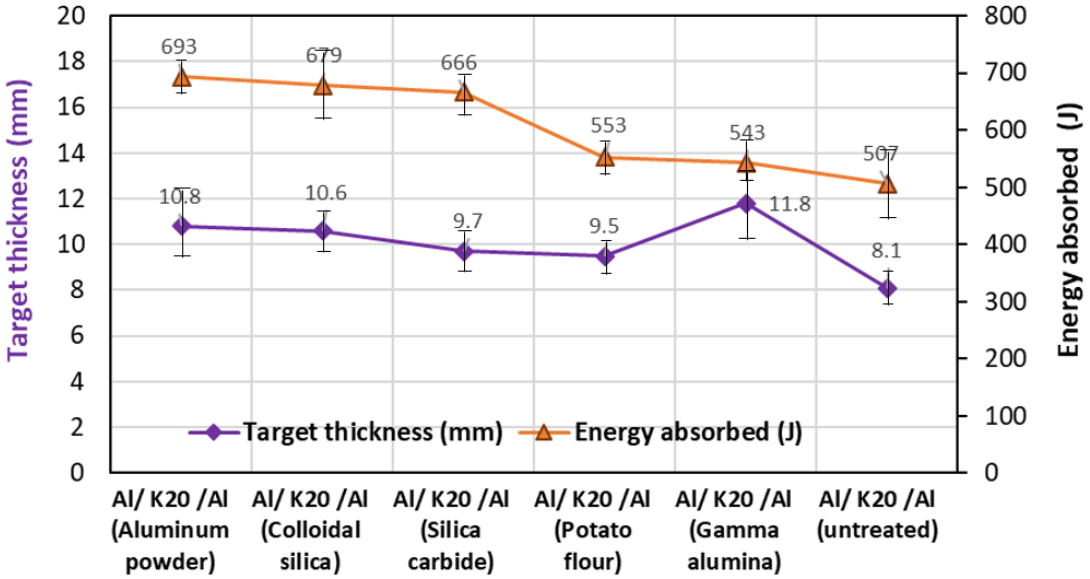

Fig. 5.9. Relation between the absorbed energy and targets' thickness.

5.5.5 Microstructural analysis and mechanisms of energy absorption

Figure 5.10 shows the results of the scanning electron microscopic (SEM) evaluation of the impregnation of the Kevlar® fabrics with nano-powders. Figure 5.10a shows Kevlar® fabric neat (with no nano-powder impregnation) indicating void spaces between fibers bundles. When joined with other layers of Kevlar® fabrics by using epoxy resin, the loops were filled with only resin. This suggests that the hybrid laminate structure containing Kevlar® neat can be less effective in resisting ballistic impact damage. Targets built with Kevlar® containing impregnated nano-fillers show fewer voids between fibers bundles and between fiber layers. The properties of the nano-fillers, the surface morphology of the Kevlar® fibers, and the fiber size are factors that have significant effects on the impregnation state of the nano-powders. The nano-powder filled the gaps existing between Kevlar® fiber fabrics and provide extra reinforcement for the hybrid composite laminates. This also facilitated stronger bonding of the Kevlar® fibre layers leading to strong structure with improved energy absorption capabilities during ballistic impact. Nano-fillers created a sealing coating on the Kevlar® surface as shown in Fig. 5.10.

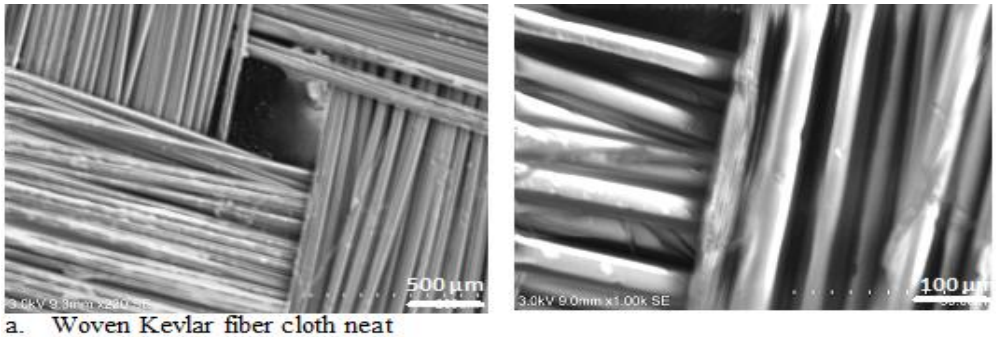

a. Woven Kevlar fiber cloth neat

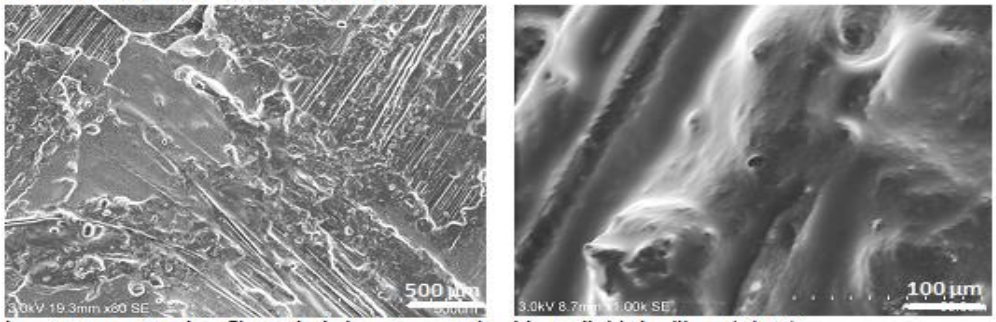

b. Woven Kevlar fiber cloth impregnated with Colloidal silica (SiO_2)

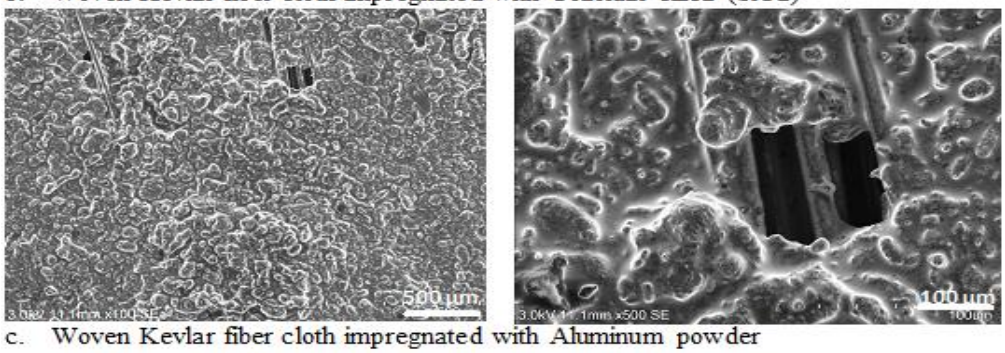

c. Woven Kevlar fiber cloth impregnated with Aluminum powder

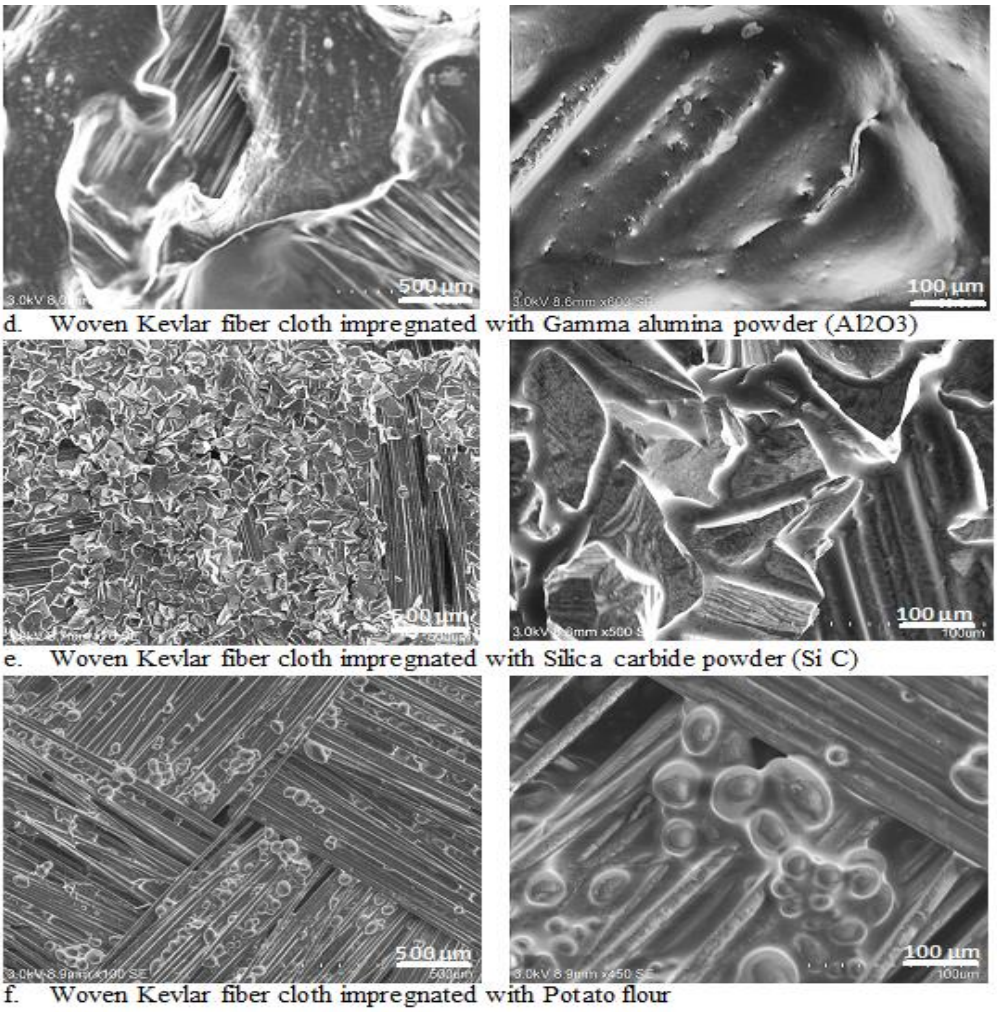

Fig. 5.10. SEM image of Kevlar® fibers impregnated with nano-powders.

Figure 5.10b shows a complete coating of the surface of the Kevlar® fiber with nano-powders of colloidal silica (SiO_2). The hard oxide particles suspended in a liquid polymer (PEG-400) behave like non-Newtonian fluid, whose viscosity increases when shear stress is applied. The homogeneity of distribution of the silica nanoparticles on the fibers is highly dependent on the size of these particles. As a result, the concentrations of the solutes (SiO_2) and solvents (PEG-400) have a direct influence on the efficiency of the impregnation of the fibers with the nano-powders and this was confirmed in an earlier study by Rao *et al.* [108]. SEM micrographs of Kevlar® impregnated with aluminum powder mixed with PEG-400 showing coated fiber with improved bonding capability with other fiber layer or aluminum plate are presented in Fig. 5.10c. Aluminum powders in the micrographs show good adherence to the fibers and sealed up the voids between fibre bundles. This may account for the highest energy absorption capacity achieved in hybrid

composite laminates infiltrated with aluminum powder. SEM micrographs of the coating of gamma alumina (Al_2O_3) powder on the Kevlar® fabric (Fig. 5.10d) indicates a partial coating on the Kevlar® fabric surface. Gama alumina is an excellent filler for plastics when mixed with resins. However, impregnation of Kevlar® fabric with alumina mixed with PEG did not produce a good adherence of the nanoparticle to the fibers, thereby contributing to the observed low ability of the laminates containing alumina nanoparticles to withstand high velocity impacts.

The coating of silica carbide particles (SiC) on the Kevlar® fabrics is continuous as in the case of aluminum powder (Fig. 5.10e). Voids within fibre bundles were completely sealed with the mixture of the particles and the solvent (PEG-400) and bonding of Kevlar® layers was enhanced leading to a good energy absorption capability. The micrographs in Fig. 5.10f suggests weak bonding between the potato flour particles and the Kevlar® fabric. Thus, a non-continuous coating of the nanoparticles on Kevlar® fabrics was obtained. The low adherence of the particle to the Kevlar® could be due to dissolution of the potato powder in the PEG-400 during mixing. Thus, the potato flour could not effectively serve as filler. Hence the poor ballistic impact resistance of hybrid targets containing potato flour.

SEM micrographs taken on the longitudinal section of the perforations in the laminates provide information on the energy absorption, deformation of various components of the laminates and the sequence of impact damage (Fig. 5.11). The deformation of the target is influenced by the projectile shape (nose), impact velocity as well as the physical and mechanical properties of the hybrid composite laminate. A terminal ballistic analysis was performed to analyze the behavior of the projectiles upon impacting the various laminates. This analysis was done on the longitudinal section of the penetration channels produced by projectiles after ballistic impacts (Fig. 5.11). The SEM micrographs provide indication of the mechanism of failure and fracture of the laminates as they were perforated by the sharp-nosed projectile. The damage in various components of the laminates was inspected and evaluated from the SEM micrographs. The damage sequence involved an initial indentation of the face of the frontal aluminum plate produced by a localized stress in the initial region of contact. These created a small puncture due to pressure exerted by the projectile. In the initial phase of penetration, a ductile crater enlargement can be observed (Fig 5.11a). Horizontal striations are produced by lands and groves that come from the rifling process of the ogive. Figure 13a shows the impression marks of the bullet as it travels through the barrel,

suggesting rotation of the bullet in the barrel. Also, vertical striations are shown in the Fig 5.11a that can be traced to the initial reaming of the barrel.

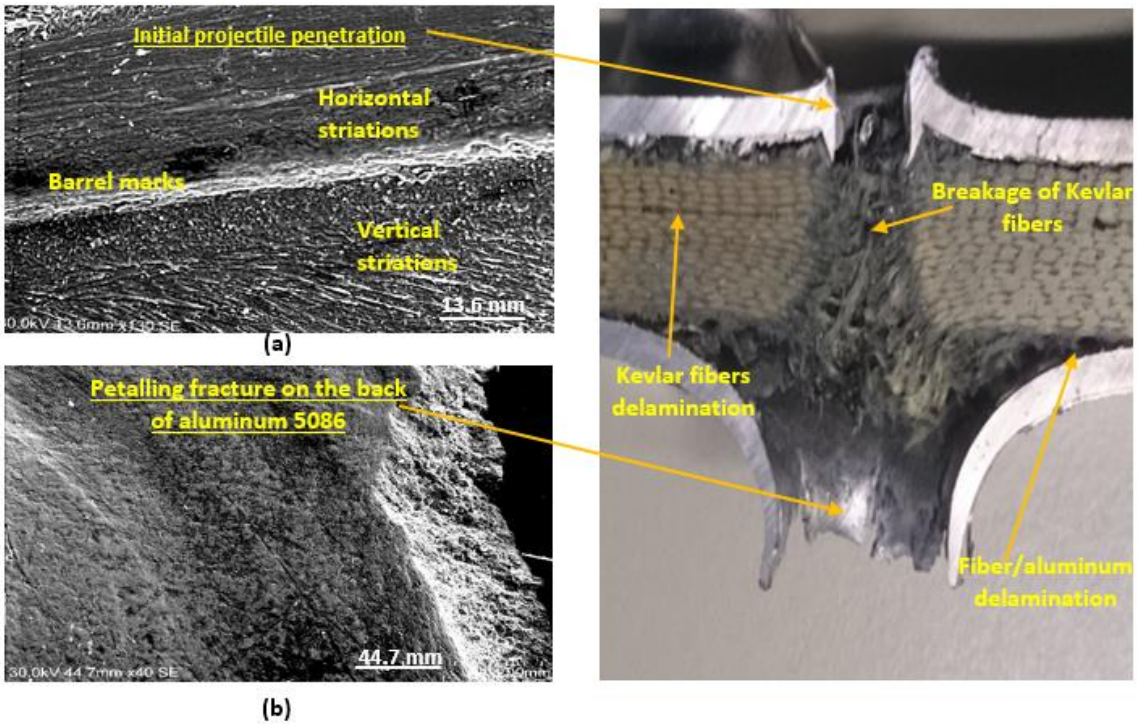

Fig. 5.11. Fracture surface along perforation in the target.

On piercing the frontal aluminum plate, the projectile continued the perforation of the plates with breakage of fibers layers adjacent to the frontal aluminum plate. The fibers are broken by compression force exerted by the projectile, which created an enlarged ductile crater as a result of shear plugging, and tensile fracture of the first fiber yarn. As a result, Kevlar® fibers are broken and expelled due to projectile penetration. The nature of the tensile failure of the Kevlar® fiber failure differed from one plate to the other depending on the type of nanoparticle infiltrated into the Kevlar® fabric. For instance, the untreated Kevlar® fibers (no nano-filler) suffered a high yarn pullout, debonding, plastic deformation and fracture while the fragmented fibres were expelled from the channel during the penetration. On the other hand, the amount of the fiber pull-out and delamination in the targets containing Kevlar® infiltrated with nano-fillers was less due to better fiber/Kevlar® adhesion. As a result, laminates containing nano-fillers exhibited more elongation and better resistance to projectile penetration.

Delamination between Kevlar® layers, and between aluminum plates and Kevlar® layers can be observed in Fig. 5.11. Such delamination is an effect of the elastic wave propagation and force distribution of the target plates where the fibers were working as reinforcement. Shear forces increased and a dynamic friction between layers also increases as a result of the projectile penetration. The last layers participate in this process and the deformation increased to absorb the impact energy at the maximum level. Figure 5.11b shows the back of aluminum plates after a complete projectile penetration through the hybrid laminates. Radial cracking formed by the projectile penetration leading to the formation of a sheeting of open petals. The radial fracture produces wrinkles in each petal, which end taking a form of a highly deformed tip. This shape depends on the behavior in terms of energy absorption. The more the energy absorbed by the target, the greater is the deformation produced (Fig 5.7b) on the rear face of the targets. The damage mode observed in the hybrid laminates produced in this study is similar to that observed in carbon fiber reinforced plastic in previous studies [113]. Yaghoubi and Liaw also observed similar pattern of delamination during ballistic impact study on fiber metal laminates (FMLs) plates made of aluminum plates and glass fiber fabrics [114]. Ballistic impact testing of Aluminum plates coated with polyurea also exhibited similar deformation mode showing petalling when subjected to ballistic impact [133].

5.6 Conclusions

The effects of micro or nano-fillers additions SiC, aluminum, alumina, potato flour and colloidal silica on the ballistic performance of hybrid composite laminates made of woven Kevlar® fabrics, epoxy resin and AA 5086 aluminium alloy sheet were investigated. The laminates consist of 20 layers of fiber cloth sandwiched between two aluminium alloy sheets. The result of these studies indicates that deposition of these fillers on the surface using PEG-400 offer a very promising method for depositing micro and nano fillers on Kevlar® surface to enhance ballistic impact performance of the hybrid laminate. The fiber/fiber and fiber/metal bonds were strengthened by introduction of fillers into the hybrid composite laminates. Microstructural analysis indicated that the laminates, which contain nano-fillers that are able to effectively coat fiber fabric surface and effectively seal the voids between fiber bundles, exhibits a greater energy absorption capability. Whereas aluminum powders completely sealed up the voids leading to targets with the highest capacity for ballistic impact energy absorption, the least energy absorption capacity was observed

in laminates with alumina addition which contain unfilled voids within the fiber bundles. Although the weight and thickness of the laminates vary slightly depending on the filler used, the total energy absorption and energy absorption per unit mass is highest for laminates containing Al, SiC and colloidal silica powders. Therefore, introduction of these three nanofillers to fiber surface resulted in hybrid laminates that can adequately protect against HK pistol 9 mm and Parabellum pistol 9 mm. These levels of protection can not be achieved in laminates with no nano-filler addition and those containing alumina or potato powder.

Chapter 6: The Effects of Micro- and Nano-fillers' Additions on the Dynamic Impact Response of Hybrid Composite Armors Made of HDPE Reinforced with Kevlar Short Fiber

6.1 Overview

In this chapter, another different approach is experimented, the matrix component was changed to a thermoplastic matrix HDPE. The hybridization of this matrix reinforced by the combination of short fibers and micro- and nano-fillers to produce hybrid composite armors was investigated. The developed targets were tested under dynamic and ballistic impact, and the corresponding findings are reported in this chapter. This chapter has been published as manuscript #3 in the Journal paper:

E.E. Haro, A.G. Odeshi, J.A. Szpunar, "The effects of micro- and nano-fillers' additions on the dynamic impact response of hybrid composite armors made of HDPE reinforced with Kevlar short fibers", *Polymer-Plastic Technology and Engineering*., vol. 57, no. 7, pp. 609-624, 2018 [87].

The contributions of the PhD candidate to this manuscript are: 1) experimental design, 2) preparing and processing all the samples; 3) physical, microstructural and mechanical characterization of the composites and 4) development of the manuscript for publication. The manuscript was reviewed by my supervisors before it was submitted for publication in this journal. To avoid repetition of information provided in Chapter 3, selection of the materials of composite fabrication, target preparation and composite characterization are removed from this chapter. The references of the submitted manuscript are also removed and listed at the end of this thesis. The copyright permission of use this paper is attached in the Appendix.

6.2 Abstract

Hybrid composite armors consisting of Kevlar® short fibers reinforced high density polyethylene (HDPE) were prepared and the effects of the addition of micro and nano-fillers on the dynamic impact response and the energy absorption capacity under ballistic impact were investigated. Five groups of specimens were manufactured using compression molding of pellets containing mixtures of HDPE and the reinforcing materials. The first group consist of HDPE reinforced with 10 wt.% Kevlar® pulp (KN-1). The rest are hybrid composites created by the addition of 20 wt.% of micro and nano-fillers. The natural micro-fillers used are particles of chonta palm wood (KN-2) and potato flour (KN-3). The synthetic nanofillers are colloidal silica (KN-4) and gamma alumina (KN-5). Microstructure (SEM) and compositional (EDS) analysis of the hybrid composites were carried out to evaluate matrix-reinforcements-interface. The fabricated composites plates were subjected to high velocity impact using split Hopkinson pressure bar (SHPB) system and ballistic impact, according to NIJ standard–0101.06 for ballistic resistance. Significant stiffness improvements of up to 43.5% were achieved as a result of the addition of synthetic nano-particles to Kevlar® fiber reinforced HDPE. XRD analysis revealed that the crystalline structure of the Kevlar® reinforced HDPE is unaffected by addition of the nano-particles as fillers. However, the intensity of the crystalline peaks decreased depending on the type of the added fillers. The results of dynamic impact test using SHPB revealed improved impact resistance by addition of synthetic nanofillers (silica and alumina). The results of the ballistic impact test showed the gamma alumina nano-particles (KN-5) exhibited the highest energy absorption capability. The results of these investigations indicate that hybridization of Kevlar® short fibers reinforced HDPE by micro and nano-fillers addition enhances the stiffness, impact resistance and ballistic energy absorption capability of the composites.

Keywords: Hybrid composites; micro- and nano-fillers; dynamic shocking loading, ballistic impacts; energy absorption.

6.3 Introduction

Hybrid materials are composites that consist of two or more monolithic materials at nanometer level, which are configured in such a way that the properties of individual component can be superimposed to meet the targeted service requirements [34]. The enhancement in the properties

and the performance of hybrid composites by addition of nanoparticle reinforcements depends on factors such as the bonding and size of individual components as well as the strength of the interface between the reinforcements and matrix [51]. In hybrid composites, nanoparticles in low concentrations can improve the strength of the interface between fibrous reinforcements and the matrix. The interfacial strengthening effect leads to improved mechanical properties such as strength and stiffness without compromising the density or the ease of the manufacture [117-119]. In a review article, Saba *et al.* [51] outlined the importance of using suitable and proper filler additions to obtain an efficient interaction between matrix and reinforcements leading to enhancement the performance of the resulting hybrid composite materials. This has led to increase application of hybrid composites in wide fields, which include construction, automotive, military, aerospace, and packaging industries. For example, the mixture of synthetic glass fibers and natural oil palm fruit fibers as reinforcements for HDPE, reduces the use of synthetic fibers while at the same time retaining similar mechanical properties of glass fiber reinforced HDPE [134].

Different types of micro and nano-fillers have been used to improve thermal, mechanical and other properties fiber reinforced plastic by increasing the interfacial adhesion between the matrix and fibrous reinforcements [135, 136]. The use of glass and carbon fibers as reinforcement for polymers have been widely investigated. However, Kevlar® fibers have proved to be a better choice of reinforcement in development of polymer matrix composites with improved toughness and damage tolerance compared to glass and carbon fibers [137]. A study by Li [138] indicated an increase in the tensile strength and wear resistance of thermoplastic polyimide with an addition of 15 vol % Kevlar® pulp as reinforcement. In another study, it was reported that the pre-treatment of Kevlar® pulp with a reactive compatibilizer (anhydride-grafted-polypropylene (MA-g-PP)) improved the Young modulus, tensile strength and the percentage elongation to failure of the short Kevlar® fiber reinforced Santoprene composites [139]. A 45 % increase in tensile strength was achieved by the use of Kevlar® short fiber to reinforce maleic anhydride grafted poly-styrene-*b*-(ethylene-*co*-butylene)-*b*-styrene (MA-g-SEBS). The maleic anhydride produced a self-reinforcing effect that enhanced the interfacial adhesion between the fiber and the matrix [140].

Although fiber reinforcement enhances the mechanical properties of polymers, nanofillers are usually added to fiber reinforced plastic to improve the interfacial contact between the fiber and the matrix. This often leads to a further increase in strength and stiffness of the fiber reinforced

plastic. Based on their origin, micro and nano-fillers are broadly classified into synthetic (inorganic) and natural (organic) fillers. Inorganic fillers commonly used include glass, silica (SiO_2), titanium dioxide (TiO_2), calcium carbonate ($CaCO_3$), or polyhedral oligomeric silsesquioxane (POSS). Organic fillers include coir micro-fillers, hardwood powders, carbon black and cellulosic nano-fillers [51]. A study on the hybridization of oil palm empty fruit bunch (EBF) microfillers in a glass fiber reinforced recycled polypropylene indicated that the composite containing 70 % EBF and 30 % glass fiber show superior behaviour compared with those containing no filler [134]. In a similar study, Valente *et al.* [141] reported enhanced properties of hybrid composites consisting of wood particles, recycled glass fibers and thermoplastic matrices. Fu *et al.* [83-86] also developed and investigated the properties of hybrid composites consisting of varieties of particle/short-fiber/polymer and reported improvements in strength, stiffness, fracture and impact resistance as a result of particles addition when compared to the polymer reinforced with only short fibers.

Although, there are several studies on hybridization of thermoplastic or thermosetting polymer matrices reinforced with combination of fiber and particulate reinforcements to produce hybrid composites with improved mechanical properties, information on their dynamic impact response and energy absorption behavior are limited. Therefore, the performance evaluation of hybrid materials made from addition of different types of micro- and nano-fillers to Kevlar® short fibers reinforced HDPE under dynamic and ballistic impact load was carried out. The effects of filler addition on the mechanical properties, water absorption, degree of crystallinity, impact resistance and energy absorption behavior of these specimens have been determined and reported in this paper.

6.4 Results and Discussions

6.4.1 Target configuration

SEM and EDS images showing microstructural morphology and the interphase between components of the hybrid composites developed are presented in Fig. 6.1. A uniform distribution of Kevlar® short fibers can be observed in all the samples. Organic micro-particles (chonta palm and potato flour) are very distinct in samples KN-2 and KN-3 (Fig. 6.1b, c). The interphase between the components can be observed to be related to their particle size and form of fillers, and

the extent of bonding between Kevlar® short fibers and the HDPE. Due to poor contrast, the synthetic nano-fillers in the samples KN-4 and KN-5 could not be imaged properly using SEM. Therefore, EDS analysis was performed to determine the distribution and intensity of the colloidal silica and gamma alumina in these samples. The uniform distribution of the nano-particles and Kevlar® pulp within the HDPE matrix can be observed in Figs. 6.1d and 6.1e.

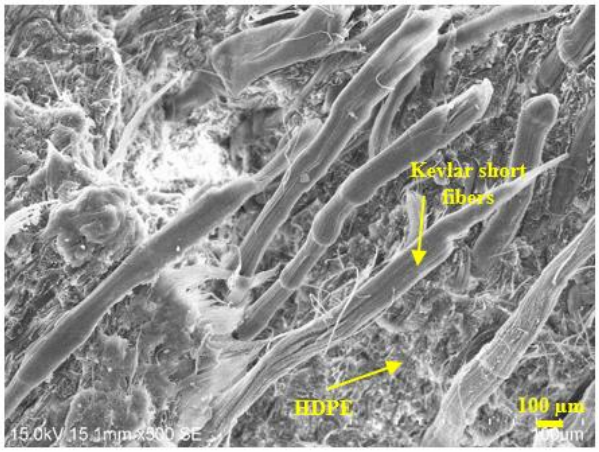

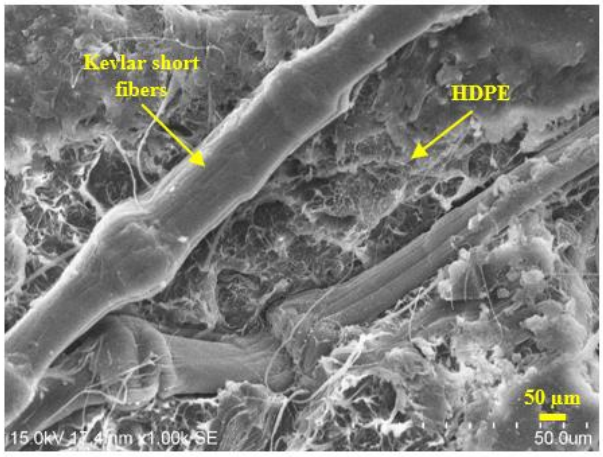

a. KN-1

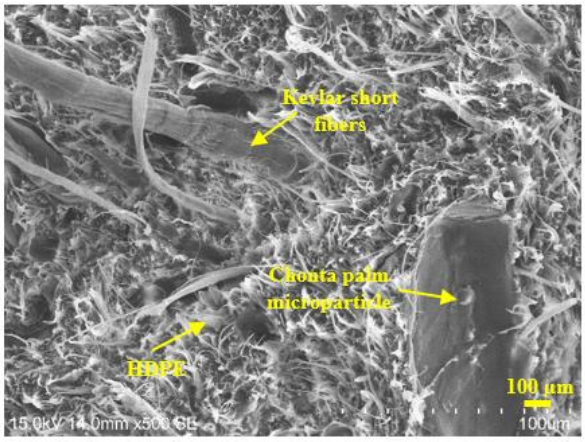

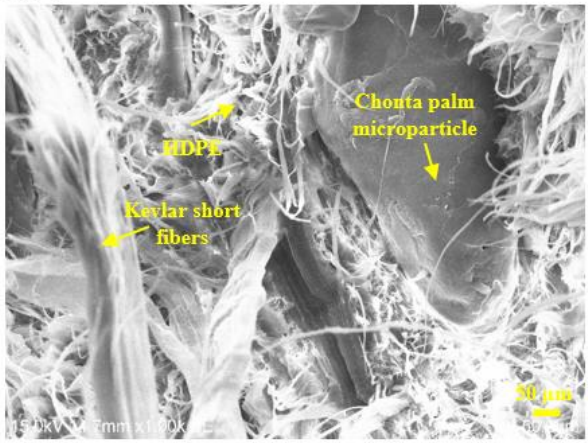

b. KN-2

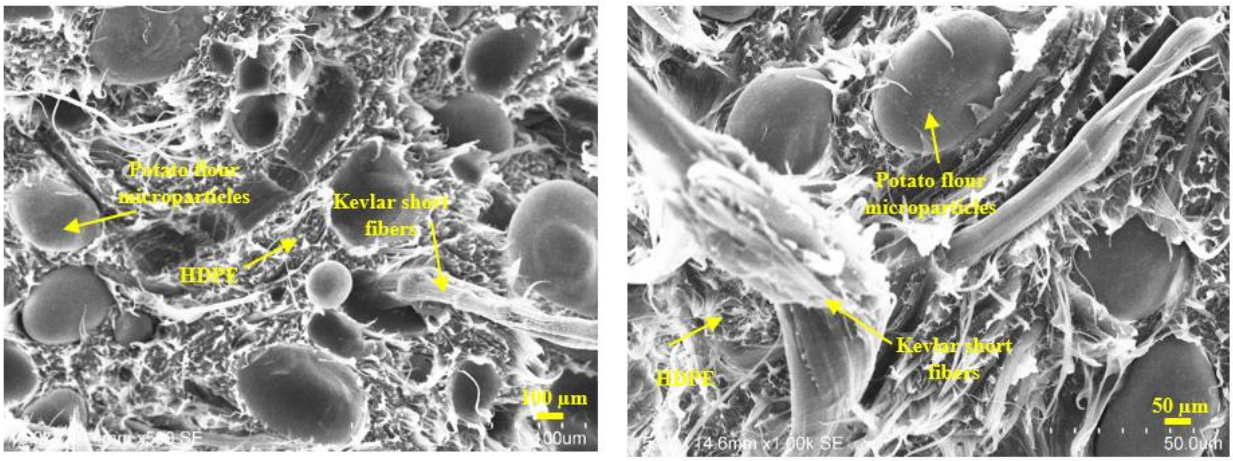

c. KN-3

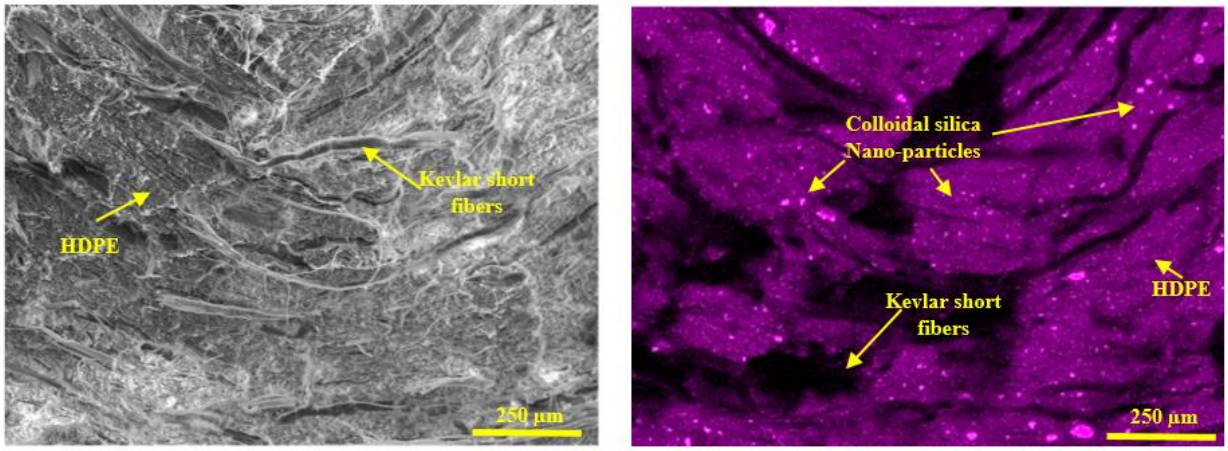

d. KN-4 (SiO_2) - EDS Analysis

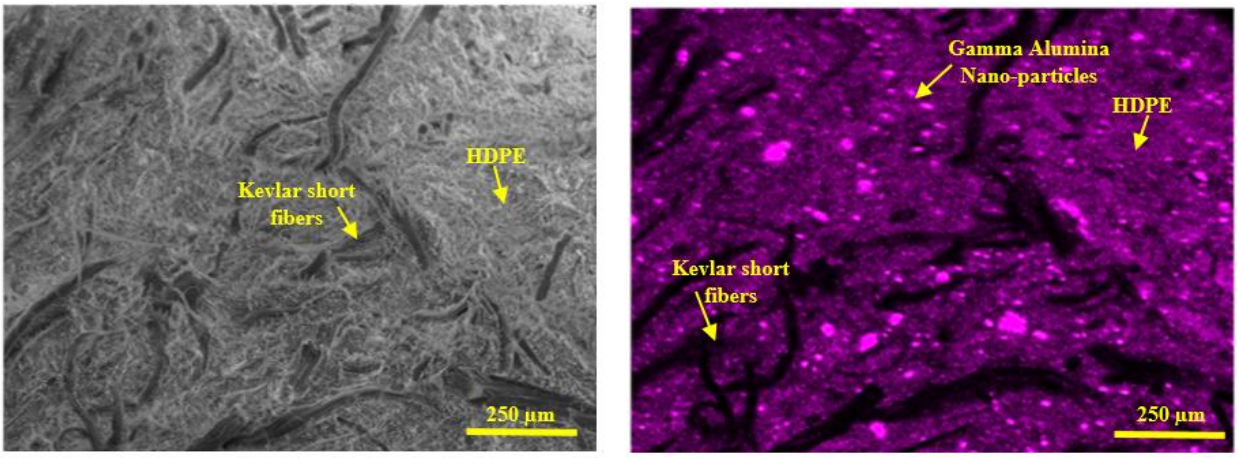

e. KN-5 (Al2O3) - EDS Analysis

Fig. 6.1. SEM and EDS images showing the microstructure and phase distribution in the developed hybrid composites.

The physical properties of the composite plates developed in this study are presented in Table 6.1. The slight variations in the density measurements of the various hybrid composites are mainly due to the differences in the density of the applied fillers.

Table 6.1. Experimental data sheet showing composition, configuration and physical properties of hybrid composites.

Targets configuration	KN-1	KN-2	KN-3	KN-4	KN-5
Kevlar pulp (wt.%)	10%	10%	10%	10%	10%
HDPE 2990 (wt.%)	90%	70%	70%	70%	70%
Chonta palm wood micro-particles (wt.%)		20%			
Potato flour (wt.%)			20%		
Colloidal Silica (SiO_2) (wt.%)				20%	
Gamma Alumina (Al_2O_3) (wt.%)					20%
Target weight average (g)	194.4±1.3	202.0±0.7	197.1±0.6	205.7±0.5	204.9±0.3
Target thickness average (mm)	5.5±0.1	4.8±0.2	5.3±0.2	4.7±0.3	4.8±0.2
Target areal density (g/cm^2)	0.49	0.51	0.49	0.51	0.51
Target density (g/cm^3)	0.88	1.05	0.94	1.09	1.07

Nomenclature:

- KN-1 = HDPE containing (10 wt.%) Kevlar pulp
- KN-2 = HDPE containing (10 wt.%) Kevlar pulp and (20 wt.%) Chonta palm micro-particles
- KN-3 = HDPE containing (10 wt.%) Kevlar pulp and (20 wt.%) Potato flour micro-particles
- KN-4 = HDPE containing (10 wt.%) Kevlar pulp and (20 wt.%) Colloidal Silica (SiO_2) nanoparticles
- KN-5 = HDPE containing (10wt.%) Kevlar pulp and (20 wt.%) Gamma Alumina (Al_2O_3) nanoparticles

The results of water absorption test are presented in Fig. 6.2. The amount of water absorbed by the composite test specimens was determined to be less than 0.02 % for samples containing Kevlar® pulp reinforcements (KN-1) and those containing potato flour (KN-3) or gamma alumina particles (KN-5) after being soaked for 2 and 24 hours. This implies water absorption saturation was achieved after 2 hours of immersion, suggesting stability against further water infiltration. KN-4 samples containing Kevlar® pulp and silica particles absorbed 0.01 % water after 2 hours and 0.04 % water after 24 hours' exposure time. Samples KN-2 with chonta palm wood micro-fillers exhibited highest values of water absorption in comparison with the other samples. Those samples absorbed 0.03 % water after 2 hours and 0.05 % water after 24 hours. This is mainly due to the cellulosic particles (wood flour) with a higher particle size leading to decreased HDPE coverage and consequently a greater tendency for wood microparticles to contact water and absorb it (Fig. 6.1b).

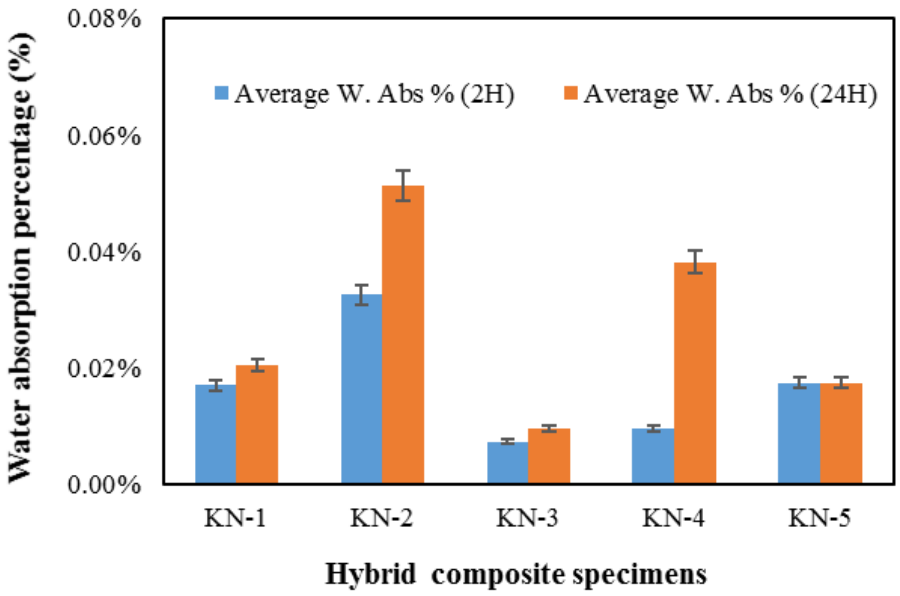

Fig. 6.2. Water absorption behavior of hybrid composite specimens.

A number of previous investigations have also reported that the water resistance of HDPE composites is influenced by the type of natural fiber used as reinforcement, the fiber weight fraction, micro voids formed at the interface between the components, and the fiber size [142, 143]. The recorded low water absorption values during water immersion tests show that exposure to water may not have any significant impact in the structural integrity of the material, or on their performance. This is also an evidence of the good adhesion between the reinforcements and the HDPE.

6.4.2 Tensile test results

Figure 6.3 shows the stress-strain curves of the hybrid composites under quasi-static tensile load while the summary of the tensile test data is presented in Table 6.2. Discontinuities observed in the stress curves occurred when the tensile machine was stopped at the end of elastic deformation and the extensometer used for precise strain measurement was removed. During the tensile testing this extensometer was removed at the point of maximum elastic deformation. Subsequent determination of elongation was based on the crosshead movement. The use of extensometer enables accurate determination of the yield point and Young modulus of the material.

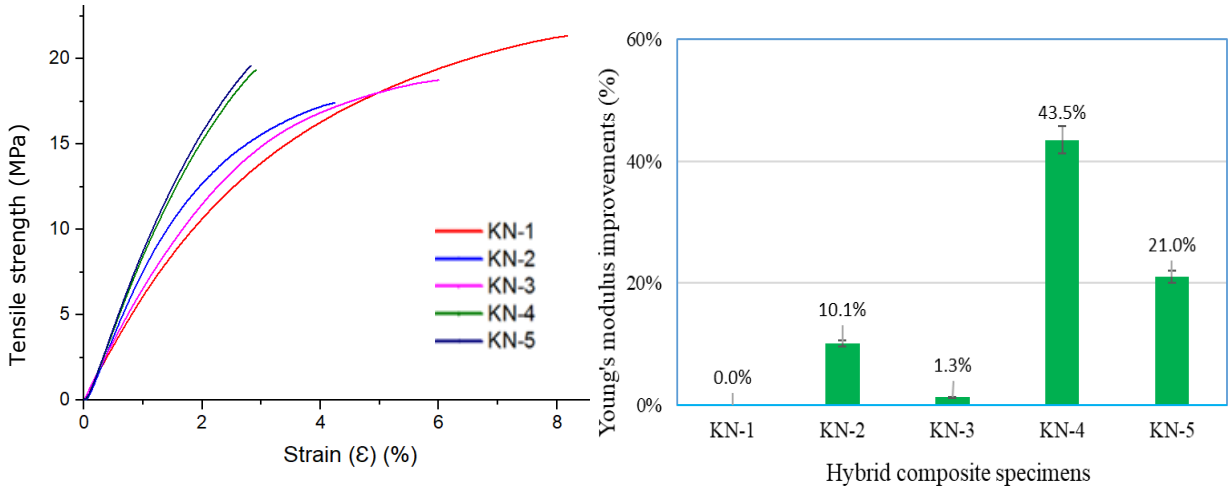

Fig. 6.3. Typical tensile stress-strain curves and Young's modulus improvements of the developed hybrid composites.

Table 6.2. Tensile strength and Young modulus of hybrid composites.

Hybrid composite specimens	Tensile strength σr (MPa)	Strain (Ɛ) (%)	Young's Modulus (MPa)
KN-1	22.16 ± 0.6	7.71 ± 1.0	615.7 ± 9.1
KN-2	17.42 ± 0.4	4.02 ± 0.2	677.9 ± 29.2
KN-3	17.71 ± 0.1	4.57 ± 0.4	623.7 ± 9.7
KN-4	20.10 ± 0.9	2.73 ± 0.3	883.7 ± 30.3
KN-5	19.32 ± 0.3	3.33 ± 0.1	745.2 ± 32.5

The highest values of tensile strength were recorded for KN-1 specimens containing only Kevlar® pulp reinforcements. This can be attributed to a more efficient load transfer across the fiber/matrix interphase, leading to the observed least tendency of the composites to fracture under tensile loading. Additions of fillers to Kevlar® fiber reinforced HDPE did not result in further increase in tensile strength. It can be observed from the strain data in Table 6.2 that addition of the micro- and nano-fillers reduced the ductility of the Kevlar® short fiber/HDPE composites and this might account for the decrease in strength properties. However, the addition of micro- and nano-fillers led to increase in Young modulus of the hybrid composites containing micro- and nano-fillers (KN-2 - 5). The highest value of Young modulus was observed for hybrid composites containing colloidal silica (KN-4) nano-fillers with a 43.5 % increase when compared to Kevlar® reinforced

HDPE containing no filler. An improvement of 21 % in stiffness also was achieved in specimens containing gamma alumina nano-particles (KN-5). 10.1 and 1.3 % increase in Young modulus was recorded for specimens containing organic chonta wood particles (KN-2) and potato flour (KN-3) respectively. These results indicate that the addition of synthetic nano-fillers enhances in higher percentage the stiffness of the hybrid composites. The nano-particle size and the higher modulus of rigidity modulus of the ceramic fillers account for the better stiffness response of the hybrid composites containing gamma alumina and colloidal silica particles. Previous investigations have reported that filler particles size in nanoscale have more pronounced effect on increasing the Young modulus of vinyl ester resin compared to micro-particles [144]. Also, Ozsoy *et al.* [145] reported that as the contents of nano- and micro-fillers in epoxy composites was increased, the strength decreased while the modulus increased, which is in agreement with our current findings on the effect of nano- and micro-filler addition to Kevlar® short fibers reinforced HDPE.

6.4.3 X-Ray Diffraction (XRD) analysis

Figure 6.4 shows the XRD patterns of the various hybrid composites produced in comparison with the control sample (KN-1). The diffraction pattern for control sample (Fig. 5e) exhibits sharp diffraction peaks corresponding to the crystalline region and small broad (diffused) peaks which are characteristics of a polymer matrix. The most prominent peaks appeared at scattering angles (2θ) of 32.3^{o}, 36^{o}, and 55.1^{o}, which correspond to the reflections from (110), (200), and (020) planes, respectively. The absence of new peaks, as well as the similarity in the X-ray patterns of the hybrid composites, is an indication that the addition of micro- and nano-fillers had no profound effects on the crystallinity of the control samples. However, the intensity of the crystalline peaks decreased as a result of the reinforcements. The peak intensity of samples (KN-2 and KN-3) containing organic micro-particles (Fig. 6.4 c, d) is higher than those of samples (KN-4 and KN-5) containing synthetic nano-particles (Fig. 6.4 a, b). The reduction in the main peak ($2\theta=32.3^{o}$) and in the secondary peak ($2\theta=55.1^{o}$); as well as, the variation in intensity peaks of the (200) peak ($2\theta=36^{o}$), are the result of the change of filler type, and the size of the fillers contained in the hybrid composites. These results are consistent with those obtained by Deka and Maji [135, 136], who studied the effect of silica nano-powder addition on wood flour composites and found that the intensity of the crystalline peaks of polypropylene matrix decreased with the increase in silica or

wood flour addition. Similar results were obtained by other researchers [146, 147] in XRD analysis of other types of fiber-reinforced wood flour/HDPE composites.

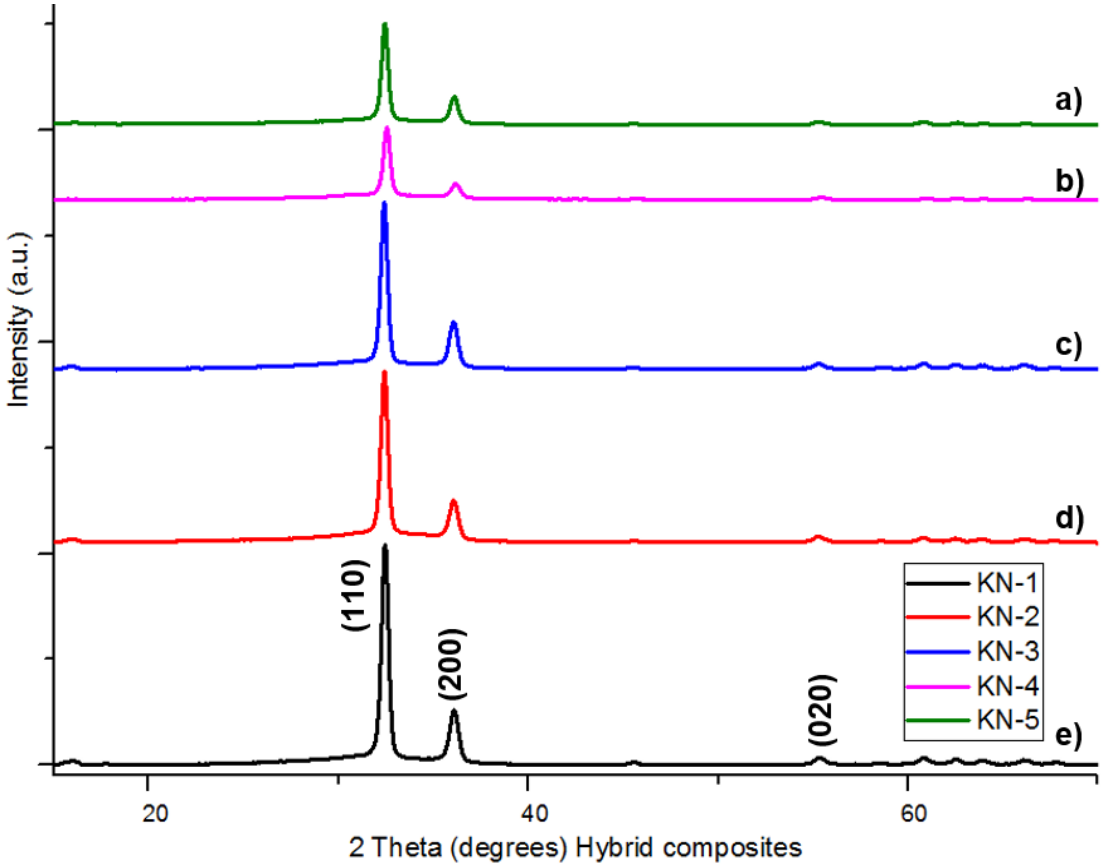

Fig. 6.4. X-ray Diffraction curves obtained for the hybrid composite specimens.

6.4.4 Dynamic mechanical behavior under impact loading

The results of the dynamic impact loading of the hybrid composites are presented in Table 6.3. The strain rates of the test specimens varied between 940 and 2800 s^{-1} depending on the impact momentum, which is dependent on the firing pressure of the striker bar. The maximum flow stress, in most of the cases, is observed to be higher for the hybrid composites compared with the control samples KN-1. The average percentage increase in maximum flow stress achieved in average by KN-2, KN-3, KN-4, and KN-5 specimens were determined to be 0.5, 9.5, 12.4, and 22.8 % respectively. The maximum flow stress is higher with samples containing synthetic nano-fillers than those containing micro-particles of chonta palm wood or potato flour.

Table 6.3. Dynamic impact properties of hybrid composites.

Pressure	Specimens	Max Strain rate (s^{-1})	Max Stress (MPa)
50KPa 4.0 kg.m/s	KN-1	947	247
	KN-2	1067	291
	KN-3	943	280
	KN-4	1219	310
	KN-5	1283	354
60KPa 6.8 kg.m/s	KN-1	1927	354
	KN-2	1765	325
	KN-3	2089	396
	KN-4	1887	415
	KN-5	2031	432
70KPa 8.7 kg.m/s	KN-1	2603	390
	KN-2	2408	359
	KN-3	2801	403
	KN-4	2697	367
	KN-5	2763	401

The stress-strain curves of the hybrid composites for various impact momentums of the projectile (4, 6.8, and 8.7 kg.m/s) are presented in Figure 6.5. The stress-strain curves indicate the yield point to be about 100 MPa or below, depending on the impact momentum. Beyond the elastic limit the stress-strain curves become non-linear. The curves show that the stress increases steadily with strain up to a maximum stress and after reaching the maximum value, the stress begins to drop. These compressive stress results obtained here are consistent with the findings of Firdaus *et. al.* [92] for jute and kenaf fibers reinforced composites that introduction of fillers also enhanced the flow stress of both composites when subjected to dynamic load.

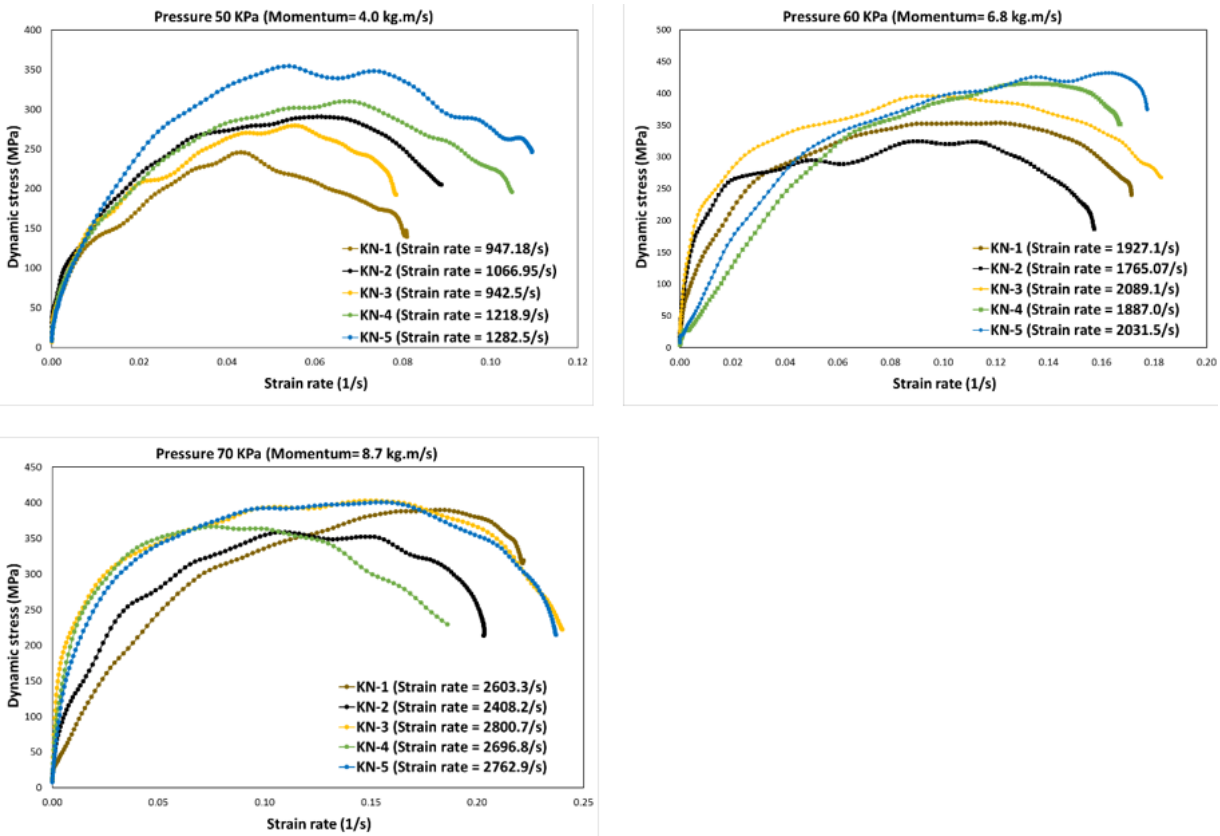

Fig. 6.5. Dynamic stress–strain curves of hybrid composites under dynamic impact loading.

Scanning electron microscope micrographs of the specimens impacted at 8.7 kg.m/s are presented in Figure 6.6. At this firing pressure, the specimens were severely deformed and ruptured. The KN-4 and KN-5 specimens experienced lower cracking tendency under impact loading than the KN-1, KN-2, and KN-3 specimens. Crack initiations were observed to occur in samples KN-1, KN-4, and KN-5 in the regions of short fiber accumulation (Fig. 6.6a, d, e), and the crack propagation was seen along the direction of the alignment of the accumulated short fibers. Exposed Kevlar® fibers can be observed along the cracks of these specimens. On the other hand, the crack initiation in samples KN-2 and KN-3 (Fig. 6.6b, c) was observed to occur at the region of agglomeration of the organic micro-particles. For both specimens, the cracks extended along the path of alignment of the micro-particles. This suggests detrimental effect of excessive accumulation of short fibers or particle fillers within the thermoplastic matrix on resistance to dynamic impact failure. This excessive accumulation of reinforcements in an area may result in weak interphase between components, thereby promoting initiation and propagation of the cracks as well as fracture during impact loading.

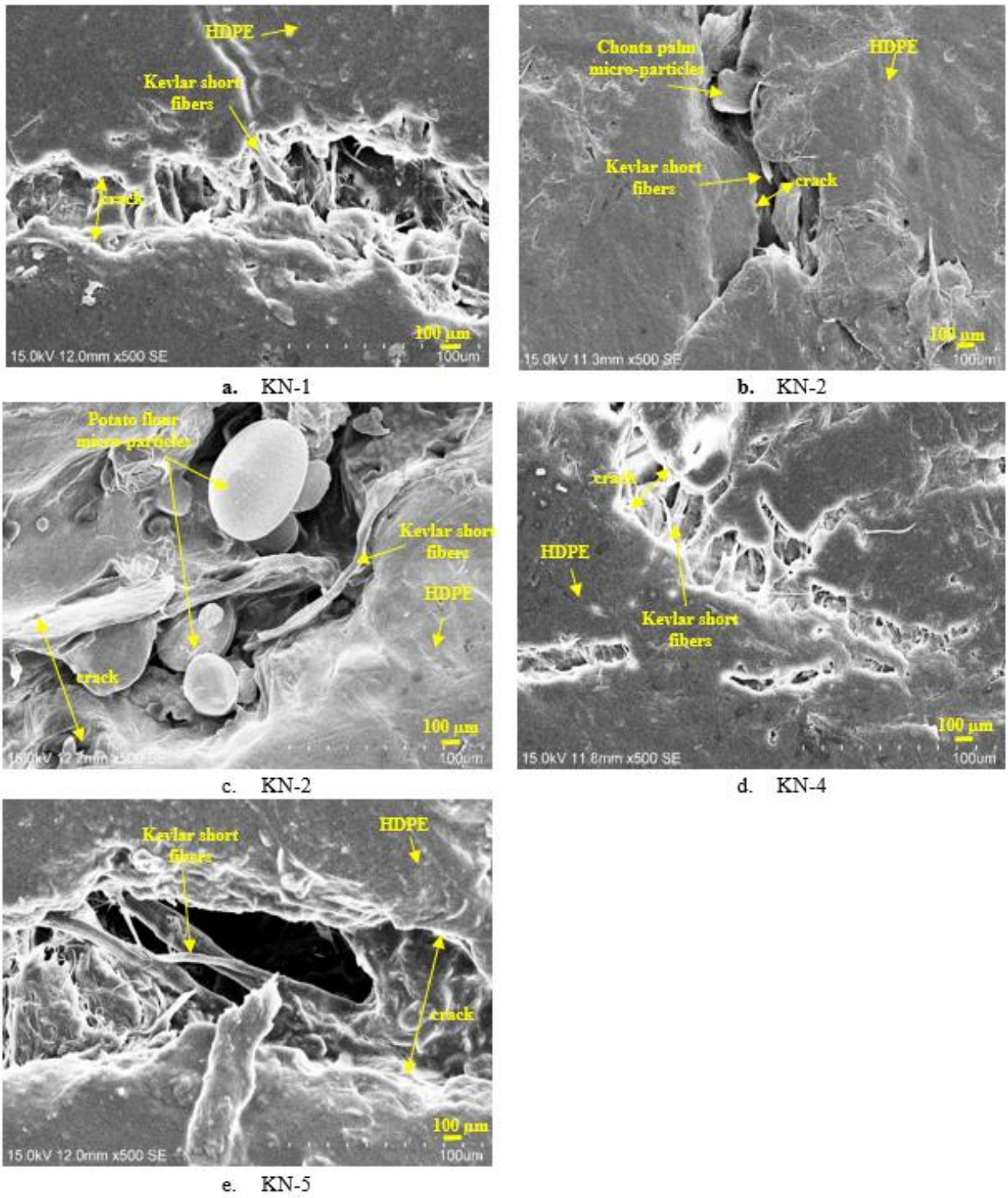

Fig. 6.6. SEM micrographs of deformed and fractured specimens after dynamic impact loading (Impact momentum = 8.7 kg.m/s).

Specimens KN-1, KN-2, and KN-3 ruptured extensively while the specimens containing gamma alumina nano-particles (KN-5) and colloidal silica (KN-4) still maintained their structural integrity

when impacted at 8.7 kg.m/s. This suggests that composites containing gamma alumina and colloidal silica possess better resistance to impact damage compared to those containing chonta palm wood or potato flour micro-particles. Matrix cracking, fiber pull out and matrix debonding were observed along the fracture path in the SEM images of the ruptured specimens after impact loading. Boudenne *et al.* [15] reported that the typical failure modes in polymer matrix composite can include, matrix deformation and cracking, fiber-matrix debonding, delamination, fiber breakage or combination of two or more of these failure modes. The results of this current study are also in agreement with those of Fu *et al.* [86], who observed failure in short fiber reinforced polymer under impact loading to occur as a result of a fiber-matrix interfacial debonding, matrix plastic deformation, fiber rupture, and matrix fracture, which have direct correlation with the fiber volume fraction, fiber orientation, and the fiber length.

6.4.5 Energy absorbed by hybrid composite targets after ballistic impact tests

According to Shaktivesh *et al.* [32], structural materials for high-performance applications in defense or aerospace structures must have good resistance to ballistic impact from a projectile of low mass traveling at high velocity. Table 6.4 provides the results of the ballistic impact test indicating the initial and exit velocities of the projectile after penetration of the various hybrid composites developed in this study. The average initial velocity of the projectile was determined to be 385 m/s that is an average of six shots with a standard deviation of 6.2 m/s. This initial velocity is comparable to the muzzle velocity of 381 m/s for the same ammunition as provided in NATO specifications. In addition, the average initial energy of the six shots was estimated to be 593 J with a standard deviation of 19 J, which is also consistent with the original muzzle energy value of 582 J for that ammunition in the NATO specifications. Moreover, all the samples were tested under similar conditions. Here, the absorbed energy from the target represents the loss in kinetic energy through elastic and plastic deformations while the residual kinetic energy is the projectile energy that remains after the ballistic impact [131].

Table 6.4. Ballistic impact data sheet for various hybrid composite targets.

Targets	Initial velocity measured before impacts average (m/s)	Initial Energy average (J)	Velocity measured after impacts average (m/s)	Energy absorbed at targets average (J)
KN-1	385 ± 6.2	593 ± 19	367.9 ± 5.6	52.2 ± 16.3
KN-2	385 ± 6.2	593 ± 19	365.6 ± 3.1	59.1 ± 9.0
KN-3	385 ± 6.2	593 ± 19	366.4 ± 3.2	56.9 ± 9.5
KN-4	385 ± 6.2	593 ± 19	366.0 ± 3.0	58.0 ± 8.7
KN-5	385 ± 6.2	593 ± 19	364.4 ± 2.2	62.7 ± 6.5

Figure 6.7a shows the absorbed energy for the various targets with similar areal density. The control specimens (KN-1) showed the lowest energy absorption (52.2 J). However, a significant enhancement was achieved in the ballistic impact performance of the hybrid composite plates incorporated with micro- and nano-fillers. For example, specimens containing 20 wt.% of gamma alumina nano-fillers (KN-5) exhibit the highest energy absorption of 62.7 J, which is equivalent to 20 % improvement over control specimens with similar thickness and density (Figure 6.7b). The KN-2 specimens containing 20 wt.% chonta micro-particles exhibited a 13 % increase in the energy absorption (59.1 J) over KN-1 samples. On the other hand, hybrid composites containing 20 wt.% of potato flour micro-particles (KN-3) and colloidal silica nanoparticles (KN-4) absorbed 56.9 and 58 J of energy; corresponding to 9 and 11 % improvement over the control samples (KN-1) respectively. These results indicate that introduction of nano- and micro-particles into short Kevlar® fiber reinforced HDPE composite improves the energy absorption capability of the composites. It can be concluded that the addition of 20 wt.% nano- and micro-fillers offers a promising way to considerably enhance the ballistic impact resistance of short Kevlar® fiber reinforced HDPE.

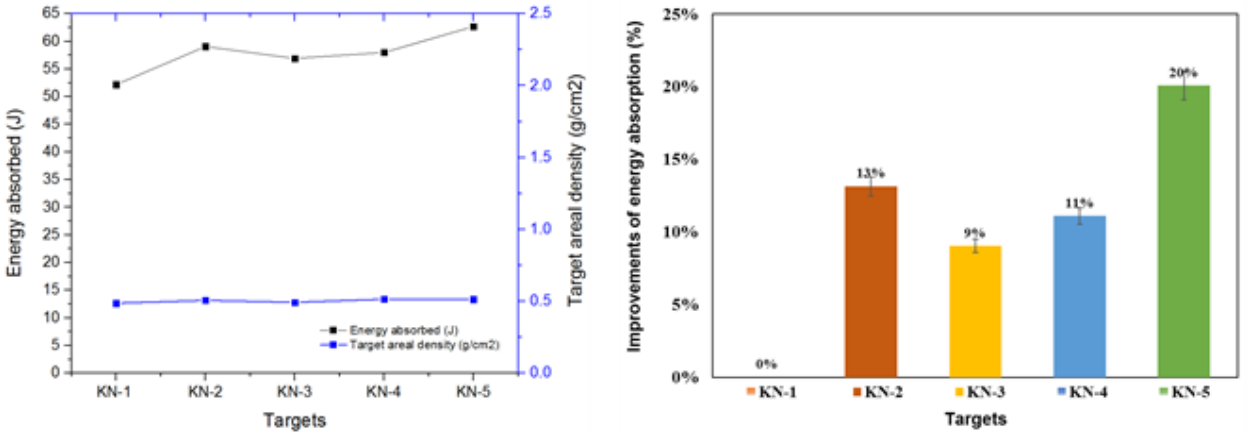

a) Energy absorbed at targets after ballistic testing

b) Improvements of the impact energy absorbed by targets (%)

Fig. 6.7. Energy absorbed by hybrid composite targets containing micro and nanoparticles.

The average sizes of perforations in the targets during ballistic impact test are presented in Figure 6.8. These are averages for ten measurements around the entry and exit holes perforated by the projectile on six targets of the same material. The difference between entry orifice and exit orifice is noticeable. The average diameter of the crater (after perforation) at the entry side was measured to be 10 mm with a standard deviation of 0.2 mm for all targets, which shows a similar behavior of bullet entry penetration. On the other side, the exit diameter of the crater on the back side ranged between 12.4 and 17.2 mm with standard deviations of 0.5 and 1.1 mm, depending on the target configuration (type of reinforcement) and material detachment. The difference in exit orifice can be traced to the difference in the penetration resistances of the targets which determines the differences in the amount of detached materials as the bullet penetrated the target. However, the relationship between energy absorbed and material detachment in the targets is not linear.

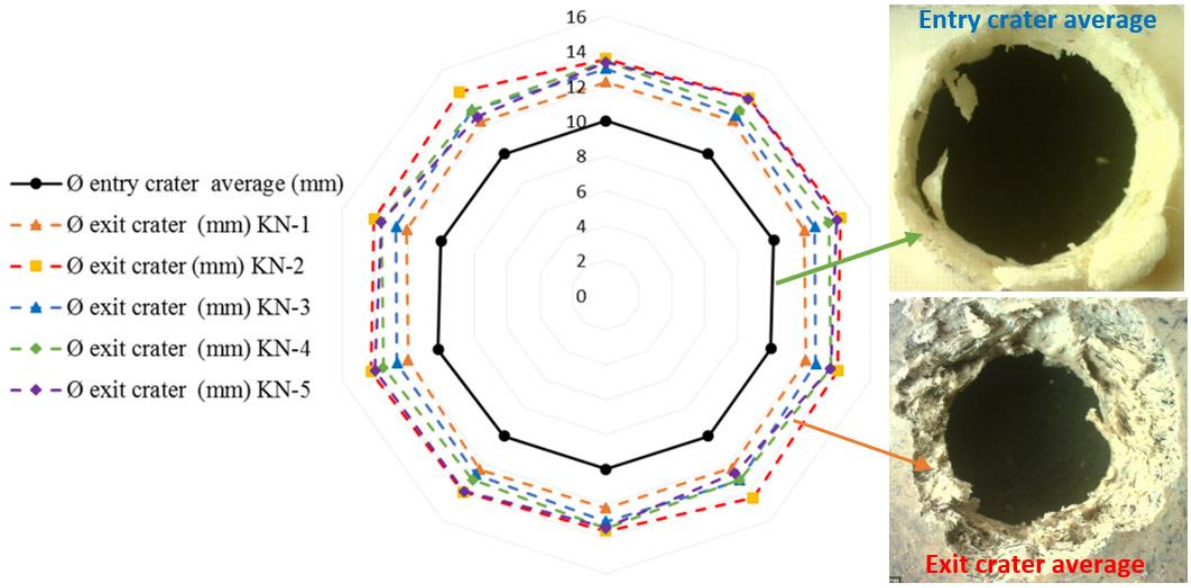

Fig. 6.8. Penetration behavior of the projectiles on the entry and exit sides of the targets.

Figure 6.9 shows the SEM micrographs of the longitudinal section of the perforations in the hybrid composites. These micrographs provides information on the deformation, penetration and the sequence of impact damage in the targets as bullets perforated them during ballistic impact. The deformation of the target is influenced by the projectile shape (round nose), impact velocity and the properties of the targets. The damage sequence involved an indentation on the frontal face of the plate, produced by a localized stress in the region of initial contact. The pressure exerted by the projectile creates a small puncture. At the initial stage of penetration, a ductile crater enlargement can be observed at the bullet entry orifice (Figure 6.9). Horizontal striations were observed in the targets, which occurred by lands and grooves that come from the rifling process of the ogive, the impression marks are characteristics of the bullet as it travelled through the barrel. Also, at the initial penetration, it is posible to observe the organic micro-particles in the samples KN-2 and KN-3, which were deformed during the bullet penetration (Figure 6.9b, c). Also, Figure 6.9 shows the bullet exit orifice, with a large material detachment, and an extensive exposure of Kevlar® short fibers and micro-particles, as a characteristic nature of the fracture associated with the projectile exit. Difference in behavior in terms of material detachment and Kevlar® pulp exposure (fiber pull-out) was observed in the targets. For example. the amount of fiber-pull out and material detachment in the KN-4 and KN-5 targets, containing synthetic ceramic partilces, were observed to be lower than for other specimens. The improved resistance to material

detachment during perforation can be considered to be responsible for the greater energy absorption and better resistance to projectile penetration in these specimens. It has been reported in a number of previous studies that energy absorbing capacity can be determined from analysis of various stages in projectile penetration: initial indentation, projectile compression in the region surrounding the impacted zone, tensile deformation and failure of primary and secondary yarns and the material detachment [99, 116].

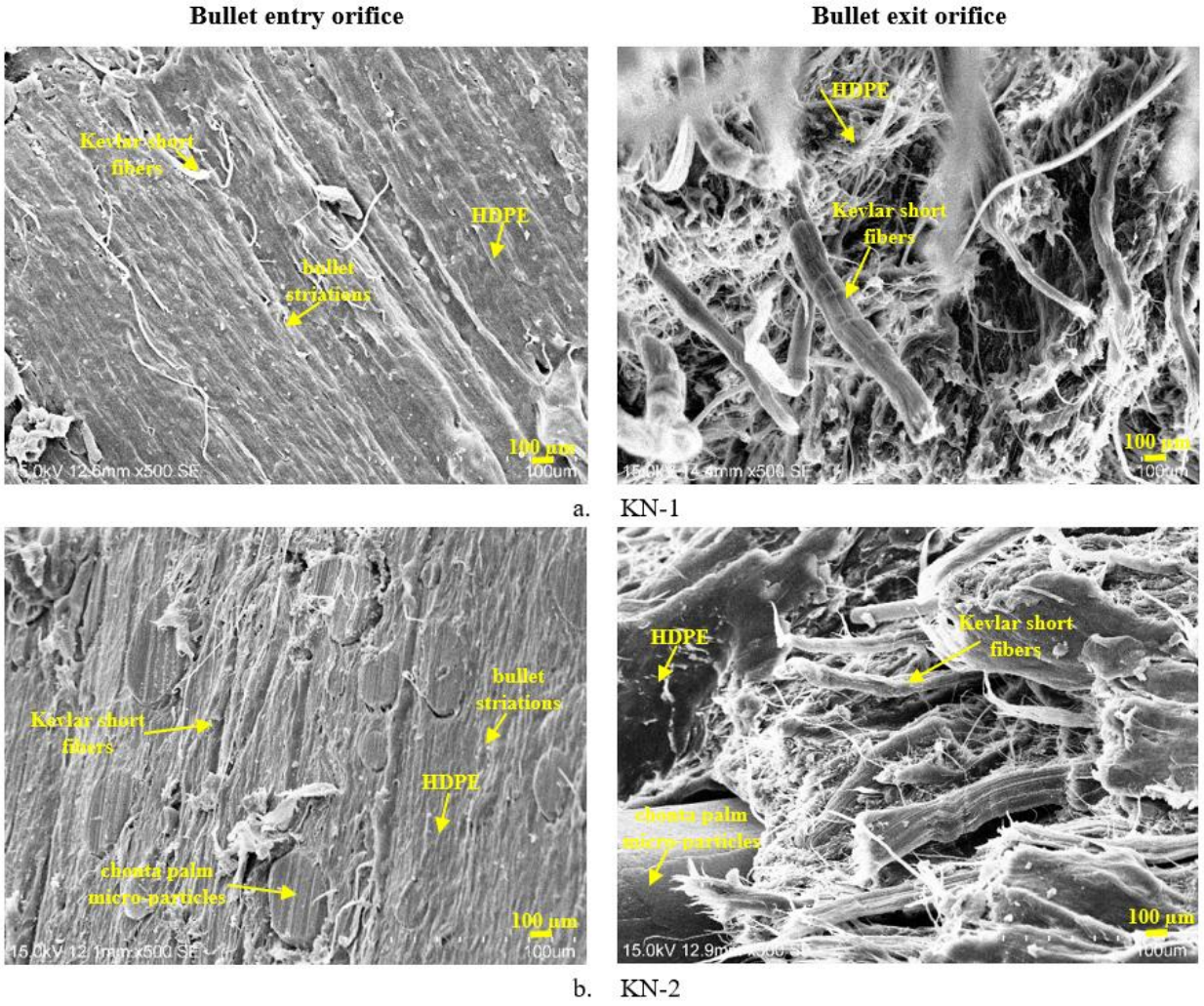

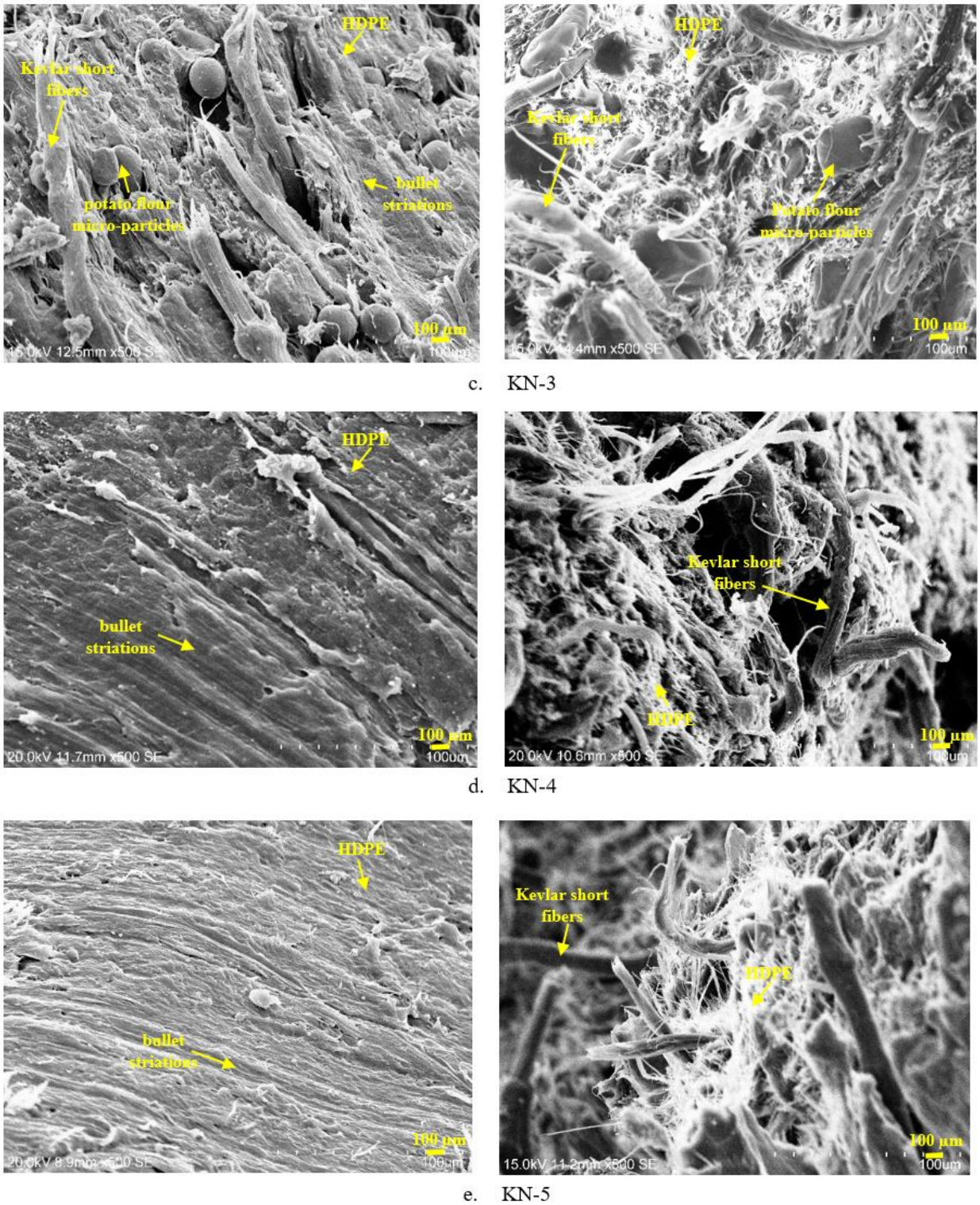

Fig. 6.9. Longitudinal sections, showing the morphology of projectile penetration channels inside the targets.

6.5 Conclusions

Hybrid composites were prepared by incorporating micro- and nano-fillers into Kevlar® short fibers reinforced HDPE (the controlled sample). The fillers used are natural chonta palm wood and potato flour micro-particles, and synthetic colloidal silica and gamma alumina nano-particles. The effects of filler addition on the crystallinity, quasi-static tensile strength, dynamic compressive strength and ballistic impact resistance of the hybrid composites were investigated. The crystalline structure of control samples is unaffected by the addition of particulate fillers. However, the intensity of the crystalline peaks decreased in different proportions depending on the added reinforcement and fillers. The addition of the micro nano-fillers Kevlar® short fiber reinforced HDPE result in increase in dynamic impact resistance and energy absorption during ballistic impact. On the other hand, the addition of this nano fillers led to loss ductility and decrease in tensile strength. Since the hybrid plates is designed for use in application requiring good resistance to dynamic shock loading, the most crucial properties of the Kevlar® reinforced HPDPE are enhanced by additions of nanofillers. Addition of nanofillers of gamma alumina and colloidal silica led to greater performance under dynamic and ballistic impact loading. An excessive accumulation of fibers or filler particles in any specific areas of hybrid composites can have detrimental effect on the quasi-static or dynamic mechanical behavior of the composite. Cracks will readily nucleate at the weak interphase between agglomerated fibers or particles with the thermoplastic matrix. Reinforcing a matrix HDPE with Kevlar® short fibers and nano-fillers result in hybrid composites with an enhanced performance under both static and dynamic mechanical loading. Therefore, these novel hybrid composites can be promising materials for automotive, military and aerospace applications.

Chapter 7: Reinforcing Effects of Natural Micro-particles on the Dynamic Impact Behaviour of Hybrid Bio-composites Made of Short Kevlar Fibers Reinforced Thermoplastic Composite Armor

7.1 Overview

Hybrid bio-composites are developed by the hybridization of Kevlar pulp with natural micro-particles (chonta palm wood), which was subsequently used in reinforcing high density poly ethylene (HDPE) matrix. Specimens cut from these bio-composites were subjected to high strain-rate compressive and ballistic impact loading conditions to understand their responses to massive and rapid loading. The findings are discussed in this chapter, which has been submitted for publication as manuscript #4 to the Journal of *Dynamic Behavior of Materials* as follows:

E.E. Haro, A.G. Odeshi, J.A. Szpunar, "Reinforcing effects of natural micro-particles on the dynamic impact behaviour of hybrid bio-composites made of short Kevlar fibers reinforced thermoplastic composite armor".

The paper has been reviewed while the request for mandatory revision has been done. As at the time of writing this thesis the final decision of the editor is being awaited. The contributions of the PhD candidate to this manuscript are: 1) experimental design, 2) preparation of raw materials and processing of bio-composite samples, 3) physical, microstructural and mechanical characterization of the composites and 4) development of the manuscripts for publication. The manuscript was reviewed by my supervisors before it was submitted for publication in this journal. To avoid duplication for the information, provide in Chapter 3, selection of the materials, target preparation, and composite characterization have been removed from this chapter. The list of references in the submitted manuscript are also removed and listed at the end of this thesis.

7.2 Abstract

Hybrid bio-composites are developed for use in protective armor through positive hybridization offered by reinforcement of high density polyethylene (HDPE) with Kevlar® short fibers and palm wood micro-fillers. The manufacturing process involved a combination of extrusion and compression molding techniques. The mechanical behavior of Kevlar® fiber reinforced HDPE with and without palm wood filler additions are compared. The effect of the weight fraction of the added palm wood micro-fillers is also determined. The Young modulus was found to increase as the weight fraction of organic micro-particles increased. However, the flexural strength decreased with the increasing weight fraction of added micro-fillers. The results of X-ray diffraction analysis on the composites revealed that the crystalline structure of the Kevlar® fiber reinforced HDPE remained unchanged with the addition of reinforcements. However, the intensity of the crystalline peaks decreased with increasing weight fraction of the added organic micro-fillers. The interfacial interactions between the components was investigated using scanning electron microscopy. The influence of the size, random alignment and distribution of the natural micro-particles was evaluated. Ballistic impact and dynamic shock loading tests were performed to determine the optimum proportion of Kevlar® short fibers and organic micro-fillers needed to improve impact strength of the HDPE. These results indicate a positive hybridization by deposition of organic micro-fillers on the surface of short Kevlar® fibers used in reinforcing in a thermoplastic matrix enhanced the mechanical and dynamic properties of these materials. Therefore, these novel hybrid bio-composites can be promising materials for different applications including protective armor against ballistic impacts.

Keywords: Hybrid bio-composites; organic nano-fillers; dynamic shocking loading; ballistic impacts; energy absorption.

7.3 Introduction

Natural fiber reinforced polymeric matrix composites are gaining considerable attention in the construction, military and automotive industries. These natural fiber composites are biodegradable and may contain organic fillers, which can further enhance their mechanical properties. Obtaining a strong interface between organic fillers and the polymer matrix has been a challenge that is being overcome with the addition of compatibilizers such as maleic anhydride. Earlier studies indicated

that lack of good compatibility between natural fillers and polymer matrix adversely affect mechanical properties such as impact and tensile strength of the organic filler reinforced plastic composites [141]. The hybridization of organic fiber reinforced composites by using inorganic fillers has also proved to be a promising method to enhance the interface between components and improve the mechanical strength and impact properties of polymer matrix composites [148, 149]. Hybrid composites containing more than two types of reinforcements (fibers and micro-fillers) have been developed and reported to exhibit improved performance [150]. These composites named hybrid bio-composites can be prepared using natural reinforcements (coir, bast, leaf, hardwood, cellulosic fillers) and synthetic fibres (glass, carbon, Kevlar®, boron) incorporated in a polymer matrix [134, 135]. For example, Burgueno *et al.* [151] experimented with hybrid bio-composites made of green and raw hemp particles incorporated in a single polymer resin, and then impregnated the mixture into short jute fibers, glass strand mat and unidirectional carbon fibers. This resulted in composites with improved stiffness and strength.

In another study, the hybridization effects of short glass fibers and wood flour as reinforcements in thermoplastic matrix composites was evaluated by Valente *et al.* [141]. They reported improved flexural strength as a result of hybridization of glass fiber (20 wt.%) reinforced polymer LDPE (50 wt.%) with wood flour (30 wt.%). However, increasing the wood flour content above 30 wt.% led to a decrease in flexural strength. Hybridization of inorganic particles and short-fibers in a thermoplastic matrix is widely studied. For example, short-glass-fiber (SGF) reinforced polypropylene (PP) and short-carbon-fiber-reinforced polypropylene (PP) composites were investigated by Fu *et al.* [83-86]. The results of these studies confirm improvement of composites' strength, fracture resistance and impact capability in comparison to their polymer matrix. Fu and Lauke [83] investigated the effects of inorganic particles (calcite) and short glass fibers reinforced Acrylonitrile-butadiene-styrene (ABS) terpolymer matrix, they concluded that toughness and strength of the composites can be enhanced by incorporation of glass short fibers and addition of calcite particles to ABS resin.

Yeung and Rao [137] investigated the mechanical behaviour of Kevlar® fibers reinforced thermoplastic composites using Styrene Acrylonitrile, Acrylonitrile Butadiene Styrene and Polyethylene Resins as matrices and reported significant improvement in the tensile, compressive and flexural strength of the thermoplastic as a result of reinforcement with Kevlar®-49 [137].

Kevlar® fibers have also been used to reinforce polypropylene (PP) to develop thermoplastic composites with improved ballistic resistance for use in protective armors [152]. The use of Kevlar® pulp as reinforcement for thermoplastic polyimide composites was studied by Li [138, 153], and the results indicated improved tensile strength and wear resistance, which is optimum when the content of Kevlar® pulp is 15 wt.%. The objective of this research project is to evaluate the effects of the addition of organic microparticles (chonta palm wood) to Kevlar® short fibers reinforced HDPE on the tensile properties, impact resistance, water absorption behavior, and crystallinity of the resulting hybrid composites.

7.4 Results and Discussions

7.4.1 Microstructure and physical properties

Investigation of the microstructure of the obtained hybrid bio-composites was done using a Hitachi SU-6600 scanning electronic microscope (SEM) operating at an accelerated voltage of 15.0 kV. Specimens were gold coated using a Edwards S150B sputter coater.

Typical microstructures of the obtain hybrid bio-composites are presented in Fig. 7.1 (a-d). K-1 specimens made of HDPE containing (10 wt.%) Kevlar® pulp, show a uniform distribution of Kevlar® short fibers and good bonding between HDPE and reinforcing components (Fig 7.1a). In the hybrid bio-composite (Fig 7.1b-d), dispersed organic palm wood micro-particles of different ranging sizes (0.5 – 0.75 mm) are observed clearly. There is a random orientation of the micro-particles and short Kevlar® fibers, it is possible to differentiate the increasing weight fraction of the added chonta palm micro-particles. The interphase region in the hybrid bio-composites developed is formed by the interaction between Kevlar® short fiber/HDPE and wood palm micro-particles/HDPE. Similar characteristics were observed for all developed plates, i.e. they all exhibited a random orientation of both short Kevlar® fibers and chonta palm wood micro-particles as well as uniform distribution of the reinforcements. Since composite plates were maintained under pressure as the plates cooled from molding temperature to room temperature to ensure dimensional stability, uniform material properties at different locations in the plates is assumed. Moreover, test specimens were cut from the central regions while ballistic shots were also fired at central region to eliminate any possible effect of property variation at the edge of the plates.

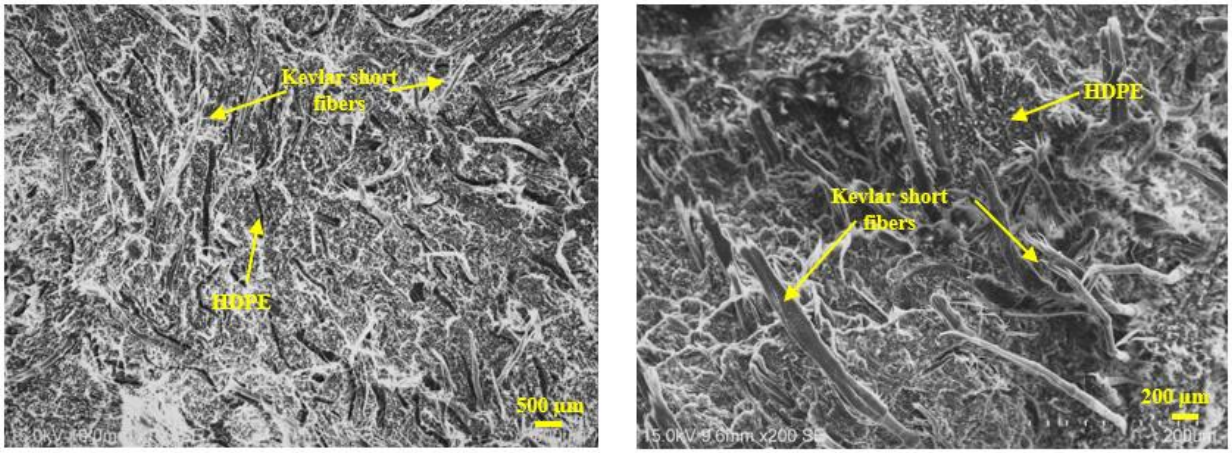

a. K-1 (HDPE containing 10 wt.% Kevlar pulp)

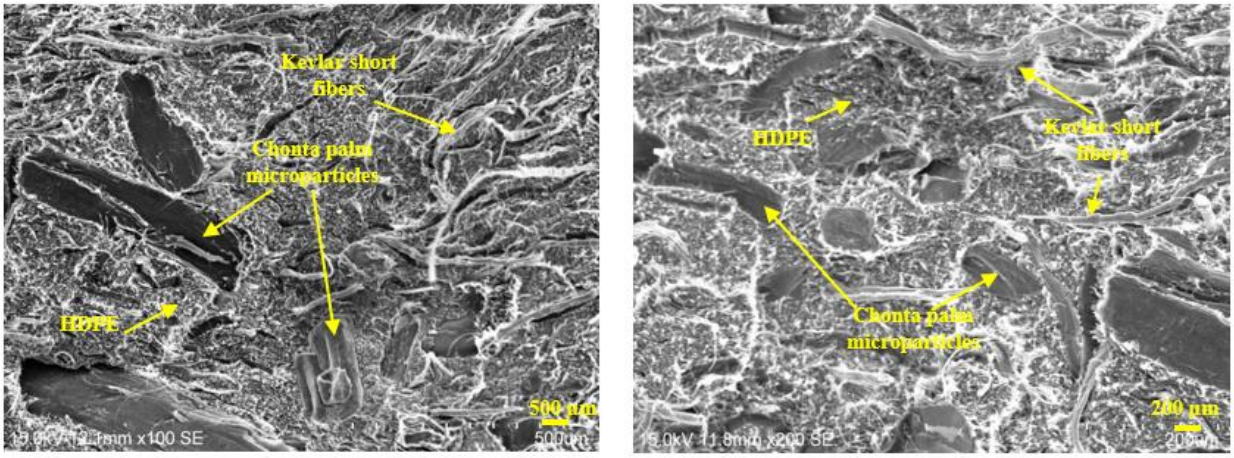

b. KCh-10 (HDPE containing 10 wt.% Kevlar pulp and 10 wt.% chonta palm micro-particles)

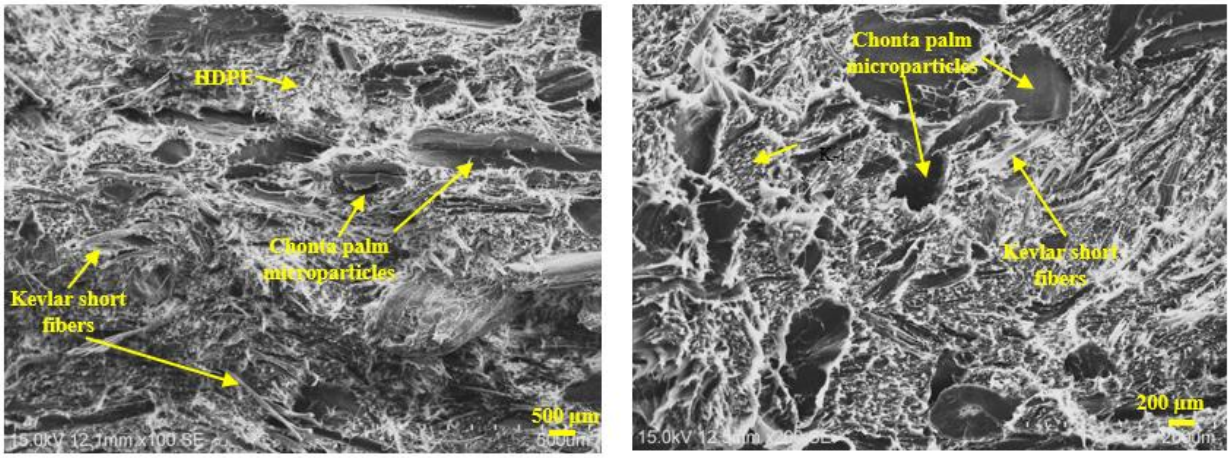

c. KCh-20 (HDPE containing 10 wt.% Kevlar pulp and 20 wt.% chonta palm micro-particles)

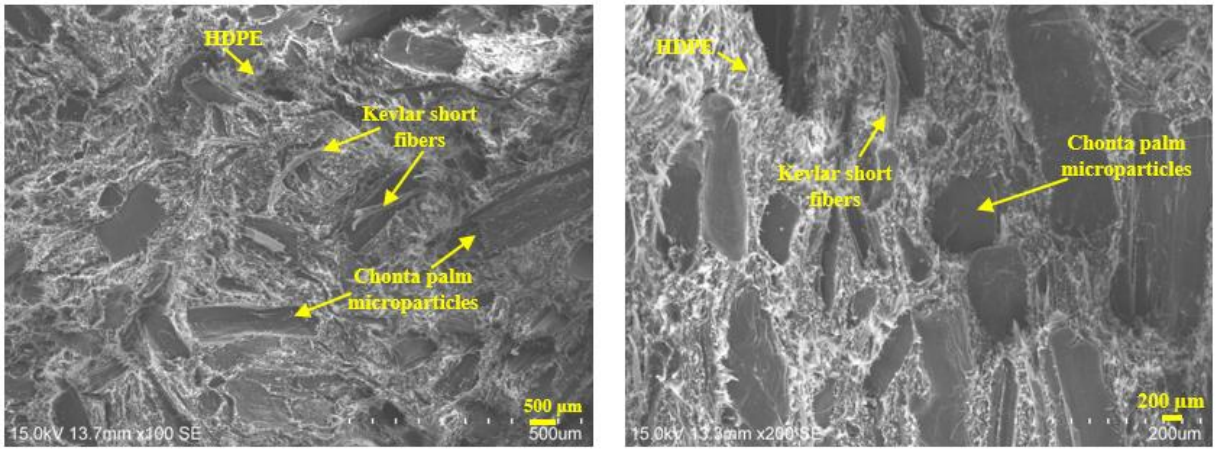

d. KCh-30 (HDPE containing 10 wt.% Kevlar pulp and 30 wt.% chonta palm micro-particles)

Fig. 7.1. SEM micrographs showing the transverse section of the hybrid bio-composites.

The physical properties of the hybrid composites developed in this study are presented in Table 7.1. The density variations observed for the various category of hybrid bio-composites are mainly due to the difference in the densities of the organic micro-particles contained in the specimens.

Table 7.1. Experimental data sheet showing composition and physical properties of the synthesized hybrid bio-composites.

Targets configuration	K-1	KCh-10	KCh-20	KCh-30
Kevlar pulp (10%)	10%	10%	10%	10%
Chonta palm wood micro-particles (wt.%)	-	10%	20%	30%
HDPE 2990 (wt.%)	90%	80%	70%	60%
Target weight average (g)	194±1.3	200±0.8	202±0.7	204±0.4
Target thickness average (mm)	5.5±0.1	5.1±0.1	4.8±0.2	4.7±0.2
Target areal density (g/cm^2)	0.49	0.50	0.51	0.51
Target density (g/cm^3)	0.88	0.99	1.05	1.09

Nomenclature:

- K-1 = HDPE containing (10 wt.%) Kevlar pulp
- KCh-10 = HDPE containing (10 wt.%) Kevlar pulp and (10 wt.%) Chonta palm micro-particles
- KCh-20 = HDPE containing (10 wt.%) Kevlar pulp and (20 wt.%) Chonta palm micro-particles
- KCh-30 = HDPE containing (10 wt.%) Kevlar pulp and (30 wt.%) Chonta palm micro-particles

The results of water absorption test performed on the composites are summarized in Fig. 7.2. From these results, it is possible to observe that there exists a slight increase in water absorption with increase in the content of organic micro-fillers (wood palm flour). Water absorption was

determined to be less than 0.06 % for all samples after soaking for 2 and 24 hours. This amount of water absorbed during this period is small and may not have significant effect on performance of the material. Samples K-1 and KCh-10 achieved the water absorption saturation of less than 0.03 wt.% after 2 hours of immersion and no further increase in weight due to absorbed water was observed after the 2-h exposure time. On the other hand, samples containing 20 and 30 wt.% chonta wood micro-particles (KCh-20 and KCh-30) absorbed more water in comparison to the other samples containing only Kevlar® pulp (K-1) and those containing 10 wt.% wood particles (KCh-10). This can be attributed to exposure of higher content of the cellulosic particles which have greater tendency to absorb water. It has also been reported in previous investigations that the water resistance of HDPE composites are affected by the type, weight fraction and the size of natural fiber used as reinforcement [142, 143].

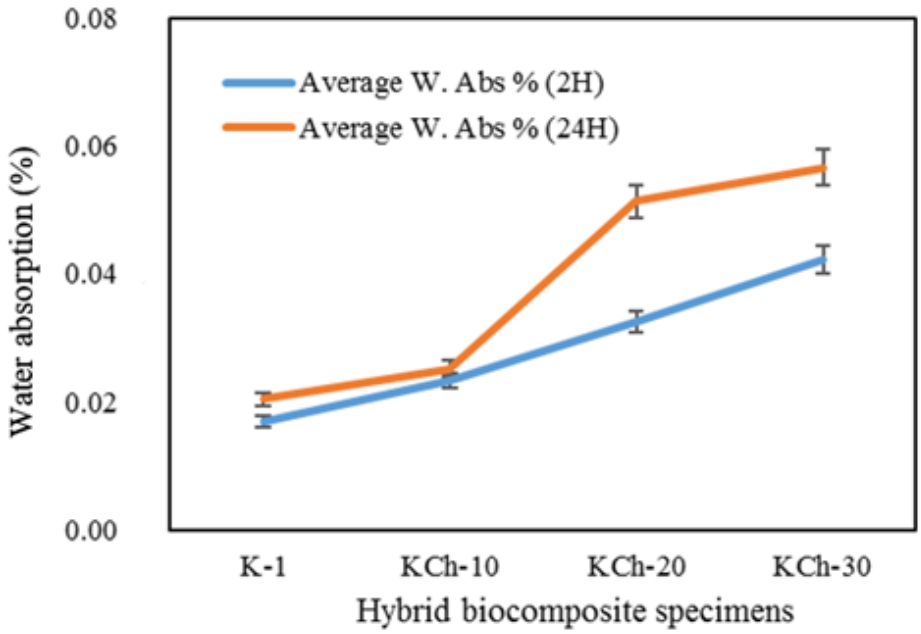

Fig. 7.2. Water absorption by hybrid bio-composite specimens.

7.4.2 Mechanical properties of hybrid bio-composites

The stress-strain curves of the hybrid bio-composites under quasi-static tensile loading are presented in the Fig. 7.3a, and tensile test results are summarized in Table 7.2. Discontinuities can be observed in the stress-strain curves, which occurred when the tensile machine stopped at the end of elastic deformation and the extensometer used for precise strain measurement was removed. During the tensile testing, this extensometer was removed at the point of maximum elastic

deformation, and subsequent elongation as the tensile load was further increased was based on the crosshead movement of the machine. The use of this extensometer enables accurate determination of the yield point and Young modulus of hybrid bio-composites.

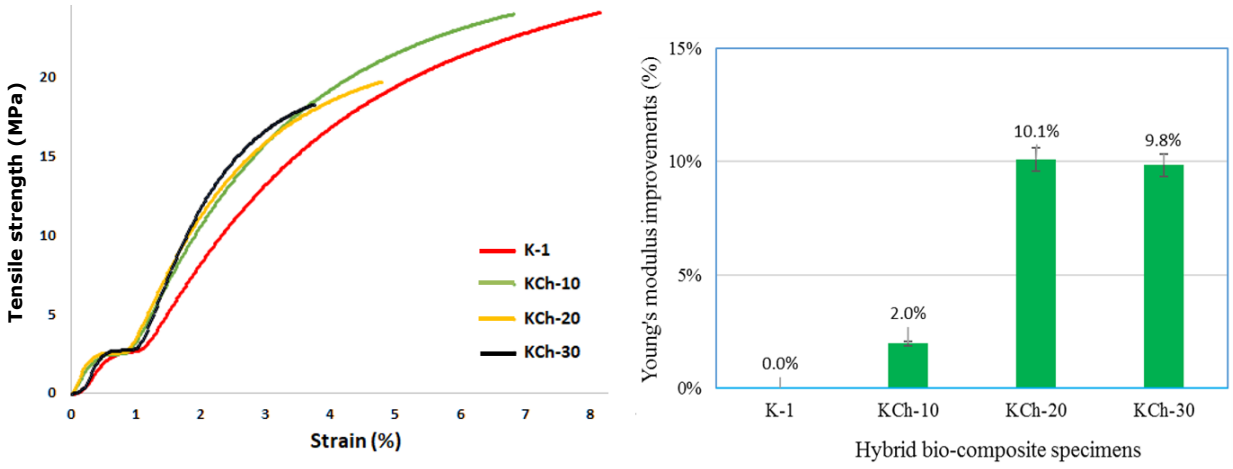

(a) (b)

Fig. 7.3. (a) Typical stress-strain curves and (b) stiffness improvements obtained for hybrid bio-composite specimens.

Table 7.2. Summary of results of the tensile test carried out on the hybrid bio-composites.

Hybrid composite specimen	Tensile strength σr (MPa)	Strain (Ɛ) (%)	Young's Modulus (MPa)
K-1	22.2 ± 0.6	7.71 ± 1.0	616 ± 9.1
KCh-10	21.6 ± 0.9	6.49 ± 0.8	628 ± 16.2
KCh-20	17.4 ± 0.4	4.02 ± 0.2	678 ± 29.2
KCh-30	16.8 ± 1.3	2.99 ± 0.6	676 ± 12.9

The highest tensile strength value was recorded for K-1 specimens (HDPE composites containing only Kevlar® short fibers), which also exhibited the least tendency to fracture under tensile loading. This suggests a more efficient fiber/matrix interaction and efficient load transfer across the short Kevlar® fiber/matrix interface. On the other hand, when a second filler (palm wood micro-particles) was added to the short Kevlar® fibres reinforced HDPE composites, a reduction

in tensile strength was observed. This result was observed to be the case with 10 % wood micro-particle addition (KCh-10) and for composites containing higher wood particle content (KCh-20 and KCh-30). This suggests that the presence of the wood particles affects the stress transfer between reinforcing Kevlar® fibers and the continuous HDPE matrix. Other researchers [154, 155] have also reported that excessive reinforcements (fibers or particles) in composite materials can lead to saturation in the matrix. This saturation is produced when the reinforcements become located very close to each other, leading to agglomeration and a weak interface between matrix and the agglomerates, thereby causing tensile strength reduction due to hindered stress transfer between matrix and the reinforcement.

With respect to material stiffness, a marginal improvement in the Young modulus (2.0 – 10.1 %) was achieved by wood particle addition to the short Kevlar® fiber reinforced HDPE (Fig. 7.3b). The highest stiffness was observed for KCh-20 specimens. This was slightly reduced as the wood particle content was raised from 20 to 30 % in the KCh-30 specimens. This suggests the optimum content of wood particle addition for enhanced stiffness is 20 %. It is evident from these findings that a positive hybridization effect can be achieved with respect to stiffness by the use of palm wood microparticle and short Kevlar® fibers as reinforcements in a thermoplastic HDPE matrix.

7.4.3 X-Ray Diffraction (XRD) analysis

Figure 7.4 shows the XRD peaks of the hybrid bio-composites produced in comparison with those of Kevlar® fibre reinforced HDPE containing no chonta wood particles (K-1 samples). The diffraction pattern of the K-1 sample exhibits sharp diffraction peaks corresponding to the crystalline region and small broad (diffused) peaks which are characteristics of amorphous polymers. The most prominent peaks for the samples appeared at the scattering angles (2θ) of 32.3^{o}, 36^{o}, and 55.1^{o}, which correspond to the reflections from (110), (200), and (020) planes, respectively (Fig. 7.4a). The absence of new peaks, as well as the lack of any difference in the X-ray patterns of the hybrid bio-composites, is an indication that the addition of palm wood microparticle fillers had no effect on the crystalline structure of the control samples (Kevlar® fiber reinforced HDPE containing no wood particle). However, the intensity of the crystalline peaks decreased as a result of the addition of the organic micro-particles. The intensity reduction in the main peak ($2\theta=32.3^{o}$), and in the secondary peaks ($2\theta=36^{o}$) can be observed in the Figures 7.4b, c,

d. This variation can be the result of the weight fraction modification of added micro-fillers to the hybrid bio-composites.

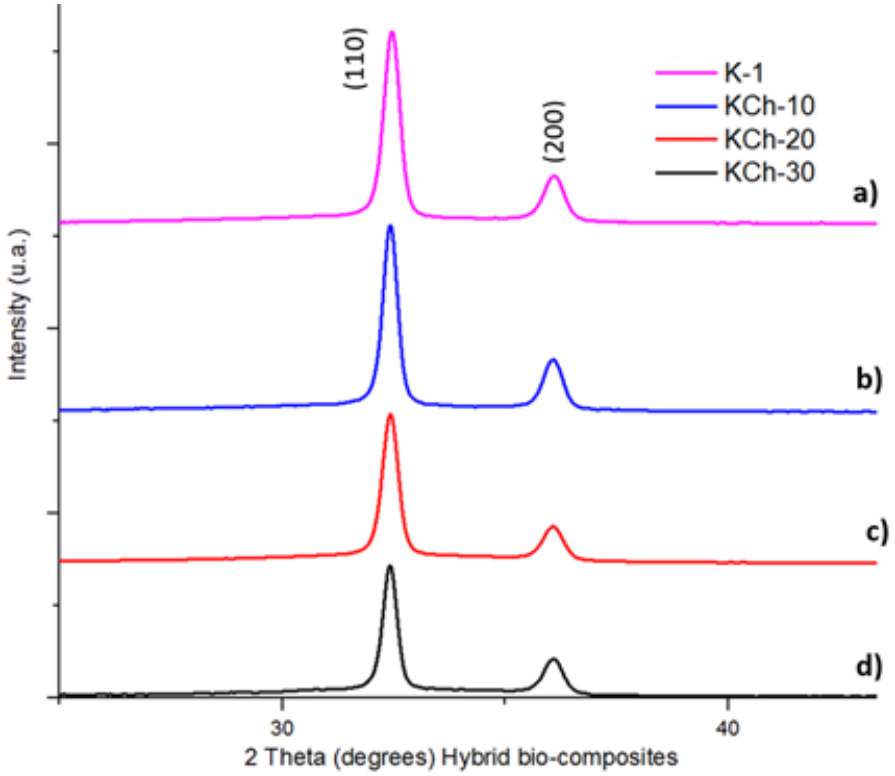

Fig. 7.4. Results of the X-ray Diffraction analysis of hybrid bio-composite specimens.

7.4.4 Dynamic mechanical behavior of hybrid bio-composites under impact loading

The results of the dynamic impact test on the specimens developed are provided in Table 7.3. The strain rates of the test specimens varied between 900 and 2700 s^{-1} depending on the impact momentum, which is determined by the firing pressure of the striker bar. The maximum flow stress is observed to be higher for the hybrid bio-composites compared with the control samples containing no wood particles.

Table 7.3. Maximum compressive stress and strain rate of hybrid bio-composites under dynamic impact loading.

Pressure	Specimens	Max Strain rate (s^{-1})	Max Stress (MPa)
50KPa 4.0 kg.m/s	K-1	900	247± 9.1
	KCh-10	1300	348± 5.8
	KCh-20	1000	291± 22.3
	KCh-30	1200	336± 16.6
60KPa 6.8 kg.m/s	K-1	1900	354± 12.4
	KCh-10	2000	368± 9.5
	KCh-20	1800	325± 18.4
	KCh-30	2100	374± 24.2
70KPa 8.7 kg.m/s	K-1	2600	390± 8.6
	KCh-10	2700	380± 11.9
	KCh-20	2400	359± 25.2
	KCh-30	2700	347± 18.1

The stress-strain curves of the hybrid bio-composites for various impact momentums of the projectile are presented in Fig. 7.5. The stress-strain curves indicate yield points that are, in most cases less than 100 MPa, depending on the impact momentum. Beyond the elastic limit, the stress-strain curves become non-linear. The curves show that the stress increases steadily with strain up to a maximum stress value and then begins to drop with further increase in strain. The drop in stress after the maximum value is attributed to softening of the matrix as the temperature increased in response to impact loading. The higher the impact momentum, the higher is the strain rate, and the higher is the maximum flow stress attained before the onset of the dominance of thermal softening. The K-1 samples exhibited the least resistance to deformation at high strain rates. The maximum flow stress is higher for samples containing 10 wt.% chonta palm microparticles. Therefore, samples KCh-10 exhibits the best performance under dynamic impact loading.

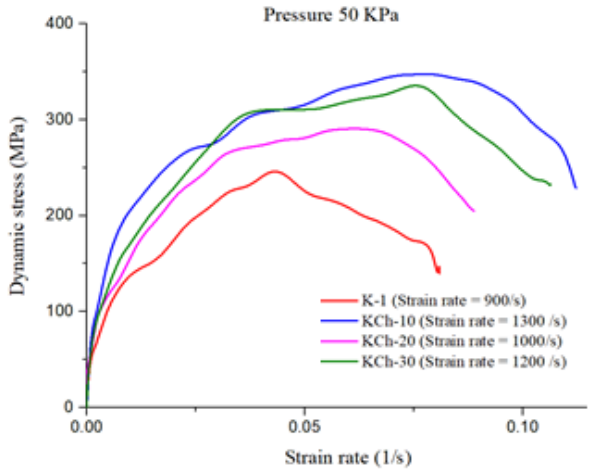

a) 50 KPa (Momentum= 4.0 kg.m/s)

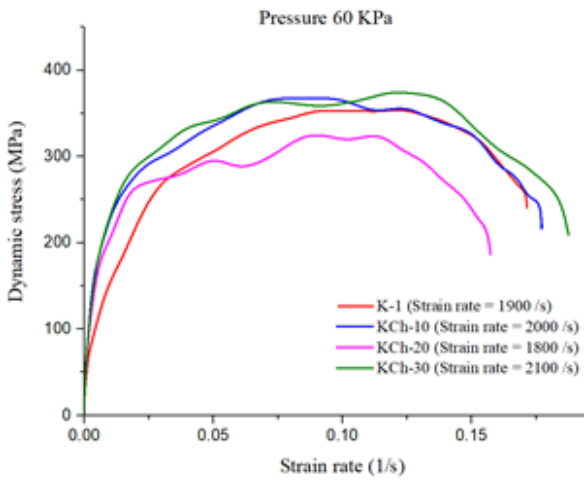

b) 60 KPa (Momentum= 6.8 kg.m/s)

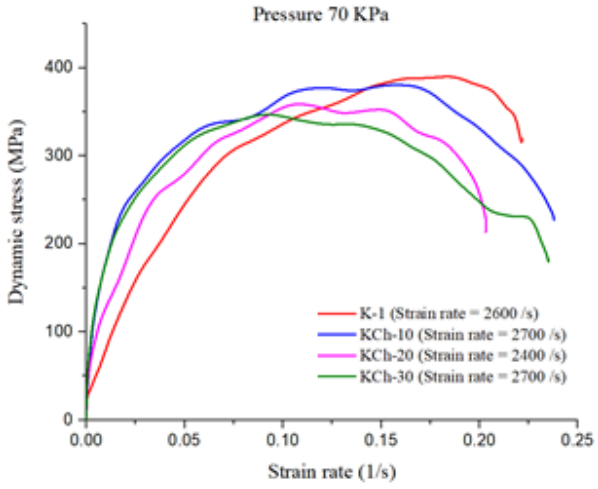

c) 70 KPa (Momentum= 8.7 kg.m/s)

Fig. 7.5. Dynamic stress–strain curves of hybrid bio-composites under dynamic impact loading.

Scanning electron microscopic micrographs of some of the damaged specimens after the impact test are presented in the Fig. 7.6. As the impact momentum increased, the intensity of damage in the specimens increased and finally specimen rupture occurred. The failure progression involved an extensive plastic deformation, crack initiation, and crack propagation until fracture. A significant increase in the areal dimensions and a considerable reduction in thickness of the impacted specimens was observed. This is attributed to the extensive plastic deformation typical of the thermoplastic matrix under mechanical load [15]. All the hybrid bio-composites experienced an extensive plastic deformation without rupture when impacted at the lowest momentum of 4.0

kg.m/s (pressure 50 KPa.). This again can be traced to the plasticity of the thermoplastic matrix. As the impact momentum was raised to 6.8 kg.m/s (pressure 60 KPa.), small cracks were observed in the specimens. Crack initiations were observed to occur where there is micro-particle agglomeration. These cracks propagated along the direction of alignment of the particle-agglomerates. This suggests that excessive accumulation of Kevlar® short fibers or organic micro-fillers within specific areas of the HDPE matrix, can affect bonding with the HDPE matrix resulting in weak interface that can promote cracking and fracture under dynamic impact loading. When the impact momentum was increased further to 8.7 kg.m/s (pressure 70 KPa.), the K-1, KCh-20, and KCh-30 specimens ruptured completely under the impact load, but specimens containing chonta palm 10 wt.% (KCh-10) kept their structural integrity. This observation aligns well with the impact stress-strain data provided in Table 7.3. Also, the SEM micrographs of the impacted specimens indicate Kevlar® fibers breakage and matrix fracture in addition to debonding between matrix and reinforcements. Fiber bridging and fiber pull-out can be observed along the crack propagation paths.

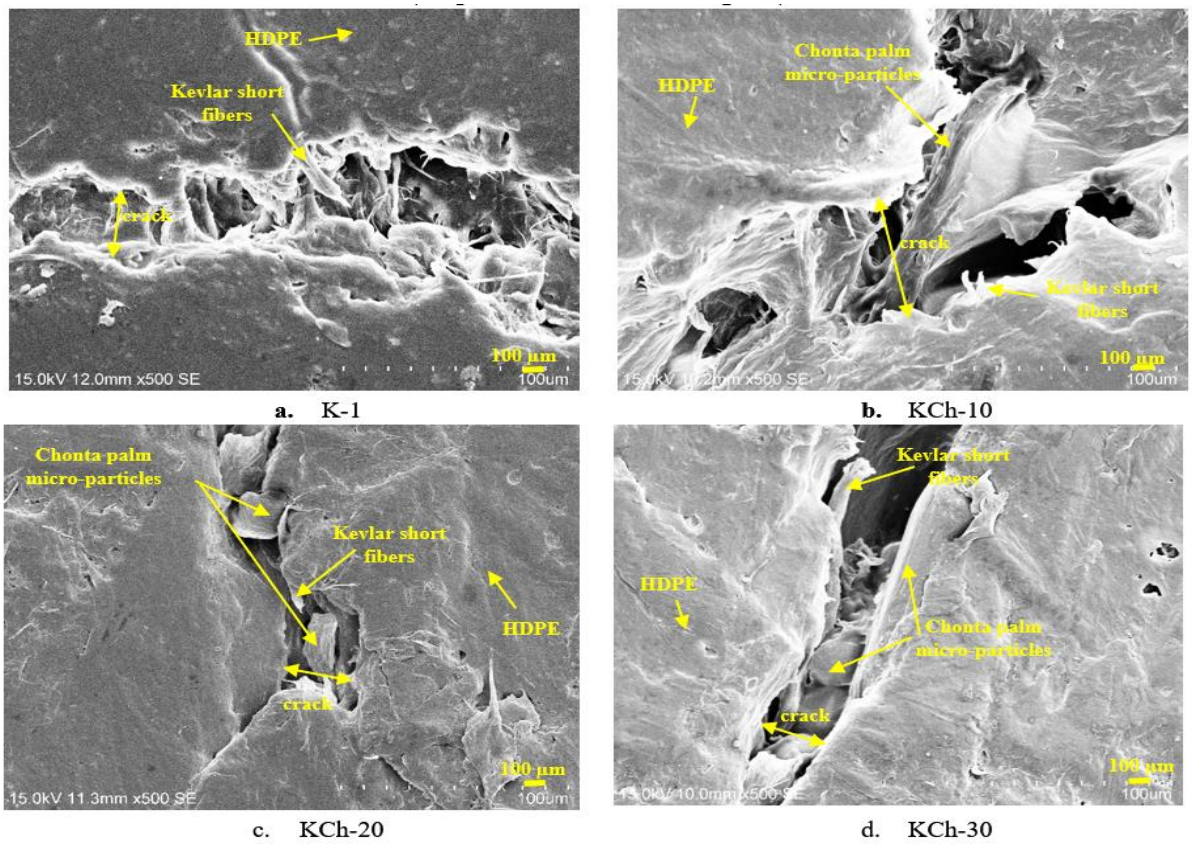

Fig. 7.6. Deformed and fractured of samples after dynamic shock loading (Impact momentum = 8.7 kg.m/s).

7.4.5 Energy absorbed at hybrid bio-composite targets under ballistic impact tests

The results of the ballistic impact test indicating the initial and exit velocities of the projectile after penetration of the bio-composite targets developed in this study are provided in Table 7.4. The average initial velocity of the projectile was determined to be 385 m/s, which is an average of six shots with a standard deviation of 6.2 m/s. The initial velocity is comparable to the muzzle velocity of 381 m/s for the same ammunition as provided in NATO specifications. In addition, the initial average energy of the six shots was estimated to be 593 J, with a standard deviation of 19 J, which is also consistent with the original muzzle energy value of 582 J for that ammunition in the NATO specifications. Moreover, all the samples were tested using the similar conditions of distance, temperature, and firing. Here, the absorbed energy from the target represents the loss in kinetic energy as the projectile perforates the target while the residual kinetic energy is the projectile energy that remains after the target is perforated by the projectile [131].

Table 7.4. Ballistic impact data sheet for the various hybrid bio-composite targets produced.

Targets	Initial velocity measured before impacts average (m/s)	Initial Energy average (J)	Velocity measured after impacts average (m/s)	Energy absorbed at targets average (J)	Energy absorbed above that K-1 control samples
K-1	385 ± 6.2	593 ± 19	367.9 ± 5.6	52.2 ± 16.3	0%
KCh-10	385 ± 6.2	593 ± 19	364.5 ± 3.1	62.4 ± 9.0	20%
KCh-20	385 ± 6.2	593 ± 19	365.6 ± 3.1	59.1 ± 9.0	13%
KCh-30	385 ± 6.2	593 ± 19	369.1 ± 2.2	48.8 ± 6.5	-6%

Figure 7.7a shows the energy absorbed by the various targets having similar target areal density. The plot of percentage increase in energy asorbed against the weight fraction of added wood particle is presented in Fig.7.7b. The energy absorbed by the control specimens, Kevlar® pulp reinforced HDPE (K-1), is estimated to be 52.2 J. A significant ballistic resistance enhancement was achieved in the hybrid bio-composite plates containing 10 wt.% of chonta palm microparticles (KCh-10), which exhibit the highest energy absorption of 62.4 J. This is equivalent to 20 % improvement over control specimens K-1 with similar thickness and density. The KCh-20 specimens containing 20 wt.% chonta palm micro-particles exhibited a 13 % increase in the energy

absorption (59.1 J) over K-1 samples. These results can also be related to the improvements achieved in material stiffness. On the other hand, hybrid bio-composites containing 30 wt.% chonta palm micro-particles (KCh-30) absorbed only 48.8 J of impact energy which is 6 % lower than the energy absorbed by composites containing no wood particle addition. Therefore, around 10 % chonta wood particles addition to Kevlar® pulp/HDPE composite may be considered an optimum wood particle content for best resistance to ballistic penetration. Higher amounts of the second reinforcement (milled wood fibers) can lead to an excessive accumulation of fibers or filler micro-particles in any region within the matrix. This will have detrimental effects on the impact resistance of the hybrid bio-composites. The saturation of wood particles is produced when the reinforcements become located very close to each other, leading to agglomeration, poor bonding, and a weak interface between agglomerated particles and the matrix. This accounts for the reduction energy absorbed observed for composite containing 20 and 30 wt.% wood particles.

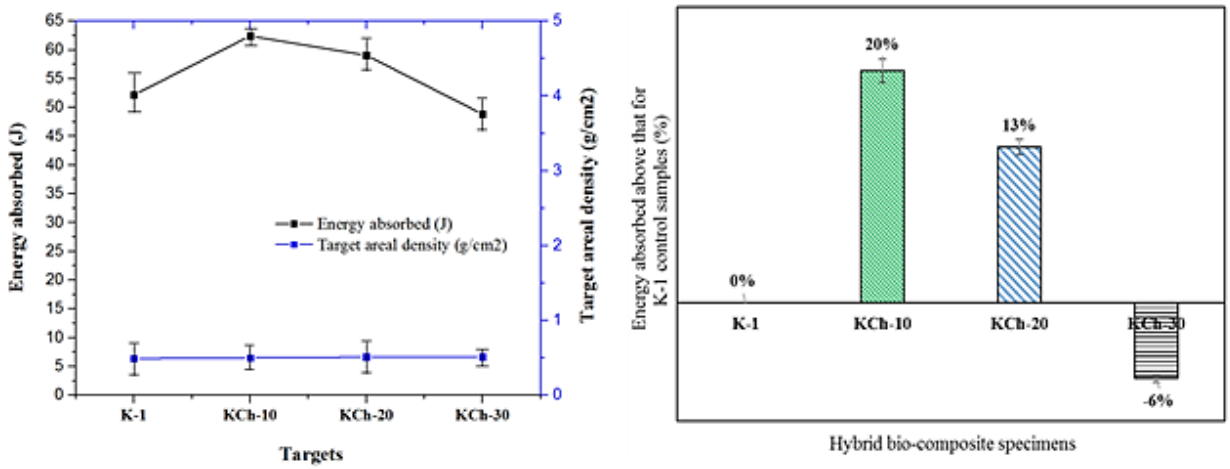

a) Energy absorbed by targets during ballistic testing of composites with similar density

b) Improvements of the energy absorption compared to K-1 control sample (% increase)

Fig. 7.7. Energy absorbed by hybrid bio-composites containing chonta palm microparticles.

The results of the SEM investigations of the transverse section of the perforations in the targets after the ballistic impact testing are presented in Fig.7.8. These micrographs provides information on the deformation, penetration and the sequence of damage in the targets during ballistic impact. The deformation and penetration of the targets are influenced by the projectile shape (round nose), impact velocity as well as physical and mechanical properties of the targets. The damage sequence starts with an indentation on the frontal face of the target, which is produced by a localized stress at the point of impact. The pressure exerted by the projectile creates a small puncture. A ductile

crater enlargement can be observed at the bullet entry orifice. Horizontal striations were observed on target perforation surface (Fig.7.8 bullet entry orifice), which ocurred by lands and grooves that come from the rifling process of the ogive. The impression marks are charactheristics of bullet as it travels through the target. Figure 7.8 also shows the bullet exit orifice, exhibiting a large material detachment indicated by short Kevlar® fibers and chonta palm microparticles exposure. This fracture is associated with the projectile exit after the total penetration. Difference in behavior in terms of material detachment was observed in the targets, as a result of their different energy absorption capability and resistance against ballistic impacts. For example, the amount of fiber-pull out and material detachment in the KCh-10 and KCh-20 targets, was observed to be lower than for other specimens. This material behavior is in agreement with the energy absorption results presented in Table 7.4. The improved resistance to material detachment during perforation can be considered to be responsible for the greater energy absorption and better resistance to projectile penetration in these specimens.

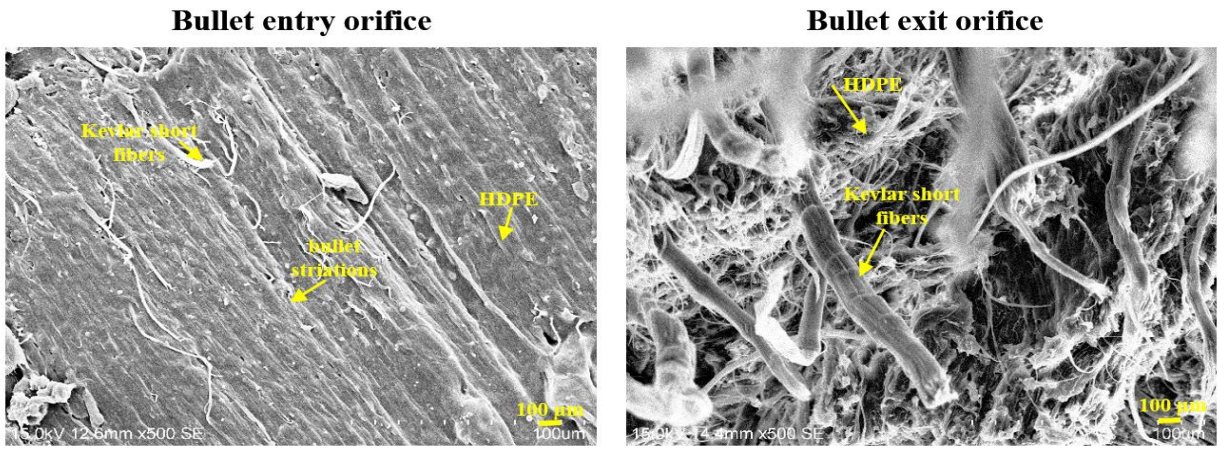

a. K-1

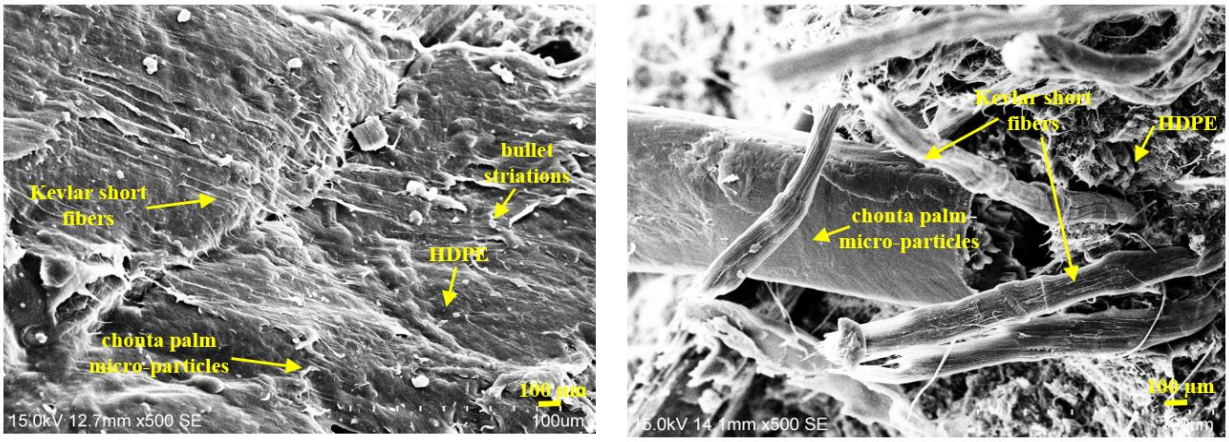

b. KCh-10

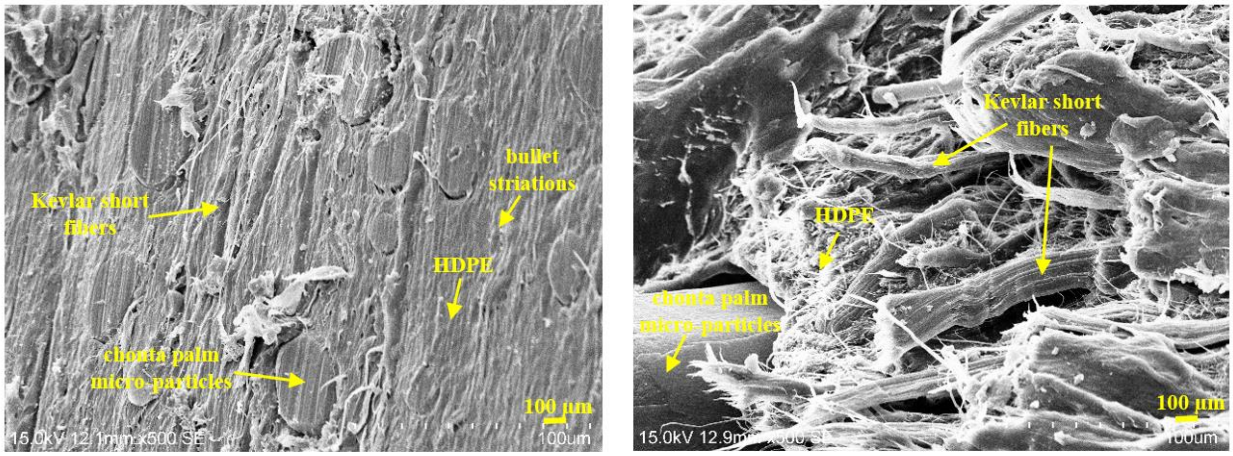

c. KCh-20

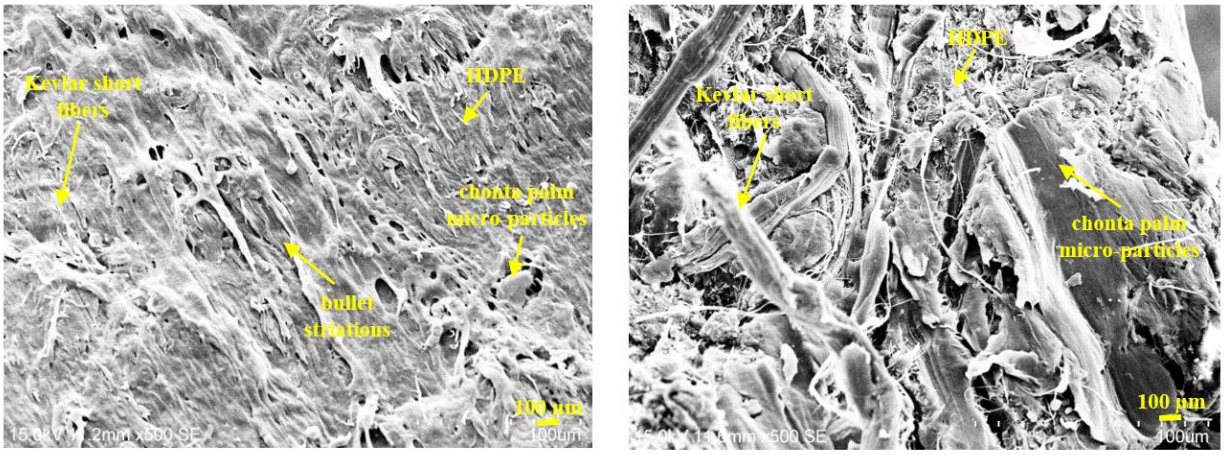

d. KCh-30

Fig. 7.8. Fracture surface along perforation on the targets (transverse section).

7.5 Conclusions

Hybrid bio-composites were prepared by incorporating organic micro-fillers into short Kevlar® fibers reinforced HDPE matrix composite. The organic fillers used as second reinforcement are organic chonta palm wood micro-particles in different proportion (10, 20, and 30 wt. %). The effects of this second filler addition on the quasi-static tensile strength, crystallinity, dynamic compressive strength and ballistic impact resistance of the hybrid bio-composites were investigated. Material characterization showed that the addition of the micro-fillers reduces the tensile strength of the Kevlar® short fiber reinforced HDPE. However, such addition improved the materials' stiffness. XRD analysis revealed that the crystalline structure of Kevlar® fiber reinforced HDPE remained unchanged with the addition of the organic wood particles. However,

the intensity of the crystalline peaks decreased with increasing content of the organic micro-fillers. Microstructural analysis indicated that the size of the organic micro-particles, their alignment and distribution could affect the bonding with Kevlar® short fibers within HDPE matrix. The dynamic shock loading test revealed optimum impact resistance by hybrid composites containing 10 wt.% Chonta wood particles in addition to the short Kevlar® fibers. An excessive accumulation of fibers or filler micro-particles in any region within the matrix will have detrimental effects on the impact resistance of the hybrid bio-composites. This can be attributed to formation of weak interface between agglomerated fibers or particles with the polymer matrix. Similarly, the results of the ballistic impact test revealed that the composites containing 10 wt.% of organic wood particles exhibited the highest capacity for energy absorption during ballistic impact. Reinforcing HDPE with Kevlar® pulp and organic micro-fillers (not more than 10 wt. %) result in hybrid bio-composites with an enhanced performance under dynamic mechanical loading.

Chapter 8: Dynamic and Ballistic Impact Behavior of Biocomposites Armors Made of HDPE Reinforced with Chonta Palm Wood *(Bactris gasipaes)* Microparticles

8.1 Overview

Bio-composites are produced with wood palm micro-particles reinforced HDPE. This is different from the composites produced and discussed in Chapter 7 in that they contain no synthetic fibre (Kevlar®). The impact resistance and energy absorption capability of the obtained bio-composites under high strain-rate compressive and ballistic impact loading conditions are presented and discussed. The research findings reported in this chapter have been published as manuscript #5 in the Journal: *Defence Technology* as follows:

E.E. Haro, J.A. Szpunar, A.G. Odeshi, "Dynamic and ballistic impact behavior of biocomposite armors made of HDPE reinforced with chonta palm wood (*Bactris gasipaes*) microparticles", *Defence Technology,* vol. 14, no. 1, pp. 238–249, 2018 [156].

The contributions of the PhD candidate to this manuscript are: 1) experimental design, 2) preparing and processing all the bio-composite samples; 3) physical, microstructural and mechanical characterization of the composites and 4) development of the manuscript for publication. The manuscript was reviewed by my supervisors before it was submitted for publication in this journal. To avoid repetition, selection of the materials, target preparation, and composite characterization have been removed from this chapter. Likewise, the references of the submitted manuscript are listed at the end of the thesis.

8.2 Abstract

The mechanical behavior of chonta palm wood (*Bactris gasipaes*) microparticles reinforced high density polyethylene (HDPE) under high strain-rate compressive and ballistic impact loading were investigated. The palm wood microparticles were introduced into the HDPE via an extrusion process using parallel twin screw extruder to produce biocomposite containing 10, 20, 25, and 30 wt.% chonta wood microparticles. In addition to mechanical tests, fractographic analysis was done to understand the failure mechanism in the biocomposites under dynamic and ballistic impact loads. The results indicate that both quasi-static and dynamic mechanical properties of HDPE are enhanced by reinforcement with chonta palm wood particles. The biocomposites containing 25 wt.% wood microparticles exhibited the highest strength, stiffness, ballistic impact resistance and impact energy absorption capability. Introduction of microparticles of chonta palm wood as reinforcement into a polymeric matrix such as HDPE therefore offers a promising method to develop biocomposites with enhanced capacity to withstand dynamic impact loading and absorb impact energy.

Keywords: Biocomposite armors; high density polyethylene; chonta palm wood microparticles; split Hopkinson pressure bar; ballistic impact.

8.3 Introduction

Development of polymer biocomposites using natural fibers or wood particles as the reinforcing components is gaining increasing attention since synthetic fibers are expensive, non-biodegradable and their production is energy consuming, with the attendant negative impact on the environment [53]. The use of wood fibers and wood flours as reinforcement in thermoplastics have been intensified due to their several advantages over the traditional synthetic fibers like glass, carbon and Kevlar® fibers. Reinforcing polymer with wood fiber or particles enables the development of innovative, lightweight, strong, and low-cost materials that can find application in different areas of engineering. Most importantly, natural fibres are renewable, recyclable and biodegradable materials [157-159], which are very crucial for environmental sustainability.

Chonta palm (*Bactris gasipaes*), also called pupunha palm, peach palm, or heart palm has origin in the tropical Latin American regions (Amazonia). Peach palm fruits are used in great proportion as food and oil products. Chonta wood palm is believed to be one of the hardest woods in the

Amazonia for its strong and durable fibers and they can be used to make crafts, building parts, and weapons for hunting and fishing [80]. Because of these properties, chonta palm fibers or wood particles offers innovative resource for reinforcement for polymer matrix composites. For example, heart palm residues have been used to build agglomerate and plywood panels, chopped fibers and polyurethane resins were mixed in a plywood mold, resulting in panels that can meet the ANSI 208.1 standard for flexural strength of particle boards [160]. Temer and Almeida [161] investigated the tensile properties of heart palm fibers and reported a low tensile strength, but a relatively high Young modulus that is superior to those of other palm fibers such as coir or piassava, and comparable to those of traditional lignocellulosic jute and sisal fibers.

Wood-plastic composites (WPCs), also called biocomposites, are polymer matrix composites containing wood fibers, whiskers or particles as organic reinforcing components. The polymer matrix could be thermoplastic such polypropylene, polyethylene among others, or even thermosetting resin such as epoxy. Chemical additives can be introduced during the manufacture process to improve the bonding between components of the WPCs. The reinforcing organic component improves mechanical and thermomechanical properties of the polymer matrices, those properties and mainly strength properties can be controlled depending of the type of natural reinforcement (particles, fibers, whiskers) and the volume fraction of the reinforcing components [49, 162-165].

Biocomposites produced using different natural fiber reinforcements such as cotton, jute, flax, hemp, ramie and sisal fibers have been widely reported. For example, jowar fibers have been used to reinforce polyester, resulting in biocomposites with higher strength and rigidity for light weight applications compared to the polymer reinforced with the conventional sisal or bamboo fibers [162]. Reinforcement with oil palm empty fruit bunch fibers (OPF) has been reported to improve the tensile modulus and impact resistance of polypropylene and polyester resin, although the tensile modulus of epoxy resin decreased as a result of reinforcement with OPF [166]. Reinforcing polymer with Kenaf (KE) and palm empty fruit bunch fibres (EFB) resulted in increased tensile strength and flexural strength of polymer and the strength of the resulting composite increase as the weight fiber was increased to 40 %. However, increasing fiber content in excess of 60 % led to deterioration of properties, which was attributed to excessive clustering of fibre leading to debonding under mechanical load [167]. It was reported that the flexural strength of polypropylene

increased while the Charpy impact strength dropped when the polymer was reinforced with the heart-of-peach waste residue [81]. On the other hand, Farias *et al*. [168] reported 157% increase in Izod impact strength of polyester when reinforced with leaf stalk fibers extracted from peach palm. Santos *et al*. [169] reported no significant improvement in tensile and impact properties of peach palm fiber reinforced polyester as a result so surface treatment of the fiber with NaOH or C_3H_3N. However, the composite's impact strength improved after surface treatment with H_2O_2, although surface treatment of the peach palm fiber did not improve the tensile strength of the composites.

Pupunha or heart palm in different varieties such as short and long fibers, leaf-stalk, and residues after harvest have been used to reinforce different polymeric matrices [81, 160, 161, 167-169]. To the best of our knowledge, however, the dynamic impact response and the energy absorption behavior of the biocomposites produced with heart palm fiber or particles under ballistic impact loading have not yet been reported. In the current study, microparticles of chonta palm wood are used in reinforcing high density polyethylene (HDPE) to develop high performance biocomposites. The impact resistance and energy absorption capability under ballistic impact as a result of this particulate reinforcement are investigated and discussed in this paper.

8.4 Results and Discussion

8.4.1 SEM analysis of the microstructural configuration

SEM micrographs of a cross section of the composite (Fig. 8.1) show dispersion of the palm wood micro-particles within HDPE matrix. The micro-particles with sizes varying between 0.5 and 0.75 mm can be identified clearly on the micrographs. A heterogeneous particle distribution with random orientation can be observed in the microstructure of the composite. Agglomeration of chonta wood particles, caused by the excessive reinforce filler proportion, can be observed in the microstructures of Ch25 and Ch30 composites.

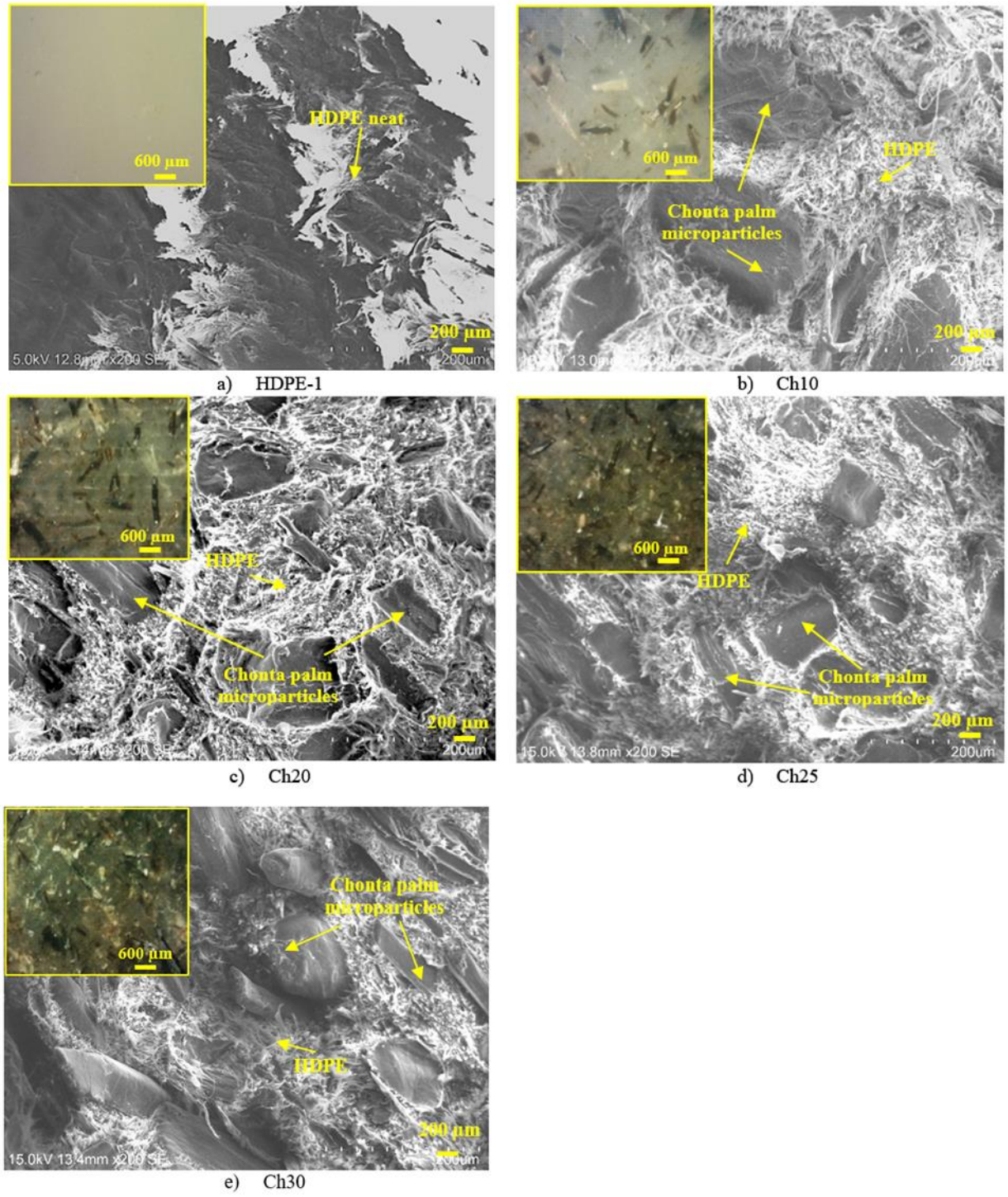

Fig. 8.1. SEM images showing microstructural morphology on the transverse section of bio-composite specimens.

The physical properties of the obtained bio-composite plates (20 x 20 cm) are summarized in Table 8.1. It was observed that color and transparency of the material varied as the volume fraction of

the chonta wood microparticles was increased, the color become darker and the transparency reduced as the content of reinforcement was increased.

Table 8.1. Experimental data sheet showing the physical properties of neat and reinforced HDPE samples (target plates: 20 x 20 cm).

Targets configuration	HDPE 1	Ch10	Ch20	Ch25	Ch30
Chonta palm wood micro-particles (wt. %)	0%	10%	20%	25%	30%
HDPE 2990 (wt. %)	100%	90%	80%	75%	70%
Target weight average (g)	193.2 ±1.2	194.5 ±1.0	187.3 ±2.3	190.7 ±4.3	191.6 ±2.4
Target thickness average (mm)	4.9 ±0.1	5.0 ±0.3	5.0 ±0.2	4.7 ±0.2	5.2 ±0.4
Target areal density (g/cm^2)	0.48	0.49	0.47	0.48	0.48
Target density (g/cm^3)	0.95	0.95	0.94	1.00	0.91

The results of water absorption test on the composite materials are presented in Fig. 8.2. Water absorption was determined to be less than 0.2 % for all samples after soaking in water for 2 and 24 hours. HDPE-1 specimens did not show any indication of water absorption at all. This is not unexpected as it is 100 % polymer with no wood particle reinforcement or porosity. After about 2 and 24-hour immersion in distilled water, it was observed that the amount of water absorbed increased gradually as the weight fraction of the wood particles was increased to 25 %. The increase only ranged between 0.002 and 0.007 % for 2 and 24-hour exposure time, which is minimal and may not have any consequential effect on the integrity of the biocomposites if exposed to water. A much steeper increase was, however, observed when the wood particle reinforcement was increased from 25 wt.% to 30 wt. %. An increase in water absorption of up to 0.040 % was recorded for Ch30 composites after 24-hour exposure. The higher content (30 wt. %) of the chonta wood particles caused a particle agglomeration leading to inhomogeneous distribution of the wood particles in the biocomposites. Debonding between agglomerated particles and pores between them and the polymer matrix is responsible for the greater tendency of composites containing higher particle content to absorb water (Fig. 8.1e). A number of previous investigations have also reported that the water resistance of HDPE composites is influenced by the type of natural fibre used as reinforcement, the fiber weight fraction, micro voids formed at the bonding between the components, and the fiber size [142, 143, 170].

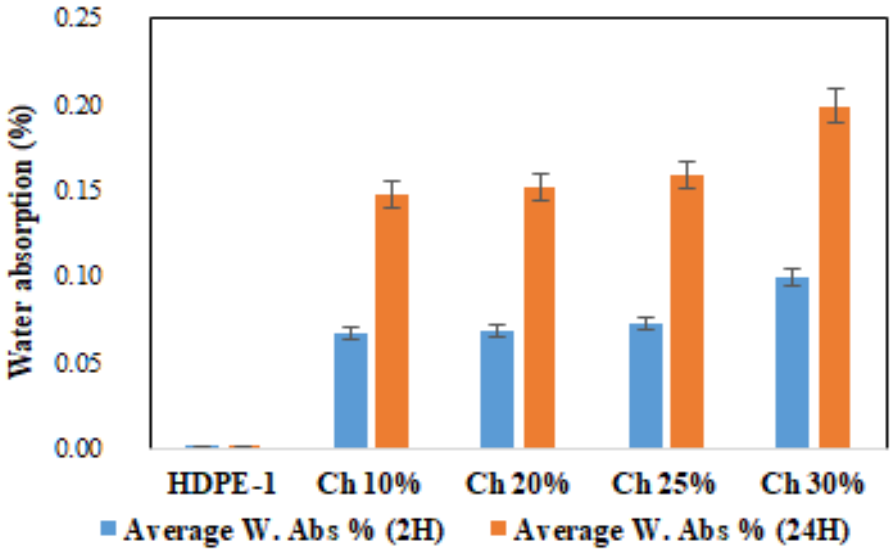

Fig. 8.2. Percentage water absorbed by HDPE (neat) and bio-composite specimens.

8.4.2 Tensile test results

The results of the tensile test of the bio-composite are summarized in Table 8.2. The plots of increase in tensile strength and Young modulus as a result of the wood particle reinforcement of the HDPE are presented in Fig. 8.3. It is evident from these plots that reinforcement of the HDPE with the chonta wood micro-particles resulted in a marginal increase in tensile strength, but in a considerable increase in Young modulus. Both strength and Young modulus increased as the weight fraction of the microparticles was increased from 0 to 25 wt. %. However, as the fraction of the particles was increased from 25 to 30 wt. %, both tensile strength and Young modulus dropped. This suggests that chonta particles fraction in excess of 25 wt.% is not beneficial in chonta palm particles reinforced HDPE bio-composites.

Table 8.2. Tensile strength and Young modulus of reinforced and unreinforced HDPE samples.

Bio-composite specimens	Tensile strength σr (MPa)	Strain (Ɛ) (%)	Young's Modulus (MPa)
HDPE 1	14.91 ± 1.77	5.38 ± 1.12	496.8 ± 21.2
Ch10	16.16 ± 1.15	5.45 ± 1.57	724.7 ± 17.4
Ch20	16.47 ± 1.05	6.00 ± 1.36	742.2 ± 13.2
Ch25	16.53 ± 0.27	4.89 ± 1.47	798.9 ± 17.3
Ch30	15.19 ± 0.83	5.13 ± 1.48	730.2 ± 12.1

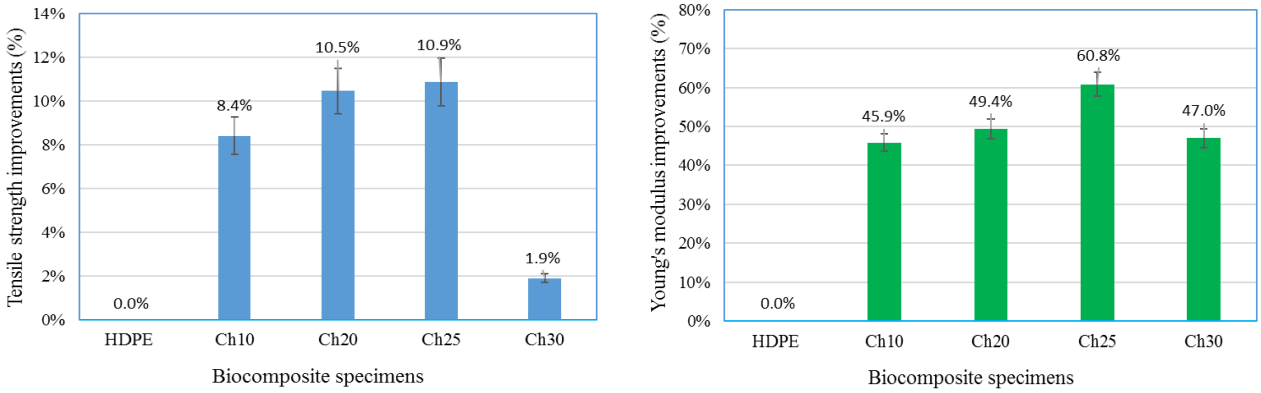

a) Tensile strength b) Young's modulus

Fig. 8.3. Tensile property improvement in the biocomposites relative to the unreinforced HDPE.

The highest tensile strength was recorded for Ch20 and Ch25 specimens, which is due to more particles available for reinforcement compared to the Ch10 composite. The lower tensile strength of the Ch30 specimens is attributable to excessive amount of particles used for reinforcement. This affected the homogeneous distribution of the fillers leading to agglomeration of micro-particle agglomerations in random areas within the polymeric matrix (Fig. 8.1e). Fracture occurred more readily in the Ch30 specimens because of the weak bong between agglomerated particles with the HDPE matrix. This impair failure resistance when loaded in tension. This explains why the tensile strength of the bio-composite dropped as the wood particle content was increased from 25 to 30 wt. %. Young's modulus increases ranging between 46 and 61 % also was observed as a result of the reinforcement of HDPE with chonta wood particles. Properties of typical thermoplastic polymers, have been reported by Ku *et al.* [171]. Their report on tensile strength of HDPE (14.5 – 38 MPa) and its elastic modulus (400 – 3800 MPa) are within the range obtained in this study.

The reduction in Young modulus as the fraction of wood particle was increased from 25 to 30 wt.% can also be traced to the uneven particle distribution caused by particle coalescence within the bio-composites. It has been reported that an excess of fibers as reinforcement in composite materials can lead to saturation of the matrix as fibers become located closer to each other, resulting in fiber agglomeration and a reduction in stress transfer between the matrix and the reinforcement [154, 155]. Similarly, in other research, an optimum flexural strength was achieved in polypropylene matrix composites containing 30 wt.% filler, and reduction in strength was observed when the filler content was raised to 40 wt.% [81]. In general, the properties of wood polymer composites (WPCs) are combinations of the individual properties of their components: wood particles, the polymer matrix, and the bonding developed between them. For example, the strength and stiffness of the matrix can be enhanced by the fillers (wood particles), if strong adhesion between the particles and the polymer is achieved during WPCs manufactured [172].

8.4.3 Dynamic mechanical behavior under impact loading

The results of the dynamic impact test on the HDPE neat and the bio-composites are summarized in Table 8.3. As it can be seen, the impact momentums generated different strain rates ranging between 895 and 2883 s^{-1} depending of the impact deformation resistance of test specimens. Therefore, depending on the weight fraction of the wood microparticles in the composite, which determine its deformation and failure resistance, the strain rates generated in the composites varied for the same impact load (momentum).

Table 8.3. Dynamic impact properties of the biocomposites and neat HDPE.

Pressure (Impact omentum)	Specimens	Max Strain rate (s^{-1})	Max Stress (MPa)
50 kPa (4.0 kg.m/s)	HDPE-1	969	247
	Ch10	1148	296
	Ch20	1202	318
	Ch25	1277	336
	Ch30	895	295
60 kPa (6.8 kg.m/s)	HDPE-1	2129	276
	Ch10	2022	347
	Ch20	2224	360
	Ch25	1953	404
	Ch30	1803	299
70 kPa (8.7 kg.m/s)	HDPE-1	2851	308
	Ch10	2642	357
	Ch20	2686	362
	Ch25	2883	372
	Ch30	2408	347

Dynamic stress-strain curves obtained from impact test of the composites are presented in Fig. 8.4. The stress-strain curves indicate initial elastic deformation region up to about 100 MPa, beyond which the stress-strain curves become non-linear. The stress continues to steadily increase with strain until a maximum stress is reached, after which the stress values begin to drop. The higher the impact momentum, the higher is the strain rate and the higher is the maximum flow stress attained before the onset of the fracture. The HDPE neat exhibited the least resistance to deformation at high strain rates. The maximum flow stress increased marginally as the mass fraction of the wood particles was raised to 25 % and decrease with further increase in the mass fraction of particles in the HDPE. The results are similar to those obtained under quasi-static tensile loading of the same biocomposite produced in this study. According to dynamic stress-strain curves and in correlation with the results obtained in Table 3, it is possible to determine that higher strain rates are obtained with the biocomposites with highest impact resistance (Ch20 and Ch25), and thus, also the elastic range achieved by these specimens are higher than the others obtained by the rest of biocomposites. Firdaus *et al.* [92] obtained similar results from dynamic compressive testing of jute and kenaf fibers reinforced unsaturated polyester using SHPB technique; highest stress values were achieved under the highest applied strain rate of 1340 s^{-1} with the jute fiber

reinforced composites (JFRC) attaining a higher maximum stress than the kenaf fiber reinforced composites (KFRC).

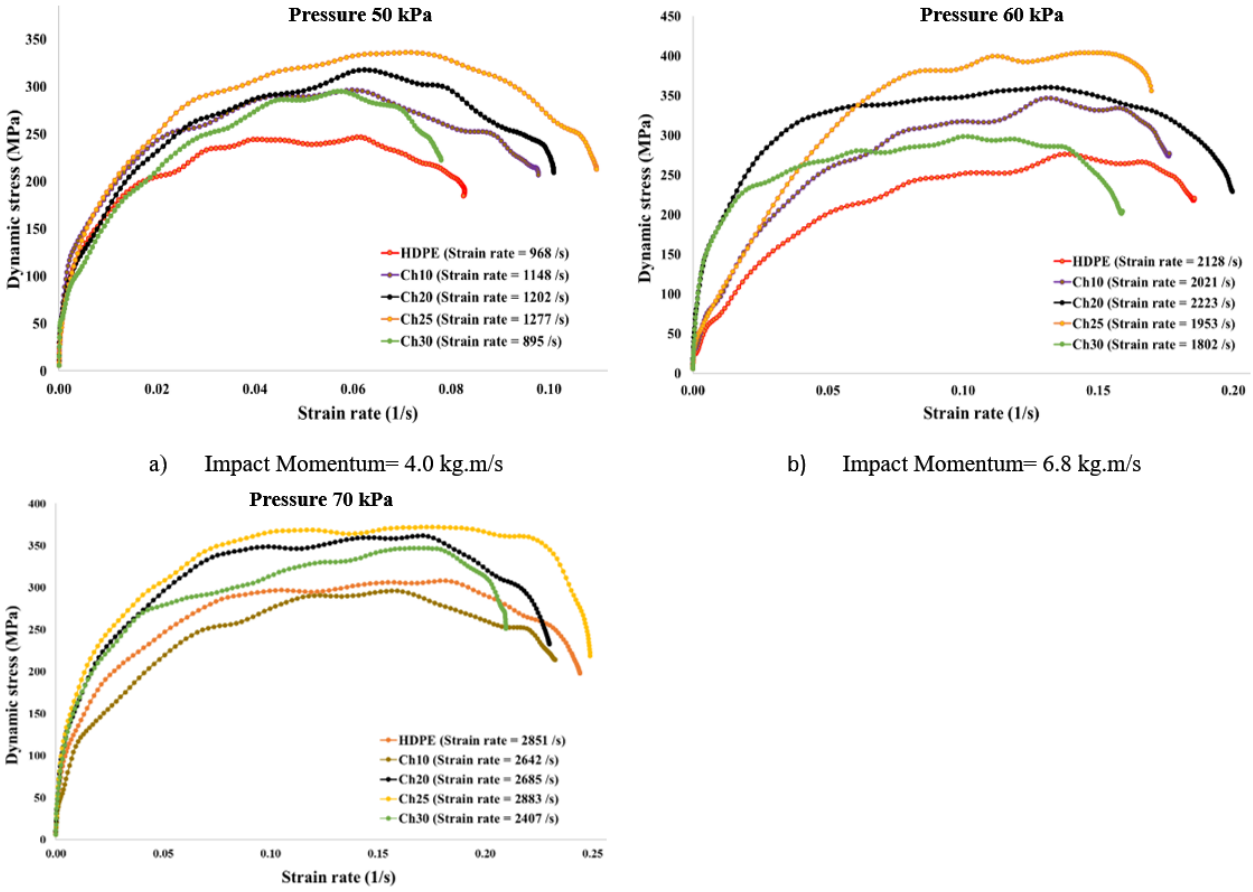

a) Impact Momentum= 4.0 kg.m/s

b) Impact Momentum= 6.8 kg.m/s

c) Impact Momentum= 8.7 kg.m/s

Fig. 8.4. Dynamic stress–strain curves of the bio-composite specimens under dynamic impact loading.

All the impacted reinforced polymers specimens were observed to experience extensive plastic deformation without rupture when impacted at the lowest momentum of 4.0 kg.m/s. The reason of this behavior can be traced to the plasticity of the thermoplastic polymeric matrix. As the impact momentum was raised to 6.8 kg.m/s, small cracks were observed in the bio-composites containing 20 and 25 wt.% wood particles (Ch20 and Ch25). However, those biocomposites containing 10 and 30 wt.% micro-particles (Ch10 and Ch30) suffered extensive cracks, which demonstrated a lower impact resistance at these conditions.

Typical SEM and optical micrographs of the impacted specimens subjected to an impact momentum of 8.7 kg.m/s are presented in Fig. 8.5. The HDPE neat specimens deformed extensively but did not rupture. However, small cracks were observed on the impacted surface (Fig. 8.5a). The extensive plastic deformation experienced by the unreinforced HDPE (neat) specimens is typical of thermoplastic matrix under dynamic load [15]. On the other hand, the bio-composites containing palm wood micro-particles fractured and ruptured at this impact momentum (Fig. 8.5 b-e). The failure tendencies of samples Ch20 and Ch25 were observed to be less severe (Fig. 8.5 c, d) when compared with those of Ch10 and Ch30 specimens that experienced extensive fracture (Fig. 5 b, e). Thus, Ch10 and Ch30 specimens exhibited lower resistance to deformation and failure under dynamic impact loading.

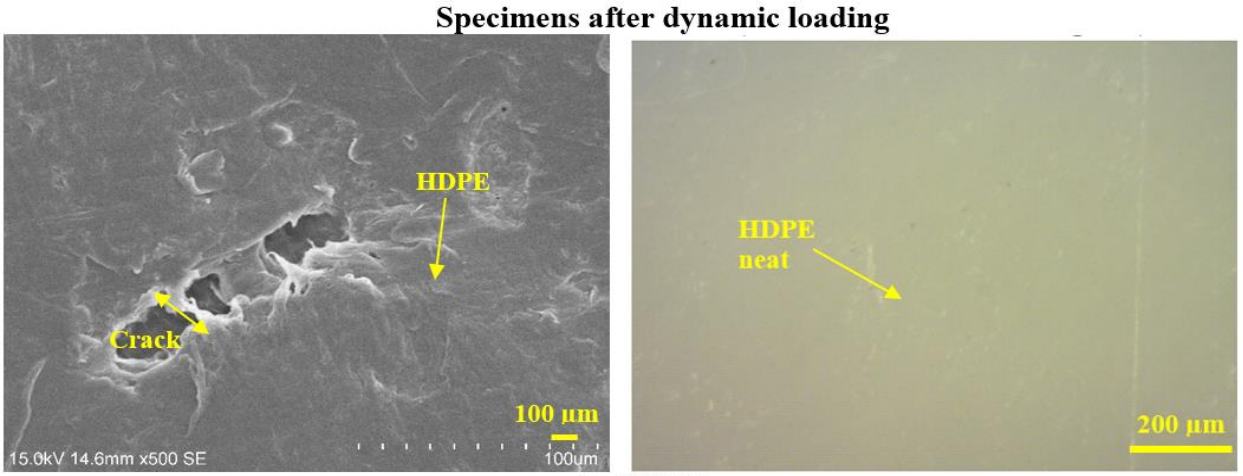

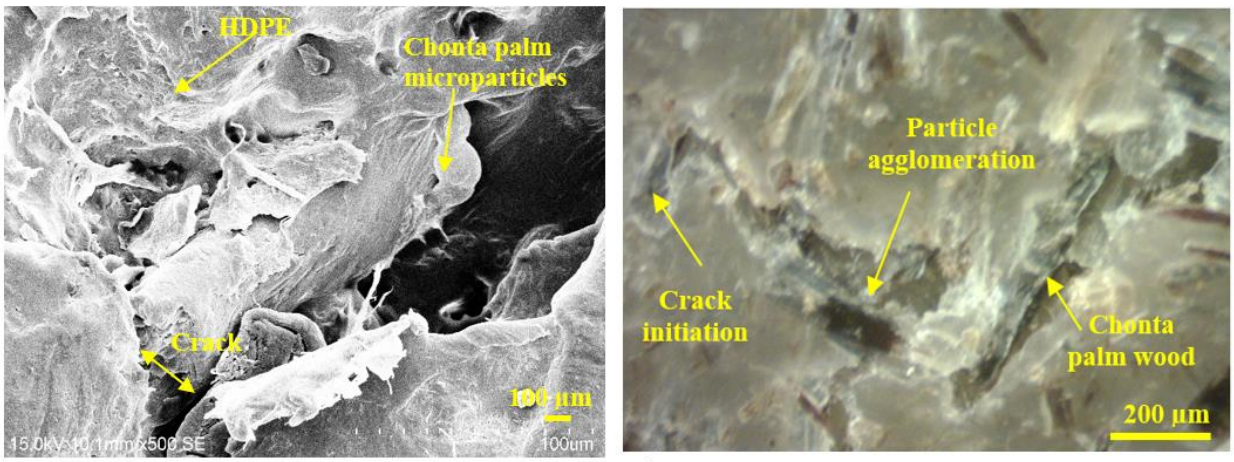

c) Ch20

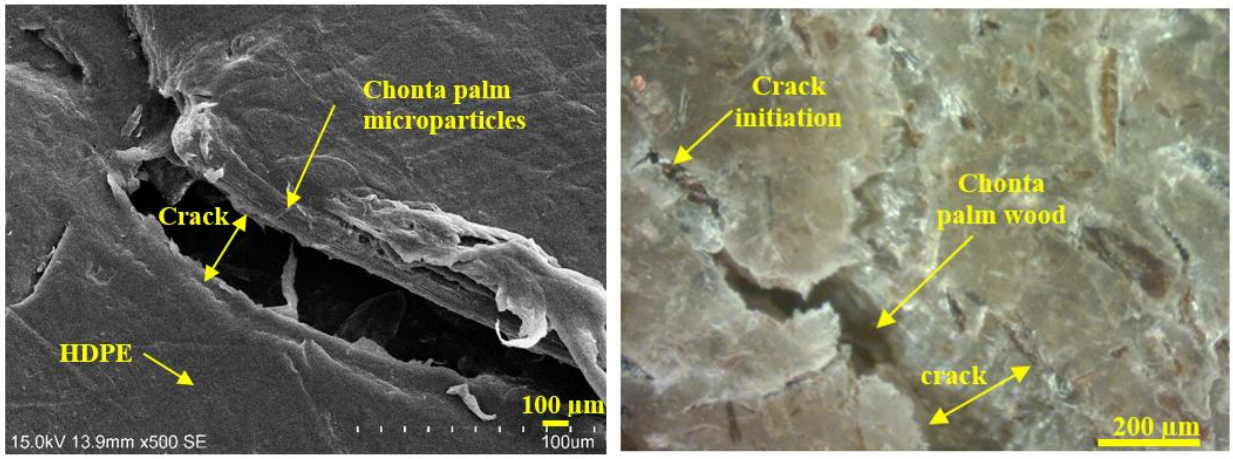

d) Ch25

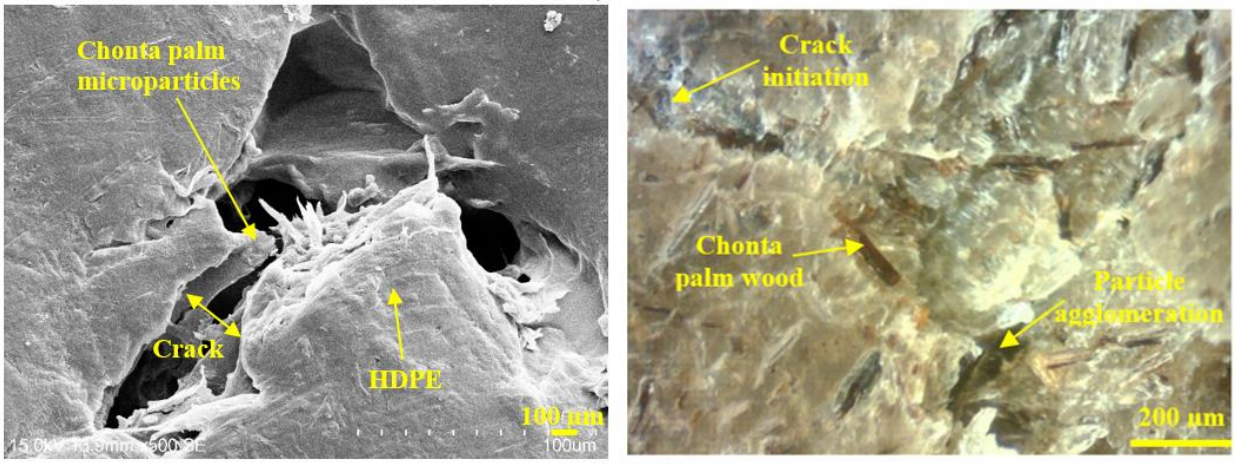

e) Ch30

Fig. 8.5. SEM and optical micrographs of deformed and fractured specimens after dynamic impact loading (average impact momentum = 8.7 kg.m/s).

In this analysis, a similar crack initiation pattern was observed in all the bio-composites and more often in small regions where agglomeration of chonta palm microparticles occurs. Particle-matrix debonding, matrix cracking and cracking bridging by the chonta wood particles were observed in the microstructure of impacted composites. Also, it was noted that the weight proportion of the reinforcements and particle size affect the crack propagation, most especially when a particle with average size 0.7 mm or higher aligns perpendicularly to the direction of impact loading (Fig. 8.5 b-e). This suggests that particle-matrix debonding between components in bio-composites can be affected by reinforcement particle size, particle orientation, and particle agglomeration in the polymeric matrix. It has also been reported in the literature that the failure modes in polymer matrix composites include: matrix deformation and cracking, fiber-matrix debonding, fiber breakage, and combination of two or more of these failure modes [15].

8.4.4 Results of ballistic impact tests

The results of the ballistic impact test conducted on the specimens, indicating initial and residual velocities of the projectile after complete penetration of the various targets by the projectiles, are summarized in Table 8.4.

Table 8.4. Ballistic impact data sheet for the various bio-composite targets produced.

Targets	Initial velocity measured before impacts average (m/s)	Initial Energy average (J)	Velocity measured after impacts average (m/s)	Energy absorbed at targets (J)	Energy absorbed (%) in relation HDPE pure
HDPE-1	385	593	372.8 ± 2.5	37.8 ± 7.3	0.0%
Ch10	385	593	371.4 ± 1.1	42.1 ± 3.1	11.5%
Ch20	385	593	370.6 ± 1.8	44.5 ± 5.2	17.6%
Ch25	385	593	367.6 ± 1.4	53.4 ± 4.2	41.3%
Ch30	385	593	371.6 ± 1.5	41.4 ± 4.4	9.5%

The six shots were fired on each target, which maintained a dimensional stability after being penetrated by the projectiles. The orifices of entrance and exit of the projectiles were measured; the penetration diameters at the bullet entry side of the target ranged from 10 to 12 mm. The diameter of perforated hole at the exit side of the plate range between 14 and 18 mm (Fig. 8.6).

The average distance between shots also was recorded to range from 15 to 28 mm (measured from edge to edge of the exit orifices).

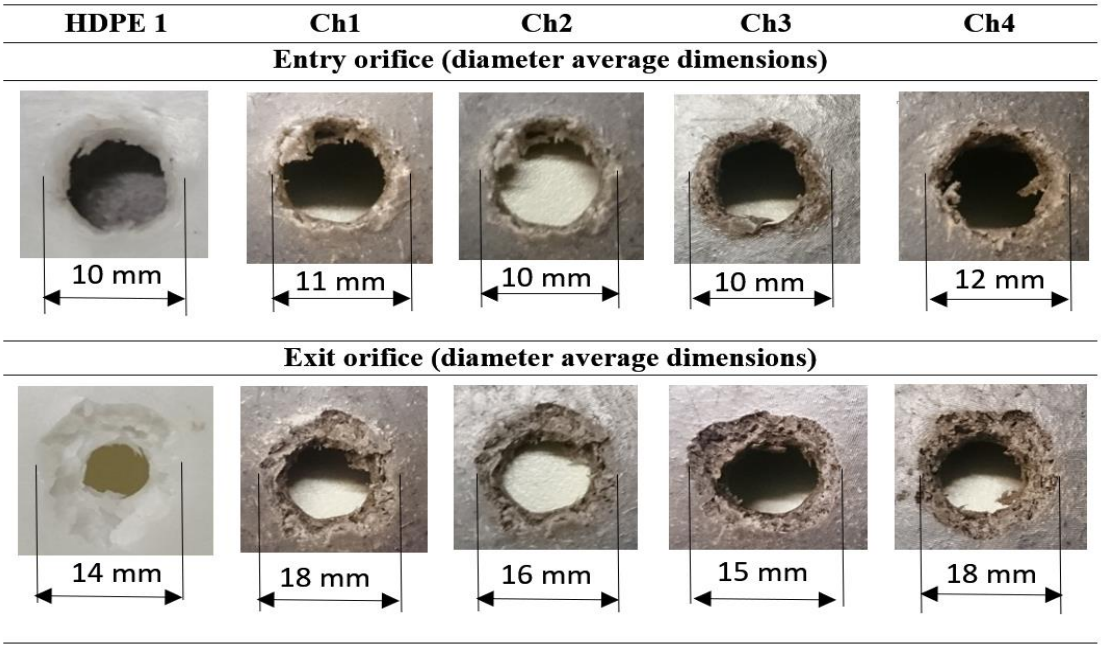

Fig. 8.6. Average diameter of the projectile orifices at the entrance and exit of targets after the ballistic impact tests.

The average initial velocity of the projectile was determined to be 385 m/s. This is an average of six shots with a standard deviation of 6.2 m/s. This initial velocity is comparable to the muzzle velocity of 381 m/s for the same ammunition as provided in NATO specifications. This average initial velocity was determined to produce an average initial energy of 593 J, with a standard deviation of 19 J, which also satisfies the initial muzzle energy value of 582 J provided in NATO specifications. Moreover, all the samples were tested using the similar conditions of firing distance, temperature and type of riffle and ammunition used. The energy absorbed by the target represents the loss in kinetic energy as a result of elastic and plastic deformations while the residual kinetic energy is the projectile energy that remains after the target is perforated by the projectile [131].

The absorbed energy of the targets containing different proportion of chonta wood particles as micro-fillers are presented in Table 8.4. The lowest energy absorption of 37.8 J was recorded for plates made of HDPE neat (unreinforced). Similar results were obtained in an earlier study by Mohagheghian *et al.* [98], who determined the energy absorption in HDPE to range between 35

and 38 J. In the current study on the ballistic performance of the chonta wood particles reinforced HDPE, the biocomposites specimens containing 25 wt.% of fillers (Ch25) exhibited the highest energy absorption of 53.4 J, which represents a 41.3% improvement over the unreinforced HDPE specimens with similar thickness and density. This is followed by targets containing 20 wt.% chonta particles (Ch20), for which the energy absorbed was determined to be 44.5 J, representing a 17.6% improvement over HDPE neat. On the other hand, biocomposites containing 10 and 30 wt.% of palm wood fillers absorbed 42.1 and 41.4 J, corresponding to 11.5 and 9.5 % improvement over the unreinforced HDPE neat. Thus, the biocomposite targets Ch20 and Ch25 offered the best ballistic impact resistance. These results have strong correlation with the data obtained for the dynamic impact and quasi-static tensile tests. The results of the ballistic impact test suggest that introduction of wood palm microparticles into a HDPE improves its energy absorption capability. The ballistic performance of natural fiber composites has been reported to be significantly influenced by the type of the applied fibers. For example, the response of natural fibre composites made of flax, hemp, and jute fabric and polypropylene matrix was studied under ballistic impact by fragment simulating projectiles [173]. In this research, flax composites were reported to absorb more impact energy (52.5 J) than the composites made of hemp (39.0 J) and jute (30.5 J) fabrics. The results of the current study suggest that the biocomposite specimens and the HDPE samples were able to absorb about 6.3 to 9.0 % of the ballistic impact energy. There is therefore a need to couple the biocomposite with a metal, such as aluminum alloy, to form light weight hybrid material system for use as protective armor.

SEM micrographs of the fracture surface of the biocomposites along the longitudinal section of perforation after projectile penetration are presented in Fig. 8.7. These micrographs provide information on the deformation and the sequence of ballistic impact damage of the targets during projectile penetration. The damage sequence involves an indentation on the impact surface produced by a localized stress in the region of initial contact. The pressure exerted by the projectile creates a small puncture. At the initial stage of penetration, a ductile crater enlargement can be observed at the initial entry orifice (Fig. 8.7 a-e). Horizontal striations were observed, which are characterized by lands and grooves that come from the rifling process of the ogive. The impression marks of the bullet are unique characteristics of a typical projectile as it travels through the barrel. At the bullet exit orifice, characterized by large material detachment, exposure of chonta palm micro-particles, plastic deformation, and matrix fracture due to projectile perforation can be

observed (Fig. 8.7 a-e, final exit orifice). These results suggest that the amount of material detachment during ballistic penetration is influenced by the impact resistance of the target. For example, Ch20 and Ch25 plates, which have the highest impact resistance, also exhibited the lowest amount of material detachment compared to the other targets (Fig. 8.7 c, d, final exit orifice). The improved mechanical and dynamic properties are responsible for the greater energy absorption and better resistance to projectile penetration in these specimens. Thus, these results suggest that incorporation of chonta palm wood microparticles into a polymeric matrix such as HDPE can improve the energy absorption capability of the polymer resulting biocomposites with enhanced energy absorption capability on exposure to ballistic impact.

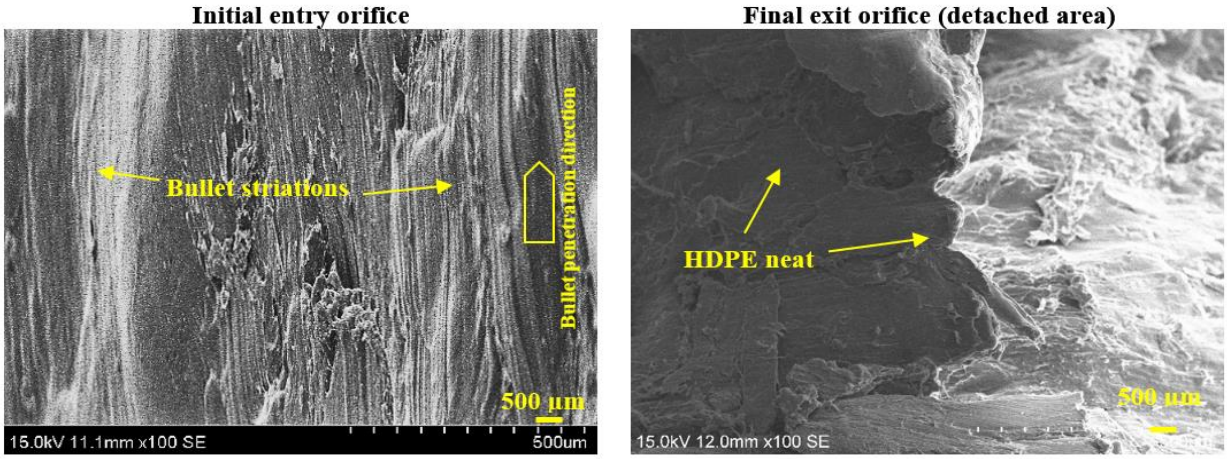

a) HDPE-1

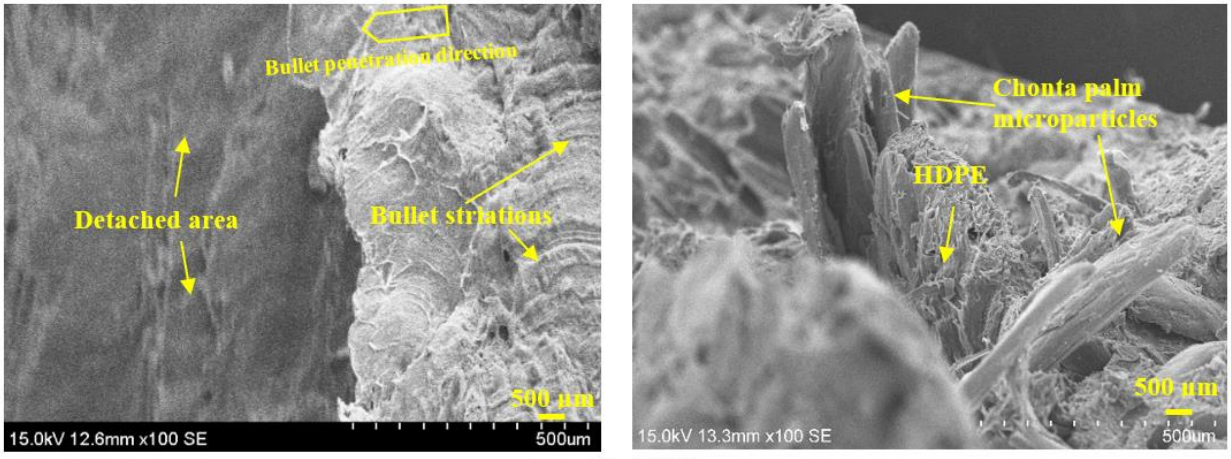

b) Ch10

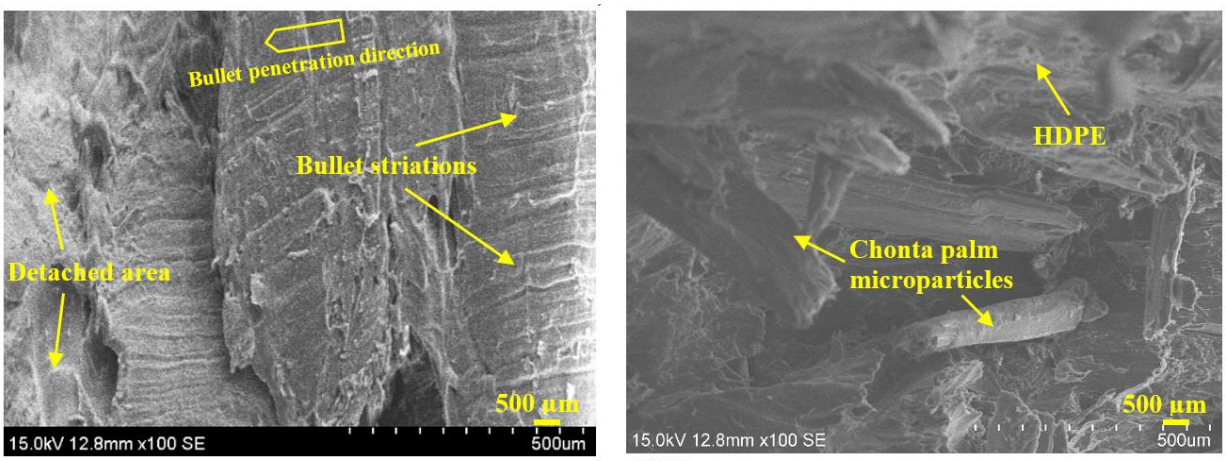

c) Ch20

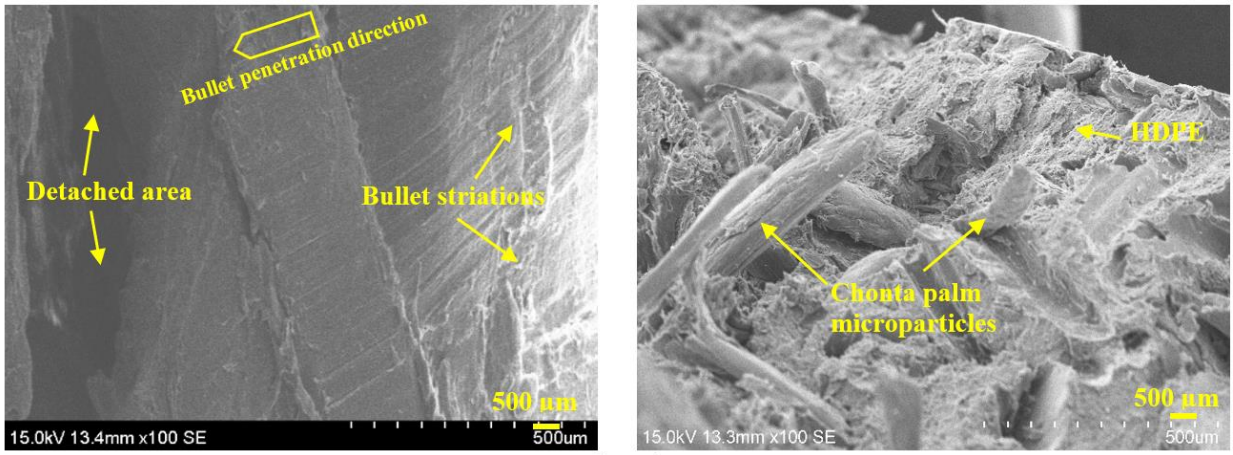

d) Ch25

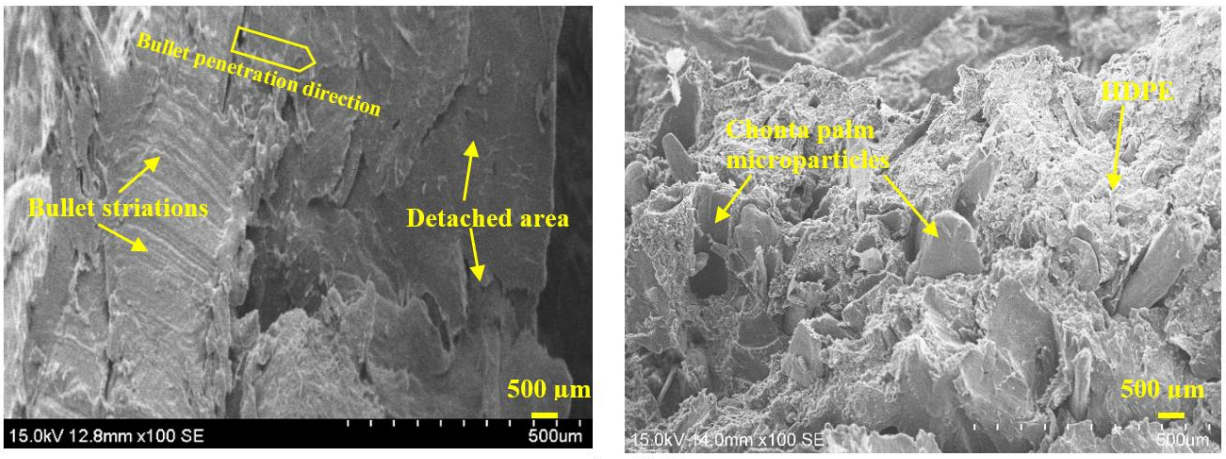

e) Ch30

Fig. 8.7. Longitudinal section showing the morphology of projectile penetration channels inside the targets.

8.5 Conclusions

Biocomposites consisting of high density polyethylene reinforced with microparticles of chonta palm wood (*Bactris gasipaes*) were developed and characterized under both quasi-static and dynamic mechanical loading. The specimens investigated include HDPE neat (unreinforced), as control sample, and biocomposites containing 10, 20, 25, and 30 wt.% of chonta wood palm microparticles as reinforcements in HDPE. The density of the biocomposites only varies slightly from one another. The tendency of the biocomposite to absorb water increased only slightly as the weight fraction of the wood particle was increased to 30 wt.%. The strength and stiffness of the HDPE are enhanced by reinforcement with chonta wood particles. However, reinforcement with chonta wood particles has a more pronounced effect on Young modulus than tensile strength. Both strength and young modulus increase as the wood particle content increases up to 25 wt. %. Increasing wood particle content beyond 25 wt.% to 30 wt.% will result in decrease in both tensile strength and Young modulus. The loss in strength and modulus as the wood particle content is increase to 30 % is due to particle agglomeration at higher particle content which leads to poor bonding between agglomerated particles and the matrix and debonding at particle-particle interface during mechanical loading. The recommendable amount of chonta wood particles for optimum reinforcing effect on HDPE are around 20 and 25 wt. %. Bio-composite containing these weight fractions of chonta microparticles exhibited the highest ballistic impact resistance, and the best mechanical performance under both quasi-static tensile and dynamic compression loading. These results suggest that addition of wood palm microparticles in a polymeric matrix (HDPE) improves the mechanical properties and the ballistic resistance of the polymer resulting in biocomposites with improved performance compared to the unreinforced HDPE.

Chapter 9: Summary, Conclusions, Contributions and Future Works

9.1 Summary

In this thesis, the results of experimental studies on the synthesis and characterization of hybrid and bio-composite materials are presented and discussed. These materials are tested for application in protective armors. The obtained composites were subjected to both dynamic impact loading using split Hopkinson pressure (SHPB) system and the ballistic impact test to characterize their dynamic impact behavior. Results of microstructural evaluation of the composites before and after mechanical test are discussed to understand the failure mechanisms of the developed composite materials. The mechanical properties and impact resistance of the composite armors are improved by the addition of micro- and nano-particles used as reinforcing fillers in thermosetting (epoxy) and thermoplastic (HDPE) matrices.

In the first chapter of this thesis, the objectives and motivations are defined. This is followed by literature review in Chapter 2. In this chapter, research findings in some of the previous works on the development and characterization of improved composite armor are provided. The protection levels of ballistic plates are also discussed in this section. The protection is evaluated based on the energy dissipated in the investigated material by low caliber weapons. Various matrices and reinforcements used in composite armor fabrication are reviewed and the knowledge gap is identified. The materials used in composite fabrication, the manufacturing procedures and materials characterization techniques are discussed in the Chapter 3. In addition, the equipment used in microstructure analysis, water absorption measurements, crystallographic structure characterization, tensile strength measurements, dynamic shock loading, and ballistic impact tests are described in detail.

The investigations carried out to determine the effects of shear thickening fluid impregnation of Kevlar® fibers on the ballistic impact resistance and energy absorption are discussed in Chapter 4. Hybrid composite laminates consisting of alternate layers of Kevlar® fiber reinforced epoxy

and 5086-H32 aluminum alloy plate were manufactured and tested. The hybrid composite materials were developed to have alternate layers of aluminum alloy plate and Kevlar® fiber (neat or impregnated with STF) reinforced epoxy. The ballistic performance of hybrid material containing no STF was compared with those containing STF impregnation. The results of ballistic tests made on the hybrid composite plates indicate that impregnation of STF into the woven Kevlar® fibers during fabrication increase its impact energy absorption performance when compared to those of the samples made of Kevlar® neat fabrics (containing no STF).

The impact energy absorption of hybrid composite laminates consisting of alternate layers woven Kevlar® fiber reinforced epoxy and AA 5086-H32 aluminum alloy, produced by impregnating the woven Kevlar® fibers with different types of nano-fillers (silicon carbide, aluminum powder, colloidal silica, gamma alumina and potato flour) during fabrication of the hybrid materials, is addressed in Chapter 5. In this study, the impact energy absorption capabilities of the developed hybrid plates were compared to determine which of the selected nano-fillers will lead to improved resistance to ballistic impact. The protection armor level of each plate (with different nano-fillers) were determined and found to be dependent on the type of nano-filler added.

The results of research findings focusing on the manufacture and characterization of hybrid composite plates for armor protection using high density polyethylene (HDPE) matrix and reinforcements consisting of combinations of Kevlar® short fibers and micro/nano-fillers are discussed in Chapter 6. SEM and EDS analysis were carried out on specimens to determine the microstructure and distribution of filler particles in the hybrid materials. Tensile strength, Young's modulus, impact behavior, ballistic resistance and water absorption behavior were determined to establish which hybrid plate configuration produces hybrid composite plates best hybridization effect on mechanical and physical properties.

The effects of the addition of micro-particles of chonta palm wood and Kevlar® short fibers as reinforcement components for a thermoplastic matrix are addressed in Chapter 7. HDPE was used as the thermoplastic matrix. In this case, material mixture consisting of 10 wt.% Kevlar® short fibers, 0 - 30 wt.% wood palm micro-particles and HDPE were compounded in a twin-screw extruder, pelletized and then compressed into 20 cm x 20 cm x 0.5 cm plates. The resulting composite plates were characterized using tensile, flexural, impact and ballistic tests. The water

absorption test was performed to ascertain the stability of the plates on exposure to water. The content of natural filler for optimum performance under various loading conditions determined.

The effects of chonta palm wood particles, as reinforcement, on the strength and impact resistance of high density polyethylene (HDPE) are reported in Chapter 8. The HDPE in this study was reinforced with natural fillers with no addition of Kevlar® short fibers. Tests were conducted to obtain information on the energy absorption during ballistic impact test for the obtained bio-composites containing 10, 20, 25, and 30 wt.% of chonta wood palm micro-particles. The effect of filler content on water absorption, strength and stiffness of the bio-composites were investigated to determine the optimum filler (chonta wood particles) content for enhanced performance. The results of microstructural investigation of the bio-composites before and after mechanical tests are also presented and discussed.

9.2 Conclusions

Based on the results obtained in these research investigations, the following conclusions can be drawn:

1. Impregnation of Kevlar® fiber used in the manufacture of hybrid composites with shear thickening fluid made of colloidal silica particles results in composite materials with improved ballistic resistance. The results indicate that most of the Kevlar® fiber reinforced epoxy /5086-H32 aluminium laminates developed meet the protective requirements for levels IIA, II, and IIIA threats. This means that they are able to resist impact damage from pistols of 9 mm calibre with an energy absorption ranging from 507 to 1037 J. The tendency of Kevlar® fibers to rupture during projectile penetration decreases when impregnated with STF.

2. The impregnation of micro or nano-fillers (silica carbide, aluminum powder, gamma alumina, potato flour and colloidal silica) on Kevlar® surface to develop hybrid composite laminates influences the ballistic resistance of the laminates. The energy absorption capacity is highest for laminates containing Al, SiO_2 and SiC nano-powders. The hybrid laminates built with these nano-fillers can adequately protect against HK pistol 9 mm and Parabellum pistol 9 mm. These levels of protection cannot be achieved in laminates with no nano-filler addition and those containing alumina or potato powders.

3. The addition of 20 wt.% micro- and nano-fillers (chonta palm wood, potato flour, colloidal silica and gamma alumina) to Kevlar® short fibers used in reinforcing HDPE enables development of hybrid composites with an enhanced stiffness under quasi-static tensile load and improved performance under dynamic compressive and ballistic impact loads. However, the addition of these nano-fillers led to loss in ductility and decrease in tensile strength. The highest energy absorption of 62.7 and 59.1 J was achieved for hybrid composites containing additions of gamma alumina and colloidal silica nano-fillers respectively. Microstructural analysis indicated that an excessive accumulation of fibers or filler particles in any specific areas of the hybrid composites has detrimental effects on the quasi-static or dynamic mechanical behavior of the composites. When targets are subjected to high velocity impact, cracks will appear and readily nucleate at the weak interphase between agglomerate fibers or particles with the thermoplastic matrix.

4. Hybrid bio-composites prepared by the hybridization of 10 wt.% Kevlar® pulp with varying proportion of organic micro-fillers (10, 20, and 30 wt.% chonta wood microparticles) in a HDPE matrix were characterized under tensile, flexural, impact and ballistic loading conditions. The addition of the micro-fillers reduces the tensile strength but improves the polymer stiffness. Microstructural analysis indicated that the size of the organic micro-particles, their alignment and distribution affect bonding of Kevlar® short fibers with the HDPE matrix. The results of ballistic impact test revealed that the composites containing 10 wt.% of organic wood micro-particles exhibited the highest ballistic impact energy absorption capacity.

5. Biocomposites made of HDPE reinforced with a variable amount of micro-particles of chonta palm wood (10, 20, 25, and 30 wt. %), were characterized and compared under both quasi-static and dynamic mechanical loading. The results suggested that such deposition of wood palm micro-particles in a polymeric matrix (HDPE) improved the strength, stiffness and the ballistic resistance of the resulting biocomposites. A negligible tendency to absorb water is observed (< 0.5 %), which increases very slightly with increasing weight fraction of the wood particles. The strength and stiffness of the HDPE are optimized in bio-composites containing between 20 and 25 wt.% chonta wood micro-particles. Increasing wood particle content beyond 25 wt.% to 30 wt.% results in decrease in both tensile strength (9 %) and Young modulus (13.8 %) due to particle agglomeration, which leads to poor bonding between

agglomerated particles and the matrix. The ballistic performance of the biocomposites containing 25 wt.% of fillers exhibited the highest energy absorption of 53.4 J, which represents a 41.3% improvement over the unreinforced HDPE specimens with similar thickness and density. Therefore, the recommendable amount of chonta wood micro-particles for optimum reinforcing effect on HDPE are between 20 and 25 wt. %. This allows optimum, strength, stiffness and ballistic impact resistance.

In summary, it can be concluded that hybrid composite laminates consisting of layers of Al 5086-H32 and Kevlar 49/epoxy impregnated with nano-fillers of colloidal silica, aluminum powder can offer an optimal ballistic impact resistance and energy absorption capability of between 679 up to 693 J. This for a laminate with an average thickness of between 9.7 and 10.8 mm and an areal density ranging between 1.7 and 1.9 g/cm^2. These protective armors can meet the protective requirements for levels IIA, II, and IIIA to resist the impact from pistols caliber 9mm, HK and Parabellum.

9.3 Scientific contributions

The research findings in this study has made significant and original contributions to knowledge in this field. These include:

1) New armor materials for ballistic protection have been produced, which offer advancements in armor plate technology for body armors.

2) The information gaps identified in the Chapter II, have been filled with the results obtained in this investigation.

3) The results of this investigation have been shared in several scientific publications, which are being used by other researchers designing composite armor plates and developing new research projects related to hybrid composite armors.

4) The developed research is providing a new solution to a critical problem in Ecuadorian Army, as detailed in the Chapter I. It offers effective solutions for the mandatory use of body armors by soldiers and law enforcement agents as well as for ballistic armor plates for tactical vehicles.

These new solutions will provide possibility to reduce the risk of lost of lives and serious injuries of soldiers engaged in high-risk missions.

9.4 Recommendations for future works

Although the main objectives of current research project are realised, there are still more work to be done for further improvement of protective armors. These include the following:

1) Dynamic impact behavior of closed cell aluminum foam composite armors made by impregnation of aluminum foams with Kevlar® short fibers and nano-fibers should be studied. This study will allow to compare what fiber impregnation and what percentage can produce hybrid composites with the most improved resistance against ballistic impact failure.

2) The effects of impregnation of shear thickening fluid, Kevlar® short fibers and carbon nano-fibers into aluminum foam to produce new hybrid polymer composites materials need to be investigated. Conducting this investigation will enable the understanding of whether or not the impregnation of colloidal silica nanoparticles can produce a positive hybridization with Kevlar micro-fibers or carbon nano-fibers and epoxy resin in the manufacture of hybrid composites made of aluminum foam plates. The optimal configuration of the hybrid composite plates can be determined from the results of ballistic testing on the plates.

3) Ballistic impact performance of hybrid composite armors made of aluminum foam/epoxy resin containing the dispersion of shear thickening fluid made of various synthetic nano-fillers of colloidal silica, silica carbide and gamma alumina. This study will determine whether or not such impregnation of nano-particles into aluminum foam can improve the impact resistance of aluminum foams. In addition, the results will allow to determine which nano-particles will provide better hybridization effect.

References

[1] M. Grujicic, H. Marvi, G. Arakere, W. C. Bell, and I. Haque, “The effect of up-armoring of the high-mobility multi-purpose wheeled vehicle (HMMWV) on the off-road vehicle performance,” *Multidiscip. Model. Mater. Struct.*, vol. 6, no. 2, pp. 229–256, 2010.

[2] D. Gay, "Composite Materials: design and applications.", 3rd edition, *Taylor & Francis Group*, U.S., 2015.

[3] P.K. Mallick, "Fiber-Reinforced Composites: Materials, Manufacturing, and Design.", 3rd edition, *Taylor & Francis Group*, U.S., 2008.

[4] U. S. A. Department of Defence, “MIL-HDBK-17-3F, Composite Materials Handbook: Volume 3. Polymer Matrix Composites, materials usage, design, and analysis.”, *Compos. Mater. Handb.*, vol. 3, 2002.

[5] U. S. A. Department of Defence, “MIL-HDBK-17-1F, Composite Materials Handbook: Volume 1. Polymer Matrix Composites, guidelines for characterization of structural materials.”, *Compos. Mater. Handb.*, vol. 1, 1997.

[6] R. Kumar, T. Singh, and H. Singh, “Natural fibers polymeric composites with particulate fillers – A review report,” *Int. J. Adv. Eng. Res. and Appl.*, vol.1, no. 1, pp. 21–27, 2015.

[7] National Institute of Justice, “NIJ Standard 0101.04, Ballistic resistance of personal body armor,” *Law Enforc. Correct. Stand. Test. Progr.*, p. 67, 2000.

[8] National Institute of Justice, “NIJ Standard 0101.03, Ballistic resistance of police body armor,” *Technol. Assess. Progr.*, 1987.

[9] Stewart James K., "NIJ Standard 0108.01, Ballistic resistant protective materials.", *Technol. Assess. Progr.*, Washington, DC: National Institute of Justice; 1985.

[10] National Institute of Justice, “NIJ Standard 0101.06, Ballistic resistance of body armor,” *Office of Justice Programs*, 2008.

[11] D. A. Jesson and J. F. Watts, “The interface and interphase in polymer matrix composites: Effect on mechanical properties and methods for identification,” *Polym. Rev.*, vol. 52, no. 3–4, pp. 321–354, 2012.

[12] D. Hull and T. W. Clyne, "An Introduction to Composite Materials (Cambridge Solid State Science Series)", 2nd edition, Cambridge: Cambridge University Press, 1996.

[13] U. S. A. Department of Defence, “MIL-HDBK-17-2F, Composite Materials Handbook: Volume 2. Polymer Matrix Composites, material properties.”, *Compos. Mater. Handb.*, vol. 2, 2002.

[14] R.M. Wang, S.R. Zheng, and Y. G. Zheng, "Polymer Matrix Composites and Technology.", *Woodhead Publishing Ltd.*, Cambridge UK., 2011.

[15] A. Boudenne, L. Ibos, Y. Candau, and S. Thomas, "Handbook of Multiphase Polymer Systems", *John Wiley & Sons Ltd.*, vol. 1. 2011.

[16] U. S. A. Department of Defence, “MIL-HDBK-17-4, Composite Materials Handbook: Volume 4. Metal Matrix Composites.”, *Compos. Mater. Handb.*, vol. 4, p. 304, 2002.

[17] N. Chawla and K. K. Chawla, ”Metal Matrix Composites.", *Springer*, 2nd edition, U.S.,

2013.

[18] G. M. Owolabi, A. G. Odeshi, M. N. K. Singh, and M. N. Bassim, "Dynamic shear band formation in Aluminum 6061-T6 and Aluminum 6061-T6/Al2O3composites," *Mater. Sci. Eng. A*, vol. 457, no. 1–2, pp. 114–119, 2007.

[19] D. L. McDanels, T. T. Serafini, and J. A. DiCarlo, "Polymer, metal, and ceramic matrix composites for advanced aircraft engine applications," *J. Mater. Energy Syst.*, vol. 8, no. 1, pp. 80-91, 1986.

[20] R. Casati and M. Vedani, "Metal Matrix Composites Reinforced by Nano-Particles—A Review," *Metals (Basel).*, vol. 4, no. 1, pp. 65–83, 2014.

[21] U. S. A. Department of Defence, "MIL-HDBK-17-5, Composite Materials Handbook: Volume 5. Ceramic Matrix Composites.", *Compos. Mater. Handb.*, vol. 5, 2002.

[22] E. Medvedovski, "Lightweight ceramic composite armour system," *Adv. Appl. Ceram.*, vol. 105, no. 5, pp. 241–245, 2006.

[23] E. Medvedovski, "Ballistic performance of armour ceramics: Influence of design and structure. Part 1," *Ceram. Int.*, vol. 36, no. 7, pp. 2103–2115, 2010.

[24] E. Medvedovski, "Alumina ceramics for ballistic protection, Part 2," *Am. Ceram. Soc. Bull.*, vol. 81, no. 4, pp. 45–50, 2002.

[25] M. Garcia-Avila, M. Portanova, and A. Rabiei, "Ballistic Performance of a Composite Metal Foam-ceramic Armor System," *Procedia Mater. Sci.*, vol. 4, no. 2010, pp. 151–156, 2014.

[26] A. K. Bandaru, V. V. Chavan, S. Ahmad, R. Alagirusamy, and N. Bhatnagar, "Ballistic impact response of Kevlar® reinforced thermoplastic composite armors," *Int. J. Impact Eng.*, vol. 89, pp. 1–13, 2016.

[27] M. F. Ashby, "Materials Selection in Mechanical Design," 3rd edition, Oxford: Pergamon Press, 2005.

[28] D. Zhang, Y. Sun, L. Chen, S. Zhang, and N. Pan, "Influence of fabric structure and thickness on the ballistic impact behavior of Ultrahigh molecular weight polyethylene composite laminate," *Mater. Des.*, vol. 54, pp. 315–322, 2014.

[29] A. R. Abu Talib, L. H. Abbud, A. Ali, and F. Mustapha, "Ballistic impact performance of Kevlar-29 and Al2O3 powder/epoxy targets under high velocity impact," *Mater. Des.*, vol. 35, pp. 12–19, 2012.

[30] L. Sorrentino, C. Bellini, A. Corrado, W. Polini, and R. Aricò, "Ballistic performance evaluation of composite laminates in kevlar 29," *Procedia Engineering*, vol. 88, pp. 255–262, 2014.

[31] P. R. S. Reddy, T. S. Reddy, V. Madhu, A. K. Gogia, and K. V. Rao, "Behavior of E-glass composite laminates under ballistic impact," *Mater. Des.*, vol. 84, pp. 79–86, 2015.

[32] Shaktivesh, N. S. Nair, C. V. Sesha Kumar, and N. K. Naik, "Ballistic impact performance of composite targets," *Mater. Des.*, vol. 51, pp. 833–846, 2013.

[33] Y. Swolfs, L. Gorbatikh, and I. Verpoest, "Fibre hybridisation in polymer composites: A review," *Compos. Part A Appl. Sci. Manuf.*, vol. 67, pp. 181–200, 2014.

[34] M. F. Ashby and Y. J. M. Bréchet, “Designing hybrid materials,” *Acta Mater.*, vol. 51, no. 19, pp. 5801–5821, 2003.

[35] M. Ashby, H. Shercliff, and D. Cebon, "Materials: engineering, science, processing and design.", 2nd edition, Oxford: Elsevier Butterworth-Heinemann, 2010.

[36] Granta Design “Granta software suitable for composite qualification,” *Reinforced Plastics*, vol. 59, no. 3. pp. 118–119, 2015. https://doi.org/10.1016/j.repl.2015.03.061.

[37] M. Sadighi, R. C. Alderliesten, and R. Benedictus, “Impact resistance of fiber-metal laminates: A review,” *Int. J. Impact Eng.*, vol. 49, pp. 77–90, 2012.

[38] A. Seyed Yaghoubi and B. Liaw, “Ballistic impact behaviors of GLARE 5 fiber-metal laminated plates,” *Conf. Proc. Soc. Exp. Mech. Ser.*, vol. 7, no. 8, pp. 189–198, 2013.

[39] A. A. Ramadhan, A. R. Abu Talib, A. S. Mohd Rafie, and R. Zahari, “High velocity impact response of Kevlar-29/epoxy and 6061-T6 aluminum laminated panels,” *Mater. Des.*, vol. 43, pp. 307–321, 2013.

[40] M. H. Ikbal, A. Ahmed, W. Qingtao, Z. Shuai, and L. Wei, “Hybrid composites made of unidirectional T600S carbon and E-glass fabrics under quasi-static loading,” *J. Ind. Text.*, vol. 46, no. 7, pp. 1511–1535, 2017.

[41] J. Zhang, K. Chaisombat, S. He, and C. H. Wang, “Hybrid composite laminates reinforced with glass/carbon woven fabrics for lightweight load bearing structures,” *Mater. Des.*, vol. 36, pp. 75–80, 2012.

[42] K. S. Pandya, C. Veerraju, and N. K. Naik, “Hybrid composites made of carbon and glass woven fabrics under quasi-static loading,” *Mater. Des.*, vol. 32, no. 7, pp. 4094–4099, 2011.

[43] M. Sayer, N. B. Bektaş, and O. Sayman, “An experimental investigation on the impact behavior of hybrid composite plates,” *Compos. Struct.*, vol. 92, no. 5, pp. 1256–1262, 2010.

[44] R. Park and J. Jang, “Impact behavior of aramid fiber/glass fiber hybrid composite: Evaluation of four-layer hybrid composites,” *J. Mater. Sci.*, vol. 36, no. 9, pp. 2359–2367, 2001.

[45] R. Park and J. Jang, “Impact behavior of aramid fiber/glass fiber hybrid composites: The effect of stacking sequence,” *Polym. Compos.*, vol. 22, no. 1, pp. 80–89, 2001.

[46] E. Randjbaran, R. Zahari, N. A. Abdul Jalil, and D. L. Abang Abdul Majid, “Hybrid composite laminates reinforced with kevlar/carbon/glass woven fabrics for ballistic impact testing.,” *Scientific World Journal.*, vol. 2014, p. 413-753, 2014.

[47] E. Randjbaran, “The effects of stacking sequence layers of hybrid composite materials in energy absorption under the high velocity ballistic impact conditions: An experimental investigation,” *J. Mater. Sci. Eng.*, vol. 2, no. 4, 2013.

[48] T. P. Sathishkumar, J. Naveen, and S. Satheeshkumar, “Hybrid fiber reinforced polymer composites - A review,” *J. Reinf. Plast. Compos.*, vol. 33, no. 5, pp. 454–471, 2014.

[49] D. Dai and M. Fan, "Wood fibres as reinforcements in natural fibre composites: structure, properties, processing and applications.", *Natural Fibre Composites*, vol. 1, pp. 3-65, 2014.

[50] A. Hodzic and R. Shanks, "Natural Fibre Composites: Materials, Processes and Properties.", *Woodhead Publishing Ltd.*, Cambridge UK,. 2014.

[51] N. Saba, P. M. Tahir, and M. Jawaid, “A review on potentiality of nano filler/natural fiber filled polymer hybrid composites,” *Polymers (Basel).*, vol. 6, no. 8, pp. 2247–2273, 2014.

[52] C. Wretfors and B. Svennerstedt, “Report Bio fibre technology used for military applications – an overview.”, Sweden, 2006.

[53] M.S. Salit, "Tropical natural fibre composites: properties, manufacture and aplications.", *Engineering Materials*, Singapore: Springer, 2014.

[54] R. Yahaya, S. M. Sapuan, M. Jawaid, Z. Leman, and E. S. Zainudin, “Measurement of ballistic impact properties of woven kenaf-aramid hybrid composites,” *Meas. J. Int. Meas. Confed.*, vol. 77, pp. 335–343, 2016.

[55] R. Yahaya, S. M. Sapuan, M. Jawaid, Z. Leman, and E. S. Zainudin, “Quasi-static penetration and ballistic properties of kenaf-aramid hybrid composites,” *Mater. Des.*, vol. 63, pp. 775–782, 2014.

[56] F. Sarasini, J. Tirillò, M. Valente, L. Ferrante, S. Cioffi, S. Iannace, and L. Sorrentino, “Hybrid composites based on aramid and basalt woven fabrics: Impact damage modes and residual flexural properties,” *Mater. Des.*, vol. 49, pp. 290–302, Aug. 2013.

[57] R. Petrucci, C. Santulli, D. Puglia, E. Nisini, F. Sarasini, J. Tirillò, L. Torre, G. Minak, and J. M. Kenny, “Impact and post-impact damage characterisation of hybrid composite laminates based on basalt fibres in combination with flax, hemp and glass fibres manufactured by vacuum infusion,” *Compos. Part B Eng.*, vol. 69, pp. 507–515, 2015.

[58] P. N. B. Reis, J. A. M. Ferreira, P. Santos, M. O. W. Richardson, and J. B. Santos, “Impact response of Kevlar composites with filled epoxy matrix,” *Compos. Struct.*, vol. 94, no. 12, pp. 3520–3528, 2012.

[59] E. G. Koricho, A. Khomenko, M. Haq, L. T. Drzal, G. Belingardi, and B. Martorana, “Effect of hybrid (micro- and nano-) fillers on impact response of GFRP composite,” *Compos. Struct.*, vol. 134, pp. 789–798, 2015.

[60] M. Hasanzadeh and V. Mottaghitalab, “The role of shear-thickening fluids (STFs) in ballistic and stab-resistance improvement of flexible armor,” *J. Mater. Eng. Perform.*, vol. 23, no. 4, pp. 1182–1196, 2014.

[61] T. A. Hassan, V. K. Rangari, and S. Jeelani, “Synthesis, processing and characterization of shear thickening fluid (STF) impregnated fabric composites,” *Mater. Sci. Eng. A*, vol. 527, no. 12, pp. 2892–2899, 2010.

[62] A. Majumdar, B. S. Butola, and A. Srivastava, “An analysis of deformation and energy absorption modes of shear thickening fluid treated Kevlar fabrics as soft body armour materials,” *Mater. Des.*, vol. 51, pp. 148–153, 2013.

[63] Y. S. Lee, E. D. Wetzel, and N. J. Wagner, “The ballistic impact characteristics of Kevlar® woven fabrics impregnated with a colloidal shear thickening fluid,” *J. Mater. Sci.*, vol. 38, no. 13, pp. 2825–2833, 2003.

[64] A. Majumdar, B. S. Butola, and A. Srivastava, “Development of soft composite materials with improved impact resistance using Kevlar fabric and nano-silica based shear thickening fluid,” *Mater. Des.*, vol. 54, pp. 295–300, 2014.

[65] W. Callister and D. Rethwisch, "Materials science and engineering: an introduction", *John*

Wiley & Sons, Inc., U.S., 7th edition, vol. 94, 2007.

[66] J. L. Park, B. Yoon, J. Paik, and T. Kang, "Ballistic performance of Kevlar fabric panels containing STF," *Sci. Technol.*, no. 1, pp. 7–11, 2011.

[67] N. J. Wagner and Y. S. Lee, "The ballistic impact characteristics of Kevlar woven fabrics impregnated with a colloidal shear thickening fluid," *J. Mater. Sci.*, vol. 38, pp. 2825–2833, 2003.

[68] Y. Park, Y. Kim, A. H. Baluch, and C.-G. Kim, "Empirical study of the high velocity impact energy absorption characteristics of shear thickening fluid (STF) impregnated Kevlar fabric," *Int. J. Impact Eng.*, vol. 72, pp. 67–74, 2014.

[69] J. William D. Callister and David G. Rethwisch, "Materials science and engineering: An introduction.", *John Wiley & Sons, Inc.*, 7th edition, U.S., 2007.

[70] N. Saba, P. M. Tahir, M. Jawaid, and U. Putra, "A review on potentiality of nano filler/natural fiber filled polymer hybrid composites," *Polymers (Basel)*, vol. 6, no. 8, pp. 2247-2273, 2014.

[71] B. K. Deka and T. K. Maji, "Effect of silica nanopowder on the properties of wood flour / polymer composite," *Polym. Eng. Sci.*, vol. 52, no. 7, pp. 1–8, 2012.

[72] U.S. Congress, Office of Technology Assesment, "Advanced Materials by Design," OTAE-351 (Washington, DC: U.S. Government Printing Office, June 1988).

[73] A. A. Ramadhan, A. R. A. Talib, A. S. M. Rafie, and R. Zahari, "The Influence of impact on Composite Armour System Kevlar-29/polyester-Al_2O_3," *IOP Conf. Ser. Mater. Sci. Eng.*, vol. 36, p. 12028, 2012.

[74] I. H. Tavman, "Thermal and mechanical properties of aluminum powder-filled high-density polyethylene composites," *J. Appl. Polym. Sci.*, vol. 62, no. 12, pp. 2161–2167, 1996.

[75] M. G. Hamed, "Study the tensile strength for epoxy composite reinforced with fibers and particles," *J. Univ. anbar pure Sci.*, vol. 3, no. 2, pp. 1–6, 2009.

[76] P. Sarkar, N. Modak, and P. Sahoo, "Mechanical characteristics of aluminium powder filled glass epoxy composites," *Int. J. Eng. Technol.*, vol. 12, pp. 1–14, 2017.

[77] R. R. Koshy, S. K. Mary, L. A. Pothan, and S. Thomas, "Soy protein- and starch-based green composites/nanocomposites: Preparation, properties, and applications," *Adv. Struct. Mater.*, vol. 75, pp. 433–467, 2015.

[78] F. Sadegh-Hassani and A. Mohammadi Nafchi, "Preparation and characterization of bionanocomposite films based on potato starch/halloysite nanoclay," *Int. J. Biol. Macromol.*, vol. 67, pp. 458–462, 2014.

[79] A. C. Arya, R. Ario, D. Soeriaatmaja, D. Hetharia, I. Surjati, B. Nasution, R. D. Rubijono, and Y. Priadi, "Environmental friendly lightweight material from natural fibers of oil palm empty fruit bunch," *J. Mater. Sci.Chem. Eng.*, vol. 3, pp. 190–195, 2015.

[80] S. Graefe, D. Dufour, M. Van Zonneveld, F. Rodriguez, and A. Gonzalez, "Peach palm (Bactris gasipaes) in tropical Latin America: Implications for biodiversity conservation, natural resource management and human nutrition," *Biodivers. Conserv.*, vol. 22, no. 2, pp. 269–300, 2013.

[81] W. L. E. Magalhães, S. A. Pianaro, C. J. F. Granado, and K. G. Satyanarayana, "Preparation

and characterization of polypropylene/heart-of-peach palm sheath composite," *J. Appl. Polym. Sci.*, vol. 127, no. 2, pp. 1285–1294, 2013.

[82] M. F. Omar, H. M. Akil, and Z. A. Ahmad, "Effect of molecular structures on dynamic compression properties of polyethylene," *Mater. Sci. Eng. A*, vol. 538, pp. 125–134, 2012.

[83] S.-Y. Y. Fu and B. Lauke, "Characterization of tensile behaviour of hybrid short glass fibre calcite particle ABS composites," *Compos. Part A Appl. Sci. Manuf.*, vol. 29, no. 5–6, pp. 575–583, 1998.

[84] S. Fu, G. Xu, and Y. Mai, "On the elastic modulus of hybrid particle / short- fiber / polymer composites," *Compos. Part B Eng.*, vol. 33, no. 2002, pp. 291–299, 2006.

[85] S. Y. Fu, B. Lauke, E. Mader, C. Y. Yue, and X. Hu, "Tensile properties of short-glass-fiber- and short-carbon-fiber-reinforced polypropylene composites," *Compos. Part A Appl. Sci. Manuf.*, vol. 31, no. 10, pp. 1117–1125, 2000.

[86] S. Y. Fu, B. Lauke, E. Mader, X. Hu, and C. Y. Yue, "Fracture resistance of short-glass-fiber-reinforced and short-carbon-fiber-reinforced polypropylene under Charpy impact load and its dependence on processing," *J. Mater. Process. Technol.*, vol. 89–90, pp. 501–507, 1999.

[87] E. E. Haro, A. G. Odeshi, and J. A. Szpunar, "The effects of micro- and nano-fillers' additions on the dynamic impact response of hybrid composite armors made of HDPE reinforced with Kevlar Short Fibers," *Polym. - Plast. Technol. Eng.*, vol. 57, no. 7, pp. 609–624, 2018.

[88] M. Brebu and C. Vasile, "Thermal degradation of lignin—a review," *Cellul. Chem. Technol.*, vol. 44, no. 9, pp. 353–363, 2010.

[89] ASTM, "ASTM: D570, Standard test method for water absorption of plastics 1," *ASTM Stand.*, West Conshohocken, US., vol. 98, Reapproved 2010, pp. 25–28, 2014.

[90] ASTM, "ASTM: D638, Standard test method for tensile properties of plastics," *ASTM Stand.*, West Conshohocken, US., pp. 1–16, 2013.

[91] Weinong, C.; BO, S. Split Hopkinson (Kolsky) Bar: Design, Testing and Applications. Mechanical Engineering Series, Vol. 1, Springer: New York, NY, 2013.

[92] M. Firdaus, H. Akil, Z. Arifin, A. A. M. Mazuki, and T. Yokoyama, "Dynamic properties of pultruded natural fibre reinforced composites using Split Hopkinson Pressure Bar technique," *Mater. Des.*, vol. 31, no. 9, pp. 4209–4218, 2010.

[93] A. A. Tiamiyu, R. Basu, A. G. Odeshi, and J. A. Szpunar, "Plastic deformation in relation to microstructure and texture evolution in AA 2017-T451 and AA 2624-T351 aluminum alloys under dynamic impact loading," *Mater. Sci. Eng. A*, vol. 636, pp. 379–388, 2015.

[94] Arvidsson PG. NATO infantry weapons standardization. Brussels, Belgium: NATO Army Armaments Group; 2008.

[95] Fire A, Publication A. NATO/PFPUN classified NATO international staff – defence investment division allied NATO reaction-to-fire tests for materials policy for the pre-selection of materials for military applications, STANAG 4602 Allied Fire Assessment Publication (AFAP), vol. 1, edition 3, July, 2010.

[96] Safety M, Analysis I. STANAG 4241 review of the bullet impact test background. San

Diego, CA: Munitions Safety Information Analysis Center; 2013.

[97] Abrate S. Impact engineering of composite structures. CISM courses and lectures, vol. 526. New York: Springer Wien; 2011.

[98] I. Mohagheghian, G. J. McShane, and W. J. Stronge, "Impact perforation of monolithic polyethylene plates: Projectile nose shape dependence," *Int. J. Impact Eng.*, vol. 80, pp. 162–176, 2015.

[99] E. Haro Albuja, J. A. Szpunar, and A. G. Odeshi, "Ballistic impact response of laminated hybrid materials made of 5086-H32 aluminum alloy, epoxy and Kevlar® fabrics impregnated with shear thickening fluid," *Compos. Part A Appl. Sci. Manuf.*, vol. 87, pp. 54–65, 2016.

[100] L. Cannon, "Behind armour blunt trauma--an emerging problem.," *Journal of the Royal Army Medical Corps*, vol. 147, no. 1. pp. 87–96, 2001.

[101] A. C. Merkle, E. E. Ward, J. V O'Connor, and J. C. Roberts, "Assessing behind armor blunt trauma (BABT) under NIJ standard-0101.04 conditions using human torso models.," *J. Trauma*, vol. 64, no. 6, pp. 1555–1561, 2008.

[102] M. Karahan, A. Kuş, and R. Eren, "An investigation into ballistic performance and energy absorption capabilities of woven aramid fabrics," *Int. J. Impact Eng.*, vol. 35, no. 6, pp. 499–510, 2008.

[103] Sparks, E. "Advances in military textiles and personal equipment.", *Elsevier Inc*., pp. 1–325, 2012, https://doi.org/10.1533/9780857095572.

[104] A. Arbor, H. Wang, Y. Cui, D. Rose, A. Socks, and D. Ostberg, "Designing an Innovative Composite Armor System for Affordable.", University of Michigan, US. 2006.

[105] S. N. Monteiro, É. P. Lima, L. H. L. Louro, L. C. da Silva, and J. W. Drelich, "Unlocking Function of Aramid Fibers in Multilayered Ballistic Armor," *Metall. Mater. Trans. A*, vol. 46, no. 1, pp. 37–40, 2015.

[106] A. Srivastava, A. Majumdar, and B. S. Butola, "Improving the impact resistance of textile structures by using shear thickening fluids: A Review," *Crit. Rev. Solid State Mater. Sci.*, vol. 37, no. 2, pp. 115–129, 2012.

[107] A. Srivastava, A. Majumdar, and B. S. Butola, "Improving the impact resistance performance of Kevlar fabrics using silica based shear thickening fluid," *Mater. Sci. Eng. A*, vol. 529, no. 1, pp. 224–229, 2011.

[108] K. S. Rao, K. El-Hami, T. Kodaki, K. Matsushige, and K. Makino, "A novel method for synthesis of silica nanoparticles," *J. Colloid Interface Sci.*, vol. 289, no. 1, pp. 125–131, 2005.

[109] N. Wagner and E. Wetzel, "Advanced body armor utilizing shear thickening fluids," *Patent US7498276 B2*, United State Patent Office, pp. 1–6, 2007.

[110] J. L. Park, B. I. Yoon, J. G. Paik, and T. J. Kang, "Ballistic performance of p-aramid fabrics impregnated with shear thickening fluid; Part II - Effect of fabric count and shot location," *Textile Research Journal*, vol. 82, no. 6. pp. 542–557, 2012.

[111] E. D. Wetzel, P. N. J. Wagner, and Y. S. Lee, "Novel flexible body armor utilizing Shear Thickening Fluid (STF) composites," *Chem. Eng.*, pp. 1–19, July 2003.

[112] G. Sukumar, B. Bhav Singh, A. Bhattacharjee, K. Siva Kumar, and A. K. Gogia, "Ballistic impact behaviour of CEZ Ti alloy against 7.62 mm armour piercing projectiles," *Int. J. Impact Eng.*, vol. 54, pp. 149–160, 2013.

[113] G. A. O. Davies and X. Zhang, "Impact damage prediction in carbon composite structures," *International Journal of Impact Engineering*, vol. 16, no. 1. pp. 149–170, 1995.

[114] A. Seyed Yaghoubi and B. Liaw, "Influences of thickness and stacking sequence on ballistic impact behaviors of GLARE 5 FML plates: Part I-experimental studies," *J. Compos. Mater.*, vol. 94, pp. 2585–2598, 2012.

[115] A. G. Odeshi, M. N. Bassim, and M. Bolduc, "Dynamic Impact Behavior of 6061-T6 and 5083-H131 Aluminum alloys," *International Congress on Fracture* (*ICF12)*, pp. 1–9, 2009.

[116] E. E. Haro, A. G. Odeshi, and J. A. Szpunar, "The energy absorption behavior of hybrid composite laminates containing nano-fillers under ballistic impact," *Int. J. Impact Eng.*, vol. 96, pp. 11–22, 2016.

[117] E. P. Giannelis, "Polymer Layered Silicate Nanocomposites," *Adv. Mater.*, vol. 8, no. 1, pp. 29–35, 1996.

[118]S. Pavlidou and C. D. Papaspyrides, "A review on polymer-layered silicate nanocomposites," *Progress in Polymer Science (Oxford)*, vol. 33, no. 12. pp. 1119–1198, 2008.

[119] S. Sinha Ray and M. Okamoto, "Polymer/layered silicate nanocomposites: A review from preparation to processing," *Progress in Polymer Science (Oxford)*, vol. 28, no. 11. pp. 1539–1641, 2003.

[120] E. D. Wetzel, P. N. J. Wagner, and Y. S. Lee, "Protective Fabrics Utilizing Shear Thickening Fluids (STFs)," in *4th International Conference on Safety and Protective Fabrics Pittsburgh, PA*, pp. 1–23, 2004.

[121] Jaisingh SJ, SelvamV, Kumar M., "Studies on mechanical properties of Kevlar fiber reinforced iron (III) oxide naniparticles filled up/epoxy nanocomposites." *Adv. Mat. Res.*, vol. 747, pp. 409–412, 2013.

[122] P. N. B. Reis, J. a M. Ferreira, J. D. M. Costa, and M. J. Santos, "Fatigue performance of Kevlar/epoxy composites with filled matrix by cork powder," *Fibers Polym.*, vol. 13, no. 10, pp. 1292–1299, 2012.

[123] P. J. Klein, Q. Zhang, J. W. Baur, L. Dai, D. C. Lagoudas, J. Liu, and R. J. Sager, "Effect of carbon nanotubes on the interfacial shear strength of T650 carbon fiber in an epoxy matrix," *Compos. Sci. Technol.*, vol. 69, no. 7–8, pp. 898–904, 2009.

[124] E. T. Thostenson, W. Z. Li, D. Z. Wang, Z. F. Ren, and T. W. Chou, "Carbon nanotube/carbon fiber hybrid multiscale composites," *J. Appl. Phys.*, vol. 91, no. 9, pp. 6034–6037, 2002.

[125] F. An, C. Lu, Y. Li, J. Guo, X. Lu, H. Lu, S. He, and Y. Yang, "Preparation and characterization of carbon nanotube-hybridized carbon fiber to reinforce epoxy composite," *Mater. Des.*, vol. 33, no. 1, pp. 197–202, 2012.

[126] A. F. Ávila, A. S. Neto, and H. Nascimento Junior, "Hybrid nanocomposites for mid-range ballistic protection," *Int. J. Impact Eng.*, vol. 38, no. 8–9, pp. 669–675, 2011.

[127] J. S. Fenner and I. M. Daniel, "Hybrid nanoreinforced carbon/epoxy composites for

enhanced damage tolerance and fatigue life," *Compos. Part A Appl. Sci. Manuf.*, vol. 65, pp. 47–56, 2014.

[128] V. Kostopoulos, A. Baltopoulos, P. Karapappas, A. Vavouliotis, and a. Paipetis, "Impact and after-impact properties of carbon fibre reinforced composites enhanced with multi-wall carbon nanotubes," *Compos. Sci. Technol.*, vol. 70, no. 4, pp. 553–563, 2010.

[129] A. Manero, J. Gibson, G. Freihofer, J. Gou, and S. Raghavan, "Evaluating the effect of nano-particle additives in Kevlar® 29 impact resistant composites," *Compos. Sci. Technol.*, vol. 116, pp. 41–49, 2015.

[130] M. Li, Y. Gu, Y. Liu, Y. Li, and Z. Zhang, "Interfacial improvement of carbon fiber/epoxy composites using a simple process for depositing commercially functionalized carbon nanotubes on the fibers," *Carbon N. Y.*, vol. 52, pp. 109–121, 2013.

[131] H. Abdulhamid, A. Kolopp, C. Bouvet, and S. Rivallant, "Experimental and numerical study of AA5086-H111 aluminum plates subjected to impact," *International Journal of Impact Engineering*, vol. 51, pp. 1–12, 2013.

[132] H. Ahmadi, G. H. Liaghat, H. Sabouri, and E. Bidkhouri, "Investigation on the high velocity impact properties of glass-reinforced fiber metal laminates," *J. Compos. Mater.*, vol. 47, no. 13, pp. 1605–1615, 2012.

[133] D. Mohotti, T. Ngo, P. Mendis, and S. N. Raman, "Polyurea coated composite aluminium plates subjected to high velocity projectile impact," *Mater. Des.*, vol. 52, pp. 1–16, 2013.

[134] M. Rivai, A. Gupta, M. R. Islam, and M. D. H. Beg, "Characterization of oil palm empty fruit bunch and glass fibre reinforced recycled polypropylene hybrid composites," *Fibers Polym.*, vol. 15, no. 7, pp. 1523–1530, 2014.

[135] B. K. Deka and T. K. Maji, "Effect of silica nanopowder on the properties of wood flour / polymer composite," *Polym. Eng. Sci.*, vol. 52, no. 7, pp. 1516-1523, 2012.

[136] B. K. Deka and T. K. Maji, "Effect of TiO_2 and nanoclay on the properties of wood polymer nanocomposite," *Compos. Part A Appl. Sci. Manuf.*, vol. 42, no. 12, pp. 2117–2125, 2011.

[137] K. K. H. Yeung and K. P. Rao, "Mechanical properties of Kevlar-49 fibre reinforced thermoplastic composites," *Polym. Polym. Compos.*, vol. 20, no. 5, pp. 411–424, 2012.

[138] J. Li, "The Effect of Carbon Fiber Content on the Mechanical and Tribological Properties of Carbon Fiber-Reinforced PTFE Composites," *Polym. Plast. Technol. Eng.*, vol. 49, no. 4, pp. 332–336, 2010.

[139] S. Saikrasun, T. Amornsakchai, C. Sirisinha, W. Meesiri, and S. Bualek-Limcharoen, "Kevlar reinforcement of polyolefin-based thermoplastic elastomer," *Polymer (Guildf).*, vol. 40, no. 23, pp. 6437–6442, 1999.

[140] T. Amornsakchai, B. Sinpatanapan, S. Bualek-Limcharoen, and W. Meesiri, "Composite of aramid fibre (poly-m-phenylene isophthalamide)thermoplastic elastomers (SEBS): Enhancement of tensile properties by maleated-SEBS compatibiliser," *Polymer (Guildf).*, vol. 40, no. 11, pp. 2993–2999, 1999.

[141] M. Valente, F. Sarasini, F. Marra, J. Tirillò, and G. Pulci, "Hybrid recycled glass fiber/wood flour thermoplastic composites: Manufacturing and mechanical characterization," *Compos. Part A Appl. Sci. Manuf.*, vol. 42, no. 6, pp. 649–657, 2011.

[142] A. Ramezani Kakroodi, Y. Kazemi, and D. Rodrigue, "Mechanical, rheological, morphological and water absorption properties of maleated polyethylene/hemp composites: Effect of ground tire rubber addition," *Compos. Part B Eng.*, vol. 51, pp. 337–344, 2013.

[143] N. A. Mohd Ayob, M. Ahmad, and N. N. Mohd Khairuddin, "Water Resistance and Tensile Strength of High Density Polyethylene (HDPE) Composites," *Adv. Mater. Res.*, vol. 1134, pp. 34–38, 2016.

[144] J. Cho, M. S. Joshi, and C. T. Sun, "Effect of inclusion size on mechanical properties of polymeric composites with micro and nano particles," *Compos. Sci. Technol.*, vol. 66, no. 13, pp. 1941–1952, 2006.

[145] I. Ozsoy, A. Demirkol, A. Mimaroglu, H. Unal, and Z. Demir, "The influence of micro- And nano-filler content on the mechanical properties of epoxy composites," *Stroj. Vestnik/Journal Mech. Eng.*, vol. 61, no. 10, pp. 601–609, 2015.

[146] R. Ou, C. Guo, Y. Xie, and Q. Wang, "Non-isothermal crystallization kinetics of Kevlar fiber-reinforced wood flour/HDPE composites," *BioResources*, vol. 6, no. 4, pp. 4547–4565, 2011.

[147] Y. Xian, H. Li, C. Wang, G. Wang, W. Ren, and H. Cheng, "Effect of white mud as a second filler on the mechanical and thermal properties of bamboo residue," *BioResources*, vol. 10, no. 3, pp. 4263–4276, 2015.

[148] G. Cantero, A. Valea, I. Mondragon, A. Arbelaiz, and B. Ferna, "Mechanical properties of flax fibre/polypropylene composites. Influence of fibre/matrix modification and glass fibre hybridization," *Compos. Part A Appl. Sci. Manuf.*, vol. 36, pp. 1637–1644, 2005.

[149] S. Mishra, A. K. Mohanty, L. T. Drzal, M. Misra, and S. Parija, "Studies on mechanical performance of biofibre/glass reinforced polyester hybrid composites," *Composites Science and Technology*, vol. 63, pp. 1377–1385, 2003.

[150] T. P. Sathishkumar, J. Naveen, and S. Satheeshkumar, "Hybrid fiber reinforced polymer composites – a review," *Journal of Reinforced Plastics and Composites*, vol. 33, no. 5, pp. 454–471, 2014.

[151] R. Burgueno, M. J. Quagliata, A. K. Mohanty, G. Mehta, L. T. Drzal, and M. Misra, "Hybrid biofiber-based composites for structural cellular plates," *Compos. Part A Appl. Sci. Manuf.*, vol. 36, pp. 581–593, 2005.

[152] A. Kumar, V. V Chavan, S. Ahmad, and R. Alagirusamy, "International Journal of Impact Engineering Ballistic impact response of Kevlar® reinforced thermoplastic composite armors," *Int. J. Impact Eng.*, vol. 89, pp. 1–13, 2016.

[153] J. Li, "The Effect of Kevlar Pulp Content on Mechanical and Tribological Properties of Thermoplastic Polyimide Composites," *J. Reinf. Plast. Compos.*, vol. 29, no. 11, pp. 1601–1608, 2010.

[154] M. Jacob, S. Thomas, and K. T. Varughese, "Natural rubber composites reinforced with sisal/oil palm hybrid fibers: Tensile and cure characteristics," *J. Appl. Polym. Sci.*, vol. 93, no. 5, pp. 2305–2312, 2004.

[155] M. D. H. Beg, J. O. Akindoyo, S. Ghazali, and A. A. Mamun, "Impact modified oil palm empty fruit bunch fiber/poly (lactic) acid composite," *Int. J. Che. Molec. Nuclear Mat. and Metall. Eng.*, vol. 9, no. 1, pp. 165–170, 2015.

[156] E. E. Haro, J. A. Szpunar, and A. G. Odeshi, "Dynamic and ballistic impact behavior of biocomposite armors made of HDPE reinforced with chonta palm wood (Bactris gasipaes) microparticles," *Def. Technol.*, vol. 14, no. 1, pp. 238–249, 2018.

[157] M. John and S. Thomas, "Biofibres and biocomposites," *Carbohydr. Polym.*, vol. 71, no. 3, pp. 343–364, 2008.

[158] V. K. Mathur, "Composite materials from local resources," *Constr. Build. Mater.*, vol. 20, no. 7, pp. 470–477, 2006.

[159] D. Rusu, S. A. E. Boyer, M. F. Lacrampe, and P. Krawczak, "Bioplastics and Vegetal Fiber Reinforced Bioplastics for Automotive Applications," *Handb. Bioplastics Biocomposites Eng. Appl.*, pp. 397–449, 2011.

[160] B. C. Temer and J. R. M. Almeida, "Development and characterization of agglomerated panels using residues from the sustainable production of heart of palm from pejibaye (Bactris gasipaes) palms," *Polym. Renew Resour.*, vol. 6, no. 2, pp. 43–55, 2014.

[161] B. C. Temer and J. R. M. Almeida, "Characterization of the tensile behavior of pejibaye (Bactris gasipaes) fibers," *Polym. Renew Resour.*, vol. 3, no. 2, pp. 33–43, 2012.

[162] A. V. Ratna Prasad and K. Mohana Rao, "Mechanical properties of natural fibre reinforced polyester composites: Jowar, sisal and bamboo," *Mater. Des.*, vol. 32, no. 8–9, pp. 4658–4663, 2011.

[163] D. Nabi Saheb and J. P. Jog, "Natural fiber polymer composites: a review," *Adv. Polym. Technol.*, vol. 18, no. 4, pp. 351–363, 1999.

[164] D. Stokke, Q. Wu and G. Han, "Introduction to wood and natural fiber composites.", *John Wiley & Sons, Inc.*, U.S., 1st edition, Chichester, England, 2014.

[165] F. P. La Mantia and M. Morreale, "Green composites: A brief review," *Compos. Part A Appl. Sci. Manuf.*, vol. 42, no. 6, pp. 579–588, 2011.

[166] R. Mahjoub, J. Bin, M. Yatim, A. Rahman, and M. Sam, "A review of structural performance of oil palm empty fruit bunch fiber in polymer composites," *Adv. Mater. Sci. Eng.*, vol. 2013, pp. 1-9, 2013.

[167] R. S. Bacellar and J. R. M. Almeida, "Mechanical properties of pupunha (Bactris gasipaes) palm," *Chemical Engineering Transactions*, vol. 17, pp. 1771-1776, 2009.

[168] M. A. de Farias, M. Z. Farina, A. P. T. Pezzin, and D. A. K. Silva, "Unsaturated polyester composites reinforced with fiber and powder of peach palm: Mechanical characterization and water absorption profile," *Mater. Sci. Eng. C*, vol. 29, no. 2, pp. 510–513, 2009.

[169] A. S. Santos, M. Z. Farina, P. T. Pezzin, and D. A. K. Silva, "The Application of Peach Palm Fibers as an Alternative to Fiber Reinforced Polyester Composites," *J. Reinf. Plast. Compos.*, vol. 27, no. 16–17, pp. 1805–1816, 2008.

[170] N. Ayrilmis, M. Taşdemir, and T. Akbulut, "Water absorption and mechanical properties of PP/HIPS hybrid composites filled with wood flour," *Polym. Compos.*, 2015. DOI: 10.1002/pc.23647

[171] H. Ku, H. Wang, N. Pattarachaiyakoop, and M. Trada, "A review on the tensile properties of natural fiber reinforced polymer composites," *Compos. Part B Eng.*, vol. 42, no. 4, pp. 856–873, 2011.

[172] M. Bengtsson, M. Le Baillif, and K. Oksman, “Extrusion and mechanical properties of highly filled cellulose fibre-polypropylene composites,” *Compos. Part A Appl. Sci. Manuf.*, vol. 38, no. 8, pp. 1922–1931, 2007.

[173] P. Wambua, B. Vangrimde, S. Lomov, and I. Verpoest, “The response of natural fibre composites to ballistic impact by fragment simulating projectiles,” *Compos. Struct.*, vol. 77, no. 2, pp. 232–240, 2007.

Appendix

Copyright Permission of Manuscript #1:

Elsevier Science and Technology Journals LICENSE
TERMS AND CONDITIONS

Dec 14, 2017

This is a License Agreement between Edison E Haro ("You") and Elsevier Science and Technology Journals ("Elsevier Science and Technology Journals") provided by Copyright Clearance Center ("CCC"). The license consists of your order details, the terms and conditions provided by Elsevier Science and Technology Journals, and the payment terms and conditions.

All payments must be made in full to CCC. For payment instructions, please see information listed at the bottom of this form.

License Number	4247700377785
License date	Dec 14, 2017
Licensed content publisher	Elsevier Science and Technology Journals
Licensed content title	Composites. Part A, Applied science and manufacturing
Licensed content date	Jan 1, 1996
Type of Use	Thesis/Dissertation
Requestor type	Author of requested content
Format	Electronic
Portion	chapter/article
Number of pages in chapter/article	12
The requesting person/organization is:	Edison E. Haro

Title or numeric reference of the portion(s)	Ballistic impact response of laminated hybrid materials made of 5086-H32 aluminum alloy, epoxy and Kevlar fabrics impregnated with shear thickening fluid
Title of the article or chapter the portion is from	Ballistic impact response of laminated hybrid materials made of 5086-H32 aluminum alloy, epoxy and Kevlar fabrics impregnated with shear thickening fluid
Editor of portion(s)	N/A
Author of portion(s)	N/A
Volume of serial or monograph.	N/A
Page range of the portion	1-12
Publication date of portion	2018
Rights for	Main product
Duration of use	Life of current edition
Creation of copies for the disabled	no
With minor editing privileges	no
For distribution to	Canada
In the following language(s)	Original language of publication
With incidental promotional use	no
The lifetime unit quantity of new product	Up to 499
Title	Ballistic impact response of laminated hybrid materials made of 5086-H32 aluminum alloy, epoxy and Kevlar fabrics impregnated with shear thickening fluid
Instructor name	Jerzy A. Szpunar
Institution name	University of Saskatchewan

Expected presentation date	May 2018
Billing Type	Invoice
Billing Address	Edison E Haro 23 Chomyn Cres Saskatoon, SK S7K 7R2 Canada Attn: Edison Haro
Total (may include CCC user fee)	0.00 USD

Terms and Conditions

TERMS AND CONDITIONS

The following terms are individual to this publisher:

None

Other Terms and Conditions:

STANDARD TERMS AND CONDITIONS

1. Description of Service; Defined Terms. This Republication License enables the User to obtain licenses for republication of one or more copyrighted works as described in detail on the relevant Order Confirmation (the "Work(s)"). Copyright Clearance Center, Inc. ("CCC") grants licenses through the Service on behalf of the rightsholder identified on the Order Confirmation (the "Rightsholder"). "Republication", as used herein, generally means the inclusion of a Work, in whole or in part, in a new work or works, also as described on the Order Confirmation. "User", as used herein, means the person or entity making such republication.

2. The terms set forth in the relevant Order Confirmation, and any terms set by the Rightsholder with respect to a particular Work, govern the terms of use of Works in connection with the Service. By using the Service, the person transacting for a republication license on behalf of the User represents and warrants that he/she/it (a) has been duly authorized by the User to accept, and hereby does accept, all such terms and conditions on behalf of User, and (b) shall inform User of all such terms and conditions. In the event such person is a "freelancer" or other third party independent of User and CCC, such party shall be deemed jointly a "User" for purposes of these

terms and conditions. In any event, User shall be deemed to have accepted and agreed to all such terms and conditions if User republishes the Work in any fashion.

3. Scope of License; Limitations and Obligations.

3.1 All Works and all rights therein, including copyright rights, remain the sole and exclusive property of the Rightsholder. The license created by the exchange of an Order Confirmation (and/or any invoice) and payment by User of the full amount set forth on that document includes only those rights expressly set forth in the Order Confirmation and in these terms and conditions, and conveys no other rights in the Work(s) to User. All rights not expressly granted are hereby reserved.

3.2 General Payment Terms: You may pay by credit card or through an account with us payable at the end of the month. If you and we agree that you may establish a standing account with CCC, then the following terms apply: Remit Payment to: Copyright Clearance Center, 29118 Network Place, Chicago, IL 60673-1291. Payments Due: Invoices are payable upon their delivery to you (or upon our notice to you that they are available to you for downloading). After 30 days, outstanding amounts will be subject to a service charge of 1-1/2% per month or, if less, the maximum rate allowed by applicable law. Unless otherwise specifically set forth in the Order Confirmation or in a separate written agreement signed by CCC, invoices are due and payable on "net 30" terms. While User may exercise the rights licensed immediately upon issuance of the Order Confirmation, the license is automatically revoked and is null and void, as if it had never been issued, if complete payment for the license is not received on a timely basis either from User directly or through a payment agent, such as a credit card company.

3.3 Unless otherwise provided in the Order Confirmation, any grant of rights to User (i) is "one-time" (including the editions and product family specified in the license), (ii) is non-exclusive and non-transferable and (iii) is subject to any and all limitations and restrictions (such as, but not limited to, limitations on duration of use or circulation) included in the Order Confirmation or invoice and/or in these terms and conditions. Upon completion of the licensed use, User shall either secure a new permission for further use of the Work(s) or immediately cease any new use of the Work(s) and shall render inaccessible (such as by deleting or by removing or severing links or other locators) any further copies of the Work (except for copies printed on paper in accordance with this license and still in User's stock at the end of such period).

3.4 In the event that the material for which a republication license is sought includes third party materials (such as photographs, illustrations, graphs, inserts and similar materials) which are identified in such material as having been used by permission, User is responsible for identifying, and seeking separate licenses (under this Service or otherwise) for, any of such third party materials; without a separate license, such third party materials may not be used.

3.5 Use of proper copyright notice for a Work is required as a condition of any license granted under the Service. Unless otherwise provided in the Order Confirmation, a proper copyright notice will read substantially as follows: "Republished with permission of [Rightsholder's name], from [Work's title, author, volume, edition number and year of copyright]; permission conveyed through Copyright Clearance Center, Inc. " Such notice must be provided in a reasonably legible font size and must be placed either immediately adjacent to the Work as used (for example, as part of a by-line or footnote but not as a separate electronic link) or in the place where substantially all other credits or notices for the new work containing the republished Work are located. Failure to include the required notice results in loss to the Rightsholder and CCC, and the User shall be liable to pay liquidated damages for each such failure equal to twice the use fee specified in the Order Confirmation, in addition to the use fee itself and any other fees and charges specified.

3.6 User may only make alterations to the Work if and as expressly set forth in the Order Confirmation. No Work may be used in any way that is defamatory, violates the rights of third parties (including such third parties' rights of copyright, privacy, publicity, or other tangible or intangible property), or is otherwise illegal, sexually explicit or obscene. In addition, User may not conjoin a Work with any other material that may result in damage to the reputation of the Rightsholder. User agrees to inform CCC if it becomes aware of any infringement of any rights in a Work and to cooperate with any reasonable request of CCC or the Rightsholder in connection therewith.

4. Indemnity. User hereby indemnifies and agrees to defend the Rightsholder and CCC, and their respective employees and directors, against all claims, liability, damages, costs and expenses, including legal fees and expenses, arising out of any use of a Work beyond the scope of the rights granted herein, or any use of a Work which has been altered in any unauthorized way by User, including claims of defamation or infringement of rights of copyright, publicity, privacy or other tangible or intangible property.

5. Limitation of Liability. UNDER NO CIRCUMSTANCES WILL CCC OR THE RIGHTSHOLDER BE LIABLE FOR ANY DIRECT, INDIRECT, CONSEQUENTIAL OR INCIDENTAL DAMAGES (INCLUDING WITHOUT LIMITATION DAMAGES FOR LOSS OF BUSINESS PROFITS OR INFORMATION, OR FOR BUSINESS INTERRUPTION) ARISING OUT OF THE USE OR INABILITY TO USE A WORK, EVEN IF ONE OF THEM HAS BEEN ADVISED OF THE POSSIBILITY OF SUCH DAMAGES. In any event, the total liability of the Rightsholder and CCC (including their respective employees and directors) shall not exceed the total amount actually paid by User for this license. User assumes full liability for the actions and omissions of its principals, employees, agents, affiliates, successors and assigns.

6. Limited Warranties. THE WORK(S) AND RIGHT(S) ARE PROVIDED “AS IS”. CCC HAS THE RIGHT TO GRANT TO USER THE RIGHTS GRANTED IN THE ORDER CONFIRMATION DOCUMENT. CCC AND THE RIGHTSHOLDER DISCLAIM ALL OTHER WARRANTIES RELATING TO THE WORK(S) AND RIGHT(S), EITHER EXPRESS OR IMPLIED, INCLUDING WITHOUT LIMITATION IMPLIED WARRANTIES OF MERCHANTABILITY OR FITNESS FOR A PARTICULAR PURPOSE. ADDITIONAL RIGHTS MAY BE REQUIRED TO USE ILLUSTRATIONS, GRAPHS, PHOTOGRAPHS, ABSTRACTS, INSERTS OR OTHER PORTIONS OF THE WORK (AS OPPOSED TO THE ENTIRE WORK) IN A MANNER CONTEMPLATED BY USER; USER UNDERSTANDS AND AGREES THAT NEITHER CCC NOR THE RIGHTSHOLDER MAY HAVE SUCH ADDITIONAL RIGHTS TO GRANT.

7. Effect of Breach. Any failure by User to pay any amount when due, or any use by User of a Work beyond the scope of the license set forth in the Order Confirmation and/or these terms and conditions, shall be a material breach of the license created by the Order Confirmation and these terms and conditions. Any breach not cured within 30 days of written notice thereof shall result in immediate termination of such license without further notice. Any unauthorized (but licensable) use of a Work that is terminated immediately upon notice thereof may be liquidated by payment of the Rightsholder's ordinary license price therefor; any unauthorized (and unlicensable) use that is not terminated immediately for any reason (including, for example, because materials containing the Work cannot reasonably be recalled) will be subject to all remedies available at law or in equity, but in no event to a payment of less than three times the Rightsholder's ordinary

license price for the most closely analogous licensable use plus Rightsholder's and/or CCC's costs and expenses incurred in collecting such payment.

8. **Miscellaneous.**

8.1 User acknowledges that CCC may, from time to time, make changes or additions to the Service or to these terms and conditions, and CCC reserves the right to send notice to the User by electronic mail or otherwise for the purposes of notifying User of such changes or additions; provided that any such changes or additions shall not apply to permissions already secured and paid for.

8.2 Use of User-related information collected through the Service is governed by CCC's privacy policy, available online here: http://www.copyright.com/content/cc3/en/tools/footer/privacypolicy.html.

8.3 The licensing transaction described in the Order Confirmation is personal to User. Therefore, User may not assign or transfer to any other person (whether a natural person or an organization of any kind) the license created by the Order Confirmation and these terms and conditions or any rights granted hereunder; provided, however, that User may assign such license in its entirety on written notice to CCC in the event of a transfer of all or substantially all of User's rights in the new material which includes the Work(s) licensed under this Service.

8.4 No amendment or waiver of any terms is binding unless set forth in writing and signed by the parties. The Rightsholder and CCC hereby object to any terms contained in any writing prepared by the User or its principals, employees, agents or affiliates and purporting to govern or otherwise relate to the licensing transaction described in the Order Confirmation, which terms are in any way inconsistent with any terms set forth in the Order Confirmation and/or in these terms and conditions or CCC's standard operating procedures, whether such writing is prepared prior to, simultaneously with or subsequent to the Order Confirmation, and whether such writing appears on a copy of the Order Confirmation or in a separate instrument.

8.5 The licensing transaction described in the Order Confirmation document shall be governed by and construed under the law of the State of New York, USA, without regard to the principles thereof of conflicts of law. Any case, controversy, suit, action, or proceeding arising out of, in connection with, or related to such licensing transaction shall be brought, at CCC's sole discretion, in any federal or state court located in the County of New York, State of New York, USA, or in any federal or state court whose geographical jurisdiction covers the location of the Rightsholder

Copyright Permission of Manuscript #2:

Elsevier Science and Technology Journals LICENSE
TERMS AND CONDITIONS

Dec 14, 2017

This is a License Agreement between Edison E Haro ("You") and Elsevier Science and Technology Journals ("Elsevier Science and Technology Journals") provided by Copyright Clearance Center ("CCC"). The license consists of your order details, the terms and conditions provided by Elsevier Science and Technology Journals, and the payment terms and conditions.

All payments must be made in full to CCC. For payment instructions, please see information listed at the bottom of this form.

License Number	4247701137472
License date	Dec 14, 2017
Licensed content publisher	Elsevier Science and Technology Journals
Licensed content title	International journal of impact engineering
Licensed content date	Jan 1, 1983
Type of Use	Thesis/Dissertation
Requestor type	Author of requested content
Format	Electronic
Portion	chapter/article
Number of pages in chapter/article	12

The requesting person/organization is:	Edison E. Haro
Title or numeric reference of the portion(s)	The energy absorption behavior of hybrid composite laminates containing nano-fillers under ballistic impact
Title of the article or chapter the portion is from	The energy absorption behavior of hybrid composite laminates containing nano-fillers under ballistic impact
Editor of portion(s)	N/A
Author of portion(s)	N/A
Volume of serial or monograph.	N/A
Page range of the portion	1-12
Publication date of portion	2018
Rights for	Main product
Duration of use	Life of current edition
Creation of copies for the disabled	no
With minor editing privileges	no
For distribution to	Canada
In the following language(s)	Original language of publication
With incidental promotional use	no
The lifetime unit quantity of new product	Up to 499
Title	The energy absorption behavior of hybrid composite laminates containing nano-fillers under ballistic impact
Instructor name	Jerzy A. Szpunar
Institution name	University of Saskatchewan
Expected presentation date	May 2018

Billing Type	Invoice
Billing Address	Edison E Haro 23 Chomyn Cres Saskatoon, SK S7K 7R2 Canada Attn: Edison E Haro
Total (may include CCC user fee)	0.00 USD

Terms and Conditions

TERMS AND CONDITIONS

The following terms are individual to this publisher:

None

Other Terms and Conditions:

STANDARD TERMS AND CONDITIONS

1. Description of Service; Defined Terms. This Republication License enables the User to obtain licenses for republication of one or more copyrighted works as described in detail on the relevant Order Confirmation (the "Work(s)"). Copyright Clearance Center, Inc. ("CCC") grants licenses through the Service on behalf of the rightsholder identified on the Order Confirmation (the "Rightsholder"). "Republication", as used herein, generally means the inclusion of a Work, in whole or in part, in a new work or works, also as described on the Order Confirmation. "User", as used herein, means the person or entity making such republication.

2. The terms set forth in the relevant Order Confirmation, and any terms set by the Rightsholder with respect to a particular Work, govern the terms of use of Works in connection with the Service. By using the Service, the person transacting for a republication license on behalf of the User represents and warrants that he/she/it (a) has been duly authorized by the User to accept, and hereby does accept, all such terms and conditions on behalf of User, and (b) shall inform User of all such terms and conditions. In the event such person is a "freelancer" or other third party independent of User and CCC, such party shall be deemed jointly a "User" for purposes of these

terms and conditions. In any event, User shall be deemed to have accepted and agreed to all such terms and conditions if User republishes the Work in any fashion.

3. Scope of License; Limitations and Obligations.

3.1 All Works and all rights therein, including copyright rights, remain the sole and exclusive property of the Rightsholder. The license created by the exchange of an Order Confirmation (and/or any invoice) and payment by User of the full amount set forth on that document includes only those rights expressly set forth in the Order Confirmation and in these terms and conditions, and conveys no other rights in the Work(s) to User. All rights not expressly granted are hereby reserved.

3.2 General Payment Terms: You may pay by credit card or through an account with us payable at the end of the month. If you and we agree that you may establish a standing account with CCC, then the following terms apply: Remit Payment to: Copyright Clearance Center, 29118 Network Place, Chicago, IL 60673-1291. Payments Due: Invoices are payable upon their delivery to you (or upon our notice to you that they are available to you for downloading). After 30 days, outstanding amounts will be subject to a service charge of 1-1/2% per month or, if less, the maximum rate allowed by applicable law. Unless otherwise specifically set forth in the Order Confirmation or in a separate written agreement signed by CCC, invoices are due and payable on "net 30" terms. While User may exercise the rights licensed immediately upon issuance of the Order Confirmation, the license is automatically revoked and is null and void, as if it had never been issued, if complete payment for the license is not received on a timely basis either from User directly or through a payment agent, such as a credit card company.

3.3 Unless otherwise provided in the Order Confirmation, any grant of rights to User (i) is "one-time" (including the editions and product family specified in the license), (ii) is non-exclusive and non-transferable and (iii) is subject to any and all limitations and restrictions (such as, but not limited to, limitations on duration of use or circulation) included in the Order Confirmation or invoice and/or in these terms and conditions. Upon completion of the licensed use, User shall either secure a new permission for further use of the Work(s) or immediately cease any new use of the Work(s) and shall render inaccessible (such as by deleting or by removing or severing links or other locators) any further copies of the Work (except for copies printed on paper in accordance with this license and still in User's stock at the end of such period).

3.4 In the event that the material for which a republication license is sought includes third party materials (such as photographs, illustrations, graphs, inserts and similar materials) which are identified in such material as having been used by permission, User is responsible for identifying, and seeking separate licenses (under this Service or otherwise) for, any of such third party materials; without a separate license, such third party materials may not be used.

3.5 Use of proper copyright notice for a Work is required as a condition of any license granted under the Service. Unless otherwise provided in the Order Confirmation, a proper copyright notice will read substantially as follows: “Republished with permission of [Rightsholder’s name], from [Work's title, author, volume, edition number and year of copyright]; permission conveyed through Copyright Clearance Center, Inc. ” Such notice must be provided in a reasonably legible font size and must be placed either immediately adjacent to the Work as used (for example, as part of a by-line or footnote but not as a separate electronic link) or in the place where substantially all other credits or notices for the new work containing the republished Work are located. Failure to include the required notice results in loss to the Rightsholder and CCC, and the User shall be liable to pay liquidated damages for each such failure equal to twice the use fee specified in the Order Confirmation, in addition to the use fee itself and any other fees and charges specified.

3.6 User may only make alterations to the Work if and as expressly set forth in the Order Confirmation. No Work may be used in any way that is defamatory, violates the rights of third parties (including such third parties' rights of copyright, privacy, publicity, or other tangible or intangible property), or is otherwise illegal, sexually explicit or obscene. In addition, User may not conjoin a Work with any other material that may result in damage to the reputation of the Rightsholder. User agrees to inform CCC if it becomes aware of any infringement of any rights in a Work and to cooperate with any reasonable request of CCC or the Rightsholder in connection therewith.

4. Indemnity. User hereby indemnifies and agrees to defend the Rightsholder and CCC, and their respective employees and directors, against all claims, liability, damages, costs and expenses, including legal fees and expenses, arising out of any use of a Work beyond the scope of the rights granted herein, or any use of a Work which has been altered in any unauthorized way by User, including claims of defamation or infringement of rights of copyright, publicity, privacy or other tangible or intangible property.

5. Limitation of Liability. UNDER NO CIRCUMSTANCES WILL CCC OR THE RIGHTSHOLDER BE LIABLE FOR ANY DIRECT, INDIRECT, CONSEQUENTIAL OR INCIDENTAL DAMAGES (INCLUDING WITHOUT LIMITATION DAMAGES FOR LOSS OF BUSINESS PROFITS OR INFORMATION, OR FOR BUSINESS INTERRUPTION) ARISING OUT OF THE USE OR INABILITY TO USE A WORK, EVEN IF ONE OF THEM HAS BEEN ADVISED OF THE POSSIBILITY OF SUCH DAMAGES. In any event, the total liability of the Rightsholder and CCC (including their respective employees and directors) shall not exceed the total amount actually paid by User for this license. User assumes full liability for the actions and omissions of its principals, employees, agents, affiliates, successors and assigns.

6. Limited Warranties. THE WORK(S) AND RIGHT(S) ARE PROVIDED “AS IS”. CCC HAS THE RIGHT TO GRANT TO USER THE RIGHTS GRANTED IN THE ORDER CONFIRMATION DOCUMENT. CCC AND THE RIGHTSHOLDER DISCLAIM ALL OTHER WARRANTIES RELATING TO THE WORK(S) AND RIGHT(S), EITHER EXPRESS OR IMPLIED, INCLUDING WITHOUT LIMITATION IMPLIED WARRANTIES OF MERCHANTABILITY OR FITNESS FOR A PARTICULAR PURPOSE. ADDITIONAL RIGHTS MAY BE REQUIRED TO USE ILLUSTRATIONS, GRAPHS, PHOTOGRAPHS, ABSTRACTS, INSERTS OR OTHER PORTIONS OF THE WORK (AS OPPOSED TO THE ENTIRE WORK) IN A MANNER CONTEMPLATED BY USER; USER UNDERSTANDS AND AGREES THAT NEITHER CCC NOR THE RIGHTSHOLDER MAY HAVE SUCH ADDITIONAL RIGHTS TO GRANT.

7. Effect of Breach. Any failure by User to pay any amount when due, or any use by User of a Work beyond the scope of the license set forth in the Order Confirmation and/or these terms and conditions, shall be a material breach of the license created by the Order Confirmation and these terms and conditions. Any breach not cured within 30 days of written notice thereof shall result in immediate termination of such license without further notice. Any unauthorized (but licensable) use of a Work that is terminated immediately upon notice thereof may be liquidated by payment of the Rightsholder's ordinary license price therefor; any unauthorized (and unlicensable) use that is not terminated immediately for any reason (including, for example, because materials containing the Work cannot reasonably be recalled) will be subject to all remedies available at law or in equity, but in no event to a payment of less than three times the Rightsholder's ordinary

license price for the most closely analogous licensable use plus Rightsholder's and/or CCC's costs and expenses incurred in collecting such payment.

8. **Miscellaneous.**

8.1 User acknowledges that CCC may, from time to time, make changes or additions to the Service or to these terms and conditions, and CCC reserves the right to send notice to the User by electronic mail or otherwise for the purposes of notifying User of such changes or additions; provided that any such changes or additions shall not apply to permissions already secured and paid for.

8.2 Use of User-related information collected through the Service is governed by CCC's privacy policy, available online here :

http://www.copyright.com/content/cc3/en/tools/footer/privacypolicy.html.

8.3 The licensing transaction described in the Order Confirmation is personal to User. Therefore, User may not assign or transfer to any other person (whether a natural person or an organization of any kind) the license created by the Order Confirmation and these terms and conditions or any rights granted hereunder; provided, however, that User may assign such license in its entirety on written notice to CCC in the event of a transfer of all or substantially all of User's rights in the new material which includes the Work(s) licensed under this Service.

8.4 No amendment or waiver of any terms is binding unless set forth in writing and signed by the parties. The Rightsholder and CCC hereby object to any terms contained in any writing prepared by the User or its principals, employees, agents or affiliates and purporting to govern or otherwise relate to the licensing transaction described in the Order Confirmation, which terms are in any way inconsistent with any terms set forth in the Order Confirmation and/or in these terms and conditions or CCC's standard operating procedures, whether such writing is prepared prior to, simultaneously with or subsequent to the Order Confirmation, and whether such writing appears on a copy of the Order Confirmation or in a separate instrument.

8.5 The licensing transaction described in the Order Confirmation document shall be governed by and construed under the law of the State of New York, USA, without regard to the principles thereof of conflicts of law. Any case, controversy, suit, action, or proceeding arising out of, in connection with, or related to such licensing transaction shall be brought, at CCC's sole discretion, in any federal or state court located in the County of New York, State of New York, USA, or in any federal or state court whose geographical jurisdiction covers the location of the Rightsholder